UNIVERSIDAD DE CÓRDOBA

Doctorado en Biociencias y Ciencias Agroalimentarias

Implicación de las fosfatasas PP2C en la señalización MAPK y patogénesis de *Fusarium oxysporum*

Involvement of PP2C phosphatases in MAPK signaling and pathogenesis of *Fusarium oxysporum*

Director: Dra. María Concepción de la Hera Díaz de Liaño

Pedro Paulo Ferreira Lemos

Córdoba, 2018.

Fecha de depósito de tesis en el Idep: 30/10/2018

TITULO: *Involvement of PP2C phosphatases in MAPK signaling and pathogenesis of Fusarium oxysporum*

AUTOR: *Pedro Paulo Ferreira Lemos*

Campus de Rabanales
Ctra. Nacional IV, Km. 396 A
14071 Córdoba

https://www.uco.es/ucopress/index.php/es/
ucopress@uco.es

TÍTULO DE LA TESIS: Implicación de las fosfatasas PP2C en la señalización MAPK y patogénesis de *Fusarium oxysporum*

DOCTORANDO/A: Pedro Paulo Ferreira Lemos

INFORME RAZONADO DEL/DE LOS DIRECTOR/ES DE LA TESIS

(se hará mención a la evolución y desarrollo de la tesis, así como a trabajos y publicaciones derivados de la misma).

La Tesis Doctoral de D. Pedro Paulo Ferreira Lemos se ha llevado a cabo en el Departamento de Genética de la Universidad de Córdoba, en el seno del Grupo "Genética molecular de la patogénesis fúngica" (BIO-3138). Su desarrollo ha permitido al doctorando adquirir una sólida formación en Genética y Biología Molecular. Durante la realización de la Tesis, D. Pedro ha mostrado tener una gran capacidad de trabajo y aptitud para la investigación científica. En el trabajo se ha analizado el papel de las fosfatasas de la familia PP2C en la señalización y la patogénesis del hongo *Fusarium oxysporum* f.sp. *lycopersici*. Los resultados obtenidos se han comunicado en varios congresos nacionales e internacionales, y se han recogido en la siguiente publicación:

Lemos P, Ruíz-Roldán C, **Hera C** (2018) Role of the phosphatase Ptc1 in stress responses mediated by CWI and HOG pathways in Fusarium oxysporum. *Fungal Genetics and Biology* 118: 10-20. DOI: 10.1016/j.fgb.2018.05.004.

Por todo ello, se autoriza la presentación de la tesis doctoral.

Córdoba, 29 de Octubre de 2018

Firma del/de los director/es

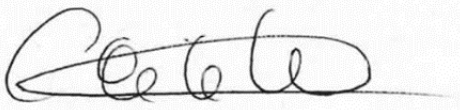

Fdo.: C. de la Hera

This work has been conducted in the Department of Genetics of the University of Córdoba and financially supported by grants BIO2013-47870R and BIO2016-78923-R from the Spanish Ministerio de Innovación y Competitividad (MINECO) and BIO-296 from Junta de Andalucia. PFL Student PhD was supported by Science Without Borders programme (CAPES, Ministry of Education and Ministry of Science and Technology), Federal Government of Brazil.

Index

List of figures

List of tables

Abstract

ABSTRACT

Reversible protein phosphorylation is crucial for cell signal transduction in stress response of eukaryotes. *Fusarium oxysporum* is a soil-borne plant pathogenic fungus that can adapt to a wide range of ecological niches and environmental conditions. Three mitogen activated protein kinase (MAPK) cascades have been shown to orchestrate the response of the fungus to external insults such as high temperature, insults on cell wall, oxidative or hyperosmotic stress in *F. oxysporum*. However, the protein phosphatases that fine-tune phosphorylation levels of different MAPKs in this fungus are unknown. In this study, we have focused on elucidating the role of type 2C protein phosphatases (PP2C) on MAPK cascade signaling pathways and pathogenesis of *F. oxysporum* f. sp. lycopersici.

There were identified seven PP2C phosphatases in the genome of *F. oxysporum*, Ptc1, Ptc3, Ptc5, Ptc5R, Ptc6, Ptc7 and Ptc7R. Gene expression analysis revealed that under stresses that activate MAPK signaling, *F. oxysporum* PP2C genes are regulated in orchestrated-like fashion. Phenotypical assays revealed that PP2C disruptant mutants are more sensitive to cell wall damaging agents in comparison to the wild type strain, suggesting roles on the cell wall integrity pathway.

MAPK immunoblot analysis demonstrated that Ptc1, Ptc5 and Ptc7 have roles in regulating the cell wall integrity (CWI) MAPK Mpk1. Moreover, Ptc1 was shown to regulates phosphorylation of the high osmolarity glycerol response (HOG) MAPK Hog1, and Ptc5 was found to be a negative regulator of the invasive growth pathway by regulating the phosphorylation level of the MAPK Fmk1. The Δ*ptc1* mutant have shown increased tolerance to osmotic stress compounds, higher expression of genes induced by osmotic stress and presented fragmented vacuoles even in absence of the osmotic stressor, supporting the involvement of Ptc1 in the negative regulation of the HOG pathway. Two mutant strains, Δ*ptc5* and Δ*ptc5R,* showed reduced virulence on tomato host. Overall, the presented results are the first report of PP2C phosphatases regulating MAPK signaling pathways in *F. oxysporum.*

RESUMEN

La fosforilación reversible de proteínas es crucial en la transducción de señales celulares en dianas de respuesta al estrés en eucariotas. *Fusarium oxysporum* es un hongo fitopatógeno y saprofito que habita el suelo y que logra adaptarse a una amplia gama de nichos ecológicos y condiciones ambientales. En *F. oxysporum* se ha demostrado que tres cascadas de proteínas quinasas activadas por mitógeno (MAPK) establecen la respuesta del hongo a variaciones ambientales tales como alta temperatura, daños en la pared celular, estrés oxidativo o hiperosmótico. Sin embargo, las proteínas fosfatasas que regulan los niveles de fosforilación en diferentes vías MAPK son desconocidas. En este estudio, nos hemos centrado en elucidar el papel de las proteínas fosfatasas tipo 2C (PP2C) en la señalización MAPK y en la patogénesis de *F. oxysporum* f. sp. lycopersici.

En el presente estudio se identificaron siete fosfatasas PP2C en *F. oxysporum*, Ptc1, Ptc3, Ptc5, Ptc5R, Ptc6, Ptc7 y Ptc7R. El análisis de la expresión génica reveló que los genes PP2C de *F. oxysporum* están regulados de forma orquestada en respuesta a estreses que activan rutas MAPK. Los ensayos fenotípicos revelaron que mutantes PP2C presentan sensibilidad a agentes perturbadores de la pared celular en comparación con la estirpe de tipo salvaje.

El nivel de fosforilación de la ruta MAPK Mpk1 demostró que Ptc1, Ptc5 y Ptc7 tienen papeles en el mantenimiento la integridad celular. Además, fue demostrado que Ptc1 regula la fosforilación de la MAPK Hog1 en respuesta de alta osmolaridad y glicerol (HOG), y se encontró que Ptc5 es un regulador negativo de la fosforilación de ruta MAPK Fmk1 de crecimiento invasivo. El mutante Δ*ptc1* ha mostrado adicional tolerancia a compuestos de estrés osmótico, incremento en la expresión de los genes inducidos por dicho estrés y vacuolas fragmentadas incluso en ausencia de agentes de estres osmótico, lo que apoya la contribución de Ptc1 en la vía de señalización HOG. Dos cepas mutantes, Δ*ptc5* y Δ*ptc5R* mostraron virulencia reducida en el huésped tomate. En conjunto, los resultados presentados indican por primera vez el papel de fosfatasas PP2C en la regulación de vías de señalización MAPK en *F. oxysporum*.

1.Introduction

1. Introduction

1.1 Fusarium Genus

Fusarium is a genus of filamentous ascomycete fungi (Sordariomycetes: Hypocreales: Nectriaceae) that includes plant pathogens of agricultural importance. Fusarium diseases occur worldwide on forest crops in both agricultural and natural ecosystems; plant symptoms include vascular browning, leaf epinasty, stunting, progressive wilting, defoliation, rots, blights, cankers, damping-off and plant death of many horticultural, field and ornamental plants. The genus collectively represents the most important group of fungal plant pathogens, causing disease on almost every economically important plant species.

As phytopathogens, Fusarium genus is mostly classified as hemibiotrophs (Agrios, 2005). Fusarium diseases may initiate in roots from soilborne inoculum or in above-ground plant parts via air or water. Initially the infection resembles that of a biotrophic pathogen that relying on the living host, but necrotrophic transition can eventually occur leading to consuming and killing host cells (Agrios, 2005).

The genus also includes non-pathogen species strains, that can be saprophytes or parasites of other organisms in natural ecosystems, including insects, humans and other animals (Vartivarian *et al.*, 1993; Guarro and Gene, 1995; Boutati and Anaissie, 1997; Odds *et al.*, 1998; Ortoneda *et al.*, 2004). Some species can be also useful to biological control, by production of ciclosporins and gibberellins (Desjardins *et al.*, 1993), and on the production of fungal biomass to obtain pectinases, celulases, and proteases useful to a broad range of industrial food processes (Wiebe, 2002). *Fusarium* infection of humans and other animals (fusarioses) are relatively rare. Nevertheless, they typically show broad resistance to antifungal drugs (Alastruey-Izquierdo *et al.*, 2008). Fusaria are suspiciously associated with some human fungal infections of the cornea (Gower *et al.*, 2010) and some isolates produce human pathogenic biofilms on plumbing surfaces (Short *et al.*, 2011).

Fusaria can also produce toxic secondary metabolites, such as mycotoxins: fumonisins and trichothecenes that can contaminate the final agricultural products (corn or wheat), making them unsuitable for food or feed. Fusaria can also colonize damaged fruits being an important post-harvest pathogen (Woloshuk and Shim, 2013). For example, reports indicated that *Fusarium graminearum* can produce secondary metabolites from eight subcategories: aurofusarin, butenolide, chlamydosporol, culmorin, cyclonerodiol, fusarins, trichothecenes, and zearalenones, while *Fusarium oxysporum* is reported to produce zearalenone, trichothecene, beauvericin and moniliformin (Marasas *et al.,* 1984; Mirocha *et al.,* 1989; Desjardins, 2006; Moretti *et al.,* 2010).

The genus *Fusarium* was first described in by Johann H. F. Link in 1824, the high number of hosts affected by a morphological similar plant pathogen lead to the scientific community to develop a precise and reliable system of classification. the first taxonomy of the genus was published in 1931 (Wollenweber, 1931) and a revised version in 1935 (Wollenweber and Reinking, 1935). Some Fusarium species produce meiotic (sexual) spores and as many as three types of mitotic (asexual) spores. The biological species concept based on sexual mating compatibility cannot be broadly applied, few examples are reported, not all spore types are known to be produced by all species becoming limited of practical use, and fewer than 20% of fusaria have a known sexual cycle and teleomorph (Ma *et al.*, 2013). Examples of plant pathogens that support biological concept are *Fusarium solani* in *Nectria haematococca*-species complex, and to *Fusarium fujikuroi* in *Giberella fujikuroi*-species complex.

During the last century the taxonomy of the genus has been extensively restructured and modified. Snyder and Hansen (Snyder and Hansen) proposed a great simplification organizing all the taxa into nine species with no varieties or forms, grouping all the taxa of section *elegans* into a single species named *F. oxysporum*. Based on their pathogenicity on different plant species it was designated 25 formae speciales (f. sp.) species. Most early-diverging *Fusarium* lineages are associated with woody plants as parasites, endophytes, or saprophytes (O'donnell *et al.*, 2013). A recent phylogenetic analysis suggests

that Fusarium originated ~91.3 Mya (Ma *et al.*, 2013), indicating that its diversification coincided with that of flowering plants (Smith *et al.*, 2010).

The concept of f. spp. become broadly adopted in Fusaria due to isolates exhibit a high degree of host specificity. In several cases, f. spp. consists of multiple, independent lineages that evolved polyphyletically through convergent evolution (Baayen *et al.*, 2000). The genus includes close to 300 phylogenetically diagnosable species, the majority of which lack formal names. Due to the complex variability on Fusaria, a simplification was proposed, “One fungus, one name”. The new criteria adopt baselines limiting taxonomical change, the definition of new species might be based on robust principles founded on monophyly, species complex, limitation of teleomorph nomenclature, and acceptation of plant pathological, medical and microbiology scientific community (Geiser *et al.*, 2013).

1.1.1 *Fusarium oxysporum* biology and life cycle

Fusarium oxysporum is a soil pathogen, considered as a species complex, that causes vascular wilt disease in a large number of field and greenhouse crops worldwide in over one hundred agronomically important plant species, causing severe yield losses in crops such as melon, tomato, cotton and banana, among others (Michielse and Rep, 2009). *F. oxysporum* isolates often exhibit a high degree of host specificity; isolates that are pathogenic on the same host are grouped into the same forma specialis (e.g., *F. oxysporum* f. sp. *lycopersici* for tomato pathogens). In several cases, *F. oxysporum* formae speciales consist of multiple, independent lineages that evolved polyphyletically through convergent evolution (O'donnell *et al.*, 1998; Baayen *et al.*, 2000).

F. oxysporum is also an emerging opportunistic pathogen of humans that can cause invasive infections in immunocompromised patients (Nucci and Anaissie, 2007; Dean *et al.*, 2012). The ability to infect mammalian hosts, converted *F. oxysporum* as a model organism to study cross-kingdom virulence factors (Ortoneda *et al.*, 2004; Lopez-Berges *et al.*, 2012; Lopez-Berges *et al.*, 2013; Schafer *et al.*, 2014). *F. oxysporum* is able to proliferate inside the

haemocoel of *Galleria mellonella* larvae and to colonize and kill the insects. Using the insect pathosystem it has been that most genes required for full virulence on immune-suppressed mice also play a significant role in *G. mellonella* infection. To reduce the need for using mammals for *in vivo studies, G. mellonella* has been used as a non-vertebrate infection model (Navarro-Velasco *et al.*, 2011; Lopez-Berges *et al.*, 2012; Alkan *et al.*, 2013; Schafer *et al.*, 2014).

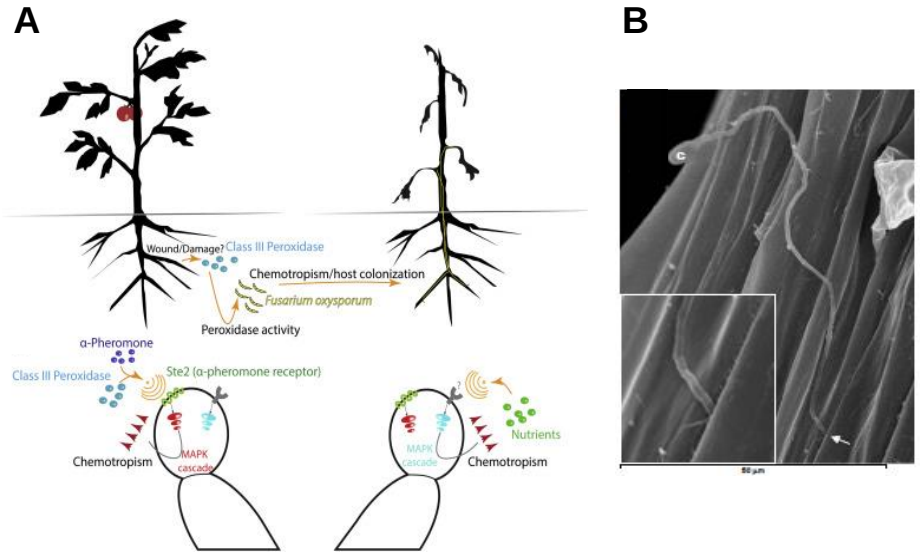

Figure 1. *F. oxysporum* sensing and penetration of plant roots prior to colonization. (A) Chemotropism and host colonization - signals from the plant host elicit the chemotropism of *F. oxysporum* toward the plant roots (Dagdas and Bozkurt, 2015), illustration by Dagdas and Bozkurt (Dagdas and Bozkurt)); (B) Scanning electron microscopy of the *F. oxysporum* penetration prior 24h germination in presence of tomato plants – conidia (c) germinates, adhere to the root and penetrate on the plant through root wounds (micrography from Pérez-Nadalez and Di Pietro (2011))

The soil is a highly dynamic environment, soilborne plant pathogens must react to contend with fluctuations in moisture, nutrients, pH, temperature, external osmolarity, and a range of potentially toxic environmental compounds. Appropriate responses to these environmental stresses must be induced for cell survival and proliferation. The worldwide distribution of *F. oxysporum* reflects the enormous potential that this pathogen has to adapt to different ecological niches. While in the soil, the primary inoculum of *F. oxysporum* can germinate and survive saprophytically in soil or plant debris producing a white cotton like mycelia (Agrios, 2005).

In response to signals from the plant host, *F. oxysporum* spores present in the soil germinate and differentiate in infection hyphae, adhere to the plant roots, and penetrate them directly through natural openings at the intercellular junctions of cortical cells or through wounds without the need for specialized infection structures (Figure1) (Pérez-Nadales and Di Pietro, 2011). Recently, tomato class III peroxidases have been described as the main chemoattractant compounds exudates of the plant roots that elicits the growth of *F. oxysporum* f. sp lycopersici toward tomato roots (Dagdas and Bozkurt, 2015).

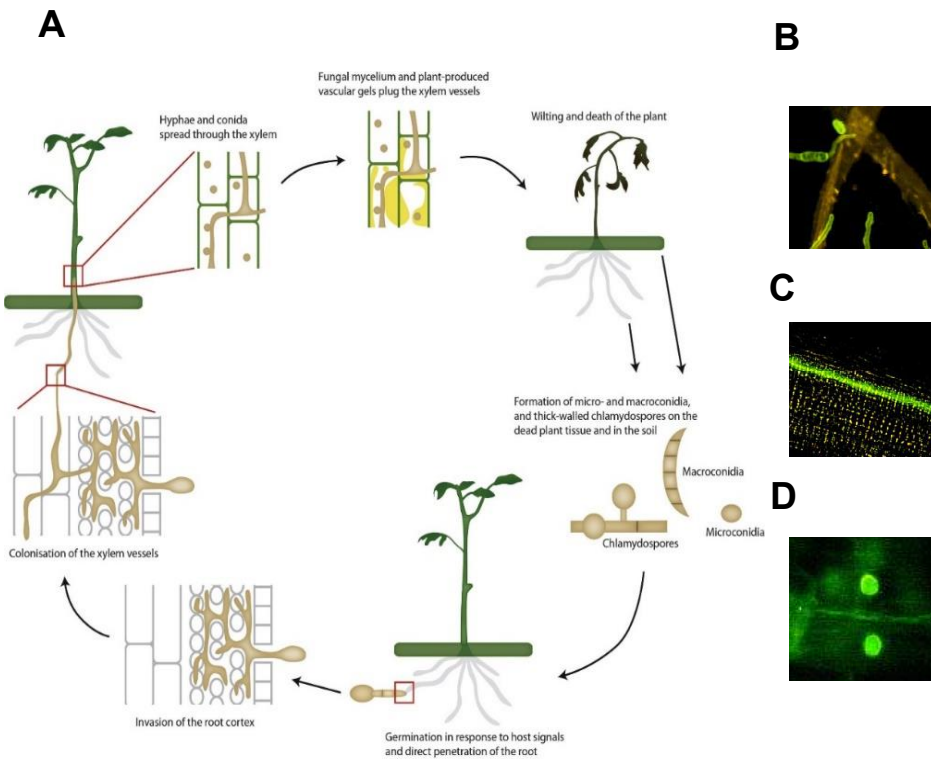

Figure 2. Life cycle of *F. oxysporum.* (A) Life cycle (B) Germination in response to host signals, adhesion and direct penetration of the root. (C) Invasion of the root cortex and colonization of the xylem vessels. (D) Formation of chlamydospores on the dead plant tissue. Figures adapted from Di Pietro et al., (2001) and Perez-Nadales, et al., (Perez-Nadales *et al.*).

Once in the root (Figure 2), hyphae grow inter and intracellularly to invade the cortex and cross the endodermis, until they reach the xylem vessels, using it as a conduit to colonize the host. Disease symptoms include wilting, chlorosis, necrosis, premature leaf loss, browning of the vascular system and

stunting, which eventually will lead to plant death (Michielse and Rep, 2009). Small oval-shaped microconidia, falcate macroconidia and thick-walled chlamydospores are formed on the dead plant tissue and in soil. *F. oxysporum* can survive in soil for extended time periods, either as chlamydospores or by growing saprophytically on organic compounds until a new cycle of infection starts (Agrios, 2005).

Microconidia spores are single-celled dispersal structures that are produced during all phases of the fungi cycle (Figure 3B), mostly produced to rapidly spread the fungi under favorable conditions. Macroconidia spores contain three to five cells gradually pointed and curved toward the ends (Figure 3C), they have relatively higher survival than microconidia, and are commonly found on the surface of dead plants killed by the pathogen. Chlamydospores formation is induced by aging or unfavorable environmental conditions such as low temperatures or carbon starvation, they are developed through the modification of hyphal and conidial cells on thick-walled cells and represent the principal structure for long-time survival during unfavorable periods in the soil (Figure 3D) and playing a vital role as primary inoculum plant root infection (Kommedahl, 1966; Smith and Snyder, 1972).

Figure 3. *Fusarium oxysporum* structures overview. (A) Mycelia grown in Potato dextrose agar medium; (B) Microconidia; (C) Macroconidia; and (D) Chlamydospores.

Although a sexual stage has not yet been described, *F. oxysporum* genome contains apparently functional mating type idiomorphs (MAT1-1 and MAT-1-2). The *mat1-1-1* gene encodes a protein carrying an α-box motif, whereas *mat1-2-1* encodes a transcription factor with a high-mobility-group (HMG) DNA binding domain. *F. oxysporum* MAT genes are expressed

and all the predicted introns are correctly processed (Arie *et al.*, 2000). These observations indicate that, like other fungal pathogens previously thought to lack sex, the presence of a cryptic sexual cycle may remain to be discovered in *F. oxysporum.*

1.1.2 *Fusarium oxysporum* plant pathogen interaction

Fungi has evolved many strategies to penetrate the plant, invade and colonize them tissues, and develop inside the plant. Aerial fungal plant pathogens have many active mechanisms to penetrate on the plant host, developing hyphae structures like appressoria and penetration peg associated with production of enzymes to degrade the cutine layer of the plant and cell wall barriers (Agrios, 2005). Soilborne plant pathogens, like *F. oxysporum,* differ from aerial plant pathogens by lacking specialized structures to infect the host (Rodríguez-Gálvez and Mendgen, 1995; Olivain and Alabouvette, 1999). After attachment/adhesion, a dense mycelial network is formed on the plant roots the hyphae penetration often occurs through wounds that are formed while the plant root is growing (Pareja-Jaime *et al.*, 2010; Pérez-Nadales and Di Pietro, 2011).

The first physical barrier of contact with the plant tissues inside the plant is the cell wall. To overcome it, *F. oxysporum* produce an arsenal of hydrolytic enzymes (polygalacturonases, cellulases, xylanases and pectinases) able to degrade this barrier allowing colonization of the plant (Di Pietro *et al.*, 2009), enzymes that degrades plant toxic compounds like tomatinases and laccases, and enzymes to reinforce the fungi cell wall structure (Canero and Roncero, 2008; Pareja-Jaime *et al.*, 2008), and subsequent production of toxins and effector proteins (Ma *et al.*, 2013).The plant responds to limit the infection, thereby producing antifungal and resistance proteins, detoxification enzymes, reactive oxygen species and activating systemic cell signaling defense mechanisms. During root invasion and colonization, *F. oxysporum* is exposed

to various plant defense mechanisms, such as physical barriers and antifungal compounds (Beckman, 1987; Vanetten *et al.*, 1994).

The genome sequence of the tomato pathogenic *F. oxysporum* f. sp. *lycopersici* isolate 4287 was published in 2010 (Ma *et al.*, 2010). A striking feature of the genome is that 28% corresponds to repetitive sequences, including many retroelements and short interspersed elements (SINEs) as well as class II transposable elements (TEs).

F. oxysporum genomes are structurally compartmentalized. The "core" genome is relatively slow-evolving, handles the housekeeping genes, and is highly syntenic between different *F. oxysporum* isolates as well as between *Fusarium* sp. such as *F. verticillioides*. The "accessory" part consists of separate chromosomes or extensions of core chromosomes not conserved in all *F. oxysporum* strains, where is observed a low gene density while repeats and transposons are found much more abundantly. The lineage specific (LS) region of the genome is not required for vegetative growth, but does contain genes encoding predicted secreted effectors, virulence factors, transcription factors and proteins involved in signal transduction that allow the fungus to invade and cause disease in its host plant (Ma *et al.*, 2010). Genes on the LS regions generally have a higher non-synonymous mutation rate (dn/ds ratio) than genes on the core genome, suggesting relaxed selection (Sperschneider *et al.*, 2015).

The recent data suggest that LS regions of *F. oxysporum* strains with different host specificities may differ considerably. Sequence analysis of genes present on the LS genome regions indicate a distinct evolutionary origin from the *F. oxysporum* core genome, suggesting that they were probably acquired through horizontal transfer from another *Fusarium* species (Williams *et al.*, 2016). This idea was experimentally supported by the finding that co-incubation of two strains of *F. oxysporum* f. sp *lycopersicy* can result in transfer of small LS chromosomes from a tomato pathogenic to a non-pathogenic strain, converting the latter in a tomato pathogen. This led to the hypothesis that horizontal chromosome transfer in *F. oxysporum* can generate new pathogenic lineages (Ma *et al.,* 2010).

Sequences of eleven additional *F. oxysporum* f. sp have recently become public. The availability of the complete genome sequences, as well as of molecular tools and well-established pathogenicity assays, has been instruments for addressing the genetic bases and evolutionary origins of pathogenicity and host range (Van Dam *et al.*, 2016; Williams *et al.*, 2016; Zhang and Ma, 2017). In summary, two classes of gene are involved in pathogenicity: specialized pathogenicity genes, which in most cases are specific to individual *Fusarium* spp. on their specific hosts; and basic pathogenicity genes, which share function in *Fusarium* and other pathogenic fungi (Ma *et al.*, 2013).

Basic pathogenicity genes are present in the core genome and encode essential components of pathways involved in sensing of exogenous or endogenous signals in *F. oxysporum*. Mutations in these genes often affect the fitness and pathogenicity of mutants. Example of this genes are components of mitogen-activated protein kinase (MAPK) signaling pathways (Di Pietro *et al.*, 2001; Prados-Rosales and Di Pietro, 2008; Rispail *et al.*, 2009 2011; Pérez-Nadales and Di Pietro, 2012; Perez-Nadales and Di Pietro, 2015; Segorbe *et al.*, 2017), cAMP pathways (Kim *et al.*, 2011), Ras proteins (Macias-Sanchez *et al.*) (Bluhmn et al., 2007; Liu et al., 2010), G-protein signaling components and their downstream pathways (Jain *et al.*, 2002; Delgado-Jarana *et al.*, 2005), components of the velvet complex (*laeA/veA/velB*) (Lopez-Berges *et al.*, 2009; Lopez-Berges *et al.*, 2013; Lopez-Berges *et al.*, 2014), transcription factors *con7-1*, *cti6, sge1, fnr1, fow2, pacC, meaB, ste12, ftf1, fow2, hapX* (Caracuel *et al.*, 2005; Divon *et al.*, 2006; Imazaki *et al.*, 2007; Ramos *et al.*, 2007; Lopez-Berges *et al.*, 2009; Michielse *et al.*, 2009; Rispail *et al.*, 2009; Lopez-Berges *et al.*, 2012; Ruiz-Roldan *et al.*, 2015), ubiquitin proteasome regulation proteins (Duyvesteijn *et al.*, 2005; Miguel-Rojas and Hera, 2013, 2015). Understanding the exact nature of the pathogen virulence mechanisms controlled by these genes is complex, pleiotropic phenotypical effects are observed in many of the fungal mutants, and a single factor can have diverse roles in metabolism processes that are important to pathogenesis.

The accessory genome of *F. oxysporum* f. sp *lycopersisci* consists of the chromosomes 1B, 2B, 3, 6, 14, and 15 (Ma, et al. 2010). These lineage-specific

(LS) regions are enriched for transposable elements and genes putatively related to host–pathogen interactions. Conversely, only 20% of the genes in the LS regions could be functionally classified based on homology to known proteins. (Ma *et al*., 2010, Ma *et al*., 2013).

Specific virulence factors, like the virulence factors genes SIX (secreted in xylem) are located on the *F. oxysporum* f. sp. *lycopersici* LS chromosome 14. Some of these genes are responsible to establish *F. oxysporum* f.sp. *lycopersici* the known gene-for-gene interaction with the tomato host. In which, three known races *F. oxysporum* f. sp. *lycopersici*, race 1, 2 and 3, defines their ability to produce vascular wilt on tomato cultivars carrying different resistance genes (Beckman, 1987). These effectors are proteins encoded by avirulence (AVR) genes that were originally identified in the xylem sap of *F. oxysporum* f. sp. *lycopersici*-infected tomato plants, and namely *avr1*, *avr2*, and *avr3* (Rep *et al.*, 2004; Houterman *et al.*, 2007; Houterman *et al.,* 2008; Houterman *et al.,* 2009).

Effectors are typically secreted proteins that promote host colonization, often by modulation of plant immunity, whereas many effectors suppress immunity, some are recognized by the plant immune system and then trigger defense activation, changing them from virulence into avirulence determinants. (Hogenhout *et al.*, 2009; Dodds and Rathjen, 2010). The effector Avr1 (Lievens *et al.*), recognized by I-1, suppresses I-2 and I-3-mediated resistance, however does not contribute to virulence on susceptible cultivars (Houterman *et al.*). Avr2 (SIX3) and AVR3 (SIX1) trigger resistance in tomato plants carrying the resistance genes *I-2* and *I-3*, respectively, and additionally to triggering resistance, both proteins are required for full pathogenicity on susceptible tomato lines (Rep *et al.,* 2005; Houterman *et al.,* 2009; Takken and Rep, 2010).

In addition to the Avr proteins, 11 other secreted-in-xylem (SIX) proteins have been identified thus far, they are are relatively small (300 amino acids), generally cysteine rich, and produced with a signal peptide for secretion (Houterman et al. 2007; Lievens et al. 2009; Ma et al. 2010; Schmidt et al. 2013). However, little is known about their function, SIX5 and SIX6 were recently shown to contribute to pathogenicity of *F. oxysporum* f sp. l*ycopesici*

by different mechanisms. SIX5 together with Avr2 (SIX3) interacts with I-2 (Ma *et al.*, 2015), while SIX6 specifically suppresses the I-2-mediated response that leads to cell death and hypersensitive response (Gawehns *et al.*, 2014).

Other specialized pathogenicity genes, belonging to different classes of secreted proteins, are produced in order to enhance root penetration and host plant colonization. Examples of these are plant cell wall degrading enzymes polygalacturonases (Di Pietro and Roncero, 1996; Garcia-Maceira et al., 1997; Garcia-Maceira et al., 2000; Garcia-Maceira et al., 2001; Roncero et al., 2003; Bravo-Ruiz et al., 2016); secreted lipases and their regulatory genes (Martinez-Rocha *et al.*, 2008; Bravo-Ruiz *et al.*, 2013); detoxification of plant defense proteins and antifungal degrading enzymes, like tomatinase, responsible to overcome the α-tomatine, a major saponin produced by tomato plants (Lairini *et al.*, 1996; Ito *et al.*, 2007; Pareja-Jaime *et al.*, 2008); secreted metalloproteases *FoMep1* and *FoSep1* responsible to overcome chitinases *SlChi1* and *SlChi13* (Jashni *et al.*, 2015); degradation of phenolic compounds through the β-ketoadipate pathway by laccases *lcc1*, *lcc3* and *lcc5* (copper-containing phenol oxidases), associated chloride channel *clc1* (Canero and Roncero, 2008) and catechol dioxygenase and carboxy-*cis*,*cis*-muconate cyclase *cmle1* (Michielse *et al.*, 2009; Michielse *et al.*, 2012)

To survive and proliferate inside living plant tissue *F. oxysporum* needs to be able to control its cell wall composition and to deal with plant-derived chemicals. Adaptation of the fungal cell wall has been shown to play a vital role during pathogenicity, reinforcement of hyphae cell wall is needed to resist damage by plant enzymes or compounds and/or by reducing the release of cell wall-derived defense elicitors. Examples of them are the absolute requirement in pathogenesis of the chitin synthases ChsV (Madrid *et al.*, 2003), and ChsVb (Martin-Udiroz *et al.*, 2004; Martin-Urdiroz *et al.*, 2008), while Chs1, Chs2 and Chs7 have minor role in pathogenesis.

Additional genes with a role in cell wall maintenance and pathogenicity are *gas1*, encoding a β-1,3-glucanosyltransferase, and *rho1*, encoding a GTPase (Caracuel *et al.*, 2005). Both *gas1* and *rho1* disruptants were severely reduced in virulence towards tomato. Increased transcription

of *chsV* and *rho1* is observed in the *gas1* disruptant (Caracuel *et al.*, 2005). Consistent with alterations in the cell wall, *gas1* and *rho1* disruptants displayed enhanced resistance to cell wall degrading enzymes. It was hypothesized that the deletion of *rho1* in *F. oxysporum* leads to significant changes in cell wall architecture, increased amount of cell wall polymers such as chitin at the hyphal surface or released to the surrounding medium (Martinez-Rocha *et al.*, 2008). These cell wall components may act as elicitor-active compounds recognized by the plant that triggers defense responses, effectively blocking pathogenic development. (Martinez-Rocha *et al.*, 2008).

1.2 Kinase signaling pathways

Reversible phosphorylation of proteins is a major mechanism regulating many biological processes; it is considered the main mechanism of posttranslational modification leading to changes in enzyme activity. Protein phosphorylation is involved in the regulation of many cellular processes (Krebs and Beavo, 1979; Klipp *et al.*, 2005; Tyson and Novak, 2008; Huber *et al.*, 2009). In eukaryotic cells, phosphorylation mainly occurs on three hydroxyl-containing amino acids, serine, threonine, and tyrosine (Shi, 2009). The phosphorylation state of a protein results from the balance of protein kinases and protein phosphatases activities.

Protein kinases (Turra *et al.*) are a major class of signaling molecules that catalyze phosphorylation of a substantial proportion of cellular proteins modulating protein activity and gene expression (Cohen, 2000). Phosphorylation can activate or inactivate a target protein by altering its conformation; (un)blocking the access of a substrate to the catalytic center; determining translocation between compartments; associating the protein to different protein complexes; or marking the protein for degradation (Cohen, 2000; Serber and Ferrell, 2007; Oliveira *et al.*, 2012). Multiple PK pathways coordinated action, orchestrate key processes of the fungal life cycle, such as isotropic or polar growth, nutrient or stress responses, and asexual or sexual development. Fungal plant pathogens have evolved an amazing diversity of infection modes and nutritional strategies. The importance of this regulatory

mechanism is evident when it is considered that it affects around 30% of the proteome of *Saccharomyces cerevisiae* (Ptacek *et al.*, 2005), and that the number of genes encoding phosphatases and kinases represents 2 to 4% of all genes in a typical eukaryotic genome (Manning *et al.*, 2002).

In *S. cerevisiae*, reversible protein phosphorylation is regulated by about 120 kinases and 40 phosphatases (Bodenmiller *et al.*, 2010). The pivotal role of fungal PKs in plant infection was discovered when key components of the mitogen activated protein kinase (MAPK), the cAMP dependent protein kinase (Turra *et al.*) and protein kinase A (PKA) pathways were shown to be essential for infection-related morphogenesis and virulence on many plant pathogens (Banuett and Herskowitz, 1994; Gold *et al.*, 1994; Mitchell and Dean, 1995; Gold *et al.*, 1997; Xu *et al.*, 1998).

Functional insights from the model *S. cerevisiae* and the availability of fungal genome sequences leaded to the identification of additional kinases with distinct roles in fungal pathogenicity on plants during the past decade (Wang *et al.*, 2011). The first functional complete kinome analysis of *Fusarium sp.* was done for *F. graminearum* (Wang *et al*., 2011) and recently dissected for *F. oxysporum* complex (DeIulio *et al.*, 2018). The comparative study identified 99 kinases that are conserved in all analyzed ascomycete fungi and suggests an evolutional driven expansion of the *F. oxysporum* kinome on the 12 isolates analyzed (including 10 plant pathogens, 1 human-pathogenic strain, and 1 nonpathogenic biocontrol strain) (DeIulio *et al.*, 2018). This convergent evolution shapes individual *F. oxysporum* isolates with their unique capacity for environmental perception and associated downstream responses (DeIulio et al., 2018).

1.2.1 Mitogen activated protein kinase cascades

Mitogen-activated protein kinases (MAPKs) are evolutionarily conserved proteins that function as key signal transduction components in fungi, plants, and mammals. MAPK cascades have long been evolutionarily conserved across the fungal kingdom (Rispail *et al.,* 2009; Hamel *et al.* 2012). MAPK cascades have been functionally characterized in nonpathogenic fungi

including *S. cerevisiae*, *Neurospora crassa*, and *Aspergillus nidulans* (Park *et al.*; Bayram *et al.*; Furukawa and Hohmann); plant pathogenic fungi such as *Magnaporthe oryzae*, *Ustilago maydis*, and *F. graminearum* (Xu, 2000; Basse and Steinberg, 2004; Jia and Tang, 2015); human pathogenic fungi such as *Candida albicans*, *Cryptococcus neoformans*, and *Aspergillus fumigatus* (Clarke *et al.*, 2001; Fernandes *et al.*, 2005), and insect pathogenic fungi *Metarhizium acridum* and *Beauveria bassiana* (Zhang et al., 2009; Jin et al., 2014).

Although MAPK signaling pathways are well conserved in eukaryotes, each pathway may have different physiological, developmental and pathological functions between species (Bardwell, 2006). Interconnections of MAPK signaling or cross-regulations within and between different transduction pathways further exacerbate the complexity of the signaling network (Chen and Thorner, 2007; Schwartz and Madhani, 2004; Smith and Scott, 2002).

Comparative genomics of MAPK cascade core components in saprophytic, plant-associated, and human pathogenic fungi also identified gene expansion in some fungi, which could be responsible for the adaptation of fungi to their respective ecological niches (Rispail *et al.*, 2009; Hamel *et al.*, 2012). A recent study, encompassing 9 fungal phyla and 231 fungal species revealed that gene structure diversification and gain/loss of MAPK cascade components are correlated with the evolution of fungal species and development of different lifestyles (Xu *et al.*, 2017).

The general cellular signaling process (Figure 4) consists in the perception of external stimuli by membrane receptors that forms complexes with intracellular components including G proteins, GTPases, Guanine nucleotide exchange factors (GEFs) and Protein Kinases that transmit sequentially the phosphorylation signal on MAPK kinases modules (Figure 4A). MAPK modules consists of three interlinked components, the protein kinases MAPKKKs, MAPKKs, and MAPKs. The MAP kinase kinase kinase (MAPKKK) phosphorylates the MAP kinase kinase (MAPKK), which in turn activates the MAPK by dual phosphorylation at the well conserved threonine-x-tyrosine

(TXY) motif (Chang and Karin, 2001; Chen and Thorner, 2007; Hamel *et al*., 2012; Turrá *et al*., 2014).

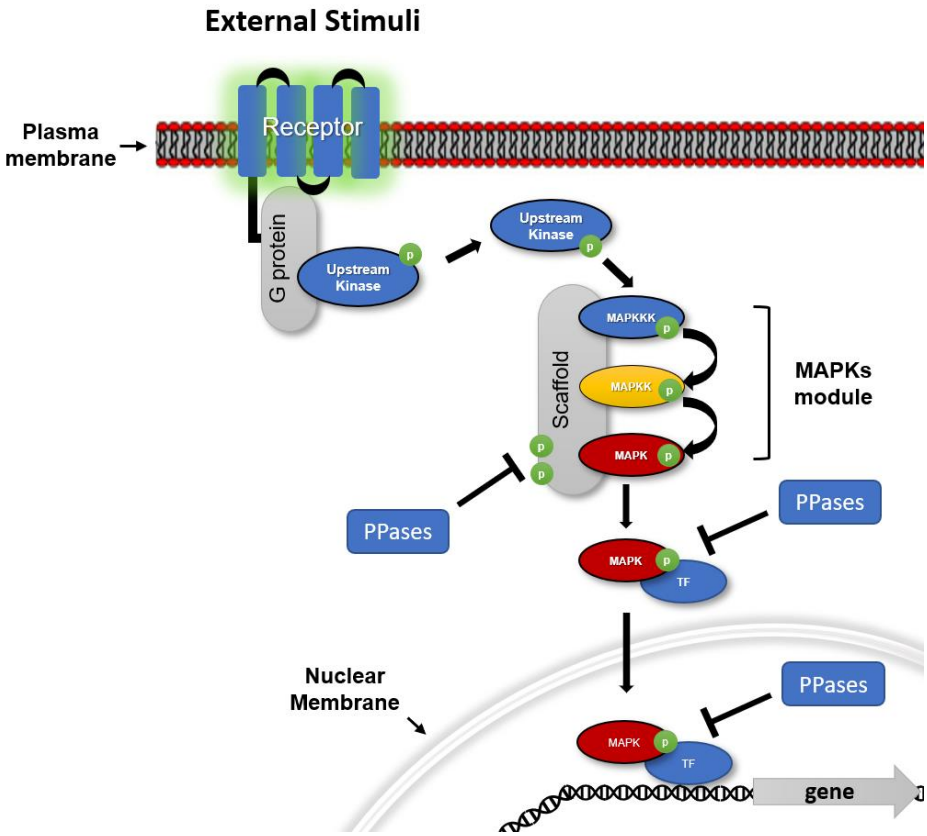

Figure 4. Mitogen activated protein kinase pathways (MAPK) general signaling mechanism. Plasma membrane receptors activate fungal MAPK cascades that modulate transcription factor (Fujioka *et al.*) activity and promote expression of gene targets associated with the response to external stimuli (Adapted from Hamel et al., 2012).

Upstream regulators can be shared between distinct MAPK signaling pathways, and specificity of each MAPK pathway is driven by different scaffolding proteins, that promotes the suitable interaction between the three tittered MAPK module (Hamel *et al*., 2012; Turrà *et al*., 2014). Finally, the phosphorylated MAPKs deliver these signals to downstream targets, including several kinases and transcription factors, which regulates gene expression responding to the external stimulus (Widmann *et al.*, 1999; Chang and Karin, 2001; Chen and Thorner, 2007). The budding yeast *S. cerevisiae* has five MAPK pathways that regulate mating, invasive growth, cell wall integrity,

osmoregulation, and ascospore formation (Chen and Thorner, 2007; Hamel *et al.*, 2012).

During interaction between phytopathogenic fungi and plants, fungal MAPKs help to promote mechanical and/or enzymatic penetration of host tissues and adaptation to the plant tissue environment (Hamel *et al*., 2012), while in plants MAPKs are required for activation of plant immunity. A highly interconnected molecular dialogue between the plant and the fungus is stablished and MAPK cascades in both organisms operate simultaneously. Pathogenesis processes controlled by fungal MAPKs lead to the activation of plant signaling, including the recruitment of plant MAPK cascades. Conversely, plant MAPKs promote defense mechanisms that threat the survival of fungal cells, leading to a stress response mediated in part by fungal MAPK cascades (Hamel *et al*., 2012).

1.2.2 Mating and invasive growth response pathway - FUS3/KSS1

In *S. cerevisiae*, the KSS1/FUS3-type MAPK cascade is essential for regulate mating, filamentous growth and invasive growth (Figure 5). The sequential MAPK module of these two pathways is composed of the MAPKKK STE11 and the MAPKK STE7 (Wang and Dohlman, 2004). Two MAPKs regulate distinct signaling outputs downstream of STE7. FUS3, is essential for mating, whereas KSS1 controls invasive growth and pseudohyphal development (Madhani and Fink, 1997).

The FUS3 MAPK cascade or pheromone pathway in *S. cerevisiae* signaling initiates when pheromone binds to the cell surface receptors STE2 and STE3. Once pheromone binds to its cognate receptor, it triggers dissociation of the G protein α subunit GPA1 from the G protein βγ subunits STE4 and STE18. The heterotrimeric βγ subunits STE4 and STE18 dissociate from Gα to transmit the signal to the downstream pathway components (Wang and Dohlman, 2004). The signal is transmitted downstream to the guanine nucleotide exchange factor CDC24 which activates the G protein CDC42. CDC42 activates the PAK-like protein kinase STE20 and the adaptor protein STE50, which cooperate in activating the downstream MAPK module. The

scaffold protein STE5 recruits the STE11–STE7–FUS3 complex to the plasma membrane (Pryciak and Huntress, 1998) stimulating phosphorelay by proximity effects, oligomerization, and conformational changes (Qi and Elion, 2005). Phosphorylated FUS3 in *S. cerevisiae* activates downstream effectors such as STE12, FAR1 or SST2, leading to cell cycle arrest, polarized growth and formation of specialized fusion tubes called shmoos (Elion *et al.*, 1993; Madhani and Fink, 1997).

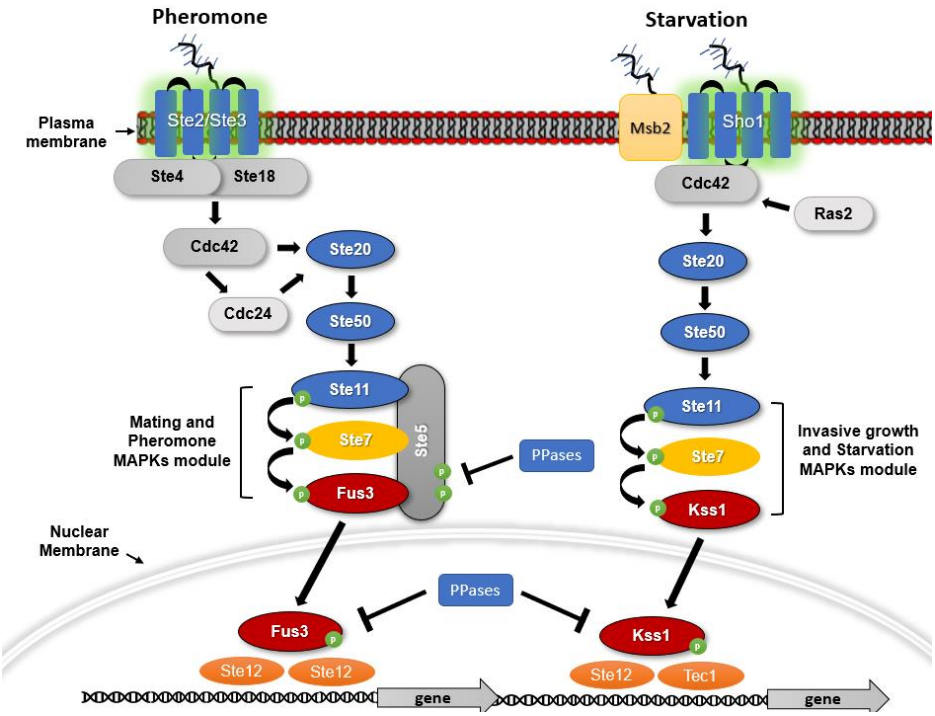

Figure 5. *S. cerevisiae* Mating and Pheromone MAPK Pathway (Adapted from Hamel et al., 2012)

This pathway is also activated under nutrient-limiting conditions by a mucin-like protein, MSB2 (Cullen *et al.*, 2004) and by other required component, the small GTP-binding protein RAS2, that is protein upstream of CDC42, STE20 and KSS1 specific for the filamentation and invasive growth pathway (Mosch *et al.*, 1996; Leberer *et al.*, 2001; Park *et al.*, 2006; Bluhm *et al.*, 2007). The KSS1 activation controls cell adhesion, cell elongation, and the reorganization of cell polarity through the transcription factors STE12 and TEC1 (Madhani and Fink, 1997). While activated yeast undergo a developmental

switch called filamentous growth, during which the cells become elongated, and mother and daughter cells remain attached to each other forming filaments of cells named pseudohyphae, this response is thought to allows yeast cells to forage for nutrient resources under unfavorable conditions. In contrast to FUS3, KSS1 can also be activated by STE7 that is not bound to the STE5 scaffold (Elion, 1998).

Orthologs of KSS1/FUS3 proteins in plant pathogens are named infection-related MAPKs, and functional analyses confirmed that this class of kinases plays important functions in establishment of various infection strategies. Strong evidences from diverse phytopathogens illustrate that KSS1/FUS3-type MAPKs are multifunctional pathogenicity factors required for virulence of biologically and taxonomically diverse phytopathogenic fungi and broadly conserved regulators of infection-related morphogenesis and invasive growth in plant-pathogenic fungi (Hamel *et al.*, 2012, Turrà *et al.*, 2014).

The orthologous KSS1/FUS3-type MAPKs are required for: appressorium formation on the plant pathogens *M. oryzae* (Xu and Hamer, 1996), *Colletotrichum orbiculare* (Takano *et al.*, 2000) *Cochliobolus heterostrophus* (Lev *et al.*, 1999), and *Pyrenophora teres* (Ruiz-Roldan *et al.*, 2001); to produce infection structures within the host mesophyll as in the cereal pathogen *Stagnospora nodorum* (Solomon *et al.*, 2005), and the wheat pathogen *Mycosphaerella graminicola* (Cousin *et al.*, 2006); to differentiate penetration and infection hyphae in *Botrytis cinerea* (Zheng *et al.*, 2000; Doehlemann *et al.*, 2006); to mating and pathogenicity as in *Ustylago maydis* (Hu *et al.*, 2007).

The activity of KSS1/FUS3-type MAPKs is also associated with virulence of several soil-borne pathogens. In *Verticillium dahliae*, disruption of the *KSS1-ortholog* also results in strains that have reduced virulence against a variety of host plants (Rauyaree *et al.*, 2005). In the necrotrophic fungus *Alternaria brassicicola*, disruption of the MAPK gene *Amk1* results in strains that are nonpathogenic on intact plants but that can still colonize damaged host tissues (Cho *et al.*, 2007). Deletion of the MAPK gene *gmpk1* hinders pathogenicity of *F. graminearum*, the causal agent of wheat head-blight disease (Jenczmionka *et al.*, 2003; Urban *et al.*, 2003), also associated with diminished

or delayed induction of enzymatic activity associated with degradation of the plant cell wall (Jenczmionka and Schafer, 2005).

In *F. oxysporum*, deletion of the MAPK gene *fmk1* (*Kss1*/Fus3 ortholog) results in strains that fail to differentiate penetration hyphae and that display reduced transcript level of the pectate lyase gene *pl1* and are nonpathogenic in tomato (Di Pietro *et al.*, 2001), but interestingly remain fully pathogenic in a murine model system (Ortoneda *et al.*, 2004). This indicates that MAPK signaling plays functionally distinct roles during infection of plants and other organisms, and that Kss1/Fus3-type MAPKs share an ancient function in pathogenicity against plants. The role of Ste12 in *F. oxysporum*, an orthologue of the yeast homeodomain transcription factor STE12 regulated by FUS3/KSS1 MAPKs was also investigated (Rispail *et al.*, 2009). Knockout mutants of *ste12* are impaired in invasive growth but not in adhesion to tomato roots, secretion of pectinolytic enzymes, or vegetative hyphal fusion, and have dramatically reduced virulence in tomato.

1.2.3 Cell wall integrity pathway – SLT2

The cell wall integrity (CWI) pathway (Figure 6) is activated by heat and various stresses on the cell wall (Levin, 2005; Fuchs and Mylonakis, 2009). This pathway is comprised of several plasma membrane sensors coupled to a G-protein, RHO1, its exchange factor ROM2, PKC1, and the downstream MAPK module of BCK1 (MAPKKK), MKK1 and MKK2 (MAPKK), and SLT2 (MAPK) (Levin 2005, Heinisch et al., 1999; Harrison et al., 2004; Hammel et al., 2012).

In *S. cerevisiae,* cell wall-associated stress sensors MID2 and WSC1 percept external stimuli (Ketela *et al.*, 1999 1997), bind to ROM2, a guanyl nucleotide exchange factor for RHO1 (Ozaki *et al.*, 1996 2001). RHO1 also binds and activates PKC1 (Kamada *et al.*, 1996, Nokada *et al.*, 1995), which in turn regulates the MAPK cascade. PKC1 phosphorylates BCK1, a MAPK kinase kinase (MAPKKK), which transmits the signal to MAPK kinases (MAPKKs) MKK1 and MKK2. These two kinases finally phophorylates the MAPK SLT2/MPK1 (Banuet, 1998). The phosphorylation of SLT2/MPK1 leads

activation of RLM1 and SBF1, SWI4 and SWI6 transcription factors, that initiate the expression of cell wall synthesis genes (Dodou and Treisman, 1997; Madden *et al.*, 1997; Watanabe *et al.*, 1997; Jung *et al.*, 2002).

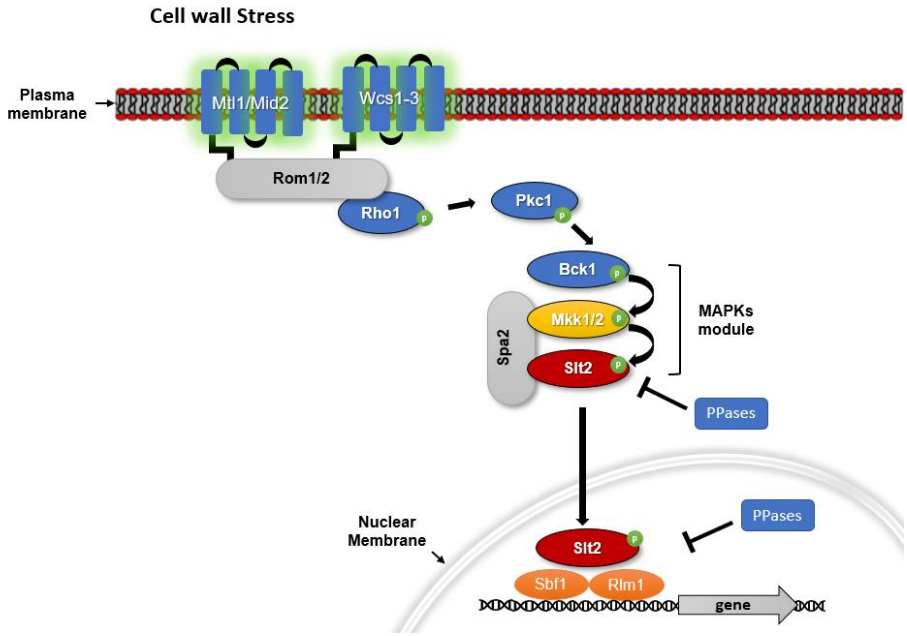

Figure 6. *S. cerevisiae* Cell Wall Integrity pathway (Adapted from Hamel et al., 2012)**.**

Among fungal pathogens, the MAPK SLT2/Mpk1 is required for fungal cell wall remodeling and integrity, which are critical during pathogenesis. Deletion of *SLT2/MPK1* orthologues in different pathogen species results in defects in host sensing, penetration and colonization, leading to decreased virulence on plant and animal hosts (Diez-Orejas *et al.*, 1997; Xu *et al.*, 1998; Kojima *et al.*, 2002; Mey *et al.*, 2002; Kraus *et al.*, 2003; Rui and Hahn, 2007; Igbaria *et al.*, 2008; Dagdas and Bozkurt, 2015), as well as, hypersensitivity to cell wall-damaging agents, such as Congo Red or Calcofluor White, and plant defense compounds such as chitinases, glucanases, antimicrobial peptides or phytoalexins (Xu *et al.*, 1998; Hou *et al.*, 2002; Mey *et al.*, 2002; Mehrabi *et al.*, 2006; Ramamoorthy *et al.*, 2007; Joubert *et al.*, 2011; Valiante *et al.*, 2015).

The SLT2 cascade also regulates developmental processes, such as hyphal growth on solid surfaces and vegetative hyphal fusion (Xu *et al.*, 1998;

Hou *et al.*, 2002; Maerz *et al.*, 2008; Dagdas and Bozkurt, 2015). In contrast to its conserved role in pathogenesis, the function of this MAPK in cell wall integrity, conidiation, and stress responses varies among fungal pathogens. SLT2/MPK1 orthologs have been demonstrated to regulate the integrity of cell walls in *A. brassicicola*, *A. nidulans*, *Claviceps purpurea*, *F. graminearum*, *M. grisea, M. graminicola, Cryphonectria parasitica, Pseudocercospora fijiensis* (Hou *et al.*, 2002; Kojima *et al.*, 2002; Mey *et al.*, 2002; Mehrabi *et al.*, 2006; Fujioka *et al.*, 2007; Valiante *et al.*, 2009; So *et al.*, 2017), but not in *B. cinerea* and *Colletotrichum lagenarium* (Kojima *et al.*, 2002; Rui and Hahn, 2007).

In *F. oxysporum* f. *sp cubense*, disruption of three cell wall integrity MAPK pathway components, FoSlt2 (MAPK), FoMkk2 (MAPKK) and FoBck1 (MAPKKK), lead to substantial attenuation in fungal virulence on banana plants associated with a reduction of the production of beauvericin and fusaric acid, crucial phytotoxins to induce wilt on the host. Similar phenotypes, abnormal hyphal growth and increased sensitivity to cell wall integrity stressors Congo Red, Calcofluor White and H_2O_2 were also observed, concomitant with their role in regulation of the genes encoding production of chitin, peroxidase. Additionally, it was found that the MAP kinase FoSlt2 was required for siderophore biosynthesis under iron-depletion conditions (Ding *et al.*, 2015).

The disruption of Slt2/Mpk1 in *F. oxysporum* f. sp *lycopersici* results in increased sensitivity towards heat stress, cell wall-targeting compounds Calcofluor White and Congo Red, showed abnormally increased ROS levels, impaired in vegetative hyphal fusion and aggregation, reduced invasive growth on apple slices and reduced virulence on tomato (Dagdas and Bozkurt, 2015; Segorbe *et al.*, 2017).

The directed growth of *F. oxysporum* f. sp *lycopersici* towards the roots of the host tomato is triggered by the catalytic activity of secreted class III peroxidases, a family of heme-containing enzymes present in all land plants. This chemotropic response requires conserved elements of the fungal cell integrity MAPK Mpk1 (Slt2 ortholog) and the seven-pass transmembrane protein Ste2, a functional homologue of the *S. cerevisiae* sex pheromone α receptor. Strikingly, this process occurs independently of the Fus3/Kss1 well

conserved pheromone pathway, *mpk1* disruption mutants were impaired in pheromone response, suggesting that the mating pheromone pathway can also be regulated by a distinct MAPK module in *F. oxysporum* (Dagdas and Bozkurt, 2015).

1.2.4 High osmolarity glycerol pathway – HOG1

The high-osmolarity glycerol pathway plays a pivotal role in the adaptive response to osmotic stress, on the accumulation of osmo-protectant molecules and the maintenance of an osmotic gradient across the stressed plasma membrane (Hamel *et al.*; Saito and Posas, 2012), and mediates sensitivity to certain fungicides, such as phenylpyrroles and dicarboximides (Dixon *et al.*, 1999; Park *et al.*, 2004; Segmuller *et al.*, 2007; Igbaria *et al.*, 2008; Lin and Chung, 2010; Van Thuat *et al.*, 2012). HOG1 has also been implicated in cellular adaptation to heat, oxidative and citric acid stresses (Alonso-Monge et al., 2003; Bilsland et al., 2004; Lawrence et al., 2004; Winkler et al., 2002). Relatively high intracellular concentrations of hydrogen peroxide (H_2O_2) has been shown to activate HOG1 in *S. cerevisiae* (Bilsland *et al.*, 2004; Haghnazari and Heyer, 2004; Staleva *et al.*, 2004). Nevertheless, how cells sense and signal the H_2O_2 stress via the HOG pathway is not well defined at the molecular level.

In *S. cerevisiae* the high osmolarity glycerol pathway signaling (Figure 7) is transduced via two alternative branches, the SHO1 and the SLN1 branches. In the SHO1 branch, osmo-stress is sensed by two mucin-like transmembrane sensors, MSB2 and HKR1 (De Nadal *et al.*, 2007; Tatebayashi *et al.*, 2007). Signals phosphorylate and activate the cytoplasmic MAPKKK STE11 via the additional transmembrane SHO1. Active STE11 subsequently phosphorylates the MAPKK PBS2, which in turn phosphorylates and activates the MAPK Hog1.

Alternatively, osmo-stress is also sensed by the plasma membrane-localized sensor SLN1 (Posas *et al.*, 1996). Under normal growth conditions SLN1 is maintained in the activated state by autophosphorylation and the

phosphoryl group is transferred to YPD1, and eventually to the receiver domain in the response regulator SSK1. Phosphorylated SSK1 is an inactive form that cannot activate the downstream MAPKKK SSK2 and SSK22 (Posas and Saito, 1998). Under osmostress a different mechanism arises to activate the pathway, osmo-stress inhibits the autophosphorylation of SLN1 and YPD1, and in consequence SSK1 become unphosphorylated. Unphosphorylated SSK1 binds to the N-terminal regulatory domain of SSK2 and SSK22 which leads to their autophosphorylation and activation (Posas *et al.*, 1996), that sequentially phosphorylate and activate PBS2, which in turn activates Hog1 (Hohmann, 2009).

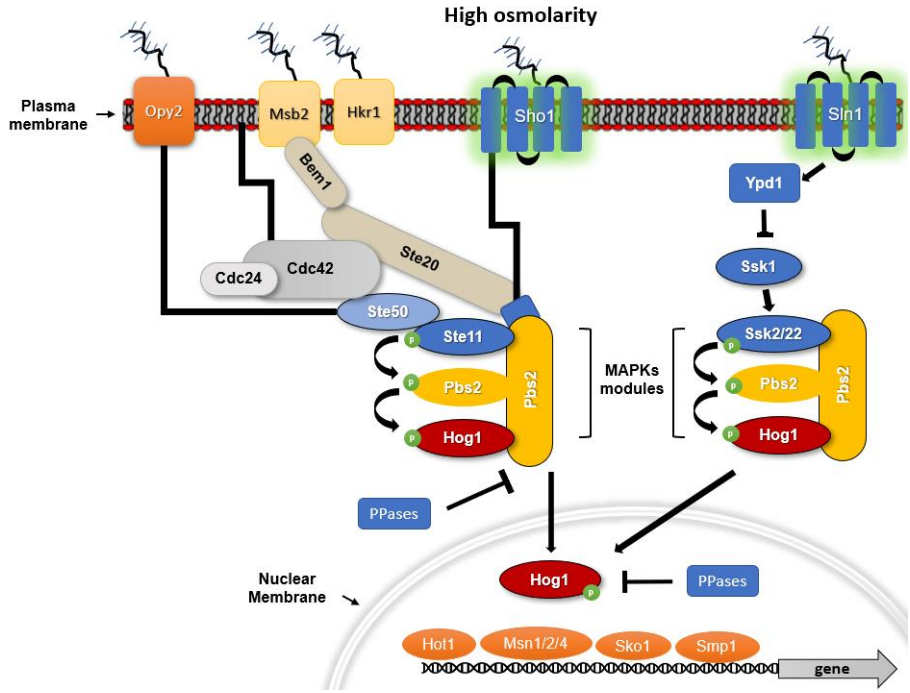

Figure 7. *S. cerevisiae* High osmolarity glycerol pathway (Brewster and Gustin, 2014).

Although there are also HOG1 targets in the cytoplasm, most of activated HOG1 translocate to the nucleus for further various functions (Saito and Posas, 2012). The transported fraction of the HOG1 MAPK into the nucleus regulates gene transcription and the cell cycle. As adaptation

proceeds, and osmotic balance is re-established, HOG1 activity is reduced to near basal levels, and HOG1 is exported back to the cytoplasm (Saito and Posas, 2012). Systematic genome-wide analyses of the binding of transcription factors and of binding of HOG1 to chromatin combined with gene expression profiling, have shown that in response to osmo-stress HOG1 can specifically regulate and integrate, the stress responses that occur at different promoters (Ni et al., 2009; De Nadal and Posas, 2015).

Upon osmo-stress HOG1 is tightly associated with the largest subunit of RNA Pol II, recruiting the basic transcriptional machinery to stress-responsive promoters (Alepuz *et al.* 2003). Contrasting with the traditional scenario in which a MAPK controls transcription indirectly by phosphorylating transcription factors, the persistent presence of HOG1 at target promoters indicates that HOG1 plays an important role in the regulation of transcription initiation (Alepuz *et al.*, 2001; Chellappan, 2001; Proft and Struhl, 2002). This effect is accomplished by HOG1 via modulation of the individual contribution of transcription factors, such as MSN2/MSN4, SKO1, and HOT1 in a promoter-specific context, results in a complex and highly specific control of gene transcriptional networks (Proft *et al.* 2005; Capaldi *et al.* 2008; Ni *et al.* 2009; Saito and Posas, 2012; De Nadal and Posas, 2015).

Immediately following the start of osmo-stress in *S. cerevisiae*, passive water efflux rapidly increases intracellular Na^+ concentration, which causes dissociation of proteins from chromatin. Activation of HOG1 in response to osmo-stress induces the phosphorylation of at least two proteins located at the plasma membrane, the NHA1 Na^+/H^+ antiporter and the TOK1 potassium channel (Proft and Struhl 2004). Activated HOG1 phosphorylates and thus stimulates NHA1 activity, leading to rapid pumping-out of excessive Na^+. This activity is crucial for the rapid and selective re-association of stress-responsive transcription factors with chromatin. Control of ionic fluxes during long-term adaptation occurs through HOG1 regulation by the expression of the Na^+ ATPase ENA1 (Benito et al., 2002; Saito and Posas, 2012).

Regardless of the redundant roles played by the two Na^+/K^+ efflux pumps, in *S. cerevisiae*, the regulatory mechanisms of ENA1 and NHA1 are

different. NHA1 is required for short-term adaptation to high salt shock and ENA1 for long-term adaptation (Proft and Struhl, 2002; Proft and Struhl, 2004). NHA1 is constitutively expressed at the plasma membrane and relieves initial osmotic shock by extruding Na^+ upon direct activation by HOG1, which results in re-assembling of transcription factors and transcription complex (Banuelos et al., 1998; Platara et al., 2006). Next, *ENA1* is transcriptionally induced, which allows cells to achieve long-term adaptation to external osmotic shock. In the human pathogen *C. neoformans* a transcriptome analysis of the environmental stress response revealed that the HOG pathway controls both basal and osmotic stress-induced expression levels of the *ENA1* and *NHA1* genes (Jung *et al.*, 2002). These examples show that HOG1 MAPK coordinates temporal spatial and distinct mechanisms to respond to stress thereby providing a rapid initial relief, which facilitates subsequent changes in gene expression that permit long-term adaptation to harsh environmental conditions (De Nadal and Posas, 2015).

HOG1 orthologues have also been identified contributing to virulence in diverse lifestyle phytopathogens as *M. oryzae* (Dixon et al. 1999) *F. graminearum* (Zheng *et al.,* 2000), *B. cinerea* (Segmuller *et al.,* 2007), *Cochliobollus heterostrophus* (Igbaria *et al.*, 2008), *C. parasítica* (Van Thuat *et al.*, 2012), *Trichoderma reseei* (Wang *et al.*, 2013), *Parastagonospora nodorum* (Leng and Zhong), *Cochliobollus sativus* (Leng and Zhong, 2015) and *Ustilaginoidea virens* (Zheng *et al.*, 2016). However, Hog1 can be dispensable for pathogenesis on other phytopatogens like *M. oryzae* (Li *et al.*, 2012), *Cochliobolus orbiculare* (Kojima *et al.*, 2004) and *Bipolaris oryzae* (Moriwaki *et al.*, 2006).

The effect on HOG1-type MAPKs in stress responses appears more universal in plant pathogens. The hypersensitivity to osmotic stress in lacking the HOG1 orthologous is reported for *M. oryzae* (Dixon *et al.*, 1999), *C. parasitica, C. orbiculare, B. oryzae, M. graminicola,* and *B. cinerea* (Kojima *et al.*, 2004; Park *et al.*, 2004; Mehrabi *et al.*, 2006; Moriwaki *et al.*, 2006; Segmuller *et al.*, 2007). In filamentous fungi, reports have also linked the activity of group III His kinases to the phosphorylation status of Hog1-type MAPKs. For instance, the *C. heterostrophus* His kinase Dic1p promotes

stress-mediated activation of Hog1 (Yoshimi *et al.*, 2005), while deletion of His kinase gene Hsk1 compromises Hog1 activation in response to stress in *Alternaria alternata* (Lin and Chung, 2010). These studies provide the first hints of how upstream regulation of the HOG pathway might be organized in phytopathogenic fungi.

In several fungal species, it has also been reported that mutants blocked in components of the HOG pathway are more resistant to a variety of fungicides (Kojima *et al.*, 2004; Motoyama *et al.*, 2005, 2008; Yoshimi *et al.*, 2005; Mehrabi *et al.*, 2006b; Moriwaki *et al.*, 2006; Viaud *et al.*, 2006). In at least three cases, treatment with fungicides also results in the activation of Hog1-type MAPKs (Kojima *et al.*, 2004; Yoshimi *et al.*, 2005; Segmuller *et al.*, 2007). This suggests that the fungicidal properties of several compounds may be due to an overstimulation of the HOG pathway, leading to uncontrolled accumulation of osmoprotectant molecules and concomitant swelling of fungal cells.

In *F. oxysporum* the role of Hog1 was recently characterized (Segorbe *et al.*, 2017). Similarly as reported previously in a number of fungal pathogens (Igbaria *et al.,* 2008; Lin and Chung, 2010; Park *et al.,* 2004; Segmuller *et al.*, 2007; Van Thuat et al., 2012), *F. oxysporum hog1* mutant display increased resistance to the dicarboximide, phenylpyrrole fungicides iprodione and fludioxonil, and are highly sensitive to hyperosmotic stress. Lack of Hog1 also leads to defects in growth at high temperature and show enhanced growth under oxidative stress caused by menadione (Segorbe *et al.*, 2017).

1.3 Protein Phosphatases as regulators of Kinase signaling in fungi

In eukaryotic cells, phosphorylation mainly occurs on three hydroxyl-containing amino acids, serine, threonine, and tyrosine, of which serine is the predominant target (Pao *et al.*, 2007; Shi, 2009). This conserved major regulation mechanism is controlled by the balanced action of kinases and phosphatases. There are two main families of phosphatases: the serine/threonine (S/T) protein phosphatases and the protein tyrosine phosphatases (PTP) (Pao *et al.,* 2007; Shi, 2009).

Although serine is the major target of phosphorylation in eukaryotes, it cannot be discarded that the regulation of tyrosine by Protein Tyrosine Phosphatases (PTPs) and Dual Specificity Phosphatases (DSPs) have also a role on kinase signaling regulation in *S. cerevisiae* and their function can overlap or have additive effects on the regulation of kinase pathways by Ser/Thr phosphatases (Fuchs and Mylonakis, 2009; Marin *et al.*, 2009; Shi, 2009).

Ser/Thr phosphatases contains three subfamilies: phosphoprotein phosphatases (PPPs), metal-dependent protein phosphatases (Zhang and Shi, 2004), and aspartate-based protein phosphatases (Shi, 2009; Zhang *et al.*, 2010). PTPs are classified into classical protein-tyrosine phosphatases (PTPs), dual-specificity phosphatases (DSPs), low-molecular-weight phosphatases (LMW-PTP), and the CDC25 class phosphatases (Andersen *et al.,* 2001; Moorhead *et al.,* 2007; Pao *et al.,* 2007).

Members of Ser/Thr phosphatases comprises a large family of enzymes, initially classified using enzymological criteria, as type 1 (PP1) and type 2 (PP2) phosphatases. PP2 enzymes were subsequently divided into three groups based on the metal ions requirement: 2A (not requiring metal ions), 2B (activated by calcium), and 2C (Mg^{2+}/Mn^{2+} dependent) (Cohen and Cohen, 1989; Shi, 2009; Arino *et al.*, 2011).

Protein phosphatases 2C (PP2C) are Ser/Thr phosphatases conserved in prokaryotes and eukaryotes organisms, involved in a wide variety of key cellular processes both in pathogenic and non-pathogenic fungi, such as cell wall integrity, filamentous growth, virulence, and environmental stress responses and they are also concerned to proliferation, metabolism, and cell death (Schweighofer *et al.*, 2004; Lammers and Lavi, 2007; Shi, 2009; Arino *et al.*, 2011).

PP2C proteins were initially associated with the negative regulation of the high osmolarity glycerol signaling pathway, inducible after osmotic stress, by dephosphorylating and inactivating the HOG1 MAPK. However, the current knowledge suggests that PP2C functions in fungi are much more diverse, playing roles in cell differentiation, growth, survival, apoptosis, and respiration metabolism (Lu and Wang, 2008; Arino *et al.*, 2011).

In contrast to other Ser/Thr phosphatases, PP2C phosphatases are monomeric enzymes and share no structural homology with PP1, PP2A, or PP2B (Schweighofer *et al.*, 2014). The conserved catalytic core domain PP2C contains a central β sandwich, with each β sheet flanked by a pair of α helices. This arrangement generates a cleft between the two β sheets, with the two Mg^{2+}/Mn^{2+} ions located at the base of the cleft. Each metal ion is hexacoordinated by amino acids and water molecules (Das *et al.*, 1996; Shi, 2009; Pan *et al.*, 2015; Si *et al.*, 2016). Dephosphorylation reaction involves the nucleophilic attack of the phosphorous atom by a metal-activated water nucleophile through an S_N2 mechanism (Barford *et al.*, 1998). Additional α helices, unique to PP2C, associate with the core domain on one side and may contribute to substrate specificity or regulation (Shi, 2009; Pan *et al.*, 2015; Si *et al.*, 2016; Bradshaw *et al.*, 2017).

PP2C phosphatases lack known regulatory subunits and their function is usually achieved by multiple catalytic isoforms, that are likely to provide the structural basis for functional specificity. The human genome has sixteen distinct PP2C genes that give rise to at least twenty-two different isoforms (Lammers and Lavi, 2007). Plants contain even more PP2C genes, eighty genes in the model plant *Arabidopsis thaliana* and seventy-eight genes in *Oriza sativa* (Xue *et al.*, 2008). In *S. cerevisiae* there are seven identified PP2C-encoding genes involved in diverse cellular functions (*PTC1-7*) (Cheng *et al.*, 1999; Jiang *et al.*, 2002; Ruan *et al.*, 2006; Guo *et al.*, 2017a, 2017b).

Homologs of several PP2Cs also play important roles in medically important fungi like *C. albicans* (Wang *et al.*, 2007; Hanaoka *et al.*, 2008; Fan *et al.*, 2009; Feng *et al.*, 2010; Yu *et al.*, 2010; Zhao *et al.*, 2010), the opportunistic human pathogen *A. fumigatus* (Winkelstroter *et al.*, 2015b, Bom*, et al.*, 2015; Dolan*, et al.*, 2015), plant pathogens like *F. graminearum* (Jiang *et al.*, 2010; Jiang *et al.*, 2011) and *B. cinerea* (Yang *et al.*, 2013), and the endophytic fungi *N. crassa* (Ghosh *et al.*, 2014).

Most information of PP2Cs came from the investigation of these enzymes in budding yeast. In the last few years, several laboratories have undertaken the study of type 2C phosphatases in organisms other than *S. cerevisiae*. A current overview of the existing PP2C enzymes in fungi, using a dataset of fungal PP2C protein sequences with similarity to *S.*

cerevisiae PTC1-7 (144 sequences from 22 different fungi species) shows that there are five major groups of PP2Cs in fungi (Arino *et al.*, 2011). The first group is formed by the family of proteins Ptc1; the second group includes the related Ptc2/Ptc3 and Ptc4 proteins; the third group includes Ptc5 and Ptc5-related proteins; the fourth group contains Ptc6 and Ptc6-related proteins; the fourth group Ptc7 and Ptc7-related proteins.

1.3.1 PP2C of the Ptc1 clade

PTC1 is the best characterized PP2C protein in *S. cerevisiae*, it is structurally and functionally distinct from the others, and is implicated in MAPK pathways such as the high osmolarity glycerol and cell wall integrity pathways, in the TOR pathway, cation homeostasis, inheritance of cellular organelles, and other functions (Arino *et al.*, 2011). PTC1 interacts with the adaptor protein NBP2 in *S. cerevisiae*, which mediates its association with multiple protein kinases (Uetz *et al.*, 2000; Ito *et al.*, 2001; Hruby *et al.*, 2011; Stanger *et al.*). Similar phenotypes patterns of the Δ*ptc1* strain and the Δ*nbp2* strain were also reported (Roeder *et al.*, 1998; Ohkuni *et al.*, 2003; Du *et al.*, 2006; Jin *et al.*, 2009).

NBP2 target the protein PBS2, that acts as scaffold for various elements of the HOG pathway such as HOG1, SHO1, STE11, and SSK2/22 (Mapes and Ota, 2004). NBP2 contains a SH3 C-terminal domain (Src homology 3), three aromatic a hydrophobic surface chains with an aromatic conserved center (tryptophan) that interacts with the protein PTC1 sites $K^{62}D^{63}$ and $H^{73}Y^{74}$ (Mapes and Ota, 2004; Stanger *et al.*, 2012).This interaction has an important role on the recruitment of PTC1 to the MAPKK protein PBS2, upstream the MAPK HOG1, and subsequent regulation of basal and stress induced levels of phosphorylation of the high osmolarity glycerol pathway (Maeda *et al.*, 1993*,* 1994; Warmka *et al.*, 2001; Mapes and Ota, 2004).

Similarly, PTC1 regulates the cell wall integrity pathway through the mediated NBP2 interaction with the protein BCK1 (Hruby *et al.*, 2011; Palacios *et al.*, 2011; Stanger *et al.*, 2012). This interaction is known to occur by the Y^{119} and F^{165} of the SH3 domain of NBP2, with the $P^{809}XXP^{812}$ of BCK1 (Mapes and

Ota, 2004). In *S. cerevisiae*, lack of *PTC1* leads to sensitive phenotypes against diverse cell wall antagonists, such as Calcofluor White or caspofungin (Ram *et al.*, 1994; Markovich *et al.*, 2004), and to conditions that activate the cell wall integrity pathway, such as alkaline pH (Serrano *et al.*, 2004; Serrano *et al.*, 2006). In agreement with the involvement of PTC1 in the CWI pathway, *PTC1* mutation is synthetically lethal with mutations in genes such as *FKS1*, *GAS1*, or *SML1*, which are crucial for cell wall construction (Lesage *et al.*, 2004).

Disruption of *PTC1* leads higher amounts of active SLT2, associated with increased expression of diverse genes that are positively regulated by the SLT2 MAPK module (MLP1, CRH1, SED1) (Du *et al.*, 2006; González *et al.*, 2006; Tatjer, Sacristan-Reviriego*, et al.*, 2016). PTC1 is also required for proper G2-M cell cycle, under stress conditions activating the CWI pathway, the Δ*ptc1* mutant displays hyperphosphorylated CDC28 kinase, and cells accumulates duplicated DNA content, indicative of a G2-M arrest (Tatjer *et al.*, 2016, Gonzalez*, et al.*, 2016).

A recent array of phenotypic tests of a collection of mutants combining the absence of PTC1 with genes encoding protein kinase catalytic or regulatory subunits identified MKK1 *(*MAPKK) as a putative additional target of PTC1 on the SLT2 MAPK module (Tatjer *et al.*, 2016, Sacristan-Reviriego*, et al.*, 2016). The double mutation Δ*ptc1*Δ*mkk1* contributed to the normalization of all phenotypes tested. It was proposed that abnormal activation of the SLT2 kinase caused by deregulation of MKK1 would be the responsible for phenotypic traits displayed by Δ*ptc1* mutant cells (Tatjer *et al.*, 2016, Sacristan-Reviriego*, et al.*, 2016).

Besides the functions on the HOG and CWI pathway, *PTC1* mutant is sensitive to zinc, to cesium, to calcium which causes hyperactivation of the calcineurin phosphatase (González *et al.*, 2006), and to lithium likely due to a Hog1-independent decrease in the expression of the Na1-ATPase *ENA1* gene (Ruiz *et al.*, 2006). PTC1-deficient cells display fragmented vacuoles, mimicking class B vacuolar protein-sorting mutants (Bonangelino *et al.*, 2002; Seeley *et al.*, 2002; Sambade *et al.*, 2005; González *et al.*, 2006; Jin *et al.*,

2009), and manifest Hog1-independent defects in the inheritance of diverse organelles (Roeder *et al.*, 1998; Du *et al.*, 2006; Jin *et al.*, 2009).

PTC1 is required for normal TORC1 signaling by regulating the SIT4 phosphatase, in a HOG-independent manner (Gonzalez *et al.*, 2009): Disruption of *PTC1* results in intense sensitivity to rapamycin, an inhibitor of the TORC1 pathway, (Parsons *et al.*, 2004; Xie *et al.*, 2005). Overlapping functions of PTC1, REG1-GLC7 and SIT4 contributes to maintenance of cell viability during growth on high glucose by the dephosphorylation of the SNF1/AMPK (Ruiz *et al.*, 2013).

PTC1 has also a role on the invasive growth and pheromone pathway in *S. cerevisiae,* by a mechanism that arises from competition between the MAPK FUS3 and PTC1 to control the phosphorylation state of four sites on the scaffold protein STE5. This competition results in a switch-like dissociation of FUS3 from STE5, a requisite for full relief and dissociation of the FUS3-STE5 complex that is necessary to generate a switch-like mating response (Malleshaiah *et al.*, 2010).

Putative orthologous of *S. cerevisiae* PTC1 have also been recently characterized in filamentous fungi. *F. graminearum* FgPTC1 was found to play an important role in the ability of mycelial growth to resist lithium toxicity (Jiang *et al.*, 2010). Deletion of *FgPTC1* attenuates *F. graminearum* virulence on wheat coleoptiles but not on wheat heads suggesting a specialized role in the virulence against specific niches on wheat (Jiang *et al.*, 2010; Jiang *et al.*, 2011).

In *B. cinerea BcPTC1* disruption lead to reduced hyphal growth, increased formation of pigment (role in melanin biosynthesis), delay of penetration on onion epidermis and increased sensitivity to osmotic stresses and cell wall degrading enzymes. The observed phenotypes cannot be attributed to the phosphorylation of BcSAK1 (Lin and Chung, 2010), since not was observed apparent increase in phosphorylation (Yang *et al.*, 2013).

A. fumigatus PtcG (PTC1 ortholog) have role on the dephosphorylation of SakA (Lin and Chung, 2010). The Δ*ptcG* strain has also been shown to be

sensitive to high temperature and iron starvation conditions, showing a higher expression of *SidG* (gene involved in the siderophore biosynthesis). A higher transcription accumulation of *ptcB* is also observed on the previously characterized *ΔptcG* (PTC3 ortholog null mutant) (Winkelstroter *et al.*, 2015), highlighting a functional redundancy of two PP2C phosphatases that can justify a lack of phenotype of the *ΔptcG* under osmotic stress.

1.3.2 PP2Cs of the Ptc2/Ptc3 clade and Ptc4 clade

S. cerevisae PTC2 and PTC3 are two proteins that are 62% identical (77% similar), that possibly arose from genomic duplication event during evolution (Wolfe and Shields, 1997; Cheng *et al.*, 1999, 1993). These two proteins differ structurally from PTC1 as they possess a carboxyl-terminal extension of around 170 residues necessary to achieve maximum activity (Young *et al.*, 2002).

PTC2 and PTC3 are also involved in the regulation of the HOG1 MAPK, nevertheless, they do not interact with NBP2 (Mapes and Ota, 2004). Their function is unable to fulfill the role of PTC1 in the HOG pathway (Maeda *et al.*, 1993), since they act to limit the maximum of activation of the HOG pathway after stress (Young *et al.*, 2002). Overexpression of *PTC2* and *PTC3* (Kobayashi *et al.*) are able to rescue the synthetically lethal phenotype of *SIT4 and HAL3* disruption, whereas overexpression of all three genes rescues the growth defect of a *SLT2* mutant strain at 37 °C (Muñoz *et al.*, 2002).

Both PTC2 and PTC3 preserve cell viability in the face of agents that compromise the integrity of DNA activating DNA checkpoints to maintain genomic stability, involving phosphorylation and activation of the protein kinase RAD53 (Marsolier *et al.*, 2000; Leroy *et al.*, 2003; Guillemain *et al.*, 2007; Seitomer *et al.*, 2008; Szyjka *et al.*, 2008; Kim *et al.*, 2011). In addition, PTC2 and PTC3 have been implicated in the regulation of the cell cycle progression since they are capable of dephosphorylating CDC28 at Thr-169, a residue essential for its activity as a cyclin-dependent kinase (Cheng *et al.*, 1999; Chen

and Thorner, 2007). Additionally, a possible role of PTC2 and PTC3 in the mechanism of downregulation of the damage checkpoint exerted by the polo-like protein kinase CDC5 has been also proposed (Vidanes *et al.*, 2010).

The putative homologs of PTC2 on *A. fumigatus* are *PtcB*, *PtcD*, and *PtcE*. The null mutant Δ*ptcB* has increased phosphorylation of the SakA (Lin and Chung, 2010) associated with increased expression of osmo-dependent genes. The Δ*ptcB* strain is avirulent in a murine model of invasive pulmonary aspergillosis, more sensitive to cell wall damaging agents, it has a remarkable effect on the cell surface and increased chitin and *β*-1,3-glucan, impaired conidia and germling adhesion, biofilm formation, and MpkA phosphorylation (Slt2/Mpk1 homolog), suggesting a role in the cell wall integrity pathway (Winkelströter *et al*., 2015b).

In *B. cinerea* lack of *BcPtc3* leaded to reduced hyphal growth, increased conidiation, and impaired sclerotium development, increased sensitivity to osmotic and oxidative stresses, and to cell wall degrading enzymes and dramatically decreased virulence on host plant tissues. Different from what it is known in *S. cerevisiae*, BcPtc3, but not BcPtc1, negatively regulates phosphorylation of BcSak1 (the homologue of Hog1) (Yang *et al.*, 2013).

Little is known about PTC4, this phosphatase lacks in filamentous fungi species (Arino *et al.*, 2011), and is still poorly characterized. In *S. cerevisiae*, PTC4 is a cytoplasmic protein of which its overexpression suppresses the lethality of a *Δcnb1Δslt2* double mutant and reduces also the level of phosphorylation and the activity of HOG1 (Shitamukai *et al.*, 2004). Recently it was also demonstrated that PTC4 binds to SLT2, GST-fused versions of PTC2 and PTC4 were co-purified with SLT2-HA, these PP2C phosphatases seem to target the MAPK of the cell wall integrity pathway, however no strong effects were observed in the *ΔPTC2ΔPTC4* strains after incubation with congo red on the phosphorylation of SLT2, suggesting that this phosphatases have a minor effect while compared to *PTC1*, possibly acting to limit hyperphosphorylation on the cascade (Sacristán-Reviriego *et al.*, 2015).

1.3.3 PP2Cs of the Ptc5, Ptc6 and Ptc7 clades

Little is known about the functions of PTC5, PTC6 and PTC7 in fungi. Nevertheless, mitochondrial PP2C phosphatases PTC5 and PTC6 regulate the reversible phosphorylation of PDA1, a E1 alpha subunit of the PDH complex that catalyzes the direct oxidative decarboxylation of pyruvate to acetyl-CoA in *S. cerevisiae* (Krause-Buchholz *et al.*, 2006; Gey *et al.*, 2008). Deletion of either PTC5 or PTC6 results in a decreased PDH activity (Gey *et al.*, 2008).

In *N. crassa*, the role of PTC5 ortholog appear to be more diverse; abnormalities in growth of basal hyphae and asexual development (but not in sexual development) and resistance to oxidative stress mediated by *t*-BuOOH were reported for the mutant Δ*pph-5* (Ghosh *et al.*, 2014). In *A. fumigatus, ΔptcF* strain grows significantly less than the wild-type in iron starvation conditions and it is sensitive to heat stress under growth at 44°, and to geldamicyn. Additionally, the expression of siderophore biosynthesis gene *sidG* was shown to be reduced compared to the wild type strain (Winkelstroter, Bom*, et al.*, 2015). The disruption of *Ptc5* on *F. graminearum* and *B. cinerea* was reported to have no different phenotypes (Jiang *et al.*, 2011; Yang *et al.*, 2013).

PTC6 is located both in the intermembrane space and in the mitochondrial matrix *in S. cerevisiae* (Tal *et al.*, 2007). The *YCR079w locus* was presumed for many years to encode a type 2C phosphatase in *S. cerevisiae* (Stark, 1996), although the first attempt to demonstrate the phosphatase activity of the recombinant protein was unsuccessful (Cheng *et al.*, 1999). It was only in 2007 that it was demonstrated the typical characteristics of a PP2C protein for YCR079w, and it was renamed PTC6 (Ruan *et al.*, 2007).

Although PTC5 and PTC6 function appear to overlap, the lack of PTC6 (but not of PTC5) results in sensitivity to rapamycin (Gonzalez *et al.*, 2009; Ruan *et al.*, 2007), suggesting additional functions for PTC6. Lack of PTC6 results in substantial attenuation of the transcriptional response to rapamycin, particularly in the subset of repressed genes encoding ribosomal proteins or involved in rRNA processing (Gonzalez *et al.*, 2013). Moreover, PTC6 is necessary for survival of stationary-phase cells, and is probably involved

through the RTG3 transcription factor, in mitochondrial mitophagy. This phenotype justifies its alias as autophagy-related protein phosphatase AUP1 (Tal *et al.*, 2007; Journo *et al.*, 2009).

S. cerevisiae cells lacking PTC6 are also sensitive to zinc ions, and somewhat tolerant to cell-wall damaging agents and to Li^+ (Gonzalez *et al.*, 2013; Sharmin *et al.*, 2014). Simultaneous disruption of *PTC1* and *PTC6* compared to single deletion results in a synergistic response to cell wall damaging agents caffeine, Congo Red and Calcofluor White (Sharmin *et al.*, 2014). The level of phosphorylated SLT2 is significantly increased after Congo Red treatment in Δ*ptc1* cells and is enhanced to higher levels in Δ*ptc1*Δ*ptc6* cells. The Δ*ptc1*Δ*ptc6* double disruptant cells restore Δ*ptc1* vacuole fragmentation under standard growth conditions, however shows vacuolar fragmentation in the presence of Congo red or Calcofluor white (Sharmin *et al*., 2014).

Similarly, to PTC5 and PTC6, PTC7 phosphatase was initially located in the mitochondria of *S. cerevisiae* (Ramos *et al.*, 2000). Lack of PTC7 do not result in growth rate or morphological characteristics defects (Jiang *et al.*, 2002). However, overexpression of *PTC7* improves growth in a low-oxygen environment on media supplied with ethanol or galactose as a carbon source. The mRNA transcript levels of *PTC7* are induced under osmotic stress in a Hog1-dependent manner (Runner and Brewster, 2003).

The existence of a functional intron in the *PTC7* gene has been discovered, resulting on two mRNAs transcripts that encode two different proteins (Juneau *et al.*, 2009). Remarkably, the different protein isoforms localize in different cellular compartments and play different roles. The protein translated from the smaller RNA, named PTC7s, is localized in mitochondria, and its expression depends on the source of carbon in the growth medium. On the other hand, the translation of the full mRNA produces a nuclear isoform, named PTC7u, that mediates the effects of actin polymerization caused by the toxin latrunculin A (Juneau *et al.*, 2009). The mitochondrial isoform of PTC7 was recently reported to regulate the PDH activity by dephosphorylation the canonical citrate synthase of the tricarboxylic acid (Lawrence *et al.,* 2004) cycle

CIT1 maintaining its proper dimerization, since dimerization of this protein is needed for its activity and is blocked by phosphorylation (Guo *et al.*, 2017).

Recently, a robust comparative study of the mitochondrial PP2Cs in *S. cerevisiae*, using technics of phosphoproteome and immunoprecipitation, dissected the role of PTC5, PTC6 and PTC7 on the pyruvate dehydrogenase complex (James *et al.,* 1995; Guo *et al.*, 2017). While PDA1 is active at a dephosphorylated state, all three phosphatase mutant strains exhibited lower oxygen consumption rates compared to the wild type. A comparative analysis of the PDC activity showed a high reduction of 90% in the PDA1 activity on the Δ*ptc6* strain*,* while Δ*ptc5* and Δ*ptc7* reduced the activity to 50%. The reduction of activity was confirmed by the observation of highest levels of phosphorylation of the PDA1 on the Δ*ptc6.* Additionally, the phosphoproteomic data also unraveled the Gpd1p as another putative target of PTC5 in the mitochondria, while this protein has augmented phosphorylation on the Δ*ptc5* strain (Guo *et al.*, 2017).

2.Aims of the Study

2. Aims of the Study

The general objective of this thesis has been to study the role of Protein phosphatases type 2C in the development of the pathogenesis of *Fusarium oxysporum* f. sp. lycopersici and signaling on MAPK pathways.

To analyze the role of PP2Cs, the following specific objectives have been proposed:

1. Identification of PP2Cs in F. oxysporum

2. Implication of the different PP2Cs in the MAPK signaling pathways.

3. Investigate the role of Ptc1 phosphatase in Cell wall integrity and High Osmolarity Glycerol pathways

3.Material and Methods

3. Material and Methods

3.1 Material

3.1.1 Webpages and Software

The bioinformatic analysis and prediction tools of the data presented in this work were processed with the webpages and software listed on table 1.

Table 1. Webpages and software tools used in this study.

Webpages	Employment
Broad institute Fusarium comparative Database (http://www.broadinstitute.org)	Protein and nucleic acid sequences sequence retrieval, BLAST algorithm
EupathDB FungiDB (http://fungidb.org)	Protein and nucleic acid sequences sequence retrieval, BLAST algorithm and genome analysis
National Center for Biotechnology Information (NCBI) (http://www.ncbi.nlm.nih.gov)	Protein and nucleic acid sequences sequence retrieval, BLAST algorithm
ExPASY – Prosite database (http://prosite.expasy.org)	Protein domain prediction
SMART (http://smart.embl-heidelberg.de/)	Protein domain prediction
ExPASY-Prosite database https://prosite.expasy.org/	Protein domain prediction and modeling
SwissModel Workspace (http://swissmodel.expasy.org/)	3D Protein Structural modeling and analysis
Emboss epestfind (http://bioinfo.nhri.org.tw/cgi-bin/emboss/epestfind)	Pest domain prediction on protein sequences

Software	Employment
MEGA7	Building, editing and alignment of DNA sequence datasets and molecular evolutionary phylogenetics analysis
FigTree v.1.4.3	Phylogenetic tree figure drawing and editing
DNAstar Lasergene v.7.0.0 - SeqBuilder	DNA sequence analysis
Oligo 6	Design and analysis of oligonucleotides
Image J	Image edition, quantification and measurement
Adobe illustrator CS5	Design of figures and image editing
Adobe photoshop CS5	Design and image editing
GraphPad Prism (v5.00)	Graphic build and statistical analysis
Image Reader LAS-3000 (FujiPhotoFilm)	Photo documentation of southern-blot and western-blot membranes by chemiluminescence
Kodak 1D Image Análisis	Photo documentation of agarose gels
Leica IM500 V1.2	Image

3.1.2 Synthetic oligonucleotides

Oligonucleotides used in amplification reactions were designed with the software Oligo version 6.0 (Molecular Biology Insights, Inc. Colorado, USA). Temperature of melting Tm; was calculated through the [2(A+T)°+4(G+C)°] method, internal stability, duplex and hairpin formation and different physicochemical were determined to avoid primer dimer during PCR reaction. The designed oligonucleotides were synthesized by Isogen Life Science, Netherlands. The oligonucleotides used in this study are listed in the table 2.

Table 2. Oligonucleotides used in this study.

Oligo name	Sequence (5´→3´)
Ptc1-1	GGCAACCTATCTGAGTATGGC
Ptc1-1N	GGCAGAGCGATTGTGGGATTA
Ptc1-2TrpC	*tttacccagaatgcacaggtacacttgtttCTGTTGATGCTGTGGAAGGCT
Ptc1-3GpdA	*tggtcgttgtaggggctgtattaggtctcgATGAGGCACTATGGACACACC
Ptc1-4	AATAGCGTCTTGGGTTCCCGT
Ptc1-4N	ACTGAGCGACGACTTAGGGTT
Ptc1-5	GAGGGTAAAAGAATCGCCGCT
Ptc1-6	GCTTCCTGGTCACTACATACG
Ptc1-9	TGCCATCTACTGTCATAAGCC
Ptc1-10	CAGGAGATTGTTTGGTTGGTC
Ptc3-1	GAACGAGAGGGGACTGTTTA
Ptc3-1N	TTAATTTAGTCTATCAATGGGGGT
Ptc3-2TrpC	*tttacccagaatgcacaggtacacttgtttGGCTGGTGAAATTGGTATTG
Ptc3-3GpdA	*tggtcgttgtaggggctgtattaggtctcgGTTGTTGTCTGAAATTACGGGG
Ptc3-4	GCAATCCCTGATATTCTAAGCCA
Ptc3-4N	CAAGTGGGCGGGCTATGTTC
Ptc3-5	CAAGGAGCACAAGATTCAGCAA
Ptc3-6	TCTCCCTCTTCCGCATCAACA
Ptc3-9 (11q)	CAGACAATGGTTATTTTGCTAT
Ptc3-10(12q)	CTCCATCTTTTGCTTTATCCATT
Ptc5-1	GTGCTTTTGGTAGGTCGGGG
Ptc5-1N	AGCATAGTAGAAGCGTAGGCG
Ptc5-2TrpC	*tttacccagaatgcacaggtacacttgtttGGGGAAACAGAAGGACGGTG
Ptc5-3GpdA	*tggtcgttgtaggggctgtattaggtctcgCCGCAGGAGAGGTTGTATGTA
Ptc5-4	CTATGGAGTGTGTCTTCTGGG
Ptc5-4N	TTATGTGCTCTTCTGACCTGG
Ptc5-5	CCTGATGGCAACAAGACCCC
Ptc5-6	TACCTCGCCTGTCTTCTCCC
Ptc5-7 (11q)	CCTGATGGCAACAAGACCCC
Ptc5-8 (12q)	TACCTCGCCTGTTCTTCTTCCC
Ptc5R-1	GTTCATCACTCCTTCCTCTGGT
Ptc5R-1N	ACAACTTTACCCGCCCAGACT
Ptc5R-2TrpC	*tttacccagaatgcacaggtacacttgtttTGATCCTGGTCTTTGGGCGAA
Ptc5R-3GpdA	*tggtcgttgtaggggctgtattaggtctcgGGTGTATTGTGAGTAAATGGTCT
Ptc5R-4	CCAATAGATCCAAAGACAGAAAG
Ptc5R-4N	CTGACTTATGAGATGGGAGATG
Ptc5R-5	TATTACCTACTCGGACTGTTCT
Ptc5R-6	CAAAAACACCCCAAAACATCCA
Ptc5R-7	ATGCTATCACAACAAAGTCCAC
Ptc5R-8	CTCTTCCTTGCTCTTGTGGAC
Ptc7-1	CTGACTTATGAGATGGGAGATG
Ptc7-1N	CGCTCAACATCATCCTCGTC

Table 2. Oligonucleotides used in this study (continuation)

Oligo name	Sequence (5´→3´)
Ptc7-2TrpC	*tttacccagaatgcacaggtacacttgtttCGATTTTATGATAGAGCAGAGG
Ptc7-3GpdA	*tggtcgttgtaggggctgtattaggtctcgGAATTGATGCGATTAGTGACGG
Ptc7-4	GTAGAGACCATCGAGCTTACG
Ptc7-4N	AGATTCCGTAAGTGAGAAAGGG
Ptc7-5 (11q)	TATTACCTACTCGGACTGTTCT
Ptc7-6 (12q)	CAAAAACACCCCAAAACATCCA
Ptc7-7	GAAGAATAGACCCGCTGTGAAT
Ptc7-8	ACTCACACATTCATAGGCTGGT
Ptc7R-1	TCACTCAGCCGCCAGAAATAC
Ptc7R-1N	GCGATTAGCACAGCCTTTTAC
Ptc7R-2Trpc	*tttacccagaatgcacaggtacacttgtttAGAGAGCAGAGCACCGTAATC
Ptc7R-3GpdA	*tggtcgttgtaggggctgtattaggtctcgGCTGGACACTGAGACATCTG
Ptc7R-4	AGCATTCCTGTCTCAACCCTG
Ptc7R-4N	TGTCCGTTTCGCCGTCGTCT
Ptc7R-5	TCAGAGGGAAAACAAACGGCG
Ptc7R-6	AGTCGCCTCAAGAGTCTGTTC
Ptc7R-7	GTGCTATCAGTTTCCCGTTGG
Ptc7R-8	AGTCAGCCAATACCTCATCCG
GpdA-15B	CGAGACCTAATACAGCCCCT
TrpC-8B	AAACAAGTGTACCTGTGCATTC
Hyg-Y	GGATGCCTCCGCTCGAAGTA
Hyg-G	CGTTGCAAGACCTGCCTGAA
Act-7q	ATGTCACCACCTTCAACTCCA
Act-9q	TGGAAGAAGGAGCAAGGGCA
Ptc1-13q	TCGCACTATGGAAGACACTCA
Ptc1-14q	GATAGCAAAATAACCATTGTCTG
Ptc3-13q	CTCAACGGAAAGACCAAGGAA
Ptc3-14q	CCATCTCATAGCCACTGTCG
Ptc5-3q	GAGACAGATAACAGCGATTGG
Ptc5-4q	CTTGTAGGTTTCGTTCAATTCG
Ptc5R-3q	CGATTGAGGATGAATGGGATC
Ptc5R-4q	TGGTAGGTGTGACGCTTGAC
Ptc6-13q	GGTCGTGAGGGCATCCATAA
Ptc6-14q	CATTTCGCTTTTGACCTCCTC
Ptc7-3q	GACGATCCACTTTCTTGCCC
Ptc7-4q	AGTCTGGAACGAGGGCACG
Ptc7R-13q	CGAGTGATTATTTCATTTGTGCC
Ptc7R-14q	CTTATCAGAGGGAAAACAAACG
Ena1-1q	GCCAAACAACGACATGAAAAGT
Ena1-2q	TCCATGACTTGATACCGAAAGA
Ena5-1q	GGCAACTGGTCTCTCTATGAT
Ena5-2q	CCAGTCTTGTCAGAGCAAATG
Nha1-1q	GAAGTCTACAACACTGAAATGG
Nha1-2q	GTCGTGGGCAGTTCATAGGT
Hog1-1q	AGGTTGATATTTGGAGTGCCG
Hog1-1qt1	CAGATCAATAGCCGAATCGTC
CatA-1q	GTGGGTTTGCGGTGAAATTCT
CatA-2q	CCCAGACGAAATCCCAGAAG

Complementary sequences of *GpdA* promoter and *TrpC* terminator to perform fusion PCR with Hygromycin resistance gene cassette (pAN7-1) are highlighted on lower case characters.

3.1.3 Biologic Material

The *Fusarium*-tomato pathosystem was studied with the plant host *Solanum lycopersicum,* cv. Monika (Syngenta seeds, Almeria, Spain) (this cultivar is susceptible to the race 2), infected with the soilborne plant pathogen *Fusarium oxysporum* f. sp. *lycopersici,* race 2. Strains are detailed in table 3.

Table 3. Fungal strains used in this study

Strain	Genotipe	Reference
4287	Wild type strain race 2	Dr. J Tello[1]
Δptc1	*ptc1*::HYG	Lemos et al., 2018, this work
CΔptc1	*ptc1*::HYG; *ptc1,* PHLEO	Lemos et al., 2018, this work
Δptc5	*ptc5*::HYG	This work
CΔptc5	*ptc5*::HYG; *ptc5,* PHLEO	This work
Δptc5R	*Ptc5R*::HYG	This work
CΔptc5R	*ptc5R*::HYG; *ptc5R,* PHLEO	This work
Δptc7	*ptc1*::HYG	This work
CΔptc7	*ptc1*::HYG; *ptc7,* PHLEO	This work
Δptc7R	*ptc1*::HYG	This work
CΔptc7R	*ptc1*::HYG; *ptc7R,* PHLEO	This work

3.1.4 Media

All media were prepared with Milli-Q deionized water and sterilized either by autoclaving at 120 °C for 20 min or by filtration (0.22 µm pore size, Millipore).

- Regeneration minimal medium: $MgSO_4$ x $7H_2O$ 0.5 g/l, KH_2PO_4 1 g/l, KCl 0.5 g/l, $NaNO_3$ 2g/l, glucose 20 g/l, sucrose 200 g/l and oxoid agar (12.5 g/l for Petri dishes and 4 g/l for top agar).

- Potato Dextrose Broth (PDB): Boil 200 g of peeled potatoes in 0.6 l of water for 60 min. Stir and add 20 g of glucose and deionized water up to 1 l. Sterilize by autoclaving.

- Potato Dextrose Agar (PDA): 39 g/l potato dextrose agar (Scharlau Microbiology). For culturing *F. oxysporum T*ransformants add hygromycin B (55 µg/ml) or phleomycin (5.5 µg/ml-1) after autoclaving.

- YPD /YPDA (Yeast extract Peptone Dextrose/Agar): yeast extract 3g/l, peptone1 g/l, glucose2 g/l, agarose 15g/l.

- Puhalla's minimal medium (MM) (Puhalla, 1968) - MgSO4 x . $7H_2O$ 0.5 g/l, KH_2PO_4 1g/l, KCl 0.5g/l, $NaNO_3$ 2g/l and sucrose 30g/l. Add oxoid agar 20g/l for solid medium.

3.2 Methods

3.2.1 In silico bioinformatic analysis

3.2.1.1 Gene search and sequence retrieval

In silico gene search and sequence retrieval of *F. oxysporum* and orthologs of other fungal species was performed with the *BLAST* algorithm (Altschul et al, 1990) from National Center for Biotechnology Information (NCBI) (http://www.ncbi.nlm.nih.gov), Broad Institute Fusarium Comparative Database (http://www.broadinstitute.org) and Fungal and Oomycete genome database - FungiDB (http://fungi.org), using as query the protein sequences of *S. cerevisiae* PP2C PTC1 (YDL006W), PTC2 (YER089C), PTC3 (YBL056W), PTC4 (YBR125C), PTC5 (Krause-Buchholz *et al.*), PTC6 (YCR079W) and PTC7 (YHR076W), and *F. graminearum* FgPTC1 (FGSG_04111), FgPTC3 (FGSG_10239), FgPTC5 (FSG_05205), FgPTC6 (FGSG_05162) and FgPTC7 (FGSG_05611) and FgPTC7R (FGSG_00435).

3.2.1.2 Phylogenetic Analysis

Phylogenetic analysis was performed by Maximum Likehood method on MEGA v.7.0 with a dataset containing protein sequences of the identified *F. oxysporum* PP2Cs, and orthologs from *Aspergillus fumigatus, Botrytis cinerea, Candida albicans, Fusarium fujikuroi, Fusarium graminearum, Fusarium verticillioides, Magnaphorthe oryzae*, and *Saccharomyces cerevisiae.* Initial trees for the heuristic search were obtained automatically by applying Neighbor-Join and BioNJ algorithms to a matrix of pairwise distances estimated using a JTT model, and the topology with superior log likelihood value was selected from 1000 replicates of bootstrap. A discrete Gamma distribution was used (5 categories +*G*, parameter). The tree was drawn with FigTree v.1.4.3 (2016), rooted on midpoint, on equal scale. All positions containing gaps and missing data were eliminated.

3.2.1.3 Domain prediction and secondary structure modeling

Predictions of domains and secondary structure models were performed with the algorithms SWISS-MODEL and ScanProsite respectively (ExPASy, Swiss Institute of Bioinformatics, Switzerland).

3.2.2 Molecular Methodology

3.2.2.1 Nucleic acid (gDNA/RNA) extraction

Genomic DNA (gDNA) was extracted from *F. oxysporum* mycelium using the CTAB method (Torres *et al.*, 1993). Briefly, approximately 100 mg of mycelium were ground to a fine powder in a mortar and pestle under liquid nitrogen and transferred to a 2 ml Eppendorf centrifuge tube with 1 ml of CTAB extraction buffer and vortexed. 4 µl of β-mercaptoethanol (Merck) and 500 µl of a chloroform: octanol 24:1 (v/v) solution were added quickly, the mix was vortexed and incubated at 65ºC for 30 minutes.

After incubating at room temperature for 15 minutes, the sample was centrifuged for 5 minutes at 12000 rpm. The supernatant was transferred to a new vial and then precipitated with 1 ml of 100% ice-cold ethanol and incubated at -20ºC for at least 10 minutes (optional overnight), followed by centrifugation for 10 min at 12000 rpm and two consecutive washes with 1 ml 75 % ethanol. Finally, the pellet was resuspended in 50-100 µl of sterile deionized water with 4 µl of RNase (10 mg/ml) and incubated at 37°C for 30 minutes.

- CTAB extraction buffer**:** 12.1 g/l Trizma base; 7.44 g/l EDTA; 81.8 g/l NaCl and 20 g/l Cetyltrimethylammonium bromide. Heat to 60 °C to dissolve and adjust to pH 8.0 with NaOH. The buffer was stored at 37ºC to avoid precipitation.

For RNA extraction, approximately 100 mg of frozen mycelium were ground to a fine powder in a mortar and pestle under liquid nitrogen and

transferred to a pre-chilled 2 ml Eppendorf centrifuge tube. Then, 1 ml (4 volumes) of TRIpure Isolation Reagent (Sigma Aldrich, St Louis, Missouri, USA), was added; the sample was homogenized by vortexing and then incubated for 5 minutes on ice. After 10 minutes (12000 rpm, 4ºC) centrifugation, the supernatant was retrieved and transferred to a new vial where 200 µl of chloroform per 1 ml of TRIpure was added. The sample was briefly homogenized by vortex for 15 seconds and incubated on ice for 3 min prior to 20 minutes centrifugation at 4ºC 13000 rpm, resulting in the formation of three phases.

The upper clear phase was transferred to a new clean 1,5 ml Eppendorf centrifuge tube pre-chilled with 750 µl Isopropanol. The tube was mixed by inversion followed by incubation on ice for 10 minutes to precipitate the RNA. The sample was centrifugated for 20 minutes at 4°C, 13000 rpm. The obtained RNA pellet was washed with 1 ml of 75% ethanol (v/v) and centrifuged at 4°C for 5 minutes and 10000 rpm. The pellet was dried for 5 minutes at speed vac and resuspended in 20-50 µl of RNase-free water.

DNA and RNA quality and quantity were measured in a Nanodrop® ND-1000 spectrophotometer (Thermo Fischer Scientific, Walthan. Massachusets, USA) at 260nm and 280 nm wavelengths, respectively. In addition, the quality of the DNA and RNA obtained was monitored by electrophoresis in a 0.7% and 1% agarose gel (w/v), respectively.

3.2.2.2 Standard PCR

PCR amplification reactions were performed in a BioRad T100 thermal cycler using the thermostable Taq DNA polymerases BioTaq™ DNA Polymerase (Bioline, London, United Kingdom), Velocity™ DNA Polymerase (Bioline, London, United Kingdom), and Expand High Fidelity PCR System (Roche Diagnostics, Basel, Switzerland) depending on the objective or fragment size.

Amplification of fragments till 2kb were performed with the thermostable BioTaq™ DNA Polymerase (Bioline, London, United Kingdom). Each PCR

reaction contained 300 nM of each primer, 2.5 mM MgCl2, 0.8 mM of dNTPs mix and 0.05 U/µl of polymerase. Genomic DNA was added at 5-10 ng/µl. The PCR cycling conditions were defined by an initial step of denaturation (5 minutes, 94°C) followed by 35 cycles of 35 seconds at 94°C, 35 seconds at the calculated primer annealing temperature and 1 minutes/Kb was stablished for DNA elongation at 72°C, and a final extension step at 72°C for 10 minutes.

Fusion PCR amplification reactions were performed with Velocity™ DNA Polymerase (Bioline, London, United Kingdom). Each PCR reaction contained 2.5 mM MgCl2, 0.8 mM of dNTPs mix and 0.05 U/µl of polymerase. A mix containing the overlapping fragments was prepared with 150ng of 5' or 3' fragments, and 300ng of resistance cassette. PCR cycling conditions were defined by an initial step of denaturation (5 minutes, 98°C) followed by 8 cycles of 15 seconds at 98°C, 35 seconds at 60°C and 75 seconds at 72°C, and a final extension step at 72°C for 10 minutes.

Amplification of fragments superior to 2kb were performed with the Expand High Fidelity PCR System (Roche Diagnostics, Basel, Switzerland). Each PCR reaction contained 300 nM of each primers, 2.5 mM MgCl2, 0.8 mM of dNTPs mix and 0.05 U/µl of polymerase. DNA was added at 10 ng/µl for genomic DNA amplification or at 5 ng/µl final concentration for plasmid DNA. The PCR cycling conditions were defined by an initial step of denaturation (5 minutes, 94°C) followed by 35 cycles of 35 seconds at 94°C, 35 seconds at the calculated primer annealing temperature and 1 minutes/Kb was stablished for DNA elongation at 72°C, and a final extension step at 72°C for 10 minutes.

3.2.2.3 Precipitation of PCR products

To eliminate oligonucleotides from PCR products and obtain a desired concentration of DNA fragments to downstream protocols, PCR products were routinely precipitated with sodium acetate, briefly, 1/10 volume of 3 M Sodium Acetate pH 5,2 was added, and 2,5 vol of 100% cold-ethanol were added and samples, the sample was briefly mixed prior to incubation at -20ºC for 30 min. Precipitated DNA was then centrifuged at 13400rpm for 30 minutes at RT. Pelleted DNA was washed with ethanol 70%, air dried and finally resuspended

with sterile ultrapure water. Similarly, DNA probes for Southern blot were precipitated with lithium chloride 8 M (Sharmin *et al.*).

3.2.2.4 Reverse transcriptase PCR

First strand cDNA was synthesized using the Transcriptor cDNA Master (Roche Diagnostics, Basel, Switzerland) from 2 µg of total RNA. The RNA samples were previously treated with DNase I (Roche Diagnostics, Basel, Switzerland). The resulting cDNA samples were diluted 1:1 on ultrapure deionized water for RT-qPCR assays. Assessment of genomic DNA contamination and quality of cDNA samples was RT-PCR tested with Act-q7 and Act-q9 (primers designed flanking an intron on the Actin gene) with Expand high fidelity Taq DNA polymerase (Roche Diagnostics, Basel, Switzerland). DNase, cDNA synthesis, and RT-PCR reactions were prepared following the manufacturer's instructions.

3.2.2.5 Real-time quantitative PCR

RT-qPCR was performed using 7.5 µl FastStart Essential DNA Green master (Roche Diagnostics, Basel, Switzerland), 5 µl of cDNA (1:1) and 0.3 µl of each gene specific primer on a final volume of 15 µl. Analyses were performed using primers flanking an intron of each gene when possible. The following PCR program was used for all reactions: an initial step of denaturation (10 min, 95 °C), followed by 40 cycles of 10 s at 95 °C, 10 s at 62 °C and 20 s at 72 °C, 5 s at 80 °C (Plate read), in a CFX-Connect Real Time System (Bio-Rad, Hercules, CA, USA).

Relative expression levels were calculated with the formula $2^{-\Delta Ct}$ (Pffafl, 2001), using *actin* as reference gene. Gene expression fold-increase levels were calculated with the formula $2^{-\Delta\Delta Ct}$ (Livak and Schmittgen, 2001) related to the non-treated wild-type strain, using *actin* as reference gene. All experiments included three biological replicates and three technical replicates for each biological sample. Data were subjected to statistical

significance test (*t-test*) comparing the expression levels with the non-treated wild-type strain level (time 0).

3.2.2.6 Fusion PCR

The *F. oxysporum* gene disruption constructs were generated by fusion PCR technique (Yang *et al.*, 2004) to perform recombination by split-marker strategy (Catlett *et al.*, 2003) (Figure 8). PCR fragments and fusion PCR were generated on a BioRad T100 thermal cycler (Biorad, Hercules, California, USA). Firstly, Upstream (5') and downstream (3') fragments were amplified with the primers pairs *PtcX*-1 *PtcX*-2*TrpC* (1.4-kb), and *PtcX*-3*GpdA PtcX*-4 (Table S1) respectively with BioTaq™ DNA Polymerase (Bioline, London, UK) standard protocol.

The fragments containing the complementary sequences of the *Aspergillus nidulans GpdA* promoter (3') and *TrpC* terminator (5') were individually fused to resistance gene cassettes hygromycin B (single mutants) or phleomycin (double mutants), previously amplified with the primers *GpdA*-8B and *TrpC*-15B from the plasmids pAN7-1 (Punt *et al.*, 1987) and pAN8-1 (Mattern *et al.*, 1988) respectively, at a molar proportion of 3:1 using Velocity DNA polymerase (Bioline, London, UK). Reactions were performed with 8 cycles of PCR with standard protocol.

The resulting fusion PCRs were used as template to amplify the overlapping fragments constructs (Figure 8) to proceed transformation of protoplasts of *F. oxysporum* as previously described (Di Pietro and Roncero, 1998). The overlapping fragments were generated with the pairs of primers *Ptc1*-1N *and Hyg*-G (5' fragment), and pair *Ptc1*-4N *and Hyg*-Y (3' fragment) using Velocity DNA polymerase (Bioline, London, UK) with standard protocol.

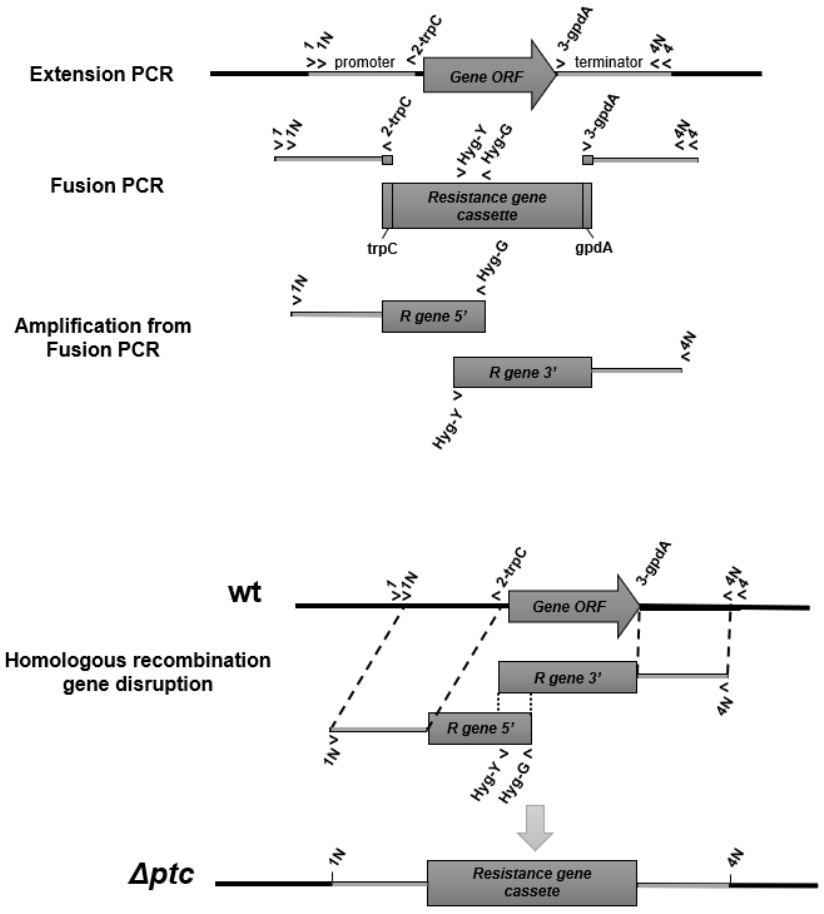

Figure 8. ***F. oxysporum*** **constructs generation by fusion PCR technique** (Yang et al., 2004) to perform gene disruption by homologous recombination split-marker strategy (Catlett et al., 2003).

3.2.2.7 Southern blot analysis

Transformants were analyzed by southern-blot analysis (Sambrook *et al.*) of DNA treated with the appropriate restriction enzyme, hybridized with a labelled probe generated with primers uptstream or downstream to the gene ORF, as described (Di Pietro and Roncero, 1998), using the non-isotopic digoxigenin labelling kit (Roche Diagnostics SL, Barcelona, Spain).

3.2.2.8 Protein purification from mycelia

Mycelial samples were obtained as described above, protein extraction and western blot analysis were performed as described previously (Miguel-Rojas and Hera, 2015 2017). 100 mg of frozen mycelia were ground to a fine powder in a mortar and pestle under liquid nitrogen and transferred to a pre-chilled 2 ml Eppendorf centrifuge tube with 1 ml of fresh prepared lysis buffer (200 µM NaOH 10 N, 0.2 % β-mercaptoethanol, on water). Simultaneously to alkaline lysis, mechanical homogenization was achieved by using by vortex. 75 µl of Trichloroacetic acid were added to each sample to precipitate proteins, and samples were thoroughly mixed with the micropipette. Extracts were incubated for 10 minutes on ice, and precipitated proteins were harvested by centrifugation at 13400 rpm for 5 minutes at 4°C. The supernatant was removed, and the pellet resuspended in 100 µl of Tris-base 1 M and 200 µl 2X loading buffer (20 mM Tris-HCl pH 6.8, 8% glycerol, 1.6 % SDS, 4% β-mercaptoethanol and 0.1 % bromophenol blue, on water).

3.2.2.9 Western blot analysis

Equal amounts of protein were loaded to a 14% Tris-glycine 10% polyacrylamide gel using standard protocols (Sambrook *et al.*, 1989). After SDS-PAGE electrophoresis separation, total proteins were transferred from the polyacrylamide gel to 0,45 µm nitrocellulose membranes (Bio-Rad, Hercules, CA, USA) in a Trans-Blot Turbo Transfer System (Bio-Rad, Hercules, CA, USA) using the Trans-Blot RTA Transfer Kit, following manufacturer's instructions. The membranes were blocked using 5% Skim-Milk (Difco, Detroit, MI, USA) on PBS-Tween for 45 min and then incubated overnight with monoclonal antibodies on 1% BSA PBS-Tween to detect the phosphorylated and total MAPK proteins Mpk1, Hog1 and Fmk1, Tubulin was used as loading control, as previously described (Miguel-Rojas and Hera, 2016, Perez-Nadales and Di Pietro, 2011, Segorbe et al., 2017).

Phosphorylated Mpk1 and Fmk1 were detected using the Phospho-p44/42 MAPK (Erk1/2) (Thr202/Tyr204) (D13.14.4E) XPV R

Rabbit monoclonal antibody (no. 4370) (Cell Signalling Technology, Danvers, MA, USA). Unphosphorylated Mpk1 and Fmk1 were detected using anti-Mpk1 (yN-19) (sc-6802) and anti-Fus3 (γN-19) (sc6772) respectively (Santa Cruz Biotechnology, Heidelberg, Germany). Phosphorylated Hog1 was detected using the Phospho-p38 MAPK (Erk1/2) (Thr180/Tyr182) Rabbit monoclonal antibody (no. 9211S) (Cell Signalling Technology, Danvers, MA, USA). Unphosphorylated Hog1 was detected using anti-Hog1 Rabbit monoclonal antibody (y-215) (sc-9079) (Santa Cruz Biotechnology, Heidelberg, Germany). Tubulin was detected using αTub Mouse monoclonal antibody (3H3087) (Santa Cruz Biotechnology, Heidelberg, Germany). Horseradish peroxidase (HRP)-conjugated anti-rabbit (no. 7074) (Cell Signalling Technology, Danvers, MA, USA), Horseradish peroxidase (HRP)-conjugated anti-mouse (no. 7076) (Cell Signalling Technology, Danvers, MA, USA), and donkey anti-goat IgG-HRP (sc2020) (Santa Cruz Biotechnology, Heidelberg, Germany) were used as secondary antibodies.

After overnight incubation, the membranes were washed three times with PBS-Tween (10 min), incubated for 1 h with the correspondent secondary antibody, washed three times with PBS-Tween (10 min), and then visualized using the ECL Select western blotting detection reagent (GE Healthcare, Madrid, Spain) on LAS-1000 Intelligent Dark-box (Fuji Photo Film co, Tokyo, Japan). Band intensity was quantified with Image J software v. 1.08 (National Health Institute, United States of America). The phosphorylation level was calculated by the ratio of phosphorylated protein versus non-phosphorylated protein. Wild-type (time 0) was used to standardize the samples.

3.2.3 Culture conditions

3.2.3.1 Fungal strains storage and conidia obtention

Fungal strains were stored as microconidia suspensions at 30% glycerol and -80ºC. To obtain mycelia for DNA extraction and fresh microconidia for colony growth assays, the fungal strains were cultured inoculating the microconidia from stock solutions on potato dextrose broth (PDB; Difco, Madrid, Spain), incubating at 28ºC, orbital shaking 170 rpm (Di Pietro and Roncero, 1998). In the case of mutant strains, appropriate antibiotics (hygromicin B at 55 µg/ml or phleomycin at 5.5 µg/ml) were added to the culture medium.

Conidia were obtained by filtration through a nylon filter (Monodur; mesh size 10 µm), harvested by centrifugation at 12000g for 10 min and resuspended in 1ml of sterile water (Di Pietro and Roncero, 1998). After measurement with a hemocytometer (Thoma 250) (Marienfield, Lauda-Königshofen, Germany), the conidial suspension density was adjusted to proper concentration for the posterior assays.

3.2.3.2 Fungal stress induction assays

To perform the invasive growth assay, $1x10^9$ microconidia were inoculated into 200 ml of PDB and incubated for 15 h at 28°C with 170 rpm. After, germlings were harvested by filtration with a monodur filter and washed with 400 ml of Puhalla Minimal Media. A sterile spatula was used to transfer germlings from the filter to a sterile 50 ml Falcon tube, on a final volume of 12 ml of Puhalla Minimal Media. Three replicates of 1ml were recovered for the timepoint 0 (non-treaded replicates) and 9 aliquots of 1ml were individually spread on Puhalla Minimal Media plates and incubated at 28°C for 15, 30, and 60 min to obtain samples to a time course analysis (three biological replicates per timepoint).

To perform the liquid stress assays, germlings were obtained similarly as described above. Aliquots of 25 ml were harvested by filtration with a monodur filter and washed with 50 ml of PDB. A sterile spatula was used to transfer germlings from the filter to a 25 ml PDB supplied with the stressor (1 replicate). Similarly, three biological replicates were harvested after transfer (non-treated) and a time course analysis of stress was performed (15, 30, 60 minutes with three biological replicates per timepoint). Immediately after harvest, samples were frozen in liquid nitrogen, and stored at -80°C. Additionally, it was performed a similar assay on PDB (without stress).

All The liquid assays were performed at 28°C, 170 rpm shaking. Cell wall and membrane stress were performed in PDB supplemented with Sodium-dodecyl-sulfate (SDS 0.0125%) prepared in water; calcofluor white (CFW 50 µg/ml) prepared in 0.5% KOH, 83% glycerol (both from Sigma-Aldrich). For oxidative stress, PDB was supplemented with caffeine (5 mM) prepared in water. For hyperosmotic stress, PDB was supplemented with Sodium chloride (NaCl 0.6M and 1.2 M), Sorbitol (1.25 M), Potassium chloride (KCl 1.2 M) and Lithium chloride (LiCl 0.3 M).

3.2.4 Protoplast generation and Genetic transformation

3.2.4.1 Generation of *F. oxysporum* protoplasts

Protoplasts were obtained following the protocol described by Powell and Kistler (1990), with some modifications. Briefly, $5x10^8$ microconidia were inoculated into 200 ml of PDB and incubated for 14 h at 28°C with 170 rpm. After, germlings were harvested by filtration with a monodur filter and washed first with 500 ml of ultrapure deionized water and then with 200 ml MgP solution. A sterile spatula was used to transfer germlings from the filter to a sterile 50 ml Falcon tube, containing 20 ml of MgP with 0.5% (w/v) Glucanex® (Novozymes, Bagsværd, Denmark) as the protoplasting enzyme. The protoplasts were incubated in the enzyme solution for 60 minutes at 30°C with

slow shaking (60 rpm), after incubation the protoplast accumulation was monitored under the microscope till reach optimal quantity.

When optimal number of protoplasts was achieved, the sample was filtered through a double layer of monodur nylon filters and washed with 400 ml of STC solution. The flow-through containing the protoplasts was collected in ice-cold pre-chilled 50 ml centrifuge tubes. Filtrates were centrifuged at 4°C and 1500g for 15 minutes to collect protoplasts, which were carefully resuspended in 1 ml STC and counted on hematocytometer. The protoplast suspension was adjusted to a final concentration of 2 x 10^7 total protoplasts on 100 µl aliquots, stored in Eppendorf tubes to be used directly for transformation

- MgP solution: 1.2 MgSO4; 10 mM Na2HPO4, pH 5.8-6.0 adjusted with orthophosphoric acid.
- STC solution: 0.8 M sorbitol; 50 mM CaCl2 y 50 mM Tris-HCl, pH 7.5.
- PEG solution: 60% polyethylene glycol MW 4000 (p/v) in 0.6 M MOPS.

3.2.4.2 Genetic transformation

Transformation was performed as described (Malardier et al., 1989), with slight modifications. 2-3 µg of transforming DNA were mixed with 10 µl of 0.1M aurintricarboxylic acid (ATA) (Sigma Aldrich, St Louis, Missouri, USA), a potent inhibitor of nucleases, in a final volume of 60 µl with TEC solution. For co-transformation experiments, 2-3 µg of full-length fragments (from the start of the promoter to the end of the terminator) were mixed with 1,0 µg of the DNA construct conferring antibiotic resistance was added. For the negative transformation control 50 µl of TEC was mixed with 10 µl of ATA in an additional tube and treated like the transformation mix in the following procedure. The mixes were incubated on ice for 20 minutes in parallel with 2 tubes of 100 µl protoplasts (2x10^7) generated as described above.

Next, protoplasts and DNA solutions were carefully mixed and incubated a further 20 minutes on ice. Then, 160 µl of PEG solution were added and mixed carefully, followed by 15 min incubation at room temperature before 1 ml of STC solution was added. The tube was centrifuged for 5 minutes at

3000 rpm to pellet protoplasts, which were resuspended in 200 µl of STC. Next, 50 µl aliquots were mixed with 3 ml of top agar at 45°C and spread onto plates containing 25 ml of solid regeneration minimal medium.

Four transformation controls were made. To calculate the protoplast regeneration 10µl of the negative control mix was diluted 10^{-4} and 10^{-5} with STC and spread on plates without antibiotic. A 10^{-5} dilution made with H_2O leads to burst of the protoplasts and allows the determination of conidia which inhibits the transformation efficiency. The antibiotic control was performed by spreading the rest of the negative control (190 µl) on regenerations media containing the appropriate antibiotic.

Plates were incubated at 28°C for 14 hours or 2 hours before addition of 3 ml of top agar containing 200 µg of hygromycin B or 160 µg of phleomycin, respectively. Incubation at 28°C was prolonged for 4-7 days until transformant colonies became visible. Colonies were transferred to PDA plates with selective medium, and transformants were submitted to two consecutive rounds of single monoconidial purification on selective PDA plates.

- TEC solution: 10 mM Tris-HCl, pH 7.5; 1 mM EDTA and 40 mM CaCl2.
- Regeneration minimal medium: 0.05% MgSO4 x 7H2O ; 0.1% KH2PO4; 0,5g KCl; 0.2% NaNO3; 2% glucose, 200g sucrose and 1,25% oxoid agar (12.5 g/l for Petri dishes and 4 g/l for top agar).

The generated transformants were purified by monoconidial isolation on PDA plates supplied with hygromycin or phleomycin as described previously (Di Pietro and Roncero, 1998). Homologous insertion of the split-marker knockout construct was checked by PCR amplification using the internal ORF primers *PtcX*-1 (primer external to the construct) and *Hyg*-G or Phl-e (internal primer of the hygromicin B, and phleomycin resistance cassettes, respectivelly).

The complementation of the mutant strains was performed with the transformation of protoplasts Δ*ptc strains* with a fragment containing the complete *ptc* gene amplified from the wild-type genomic DNA with the primers pair *PtcX*-1N and *PtcX*-4N (from promoter to terminator) by cotransformation with the phleomycin cassette (amplified from pAN8-1 plasmid with the primers

GpdA-8B and *TrpC*-15B). Phleomycin resistant transformants were selected as previously described (Di Pietro *et al*., 2001), the detection of the wild-type *Ptc* allele in the complemented strain was confirmed to be on the homologous site by PCR with the primers *PtcX*-1 and *PtcX*-4, and by southern blot analysis.

3.2.5 Phenotypical assays

3.2.5.1 Colony growth phenotypical assays

Differential growth of *F. oxysporum* strains was monitored at 3, 6 and 9 days after inoculation of $5x10^4$ fresh microconidia on PDA and MM (Puhalla, 1985) incubated at 28ºC.

For the phenotypic analysis of colony growth, water droplets from serial dilutions containing 10^4, 5×10^3, 10^3, 2×10^2, 10^2 freshly obtained microconidia were plated onto plates containing complete rich medium YPD agar. Cell wall and membrane stress were performed on YPD plates supplemented with Sodium-dodecyl-sulfate (SDS 0.0125%) prepared in water; Calcofluor White (CFW 50 µg/ml) prepared in 0.5% KOH, 83% Glycerol (both from Sigma-Aldrich); Congo Red (CR 100 µg/ml) prepared in water. For oxidative stress YPDA plates were supplemented with Menadione (20 µg/ml) prepared in DMSO and Caffeine (5 mM) prepared in water. Fungicide sensitivity assays were performed on YPDA containing Iprodione (20 µg/ml) and Fludioxonil (20 µg/ml) prepared in ethanol or DMSO respectively. For hyperosmotic stress, YPDA plates were supplemented with Sodium choride (NaCl 1.2 M), Sorbitol (1.25 M) and Potassium chloride (KCl 1.2 M). To measure metal tolerance YPD plates contained Calcium chloride ($CaCl_2$ 0.3 M) or Lithium chloride (LiCl 0.3 M).

Plates were incubated at 28 °C and scanned. Colony area was measured using ImageJ software. Relative colony growth was calculated using the formula: Relative growth (%) = (growth area on stress media / growth area on YPGA) * 100. The average of three biological replicates was used to perform statistical significance test (*t-test*) comparing the strains Δ*ptc1* and *C*Δ*ptc1* with

the wild-type strain. Heat tolerance was measured by inoculation of 5×10^4 fresh microconidia on PDA followed by incubation at 28 °C or 33 °C. For Acetic acid tolerance assays, water droplets containing 5×10^4 fresh microconidia were inoculated on PDA plates and incubated at 28 °C. All plate assays included three replica plates and were performed three times with similar results.

3.2.5.2 Conidiation and germination assays

For conidiation assays 1.25×10^8 fresh conidia were inoculated on 25 ml of PDB media and incubated 48 h at 28 °C with shaking (170 rpm). Aliquots of 1 ml were taken from each replicate to perform quantification of the conidia on a Leica DMR microscope using a hemocytometer (Marienfiend, Baden-Württemberg, Germany).

Germination was measured 13 h after inoculation of 3.19×10^6 conidia on 1 ml of diluted 1:10 minimal medium (MM) (0.05% KCl, 0.05% $MgSO_4$, 0.1% KH_2PO_4, 0.2124% $NaNO_3$, 0.1% Sacarose) (Puhalla, 1985), supplemented with 25 mM $NaNO_3$. One hundred events were counted by sample using a Leica DMR microscope (germinated or not germinated microconidia). Germination rate was calculated using the formula: Germination (%) = (germinated microconidia/total microconidia) * 100. Statistical analysis (*t-test*) was performed to compare the strains Δ*ptc1* and *C*Δ*ptc1* with the wild-type strain.

3.2.5.3 Vacuole staining and fluorescence microscopy

For vacuole analyses, 3.19×10^6 fresh conidia were inoculated on 1 ml diluted 1:10 MM supplied with 25 mM $NaNO_3$. After 13 h incubation at 28 °C 170 rpm shaking, germling aggregation was eliminated by 1 min vortexing and vacuoles were stained for 15 min in the dark using the fluorescent dye FM4-64 (T13320) (Invitrogen, Thermo Fisher Scientific co, Whaltan, MA, USA) at a final concentration of 4 mM FM4-64 dye. Samples were centrifuged for 5 min at 7000 rpm and 250 µl aliquots of the supernatant were incubated in the presence of 0.6 M NaCl. Un-treated control samples were supplemented with equal volume of fresh MM.

After 15 min treatment at 28 °C samples were observed under optical and epifluorescence microscopy analysis using the Nomarsky technique or the appropriate filter set, respectively, in a Zeiss Axio Imager M2 Dual Cam microscope (Carl Zeiss MicroImaging GmbH, Göttingen, Germany). Examination using epifluorescence was performed with UV-light 340–380 nm and a filter block (BP 560/40, FT 585, BP 630/75). Images were captured with an Evolve Photometrics PV Cam digital camera using the Axiovision 4.8 software. Images were processed using Adobe Photoshop CS3 (Adobe Systems, Mountain views, CA, USA).

3.2.6 Plant infection and Virulence related assays

3.2.6.1 Plant infection

Tomato root infection assay was performed as described (Di Pietro et al., 2001), using the susceptible cultivar Monika (Syngenta Seeds, Almeria, Spain). Briefly, 2-week-old tomato seedlings were inoculated by submerging roots for 30 min in a suspension of 5×10^6microconidia/mL of the different *F. oxysporum* strains, planted in vermiculite and maintained in a growth chamber (28 °C; photoperiod 14 h light/10 h dark). Ten plants were used for each treatment. Plant survival was recorded for 35 days. A Long-rank (Mantel-Cox) test was used to assess the statistical significance of the differences in survival among groups. Data were plotted using the software GraphPad Prism version 5. (GraphPad Software, La Jolla, CA, United States of America). $P < 0.05$ was considered to be significant. Experiments were performed three times with similar results.

3.2.6.2 Cellophane penetration assay

Invasive growth assays on cellophane membranes were performed as described (Lopez-Berges et al., 2010, Prados Rosales and Di Pietro, 2008) with some modifications, using solid MM supplemented with 50 mM $NaNO_3$ and buffered with 100 mM MES. The pH of the media (5 or 7), ph7 was adjusted

with 10 M NaOH. Cellophane sheets with the same size of a Petri dish were cut, autoclaved in deionized water and placed on the center of Puhalla's MM plates buffered to pH 5.0 or 7.0.

Drops of 5 µl of water containing $5x10^4$ microconidia were spotted onto the center of the plates, and plates were incubated at 28ºC for 3 days, respectively. Then, the cellophane sheet with the fungal colony was carefully removed and the plates incubated for more 24 hours at 28ºC. Plates were imaged before and after removal of the cellophane. All experiments included three replicates and were performed twice.

4. Results

4. Results

4.1 PP2C phosphatases in *Fusarium oxysporum*

4.1.2 *F. oxysporum* genome encodes seven putative PP2C phosphatases

Fusarium graminearum genome contains seven PP2C phosphatase genes orthologous to the PP2C genes of *Saccharomyces cervisiae* (Jiang, 2010 #247). BLASTp analysis of *F. oxysporum* genome (FungiDB and NCBI) identified seven genes showing different levels of homology to *S. cerevisiae* PP2C genes (Table 4). Single orthologues to *S. cerevisiae* PTC1, PTC3, and PTC6 were found in the screening. Additionally, we found two orthologous genes to each *S. cerevisiae* PTC5 and PTC7 (*ptc5* and *ptc5R* and *ptc7* and *ptc7R*, respectively), as it was previously described for *F. graminearum* (Jiang et al., 2010; Jiang et al., 2011). However, no *S. cerevisiae* PTC2 and PTC4 orthologues were detected in the blast analysis.

Table 4. Identification of PP2C genes on *Fusarium oxysporum* f. sp *lycopersici* 4287

Fungi Database Gene Transcript	Length (bp)	Exons (No.)	Predicted amino acids (aa)	Similarity to *S. cerevisiae* PP2Cs (reference sequence)		Similarity to *F. graminearum* PP2Cs (reference sequence)	
				Identity (%)	Coverage (%)	Identity (%)	Coverage (%)
				***PTC1* (YDL006W)**		***FgPTC1* (FGSG_04111)**	
FOXG_11525_t26_1	2781	2	576	43	50	92	100
FOXG_11525_t26_2	2983	1	576	43	50	92	100
				***PTC3* (YBL056W)**		***FgPTC3* (FGSG_10239)**	
FOXG_05154-t26_1	6479	6	423	49	66	93	96
FOXG_05154-t26_2	6419	7	403	49	66	89	91
FOXG_05154-t26_3	6086	7	315	41	62	84	83
FOXG_05154-t26_4	6094	7	451	48	66	94	96
FOXG_05154-t26_5	6034	8	431	48	66	89	91
FOXG_05154-t26_6	3202	8	451	48	66	94	96
FOXG_05154-t26_7	4738	5	315	41	62	84	87
				***PTC5* (YOR090C)**		***FgPTC5* (FGSG_05205)**	
FOXG_07981-t26_1	1785	3	594	44	59	90	94
				***PTC6* (YCR079W)**		***FgPTC6* (FGSG_05162)**	
FOXG_07912-t26_1	2839	1	662	35	54	84	88
				***PTC7* (YHR076W)**		***FgPTC7* (FGSG_05611)**	
FOXG_09277-t26_1	1765	2	394	29	44	90	94
FOXG_09277-t26_2	1801	1	412	29	44	86	90
				***PTC5* (YOR090C)**		***FgPTC5R* (FGSG_04026)**	
FOXG_11628-t26_1	2077	2	479	37	52	79	89
				***PTC7* (YHR076W)**		***FgPtc7R* (FGSG_00435)**	
FOXG_00617-t26_1	1146	3	381	28	40	86	92

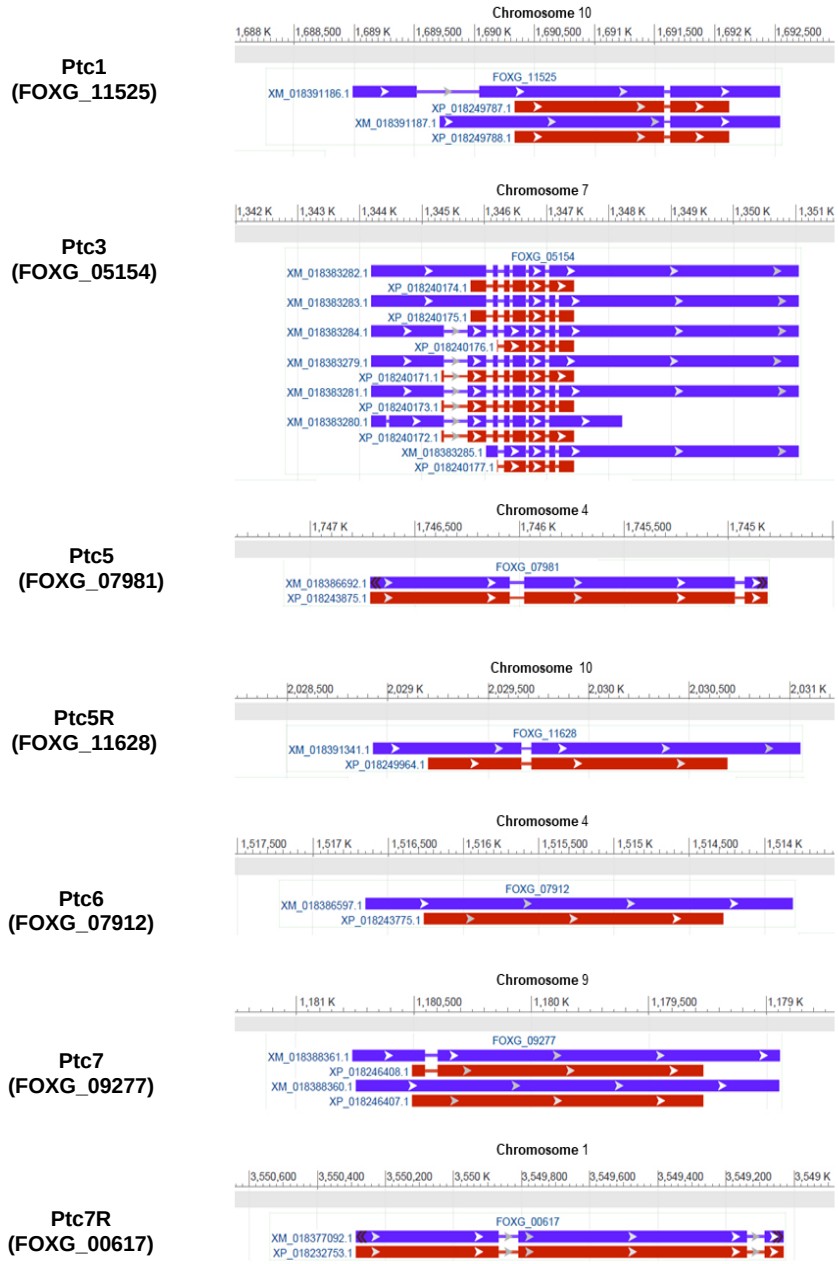

Figure 9. *Fusarium oxysporum* f. sp *lycopersici* 4287 PP2C genome localization and transcripts. Different transcripts and genome localization were identified using the GeneID search of NCBI (available at https://www.ncbi.nlm.nih.gov/gene/, National Center for Biotechnology Information, Bethesda MD, USA). Images were generated using the Printer-friendly PDF tool, and manually edited on Adobe Photoshop CS3 (Adobe Systems Incorporated, California, USA). Transcripts (highlighted in blue) and proteins (highlighted in red) are represented aligned to the gene chromosome position on the genome (scale).

Although the genomic analysis showed that all PP2C genes had a single copy on the genome, data from RNAseq analysis (available at https://www.ncbi.nlm.nih.gov/gene/ and http://fungidb.org/fungidb/) revealed the presence of putative splicing variants. Different transcripts were observed to *ptc1, ptc3* and *ptc7* genes (Table 4, Figure 9): Two *ptc1* transcripts giving the same protein, seven different *ptc3* transcripts yielding five protein isoforms and two *ptc7* transcripts that gave two different isoforms. *ptc5, ptc5R,* and *ptc7R* genes presented only one transcript, coding for single proteins.

Phylogenetic analysis was performed with a dataset containing protein sequences of the seven previously identified *F. oxysporum* PP2C phosphatases, and orthologs from *Aspergillus fumigatus, Botrytis cinerea, Candida albicans, Fusarium fujikuroi, Fusarium graminearum, Fusarium verticillioides, Magnaphorthe oryzae*, and *S. cerevisiae.*The evolutionary analysis was inferred by using the Maximum Likelihood method based on the Le Gascuel model (LG+F+I+G5) (2008) conducted in MEGA7 (Kumar et al., 2016) with 1000 replicates of bootstrap. A discrete Gamma distribution was used (5 categories - +*G*, parameter = 2.5331). The rate variation model allowed for some sites to be evolutionarily invariable ([+*I*], 21.89% sites). The analysis involved 55 amino acid sequences with 1306 amino-acid sites. There was a total of 751 positions in the final dataset. The topology with superior log likelihood value (-42736.0452) is shown (Figure 10).

F. oxysporum PP2C proteins grouped at 7 distinct clades (Ptc1, Ptc3, Ptc5, Ptc5R, Ptc6, Ptc7 and Ptc7R) (Figure 10), and have not been grouped at the clades of Ptc2 and Ptc4. This phylogeny supports the lack of these two genes on the *F. oxysporum* genome analysis. Other filamentous fungi also lack these genes, suggesting that the possible function of these proteins can be supply by Ptc3, the closest related phosphatase.

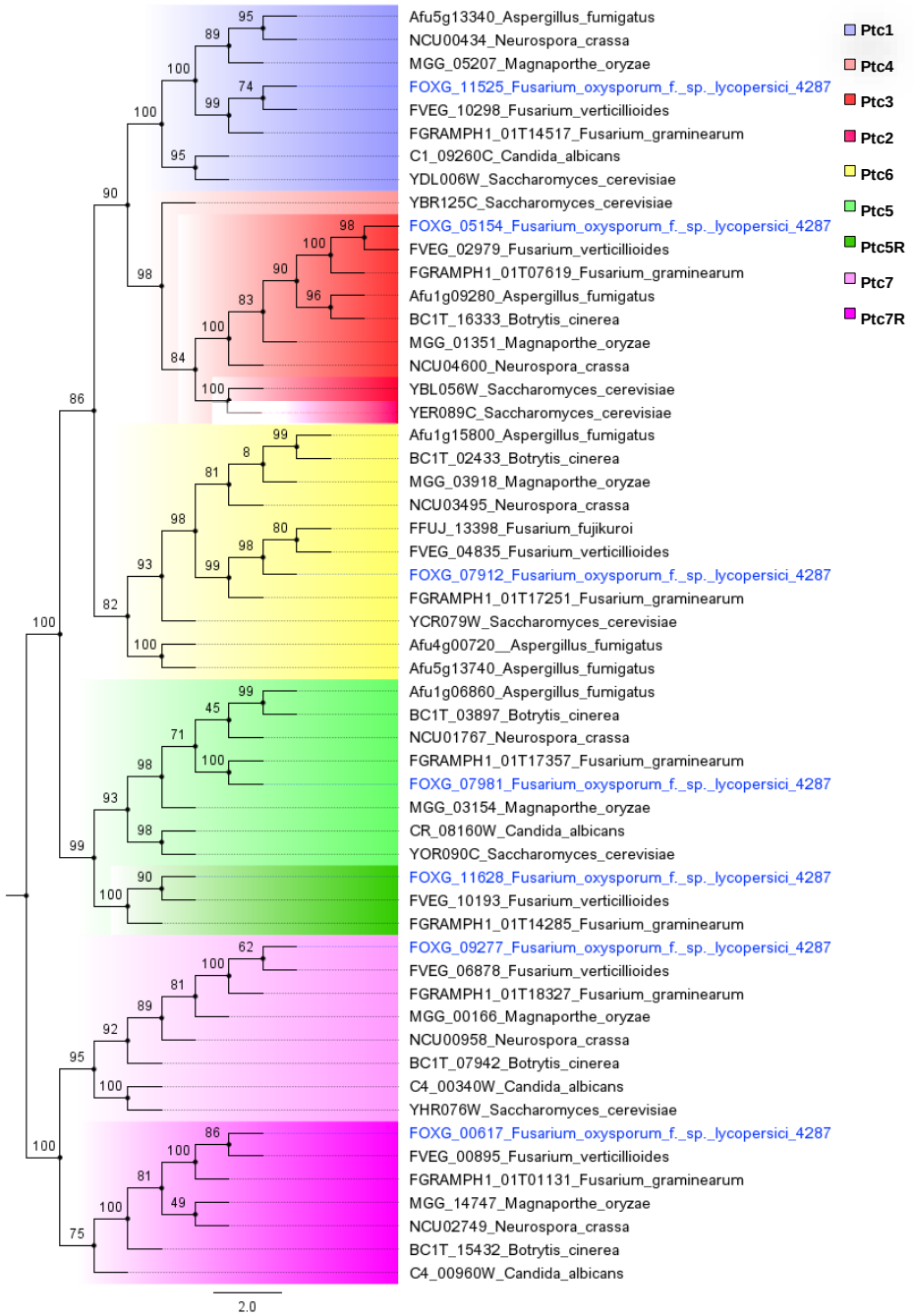

Figure 10. Molecular Phylogenetic analysis of *Fusarium oxysporum* f. sp lycopersici PP2C proteins sequences with a dataset containing fungiDB orthologs. The evolutionary history was inferred by using the Maximum Likelihood method based on the Le Gascuel model (2008) (LG+F+I+G5). The tree was drawn with FigTree v.1.4.3, rooted on midpoint, on equal scale. PP2C clades and *Fusarium oxysporum* sequences are highlighted. Evolutionary analyses were conducted in MEGA7 with 1000 replicates of bootstrap.

4.1.2 Structural analysis identifies typical core domains on *F. oxysporum* PP2C phosphatases

The model prediction performed with SWISS-MODEL (ExPASy) highlights that the predicted catalytic-core domains of *F. oxysporum* PP2Cs have also the same structure of α-helices and β-sheets typical of PP2C phosphatases. This structure plays essential functions on protein interaction, and interaction with Mn^{2+}/Mg^{2+} ions (Figure 11). Additional α-helices, known to provide substrate specificity on PP2Cs orthologues, are also present.

Structural analysis of *F. oxysporum* PP2Cs with ScanProsite (ExPASy) revealed that all the proteins contain the typical metal dependent protein phosphatase domain (PPM) present in PP2C phosphatases of other organisms (Figure 7). The analysis also detected a Serine-rich repeat between aminoacid (aa) residues 5 to 105 in *F. oxysporum* Ptc1. This region was also predicted to contain sites of N-myristoylation, N-glycosylation, Casein kinase II phosphorylation (Guillemain *et al.*), Protein kinase C phosphorylation, and cAMP- and cGMP-dependent protein kinase phosphorylation.

Differences in domain composition were found in between Ptc5, Ptc5R, Ptc6 and Ptc7. It was predicted a microbodies C-terminal targeting signal (AKL PS00342) for *F. oxysporum* Ptc5, at the position 592 – 594; this signal was not found on the other putative mitochondrial protein paralog, Ptc5R, neither in Ptc6.

However, Ptc7 codes for two protein isoforms, the intron retention resulting N-terminal amino acids (GWSHCPYNTRQSAILTVP) does not contain any domain. In both isoforms of Ptc7 it was predicted a microbodies C-terminal targeting signal SKL. The Ptc7 paralog, Ptc7R, presents a bipartite nuclear localization signal (position 23-37 aa).

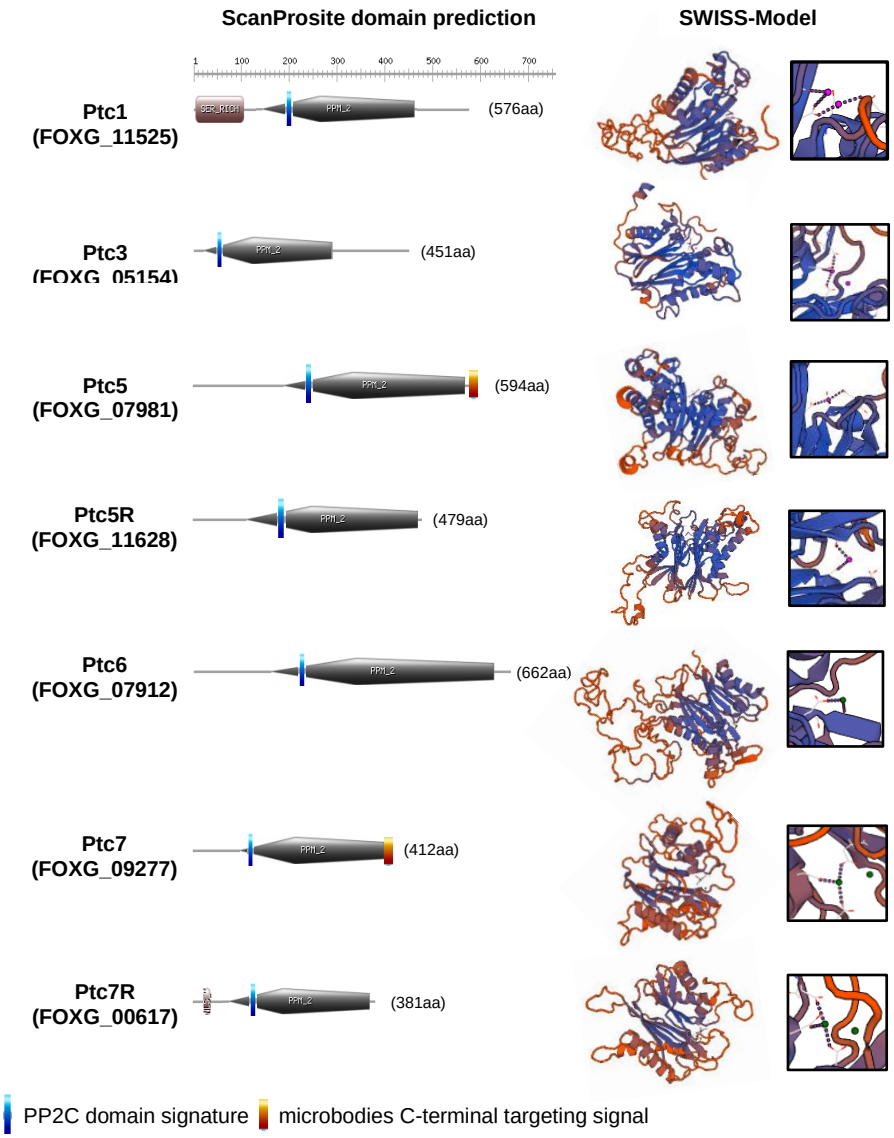

Figure 11. Graphical representation and structure models of phosphatase domains in *F. oxysporum* PP2Cs. Predictions of domains and secondary structure models with SWISS-MODEL and ScanProsite (ExPASy, Swiss Institute of Bioinformatics, Switzerland). Metal dependent phosphatase domains (PPM) (black arrows), PPM-type phosphatase domain signature (blue), Serine-rich repeats and bipartite nuclear localization signal (brown) are represented. using as prototype model the PP2Cα, the identity is represented in orange-blue, blue represents more identity. Ion ligand is represented in spheres.

F. oxysporum Ptc3 putative isoforms differ in the size of the N-terminal region (Figure 12), varying in composition of phosphorylation and N-myristoylation sites. The smallest isoform (315aa) contain just one phospho-site for the interaction with CK2 kinase; the middle size isoforms contain one additional PPM-type phosphatase domain signature (30-38aa), one Ck2 and 4 Pkc phospho-sites, and three N-myristoylation sites; the large isoform (451aa), contains three additional phospho-sites (Ck2, Pkc, and TyrK) and one additional N-myristoylation site. The medium and the large isoforms differ in one intron retention that codes for a residue that contain one N-myristoylation site, the small isoform does not contain this residue.

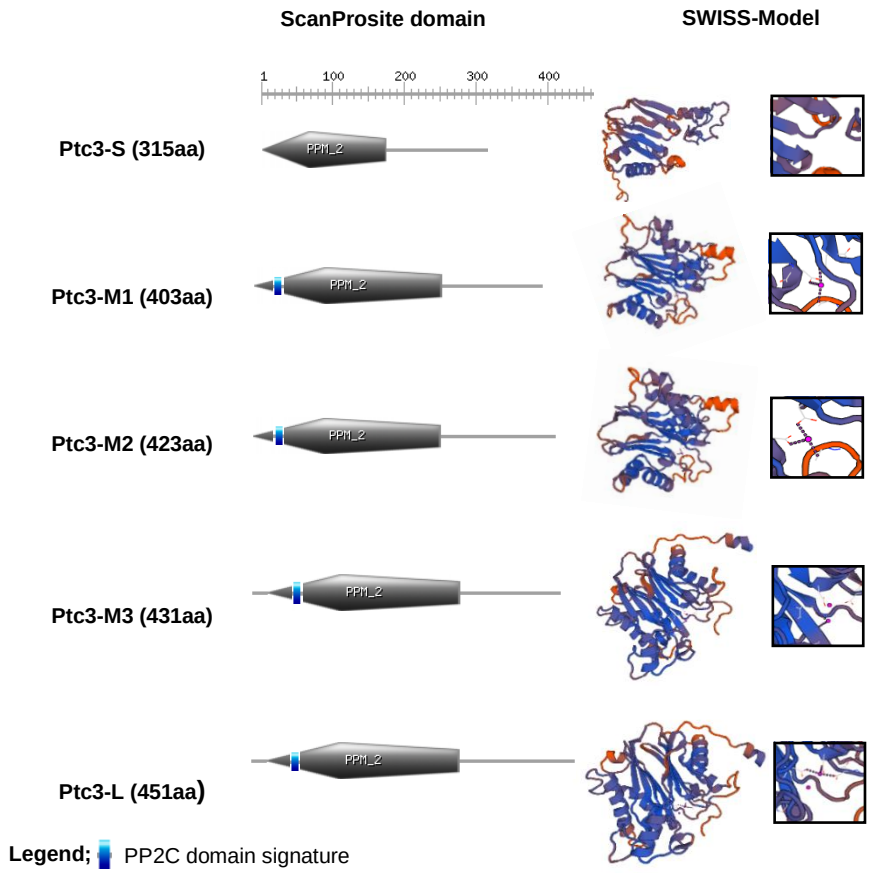

Figure 12. Structure models of *F. oxysporum* Ptc3 isoforms. Secondary structure models were performed with the algorithms SWISS-MODEL (ExPASy, Swiss Institute of Bioinformatics, Switzerland), using as prototype model the PP2Cα, the identity is represented in orange-blue, blue represents more identity. Manganese ion ligand is represented in spheres in purple

4.1.3 Gene expression analysis of *F. oxysporum* PP2C genes

4.1.3.1 Two PP2C genes show higher transcript levels on *F. oxysporum*

As a first approach to unravel the biological role of PP2Cs in *F. oxysporum*, we studied gene expression during initial stages of growth on liquid media (PDB) using RT-qPCR (Figure 13). Although expression levels were lower than actin (housekeeping reference gene), we found higher amount of mRNA for *ptc3* and *ptc7* genes.

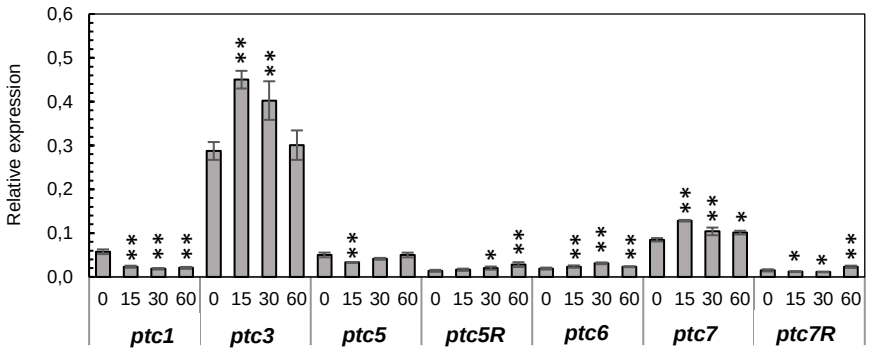

Figure 13. Relative expression of *F. oxysporum* PP2Cs during growth in liquid media. Germlings were transferred to potato dextrose broth (PDB) and mycelia were harvested at the indicated time points to perform RNA isolation. Transcript levels, indicated as relative expression, were calculated with the formula $2^{-\Delta Ct}$, using *actin* as reference gene. The results are expressed as average (± standard deviation) of three independent biological repeats. Statistics significance test (*t-test*) comparing the expression levels with untreated samples (time 0) is represented by $p<0.05$(*); $p<0.01$(**). Bars represent standard error.

In order to investigate if *F. oxysporum* PP2Cs are expressed in plant infection, RNA was obtained from infected tomato plants three, five and seven days after inoculation to perform RT-qPCR analysis (Figure 14A). Again, *ptc3* and *ptc7* transcripts were the most abundant three, five and seven days after inoculation. The expression level in plant was higher than the observed expression in liquid media, suggesting a possible role of Ptc3 and Ptc7 in plant infection.

Were then analyzed the expression of phosphatase genes in “invasive growth” conditions as previously assayed in *F. oxysporum* (Prados-Rosales

and Di Pietro, 2011). Along the time course, it was observed a downregulation of *ptc1* and *ptc7R*, a slight upregulation of *ptc3* and *ptc7*, while *ptc5, ptc5R,* and *ptc6* expression remained constant (Figure 14B).

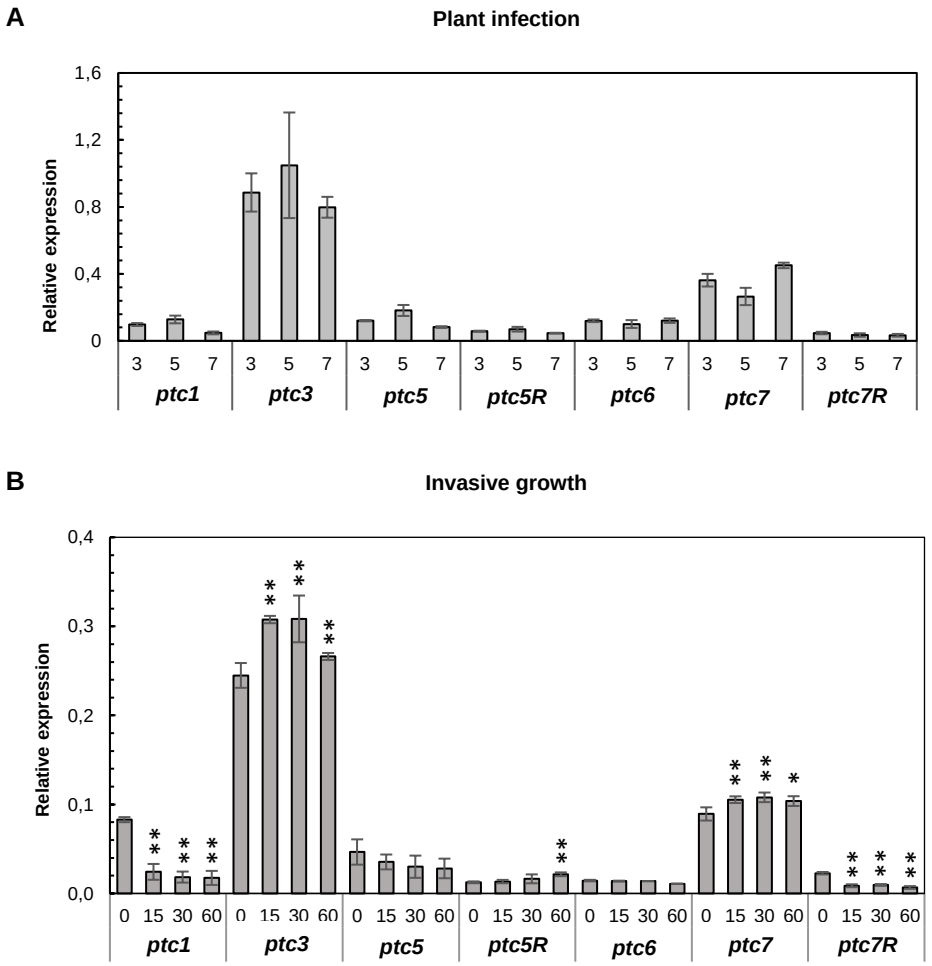

Figure 14. Relative expression of *F. oxysporum* PP2C genes during plant infection and invasive growth. Plant roots of tomato cv. Monika plant Infected with *F. oxysporum* f. sp. *lycopersici* (3, 5 and 7 days after inoculation) were used to perform RNA isolation. Three replicates were perfomed for each time point. (A-B) Transcript levels, indicated as relative expression, were calculated with the formula $2^{-\Delta Ct}$, using *actin* as reference gene. The results are expressed as average (± standard deviation) of three independent biological repeats. (B) Germlings were transferred to Puhalla Minimal Media plates and mycelia were harvested at the indicated time points to perform RNA isolation. Statistics significance test (*t-test*) comparing the expression levels with untreated samples (time 0) is represented by $p<0.05$(*); $p<0.01$(**). Bars represent standard error.

4.1.3.2 Cell wall stresses induces the expression of PP2C phosphatases

The putative role of *F. oxysporum* PP2C genes on cell wall integrity pathway was first investigated analyzing the gene expression induced by the stress compounds Sodium-Dodecyl-Sulfate (SDS) and Calcofluor-White (Sharmin *et al.*). These compounds have been widely used for the characterization of *F. oxysporum* mutants in mitogen activated protein kinase (MAPK) signaling pathway (Perez-Nadales and Di Pietro, 2011; Turra *et al.*, 2014; Miguel-Rojas and Hera, 2014; Segorbe et al., 2016). To investigate the gene expression, mycelial samples were obtained from liquid media supplemented with the stressor compounds, and RNA was isolated to perform RT-qPCR analysis.

Three out of the seven *F. oxysporum* PP2C genes were found to be upregulated during the analyzed time course (Figure 15): *ptc3, ptc6,* and *ptc7.* Small increments were observed in *ptc1* and *ptc5R* transcript levels, and slight downregulation of *ptc5* and *ptc7R* was also observed. The transcript level increase of *ptc7* was higher when compared to the other PP2C genes along all the time course, suggesting that Ptc7 might be an important regulator of cell wall remodeling during stresses.

This differential expression dynamics suggests that membrane and cell wall stress lead to an orchestrate-like expression of *F. oxysporum* PP2C genes. Fast and transient transcript level increments were observed for *ptc3* and *ptc7*, while *ptc6* increase was retained along the time course. Altogether, these results suggest that more than one *F. oxysporum* PP2C gene might have roles on cell wall integrity pathway.

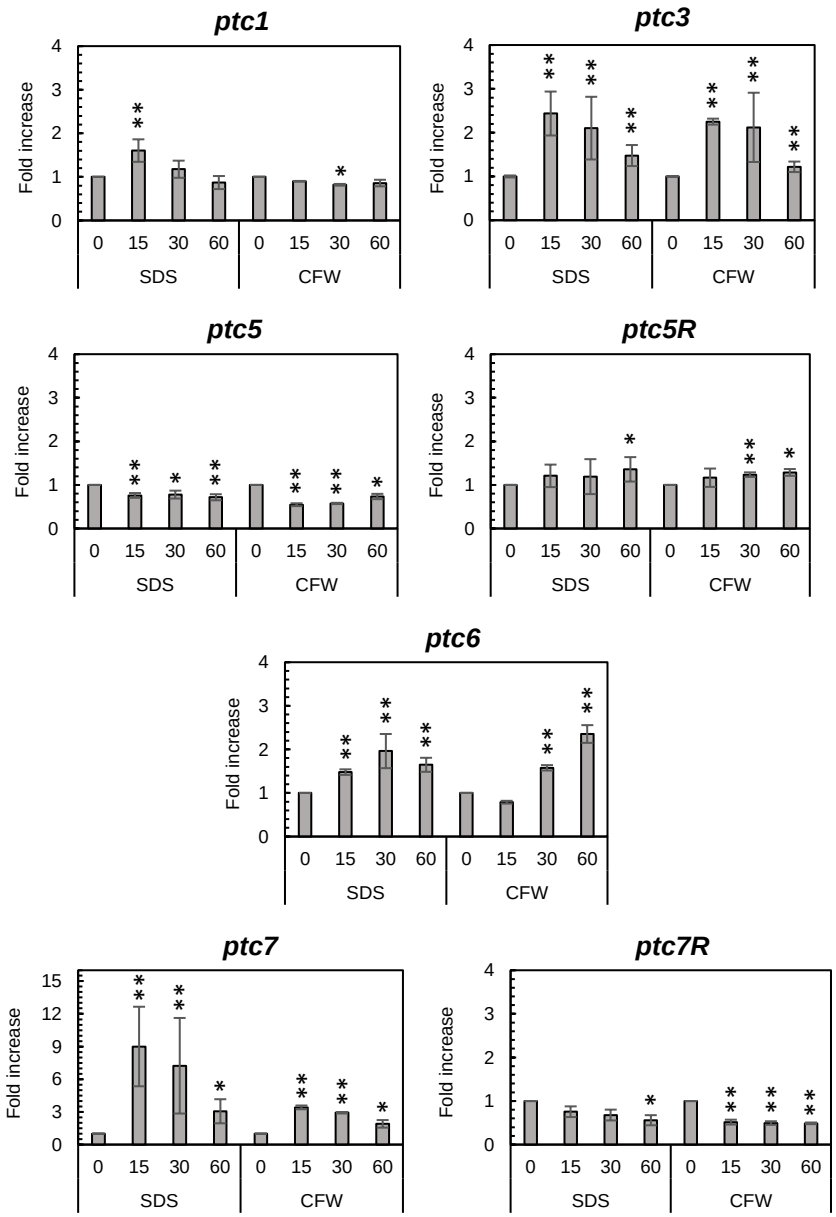

Figure 15. Expression of *F. oxysporum* PP2C genes is induced under cell wall and membrane stress responses. Germlings were transferred to potato dextrose broth (PDB) supplemented with the indicated stress compounds SDS (0.0125%) and Calcoflour White (50 µg/ml), mycelia were harvested at the indicated time points to perform RNA isolation. Transcript levels are indicated as time-fold increase were calculated with the formula $2^{-\Delta\Delta Ct}$, using *actin* as reference gene. The results are expressed as average (± standard deviation) of three independent biological repeats. Statistics significance test (*t-test*) comparing the expression levels with untreated samples (time 0) is represented by $p<0.05$(*); $p<0.01$(**). Bars represent standard error.

4.1.3.3 Osmotic stress compounds treatment upregulates some PP2C phosphatases

To investigate the gene expression dynamics during oxidative and osmotic stresses, we performed liquid assay in which Caffeine (induction of oxidative stress), Sorbitol or Potassium Chloride (induction of osmotic stress), was added to PDB media. Mycelial samples were obtained from liquid media supplemented with the stressor compounds and RNA was isolated to perform RT-qPCR analysis. (Figure 16).

Exposure to oxidative stress led to a fast and transient induction in *ptc7* transcription levels, while *ptc5R* and *ptc6* shown increased levels at the end of the time course.

The exposure to osmotic stress compounds led to high induction of the transcription levels of *ptc1, ptc7 and ptc7R*, while slight increments were observed for *ptc3,* and *ptc6* and *ptc5* expression was downregulated. As it was observed in the response to cell wall stress treatment, different dynamics of gene expression were also observed induced by osmotic and oxidative stress suggesting an orchestrate-like gene expression pattern during the adaptation of the fungus to the stressing media.

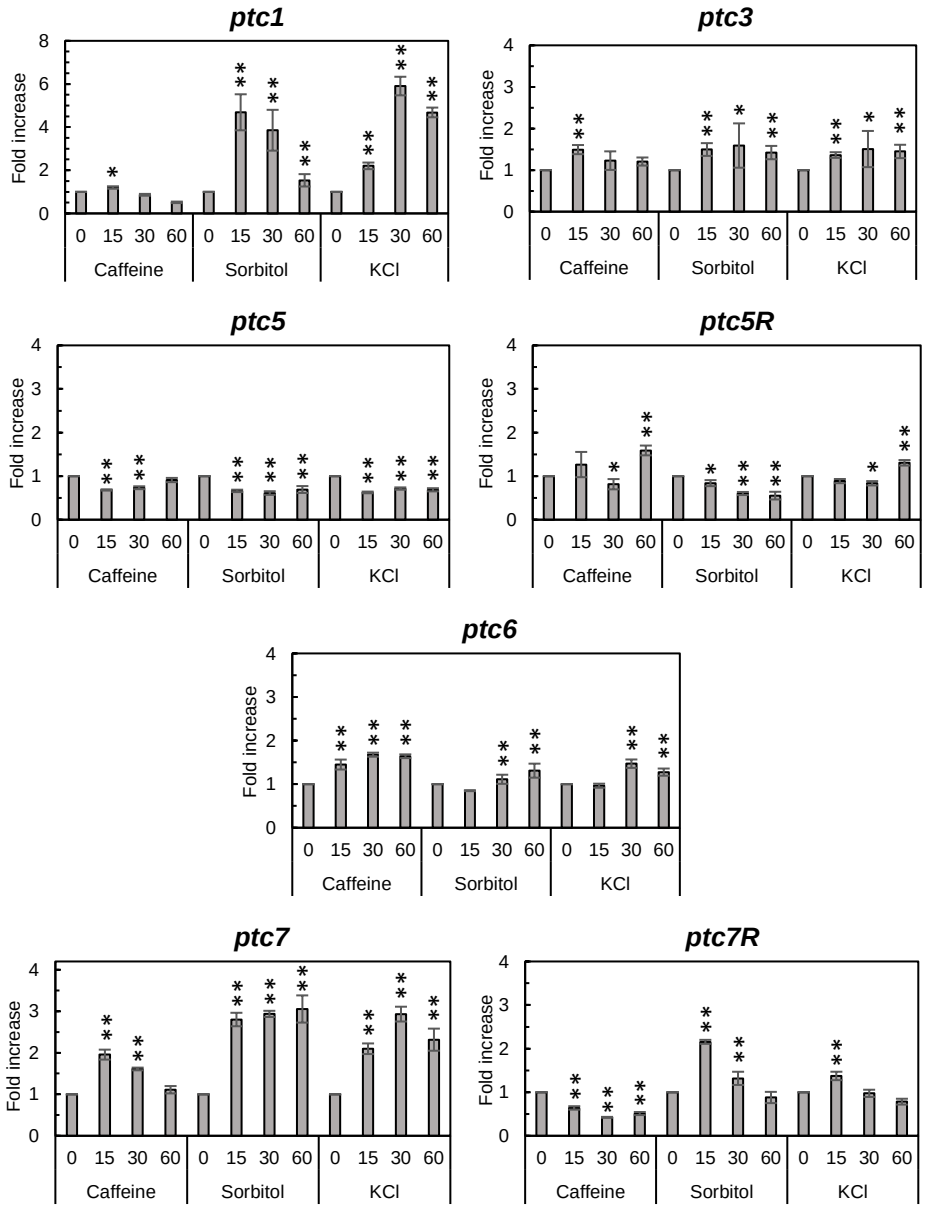

Figure 16. Expression of *F. oxysporum* PP2C genes is induced on oxidative and osmotic stress responses. Germlings were transferred to potato dextrose broth (PDB) supplemented with the indicated stress compounds Caffeine (5 mM); Sorbitol (1.25 M); KCl (1.2 M) SDS (0.0125%) and Calcoflour White (50 µg/ml), mycelia were harvested at the indicated time points to perform RNA isolation. Transcript levels are indicated as time-fold increase were calculated with the formula $2^{-\Delta\Delta Ct}$, using *actin* as reference gene. The results are expressed as average (± standard deviation) of three independent biological repeats. Statistics significance test (*t-test*) comparing the expression levels with untreated samples (time 0) is represented by $p<0.05$(*); $p<0.01$(**). Bars represent standard error.

4.1.4 Targeted disruption of *F. oxysporum* PP2C genes

To investigate the role of PP2Cs in *F. oxysporum* development and pathogenicity, fusion PCR deletion constructs were generated to replace the complete ORF with the hygromycin resistance cassette (*Hyg*^{R}) (single mutants) or phleomycin resistance cassette (*Phle*^{R}) (complemented strains) using the split-marker strategy. The constructs were used to transform protoplasts of the *F. oxysporum* wild type strain or mutant strains (complemented strains).

Transformants carrying a homologous insertion at the locus were identified by PCR analyses using pairs of primers that hybridize outside of the fragments used for transformation, and inside of the resistance cassette. The integration of single copy into the correct genome locus was verified by southern blot analysis; digoxigenin labeled probes were designed to identify restriction endonuclease fragments of different molecular weight consistent with homologous insertion of the deletion construct in transformants strains. The split marker strategy was successful for the obtention of the mutant strains Δ*ptc1* (Figure 17), Δ*ptc5* (Figure 19), Δ*ptc5R* (Figure 20) *Δptc6* (Nuñez-Rodriguez, personal communication), Δ*ptc7* (Figure 21) and Δ*ptc7R* (Figure 22).

The attempts to disrupt the *ptc3* gene failed to generate a Δ*ptc3* strain (Figure 18). Although the detection of the homologous insertion by PCR analysis resulted positive, additional bands were detected in the southern blot analysis with the probe upstream to the gene promoter. To check if the additional bands detected were due to unspecific hybridization, we performed a southern blot with a probe that hybridize with the *ptc3* ORF. Different hybridization bands were detected in all the transformants analyzed, indicating that although the integration occurred in a homologous way, the ORF was not lost. Considering that the number of analyzed transformants was high (more than one hundred) we suggested that Ptc3 could be an essential phosphatase in *F. oxysporum*.

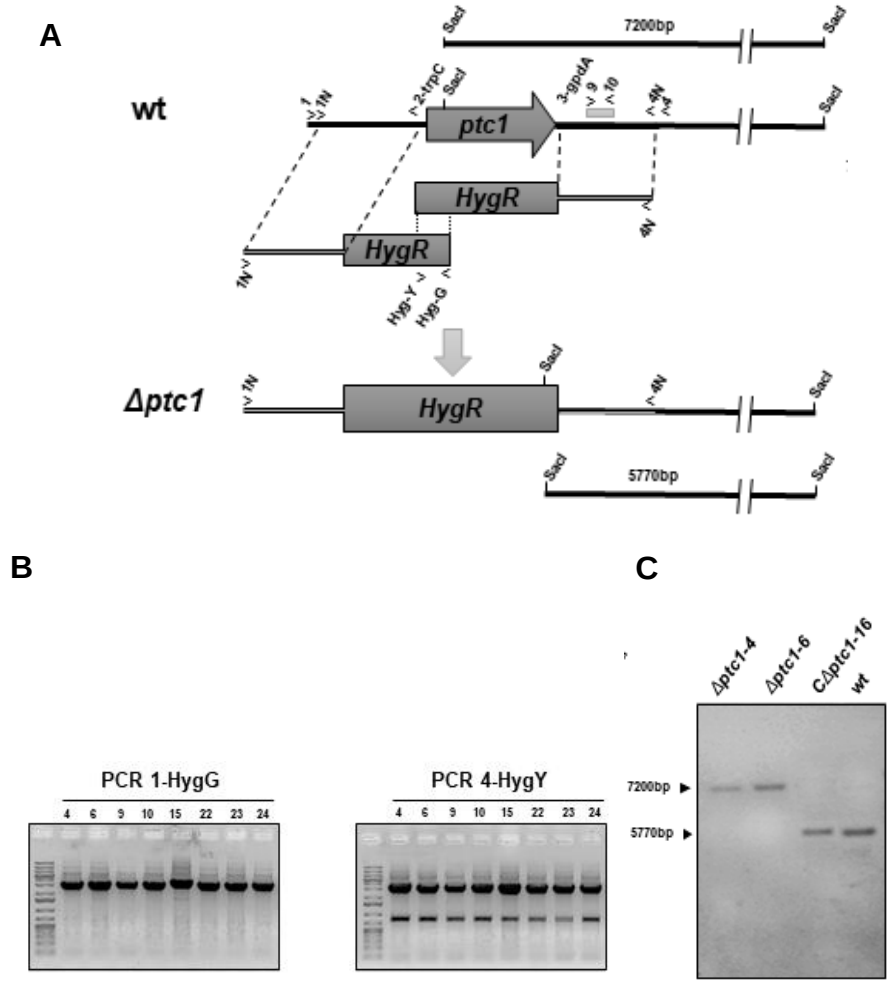

Figure 17. Disruption of *ptc1* locus in *F. oxysporum.* (A**)** Physical maps of the *Ptc1* locus and the split-marker gene replacement Δ*ptc1* allele. Relative position of the primers used for generation of the gene disruption constructs and PCR analyses of the transformants and the Southern blot probe (gray bar) are indicated. (B) PCR analyses of homologous integration of the gene disruption construct into the genome of the transformants using primers: Ptc1-1/Hyg-G (promoter region) and Hyg-Y/Ptc1-4 (terminator region) (C) Southern blot hybridization analysis of genomic DNA treated with *SacI* endonuclease of the wild type strain 4287 and Δ*ptc1* transformants and complement strain.

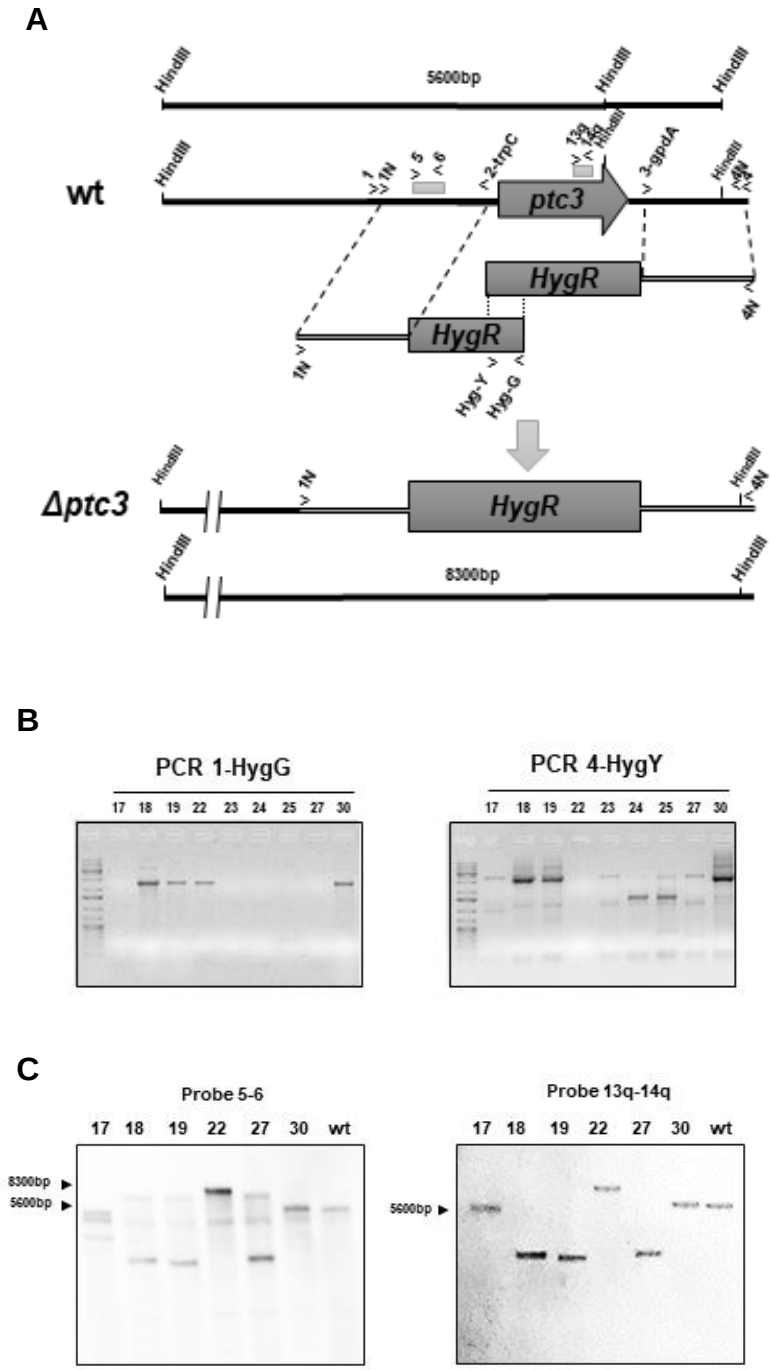

Figure 18. Disruption of *ptc3* locus on *F. oxysporum.* (A**)** Physical maps of the *Ptc3* locus and the split-marker gene replacement Δ*ptc3* allele. Relative position of the primers used for generation of the gene disruption construct and PCR analyses of the transformants and the Southern blot probes (gray bars) are indicated. (B) PCR analyses of homologous integration of the gene disruption construct into the genome of the transformants using primers: Ptc3-1/Hyg-G (promoter region) and Hyg-Y/Ptc3-4 (terminator region) (C) Southern blot hybridization analysis of genomic DNA treated with *HindIII* endonuclease of the wild type strain 4287 and transformants.

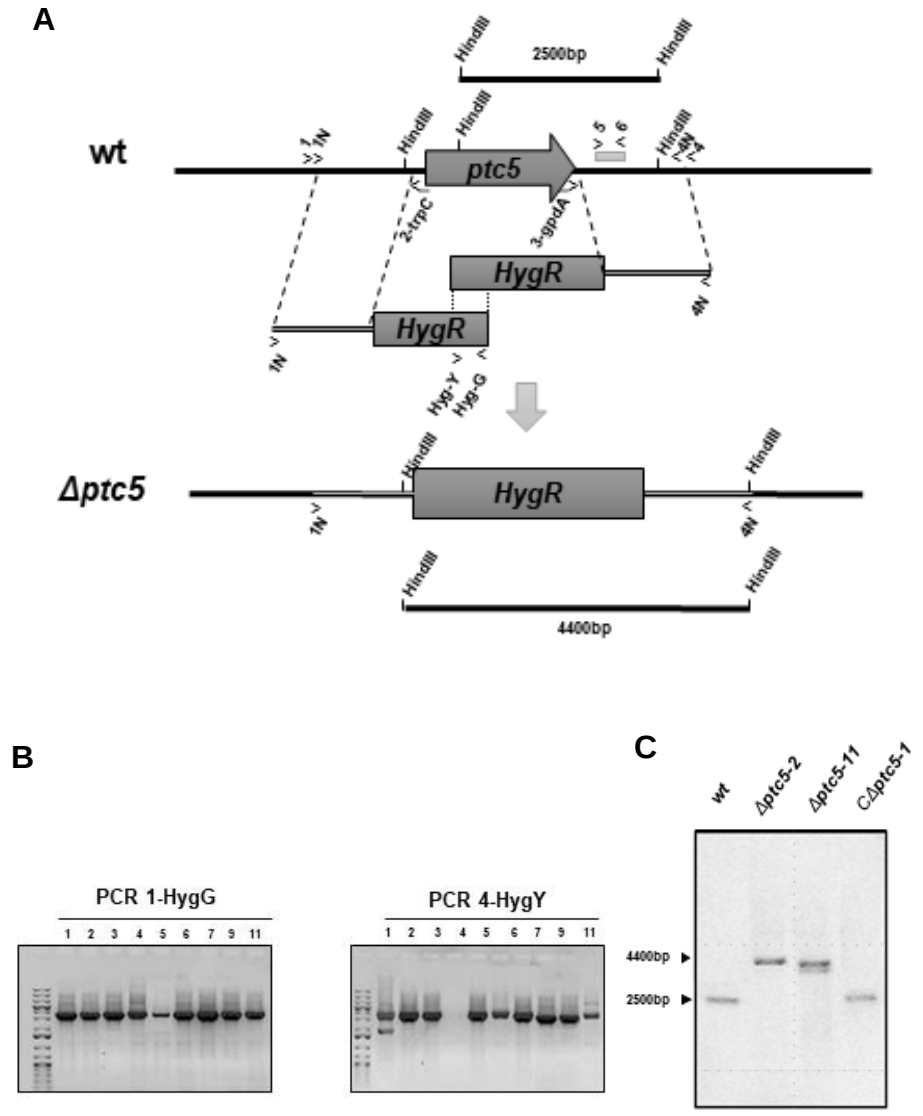

Figure 19. Disruption of *ptc5* locus in *F. oxysporum*. (A**)** Physical maps of the *Ptc5* locus and the split-marker gene replacement Δ*ptc5* allele. Relative position of the primers used for generation of the gene disruption constructs and PCR analyses of the transformants and the Southern blot probe (gray bar) are indicated. (B) PCR analyses of homologous integration of the gene disruption construct into the genome of the transformants using primers: Ptc5-1/Hyg-G (promoter region) and Hyg-Y/Ptc5-4 (terminator region) (C) Southern blot hybridization analysis of genomic DNA treated with *HindIII* endonuclease of the wild type strain 4287 and Δ*ptc5* transformants and complement strain.

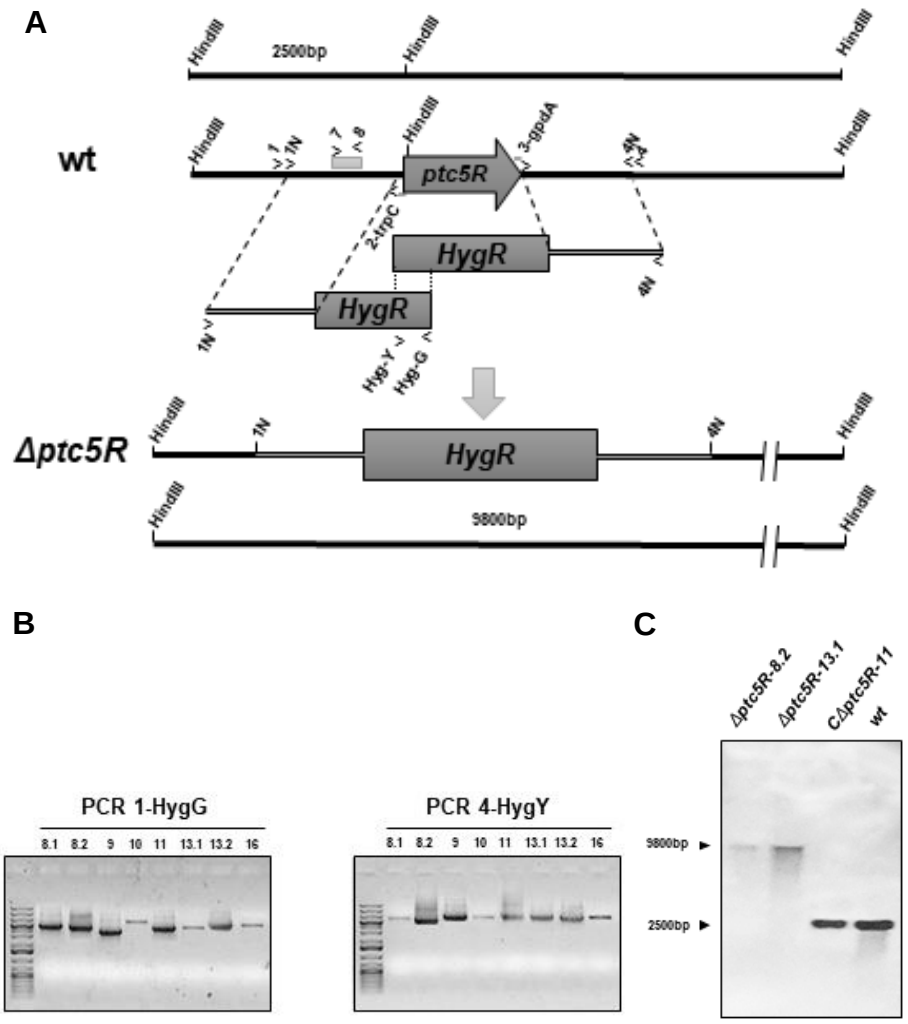

Figure 20. Disruption of *ptc5R* locus in *F. oxysporum.* (A) PCR analyses of homologous integration of the gene disruption construct into the genome of the transformants using primers: Ptc5R-1/Hyg-G (promoter region) and Hyg-Y/Ptc5R-4 (terminator region) (B) Physical maps of the *Ptc5R* locus and the split-marker gene replacement Δ*ptc5R* allele. Relative position of the primers used for generation of the gene disruption constructs and PCR analyses of the transformants and the Southern blot probe (gray bar) are indicated. (C) Southern blot hybridization analysis of genomic DNA treated with *HindIII* endonuclease of the wild type strain 4287 and Δ*ptc5R* transformants and complement strain.

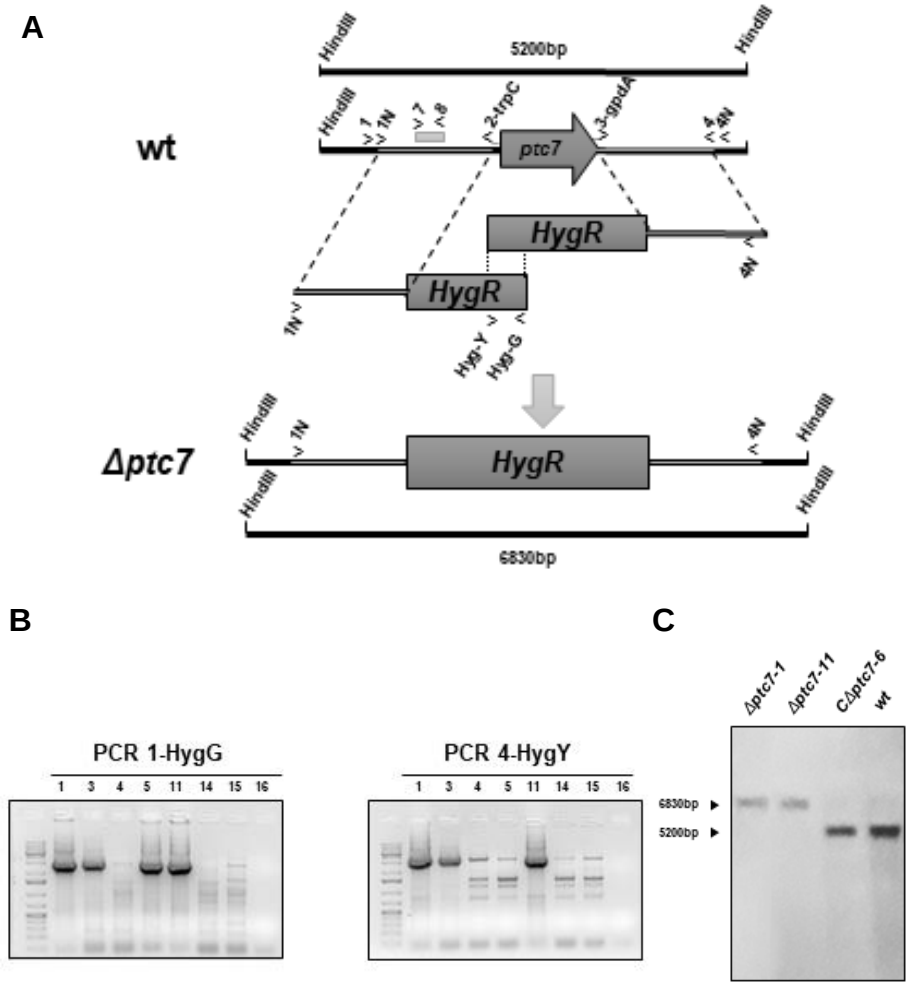

Figure 21. Disruption of *ptc7* locus in *F. oxysporum.* (A) PCR analyses of homologous integration of the gene disruption construct into the genome of the transformants using primers: Ptc7-1/Hyg-G (promoter region) and Hyg-Y/Ptc7-4 (terminator region) (B) Physical maps of the *Ptc7* locus and the split-marker gene replacement Δ*ptc7* allele. Relative position of the primers used for generation of the gene disruption constructs and PCR analyses of the transformants and the Southern blot probe (gray bar) are indicated. (C) Southern blot hybridization analysis of genomic DNA treated with *HindIII* endonuclease of the wild type strain 4287 and Δ*ptc7* transformants and complement strain.

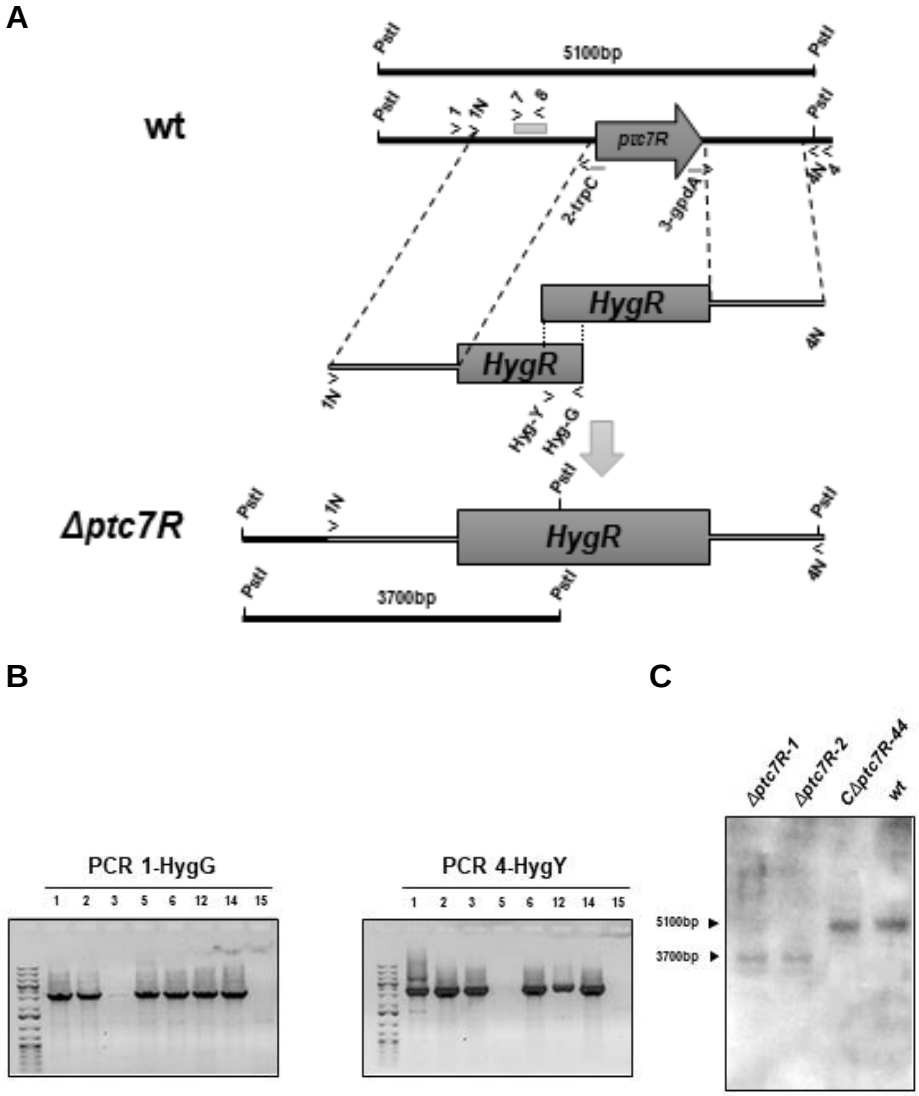

Figure 22. Disruption of *ptc7R* locus in *F. oxysporum.* (A) PCR analyses of homologous integration of the gene disruption construct into the genome of the transformants using primers: Ptc7R-1/Hyg-G (promoter region) and Hyg-Y/Ptc7R-4 (terminator region) (B) Physical maps of the *Ptc7R* locus and the split-marker gene replacement Δ*ptc7R* allele. Relative position of the primers used for generation of the gene disruption constructs and PCR analyses of the transformants and the Southern blot probe (gray bar) are indicated. (C) Southern blot hybridization analysis of genomic DNA treated with *PstI* endonuclease of the wild type strain 4287 and Δ*ptc5R* transformants and complement strain.

4.1.5 Phenotypical analysis of PP2C mutant strains

4.1.5.1 Disruption of PP2c genes affects growth on rich media

To test the role of PP2Cs in vegetative hyphal growth on solid media, colony area of the different strains was measured in nutrient-rich potato dextrose agar medium (PDA).

We observed the formation of growth sectors showing increased aerial hyphae formation in *Δptc1* and *Δptc5* mutant strain colonies (Figure 23A), leading to a reduction in the radial growth. The growth area was reduced 20% in *Δptc1* compared to the wild type strain six days after inoculation.

Considering the patterns observed, the colony growth area was reduced in the *Δptc1, Δptc5, Δptc5R, Δptc7* mutant strains and increased in *Δptc7R* mutant strain in comparison to the wild type strain (Figure 23B), suggesting that PP2Cs are somehow involved in hyphal growth.

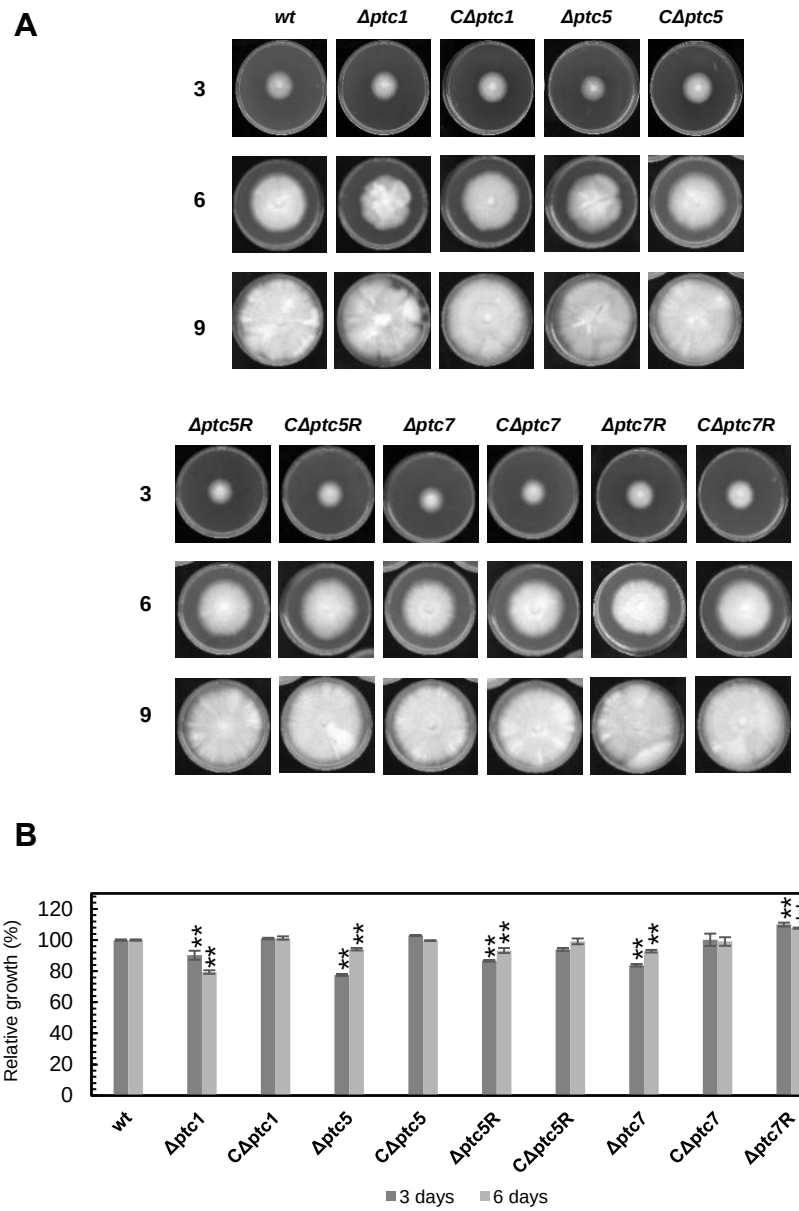

Figure 23. *F. oxysporum* PP2Cs disruption affects growth. (A) Growth on Potato dextrose agar (PDA) of *F. oxysporum* wild type and PP2c mutant strains. Plates were individually inoculated with a dot containing $5x10^4$ conidia and the growth was monitored on 3, 6 and 9 days after inoculation. (B) The mycelial growth of the strains was measured after 3 and 6 days after inoculation. Mycelial growth was measured with ImageJ software to calculate the relative growth using the formula: Relative growth (%) = [(Area of growth of mutant strain / Area of growth of wild-type) *100]. The average of three biological plate replicates were used to perform statistics significance test (*t-test*) comparing the mutant and complemented strains with the wild-type strain, represented by $p<0.05$(*); $p<0.01$(**).

4.1.5.2 Phosphatase mutant strains show differences in MAPK phosphorylation levels

PP2C phosphatases have previously been reported as strong negative regulators of MAPK pathways (Yang et al., 2002; Ariño, et al., 2011).To investigate if PP2C phosphatases are key regulators of MAPK cascades in *F. oxysporum*, we performed a western blot analysis to check the phosphorylation status of Mpk1, Fmk1 and Hog1. Total protein obtained from mycelia of the wild-type strain and knockout mutant strains Δ*ptc1*, Δ*ptc5*, Δ*ptc5R*, Δ*ptc7*, and Δ*ptc7R*, grown for 15h on PDB was analyzed. MAPK phosphorylation level status varied in-between the knockout mutant strains analyzed, suggesting putative roles of *F. oxysporum* PP2Cs on the three MAPK pathways, acting as negative or positive regulators of these cascades (Figure 24).

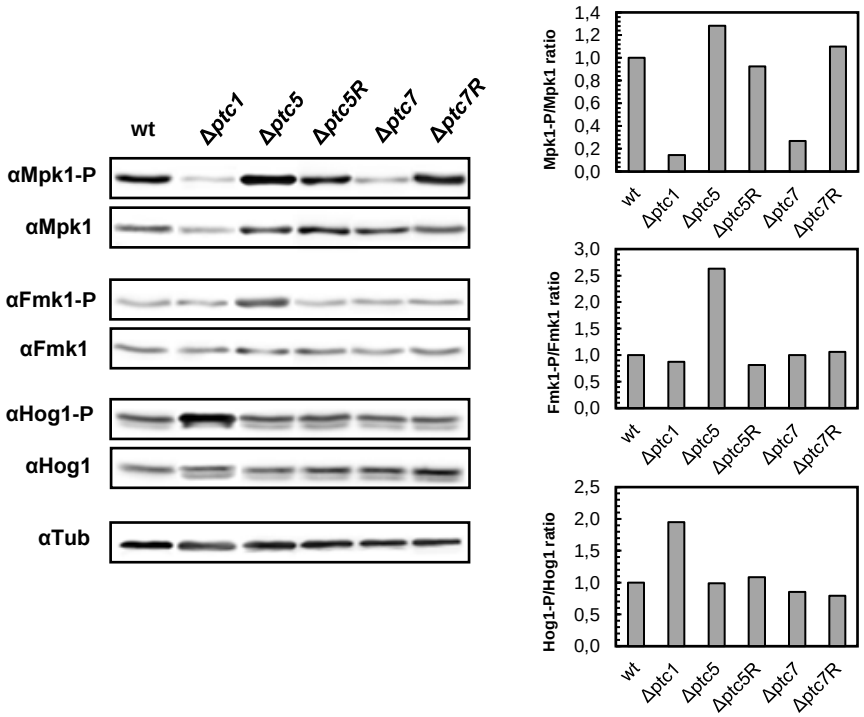

Figure 24. *Fusarium oxysporum* PP2Cs disruption alters MAPK Phosphorylation levels. Mycelia of *F. oxysporum* wild type strain and knockout mutant strains grown for 15h ($2.5x10^8$ fresh microconidia on 50ml of PDB, incubated 28ºC (170 rpm) were filtered to remove completely the media. Mycelia were recovered and frozen in liquid nitrogen to perform total protein extraction and western blot analysis. Band intensity were quantified with Image J software v. 1.08 (National Health Institute, United States of America). The phosphorylation level was calculated by the ratio (phosphorylated / total protein). Wild-type sample was used to standardize the samples. The immunoblot assay was repeated twice from two biological replicates having similar results, a representative micrography is shown.

The levels of MAPK phosphorylation on the mutant strain Δ*ptc1* changed compared to the normal levels of the wild-type strain. Mpk1 phosphorylation level ratio was highly reduced, and Hog1 phosphorylation was highly increased (Figure 24). These results suggest that Ptc1 is a positive regulator of Mpk1 and negative regulator of Hog1 pathways. The lack of *ptc1* leads to an unbalanced level of phosphorylation of Hog1 that may also affect the other MAPK phosphorylation levels in *F. oxysporum.*

The lack of *ptc5* also augmented the levels of phosphorylation of Mpk1 and Fmk1. These results suggest that Ptc5 is a negative regulator of Fmk1 cascade in *F. oxysporum* and can also have a role on limiting the hyperphosphorylation of Mpk1. No changes in MAPK phosphorylation was observed in Δ*ptc5R* (Figure 24) as observed for Δ*ptc6* mutant strain (Nuñez Rodriguez, personal communication). The lack of *ptc7* reduced substantially the basal levels of phosphorylation of Mpk1, addressing the putative role on the positive regulation of this pathway. A reverse effect was observed to *Δptc7R* strain where it was observed a slight increase of the Mpk1 phosphorylation.

4.1.5.3 Involvement of PP2Cs in the Cell Wall Integrity Pathway

As already mentioned, the implication of PP2Cs in the CWI response pathway has been reported in several fungi (Ariño et al., 2011). To investigate if the PP2C genes disruption lead to different phenotypes under membrane and cell wall stress conditions, tolerance of mutant and wild type strains to SDS and CR was determined (Figure 25).

All mutant strains were more sensitive than wild type to SDS. The Δ*ptc1* and Δ*ptc5R* strains were also sensitive to CR, while Δ*ptc5* was more resistant to CR. These results are in line with previous studies that reported that both Slt2/Mpk1 activation or inactivation leads to phenotypes of augmented sensitivity to cell wall integrity stressors (Mattison et al., 1999; Young et al., 2002, Du et al., 2006, Gonzalez et al., 2006).

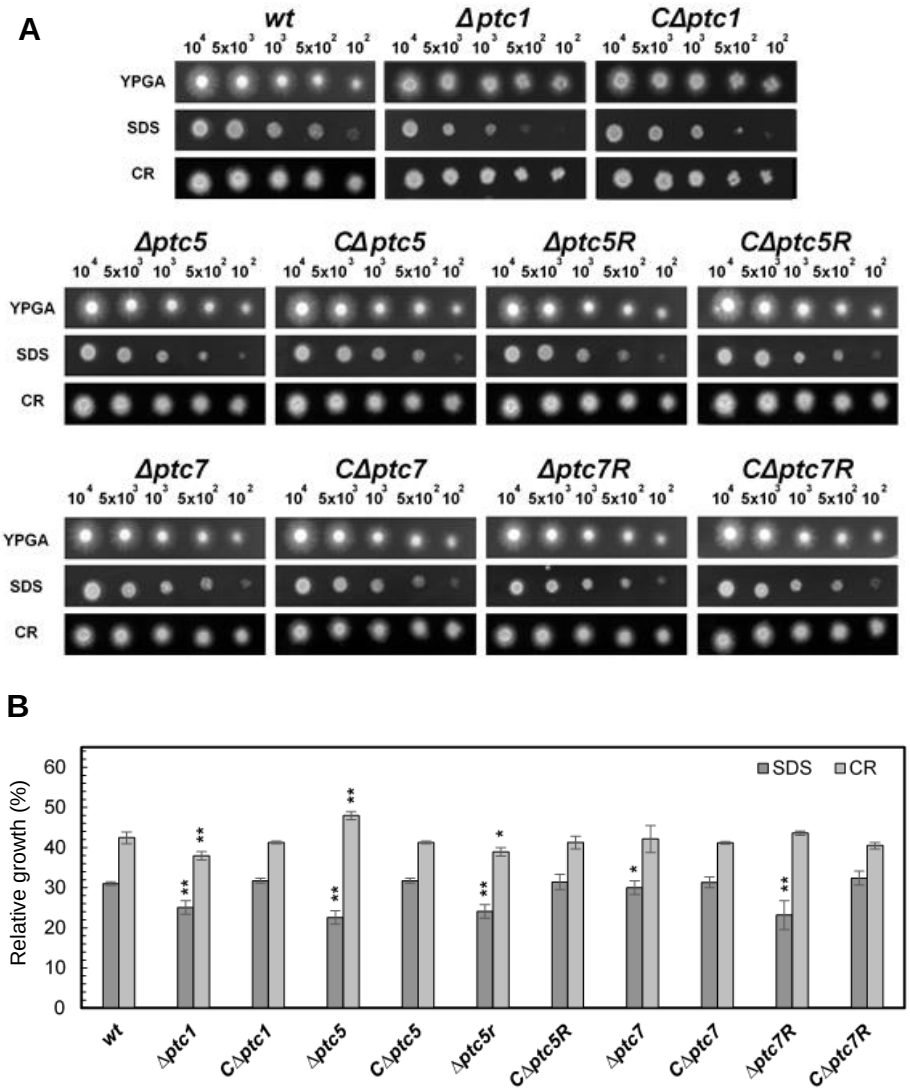

Figure 25. Multiple PP2C genes are involved in cell wall integrity (A) Phenotypical analysis on rich media the strains were performed inoculating droplets containing 10^4; $5x10^3$; 10^3; $5x10^2$; and 10^2 fresh microconidia of wild type (Jin *et al.*), PP2c mutant strains and complemented strains on YPGA supplied with stress agents. Stress agents. SDS (0.0125%) and CR (100µg/ml). Growth were monitored at 72h (B) Relative growth (%) of the different strains in the presence of the indicated stressors was calculated as the colony area on stressor-containing medium versus colony area on YPDA. Colony area of 10^3 spot was measured using the ImageJ software. Three biological replicates were used to perform statistical significance test (*t-test*) comparing relative growth of the mutant strains and complement strains with the wild-type strain, represented by $p < 0.05$(*); $p < 0.01$(**).

4.1.5.4 Disruption of *ptc5* and *ptc7R* enhances the invasive growth of *F. oxysporum*

Previous studies reported that pH is a key factor to regulation of fungal penetration into the host; the fungus needs to alkalize the surrounding environment prior to penetration (Lopez Berges *et al*., 2010; Masachis *et al*., 2017). It has been previously shown the role of the Fmk1 signaling pathway on the invasive growth of the fungus in a pH dependent manner (Perez-Nadalez and Di Pietro, 2011; Perez-Nadalez and Di Pietro, 2014).

The ability of mutant strains to penetrate on solid surfaces was analyzed by the cellophane assay (Prados Rosales and Di Pietro, 2008). This assay mimics the penetration in plant root surface by using cellophane sheets placed over the solid media. The assay evaluates the capacity of the fungus to produce enzymes that degrades cellulose polymers and the ability to hyphal penetration on the solid media. To investigate the pH dependence, the cellophane assay was performed in MES buffered plates at pH5 and 7. (Figure 26).

PP2C mutant strains *Δptc5* and *Δptc7R* were able to penetrate the cellophane sheets after 3 days even at low pH conditions (Figure 26). Since *Δptc5* strain showed the higher Fmk1 phosphorylation basal levels, it was expected that only this strain would be able to invasive growth on acid pH condition (Figure 11). Surprisingly, *Δptc7R* strain was also able to penetrate on this condition. This result suggests that not only differences in the basal phosphorylation levels influences the penetration on solid surface, but also the dynamics of Fmk1 phosphorylation and a putative crosstalk with other MAPK cascades.

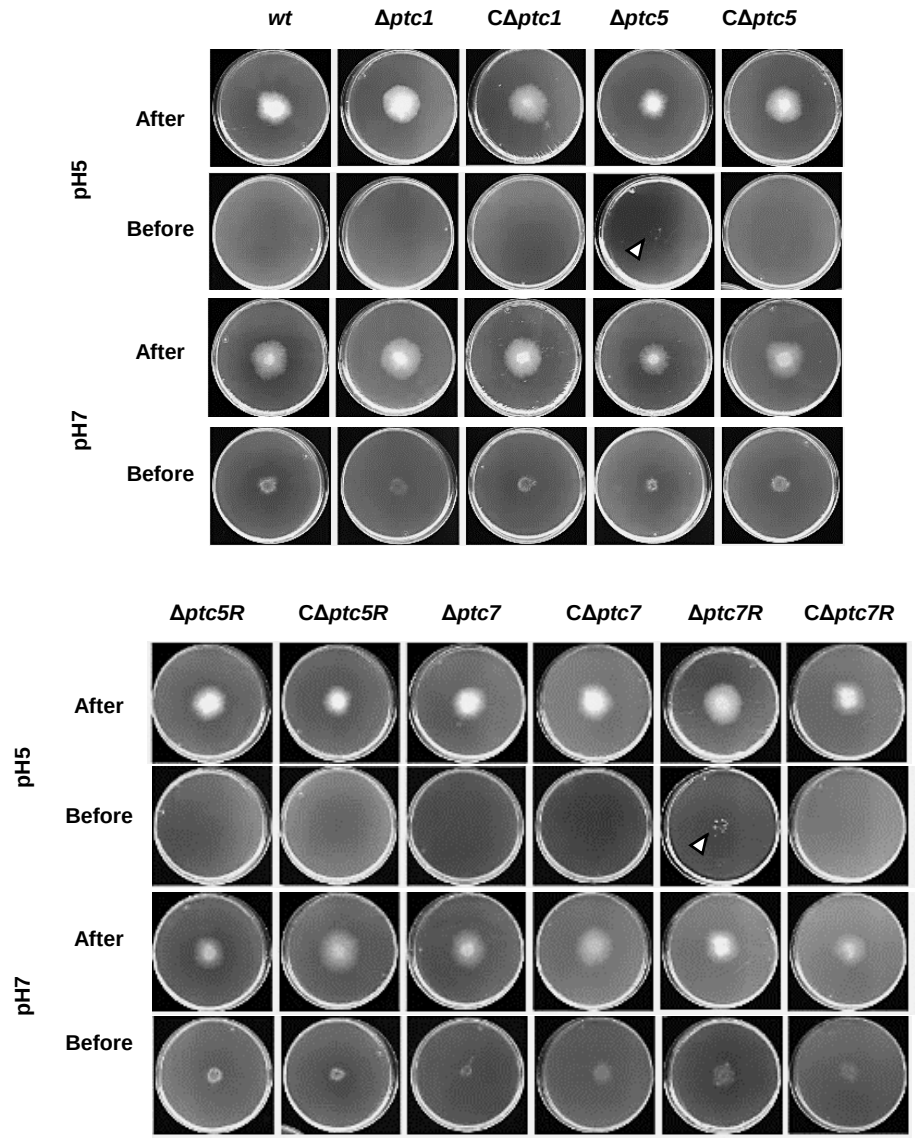

Figure 26. PP2C disruption affects invasive growth of *F. oxysporum.* wild type strain, PP2c mutant and complemented strains were subjected to cellophane penetration assay (Lopez Berges et al., 2010; Perez-Nadalez and Di Pietro, 2014) with modifications. The MM plates were buffered with 100mM MES, and the pH adjusted with 10N NaOH to obtain neutral pH (7).

4.1.5.5 Differential dynamics of MAPK phosphorylation suggests *F. oxysporum* PP2C roles on cell wall integrity and invasive growth pathways

To investigate if the penetration of the fungus into the solid surface was accompanied of differential dynamics of MAPKs phosphorylation, a time course analysis was performed as previously described (Perez Nadales and Di Pietro 2011; Miguel Rojas and Hera, 2015). The immunoblot assay showed shifts on Fmk1 and Mpk1 phosphorylation in PP2C mutant strains (Figure 27). An increase of Mpk1 and Fmk1 phosphorylation was observed on wild type strain after transfer to solid MM (Figure 27).

Interestingly, Δ*ptc5* strain presented an increase of Mpk1 phosphorylation level that was accompanied by a gradual decrease of Fmk1 phosphorylation during the time course analyzed, suggesting both, a negative and a positive role of Ptc5 on the Mpk1 and Fmk1 pathways respectively.

On the other hand, Δ*ptc5R* mutant showed an increment of the Mpk1 phosphorylation reaching the wild-type levels. In contrast, Fmk1 phosphorylation level was very low during the time course analyzed. These results support a Ptc5R negative and positive regulation of the Mpk1 and Fmk1 pathways respectively.

Opposite basal level of Mpk1 phosphorylation was observed in Δ*ptc7* and Δ*ptc7R* strains (Figure 27) but while Mpk1 phosphorylation level was slightly increased in Δ*ptc7* along the time course, Mpk1 phosphorylated was reduced in Δ*ptc7R* during the assay. The low basal phosphorylation levels of Fmk1 remained constant along the time course in Δ*ptc7*. Surprisingly, at the 15 min time point it was observed an increment at the phosphorylation level of Fmk1 in Δ*ptc7R*. This fast and transient increment could justify the fact that the Δ*ptc7R* is more invasive on the cellophane penetration assay (Figure 26), and that not only the higher basal level of Fmk1 phosphorylation is a requisite for a strain to be more invasive on penetration assays.

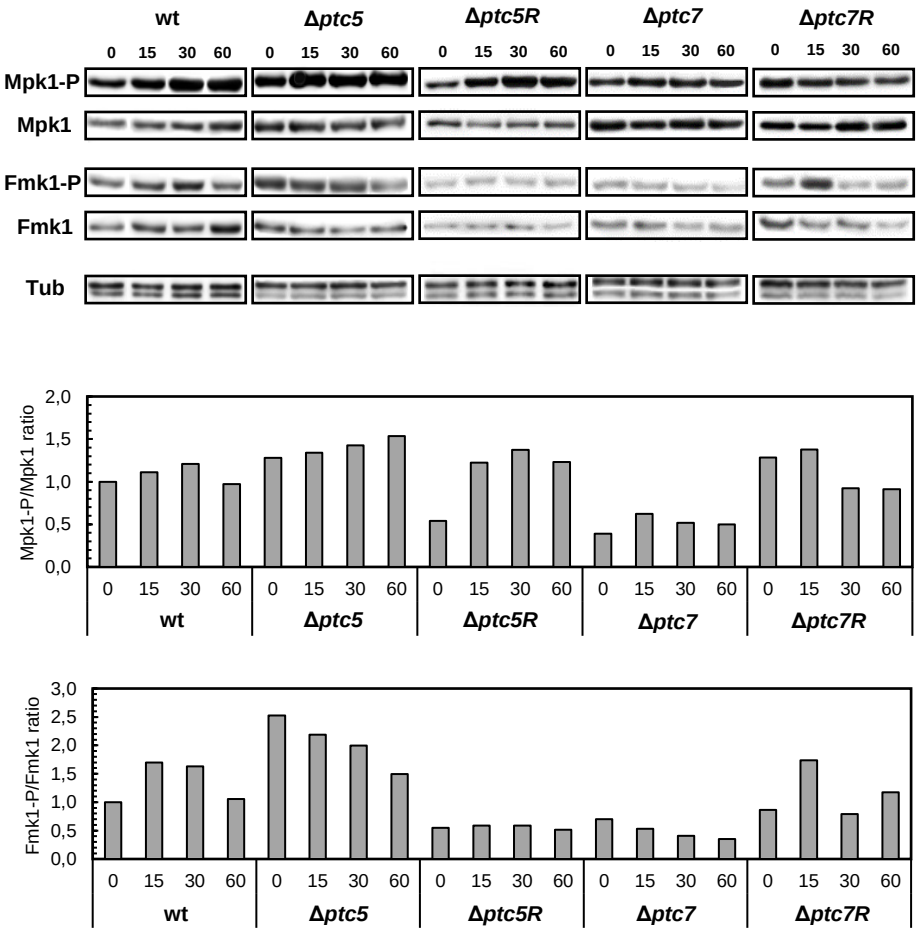

Figure 27. *Fusarium oxysporum* PP2Cs disruption alters MAPK Phosphorylation dynamics during invasive growth. Mycelia of *F. oxysporum* wild type strain and PP2c mutant strains grown for 15h ($2.5x10^8$ fresh microconidia on 50ml of PDB, incubated 28ºC 170 rpm) were filtered to remove completely the media, washed on liquid Puhalla Minimal media and then transferred to MM puhalla plates, mycelia were recovered after 15, 30 and 60 min of incubation on the plates and frozen in liquid nitrogen to perform total protein extraction and western blot analysis to access the phosphorylation status of MAPK's. Band intensity were quantified with Image J software v. 1.08 (National Health Institute, United States of America). The phosphorylation level was calculated by the ratio (phosphorylated / total protein). Wild-type sample phosphorylation status (time point 0) was used to standardize the samples. The immunoblot assay was repeated twice from two biological replicates having similar results, a representative micrography is shown.

4.1.5.6 The lack of *ptc5* or *ptc5R* reduces the virulence of *F. oxysporum*

The role of *F. oxysporum* PP2Cs in the pathogenicity of tomato was assayed as previously reported (Di Pietro and Roncero, 1998). 2-weeks-old tomato plants were root inoculated by immersion in microconidial suspensions

of the wild-type, mutant and complemented strains. Plant survival was recorded daily for 35 days (Figure 28). Most plants inoculated with the wild-type or the complemented strains were dead 30 days after inoculation (Figure 28 A, B, D and E). By contrast, mortality of plants inoculated with the Δ*ptc5* and the Δ*ptc5R* mutants was significantly reduced ($P < 0.05$), with 70% of the plants still alive after 35 days (Figure 28 B and C). The remaining mutants did not show differences in virulence compared with wild type (Figure 28 A, D, and E).

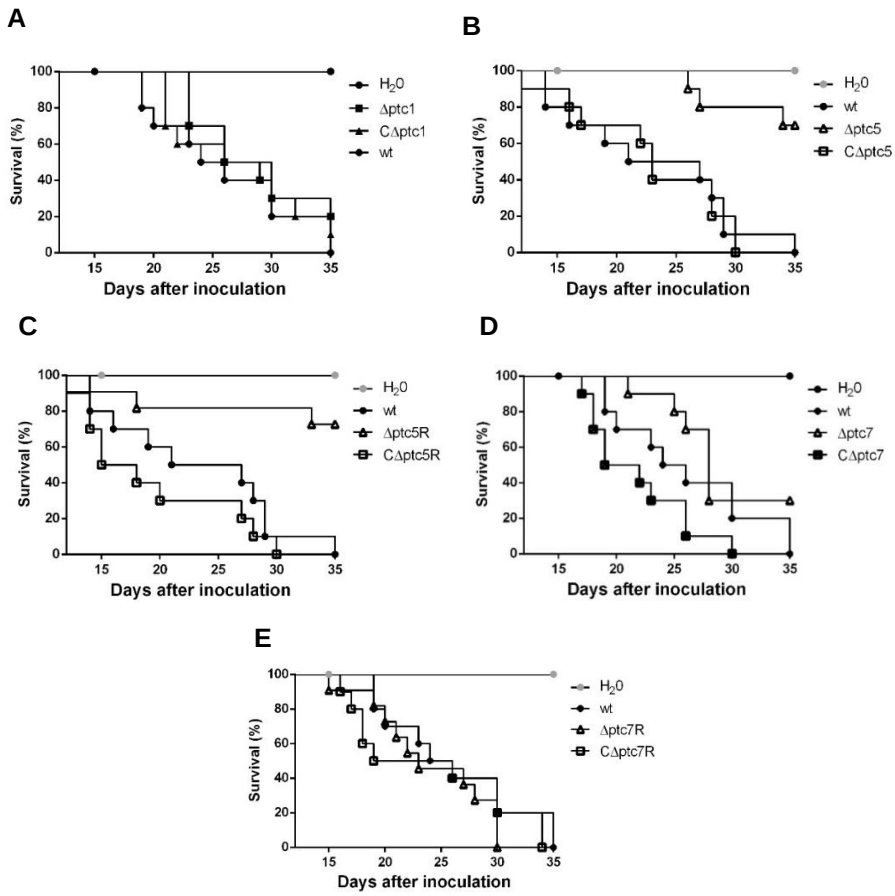

Figure 28. Role of PP2Cs on the virulence of *F. oxysporum* of tomato. Groups of ten 2-week-old tomato plants (cv. Monika) were inoculated by immersing the roots into a suspension of 5×10^6 freshly obtained microconidia ml^{-1} of the indicated strains, planted in vermiculite and maintained in a growth chamber (Di Pietro and Roncero, 1998). Percentage of plant survival recorded daily for 35 days. Experiments were performed three times with similar results. Data shown are from one representative experiment.

4.2. Role of Ptc1 on Cell Wall Integrity and High Osmolarity Glycerol pathways

The analysis of the basal level of MAPK phosphorylation indicate that the mutant strain Δ*ptc1* has an unbalanced level of phosphorylation on the CWI and HOG pathways. To gain insight of the function of *F. oxysporum* Ptc1, a series of assays to explain the effects of this unbalance and how it can influence the fungi growth were performed.

4.2.1 Deletion of *ptc1* leads to sporulation and early developmental defects

Two days after inoculation in liquid PDB medium we observed a 44% reduction of microconidia production in the *Δptc1* strain (Figure 29A). Additionally, the conidial germination rate was significantly decreased in the mutant strain (Figure 29B) suggesting a role of Ptc1 in developmental processes of *F. oxysporum*.

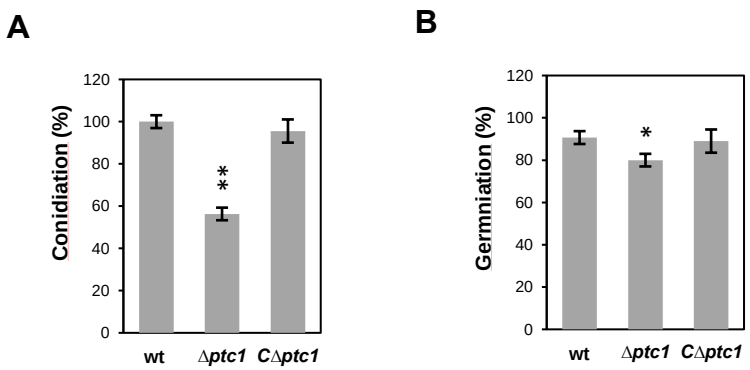

Figure 29. Deletion of *ptc1* affects conidiation and germination of *F. oxysporum*. (A) Microconidia were counted 48h after inoculation on PDB medium. Conidiation rates are referred to wt levels (100%) (B) Germination rates were determined 13h after inoculation of fresh microconidia into diluted MM supplemented with 25 mM $NaNO_3$. (B–C) The results are expressed as average (± standard deviation) of three independent biological repeats ($p < 0.05$(*); $p < 0.01$(**). Statistical significance test (*t-test*) was performed comparing Δ*ptc1* and CΔ*ptc1* with wild-type strain. Bars represent standard error.

4.2.2 Ptc1 contributes in response to cell wall, oxidative and osmotic stress

To further investigate the biological role of *F. oxysporum* Ptc1 on cell wall integrity, oxidative stress and osmotic stress, we determined the tolerance of Δ*ptc1* mutant to a range of stresses using plate dilution assays on YPGA medium supplemented with different compounds (Figure 30).

Sensitivity of the Δ*ptc1* mutant to cell wall (CFW and CR) and oxidative stresses (menadione) was increased in comparison to the wild-type and complemented strains (Figure 30). Here was found that loss of Ptc1 in *F. oxysporum* also reduced tolerance to calcium ions (Figure 30). In *S. cerevisiae*, Δ*ptc1* mutant cells are highly sensitive to calcium ions, possibly due to hyperactivation of the phosphatase calcineurin (Gonzalez *et al*., 2006).

To assay osmotic stress response, high concentration of salt (NaCl, KCl and LiCl) and osmolytes (sorbitol) was added to YPGA plates. Tolerance to the osmotic stress compounds was increased in Δ*ptc1* mutant compared to the wild-type strain. Moreover, the Δ*ptc1* mutant was more sensitive to the fungicide fludioxonil but more tolerant to iprodione (Figure 30). In several fungi, resistance to fludioxonil was linked to sensitivity to hyperosmotic stress of Δ*hog1* mutants (Liu *et al*., 2017; Segorbe *et al*., 2017). Collectively, our results suggest a role of Ptc1 in the HOG response as previously reported in yeast and other fungi (Arino *et al*., 2011; Liu *et al*., 2017).

Since addition of acetic acid at high temperature and low pH values were reported to activate the Hog1 and Slt2 pathways in yeast (Fuchs and Mylonakis, 2009, Hohmann, 2009) assays to analyze these phenotypes were performed (Figure 31). Indeed, the lack of Ptc1 resulted in increased tolerance to high temperature (Figure 31A) and that the growth of the Δ*ptc1* mutant was completely abolished on 0.05% acetic acid (Figure 31B), in contrast to the wild-type strain that was still able to germinate and form a visible colony after 4 days.

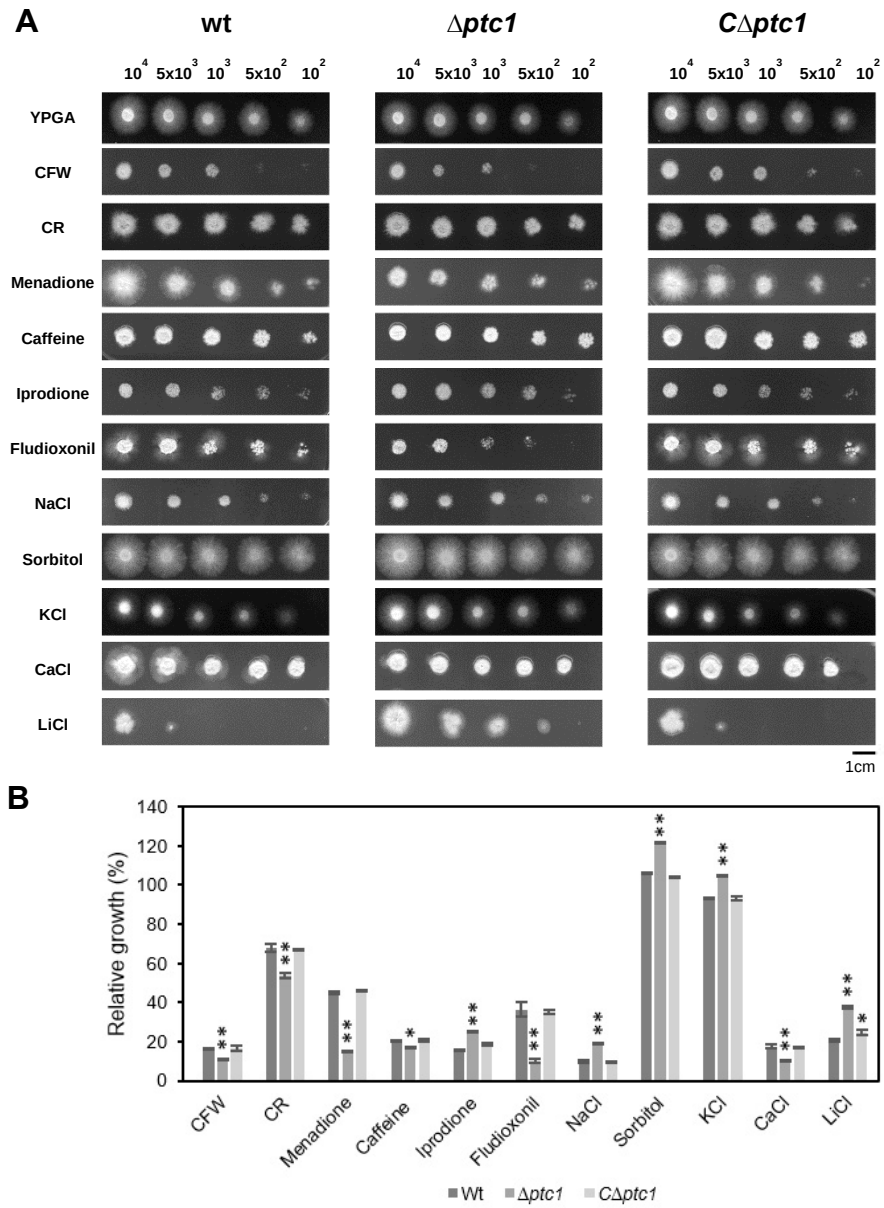

Figure 30. Ptc1 is involved in stress response (A) Phenotypical analysis on rich media of F. oxysporum strains wild type (Jin *et al.*), Δ*ptc1* and CΔ*ptc1* on YPGA supplied with stress agents. Stress agents. CFW (50µg/ml), CR (100µg/ml), Menadione (20µg/ml), Caffeine (5mM). Iprodione (20µg/ml), Fludioxonil (20µg/ml), NaCl (1,2M), Sorbitol (1.25M), KCl (1.2M), CaCl (0.3M) and LiCl (0.3M). Growth were monitored at 48h (KCl and iprodione); 72h (SDS, CFW, CR, Menadione, Caffeine, NaCl, Sorbitol and CaCl); and 96h (LiCl) (B) Relative growth (%) of the different strains in the presence of the indicated stressors was calculated as the colony area on stressor-containing medium versus colony area on YPDA. Colony area of 10^3 spot was measured using the ImageJ software v. 1.08 (LiCl was measured with 10^4) (National Health Institute, United States of America). Three biological replicates were used to perform statistical significance test (*t-test*) comparing Δ*ptc1* and *C*Δ*ptc1* with the wild-type strain, represented by $p < 0.05$(*); $p < 0.01$(**).

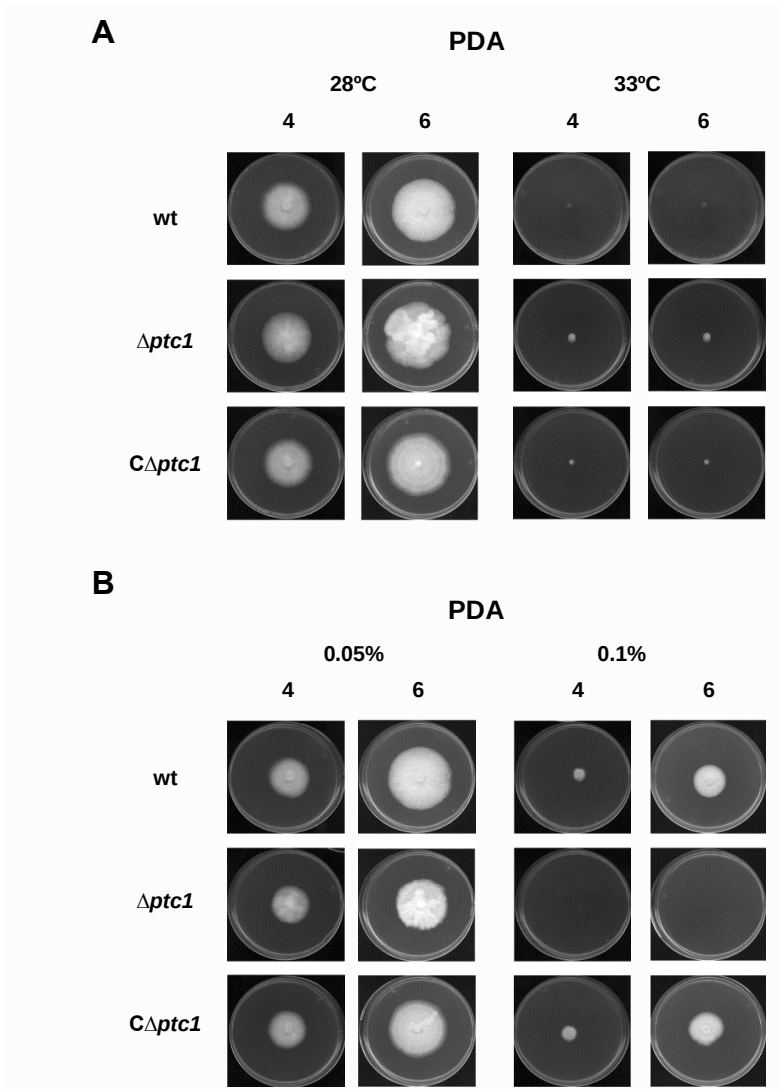

Figure 31. *F. oxysporum* Ptc1 disruption affects growth on high temperature and acid pH. Growth of the strains wild type (wt), Δ*ptc1* and CΔ*ptc1* on PDA at 28 °C or 33 °C (A), or on PDA containing 0.05% and 0.01% Acetic Acid at 28°C (B), plates were central spotted with $5x10^4$ conidia and monitored 4 and 6 days after inoculation.

4.2.3 Ptc1 regulates phosphorylation levels of the MAPKs Hog1 and Mpk1

Previous work revealed an interplay in stress responses between the three MAPK pathways in *F. oxysporum* (Segorbe et al., 2017). To investigate the role of Ptc1 in MAPK regulation, we monitored the phosphorylation status

of Mpk1 and Hog1 using western blot of total proteins from mycelia treated with 0.0125% SDS. In the wild-type strain, Mpk1 phosphorylation was rapidly induced upon treatment with SDS (Figure 32). By contrast, the Δ*ptc1* mutant showed a significant reduction and delay in the phosphorylation level of Mpk1, suggesting that Ptc1 positively regulates the Mpk1 pathway. This result is in line with the increased sensitivity of the mutant strain to SDS shown previously (Figure 25). By contrast, was observed increased phosphorylation levels of Hog1 in the Δ*ptc1* mutant, both before and after SDS treatment. The higher Hog1 phosphorylation level was continuous during the 60 min of the time course.

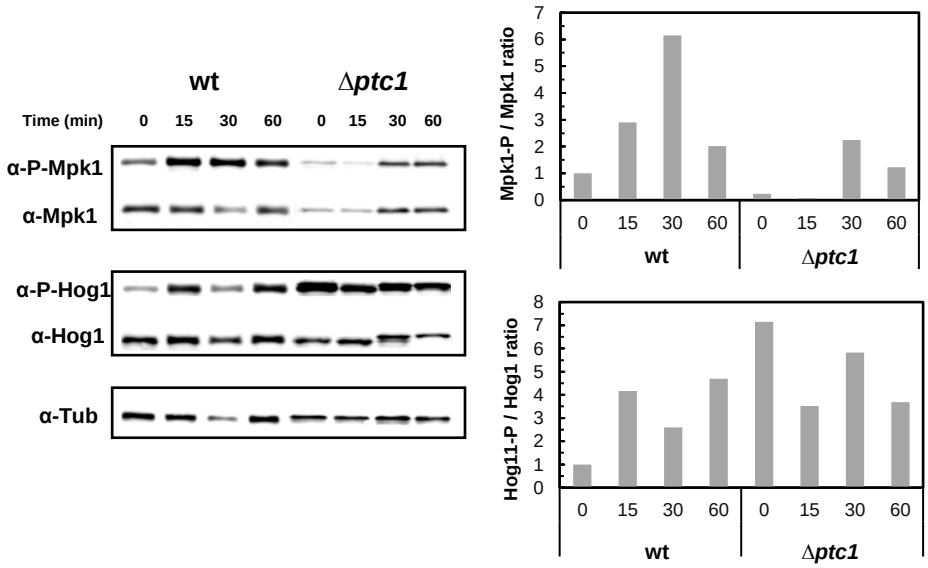

Figure 32. Ptc1 regulates Mpk1 and Hog1 phosphorylation. Germlings of the wild-type (Jin *et al.*) and Δ*ptc1* mutant strain of *F. oxysporum* were transferred to PDB supplemented with SDS (0.0125%) for 15, 30, and 60 min. Mycelia were frozen in liquid nitrogen before protein extraction and western-blot analysis to detect the phosphorylated and total MAPK levels Mpk1 and Hog1. Tubulin was used as loading control. Relative amount of phosphorylated versus non-phosphorylated are shown in the graphs. Experiments were performed twice with similar results. The figure shows results from one representative experiment. Band intensity were quantified with Image J software v. 1.08 (National Health Institute, United States of America). The phosphorylation level was calculated by the ratio (phosphorylated / total protein). Wild-type untreated sample was used to standardize the samples. The immunoblot assay was repeated twice from two biological replicates having similar results, a representative micrography is shown.

Next, Hog1 phosphorylation levels were determined after treatment with high salt concentrations, which generate osmotic stress to the cell (Figure 33). Was observed a strong induction of phosphorylation in the wild-type upon exposure to LiCl or NaCl. Similarly, in the Δ*ptc1* mutant Hog1 was constitutively phosphorylated even before induction, and the high phosphorylation level was maintained until 1 h after induction. Taken together, these findings strongly suggest that Ptc1 contributes to inactivation of the Hog1 pathway.

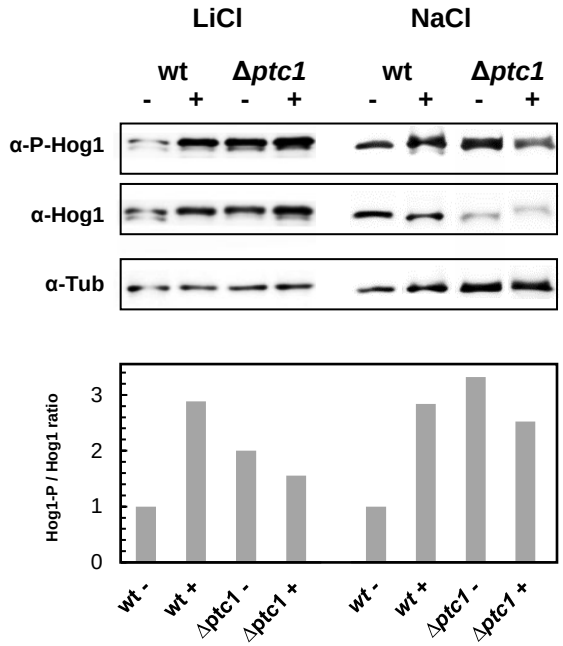

Figure 33. Ptc1 regulates Hog1 phosphorylation basal levels. Germlings of the wild-type (Jin *et al.*) and Δ*ptc1* mutant strain of *F. oxysporum* were transferred to PDB with (+) or without (-) LiCl (0.3M) or NaCl (1.2M) for 60 min. Mycelia were frozen in liquid nitrogen before protein extraction and western-blot analysis to detect the phosphorylated and total MAPK level of Hog1. Tubulin was used as loading control. Relative amount of phosphorylated versus non-phosphorylated are shown in the graphs. Experiments were performed twice with similar results. The figure shows results from one representative experiment. Band intensity were quantified with Image J software v. 1.08 (National Health Institute, United States of America). The phosphorylation level was calculated by the ratio (phosphorylated / total protein). Wild-type untreated sample was used to standardize the samples. The immunoblot assay was repeated twice from two biological replicates having similar results, a representative micrography is shown.

4.2.4 Ptc1 is associated with monovalent cation balance

The increased tolerance to salt and osmotic stress observed in Δ*ptc1* mutant strain could be correlated with the expression of sodium and lithium transporters. In *S. cerevisiae,* two main mechanisms are used for the elimination of monovalent cations. The first is based on a P-type ATPase pump encoded by the ENA system (Arino et al., 2010). ENA genes are likely to exist in all fungal genomes, often as a gene family encoding similar proteins. Ena1 is involved in tolerance to high levels of monovalent cations such as Na^+ and Li^+ or alkaline pH, both in yeast and filamentous fungi (Caracuel *et al*., 2003; Krauke and Sychrova, 2011; Petrezselyova *et al*., 2016).

A BLAST search with the Ena5 gene from *F. graminearum* was performed and identified an orthologous gene (FOXG_09046) in *F. oxysporum*, named *ena5*. A recent paper identified *FgEna5* as the most important ATPase ENA protein for extruding the excess of sodium in *F. graminearum* (Son et al., 2015). Additionally, were identified ten *F. oxysporum* genes that codes for ENA orthologs, the pairwise identity analysis with *S. cerevisiae* ENA1 (YDR040C) and FOXG_09046 revealed that these genes are copies distributed on different chromosomes or genome positions (Table 5).

Table 5. Identification of ENA genes on *Fusarium oxysporum* f. sp *lycopersici* 4287

Gene	Identity / Sequence coverage (%) with *Ena1 S. cerevisiae* YDR040C	Identity / Sequence coverage (%) with *Ena5* FOXG_09046	Ca^{++}ATPase transmembrane domain	Chromosome	Attributed name
FOXG_05702	49% / 66%	63% / 100%	yes	2	*Ena1*
FOXG_06571	42% / 60%	83% / 60%	no	3	*Ena2*
FOXG_06691	42% / 60%	83% / 60%	no	3	
FOXG_07255	42% / 60%	83% / 60%	no	6	
FOXG_10377	45% / 63%	59% / 100%	yes	7	*Ena3*
FOXG_06575	49% / 67%	83% / 100%	yes	3	*Ena4*
FOXG_06687	49% / 67%	83% / 100%	yes	3	
FOXG_07251	49% / 67%	83% / 100%	yes	6	
FOXG_09046	49% / 67%	100% / 100%	yes	9	*Ena5*
FOXG_11383	44% / 60%	49% / 100%	yes	1	*Ena6*
FOXG_20003	41% / 60%	48% / 100%	yes	9	

*Specific primers were designed to detect the transcripts of each *F. oxysporum* Ena group (1-6) based on the sequences of the genes highlighted in bold.

A second strategy of *S. cerevisiae* to extrude monovalent cations is based on the H^+/Na^+ antiporter encoded by *NHA1*, which exchanges protons with Na^+, Li^+, and K^+ cations and is expressed constitutively at low levels (Arino et al., 2010). It was predicted a single gene coding for a *NHA1* orthologue in *F. oxysporum* in the genome, FOXG_11541, named *nha1.*

To gain insight of the role of the *ena* genes in cation monovalent balance under osmotic stress, firstly we performed a 30 cycle RT-PCR analysis with samples of the wild-type strain induced with 0.3M LiCl for 2h under acid and alkaline pH (5 and 8) on PDB media (Figure 34). Specific primers were designed to detect each of the six *ena1-6* genes of *F. oxysporum.* The high identity of the proteins identified on each group was also reflected on mRNA sequence data, allowing to design the primers needed to detect transcripts belonging from each group by RT-PCR and qRT-PCR. Surprisingly, the RT-PCR analysis showed that only *ena5* and *nha1* genes were highly expressed.

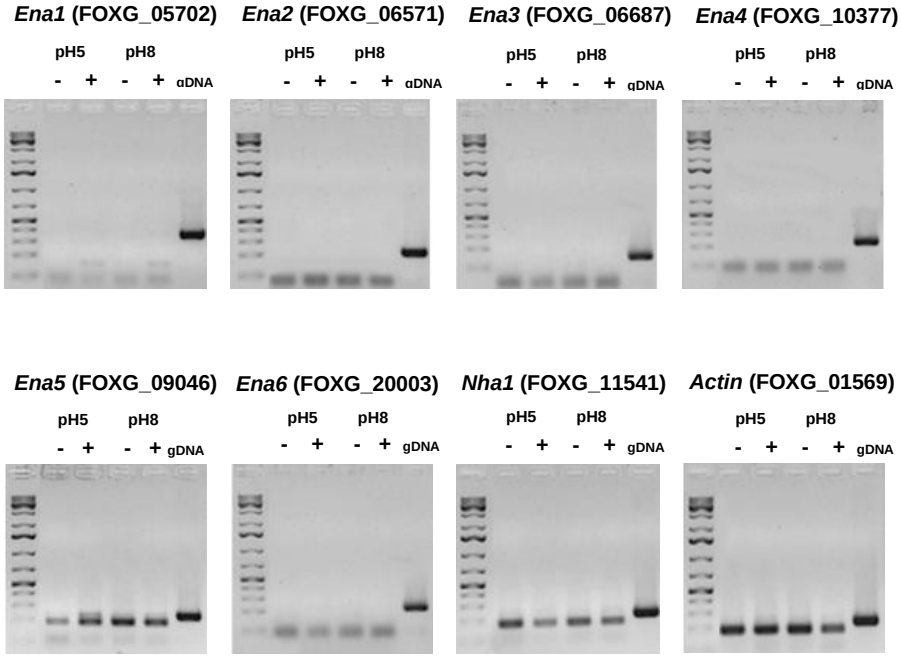

Figure 34. RT-PCR analysis of expression of *F. oxysporum* monovalent cation balance related genes. Wild-type strain germlings (15h growth) were transferred to PDB (–) or PDB supplied with 0.3M LiCl (+) for 60min. After treatment, mycelia were harvested and rapidly frozen on liquid nitrogen prior to RNA isolation. RT-PCR analysis was performed for the indicated Ena and Nha1 genes with High Fidelity Taq DNA polymerase (Roche diagnostics, Alcobendas, Spain). RT-PCR of *Actin* gene is shown reverse transcription quality control.

Since the increased tolerance to salt and osmotic stress observed in Δ*ptc1* mutant strain could be correlated with the expression of sodium and lithium transporters, a comparative time course analysis of gene expression was performed (Figure 35). A strong induction of *ena5* expression was observed 15 min after exposure to 1.2 M NaCl, showing a gradual increase during the time course analyzed (Figure 35A). The expression level was slightly but significantly higher in the Δ*ptc1* mutant in comparison to the wild-type strain.

Expression of *ena5* gene was exacerbated at lower and less toxic sodium concentration (0.6 M), reaching a maximum transcript amount 30 min after transfer to sodium containing medium in both strains. Importantly, the mutant lacking Ptc1 showed a twofold increase in *ena5* transcript levels after NaCl induction, suggesting that the Na^+-ATPase Ena5 is, at least in part, responsible for the increased tolerance of the Δ*ptc1* mutant to NaCl and LiCl. Although the transcript levels of the predicted NHA1 orthologue FOXG_11541 were low throughout the time course experiment, an increase of expression in response to NaCl treatment was observed, which was significantly higher in the Δ*ptc1* mutant than in the wild-type strain (Figure 35B).

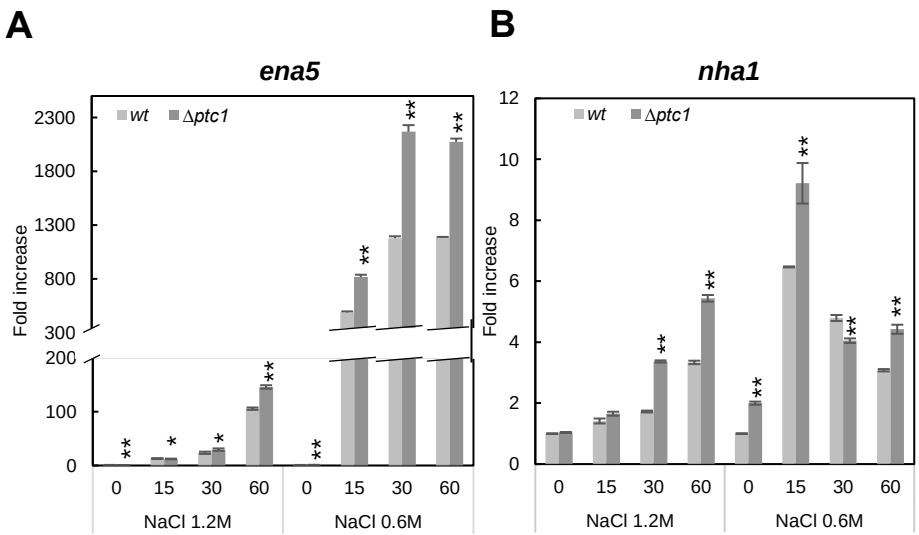

Figure 35. Expression of *ena5* and *nha1* genes is induced by NaCl and regulated by Ptc1. Germlings of the wild-type (Jin *et al.*) strain and Δ*ptc1* mutant were transferred to PDB supplemented with NaCl 1.2 M or 0.6M for 15, 30 and 60 min. RT-qPCR analysis was performed using *ena5* (A) or *nha1* (B) gene specific primers. Expression is referred as time-fold increase relative to wild-type control (time 0), using *actin* as reference gene. The results are expressed as average (± standard deviation) of three independent biological repeats ($p < 0.05$(*); $p < 0.01$(**). Bars represent standard error.

4.2.5 *F. oxysporum* Ptc1 regulates catalase gene expression.

The HOG pathway is a key signalling pathway that mediates the responses to both osmotic and oxidative stresses (Arino *et al*., 2011). There are different gene markers whose expression usually reflects the activity of the HOG pathway (Winkelstroter *et al*., 2015b). We considered a catalase gene as a marker to analyse the HOG pathway induction. Catalase plays a role in oxidative, osmotic and pH stress responses and its expression is dependent on the Hog1 pathway (Winkelstroter *et al*., 2015a). BLAST analysis with the *Aspergillus CatA* and *CatB* genes revealed the presence of two catalase orthologous genes (FOXG_08697 and FOXG_02405, respectively) in the genome of *F. oxysporum*.

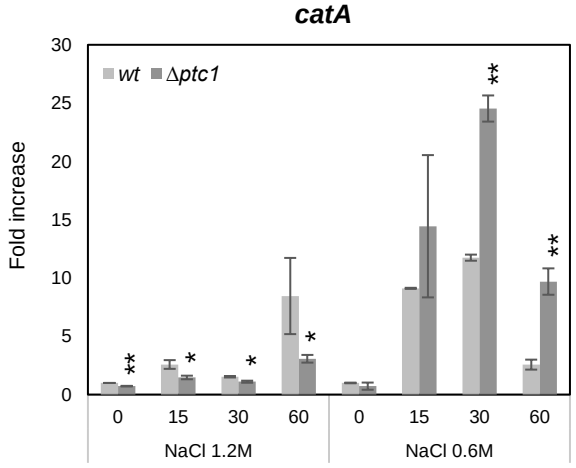

Figure 36. The *ptc1* null mutant shows higher expression of the osmotic stress dependent gene *catA*. Germlings of wt and Δ*ptc1* were transferred to PDB supplied with Sodium Choride (NaCl 1.2M or 0.6M) for 15, 30 and 60 min for RT-qPCR analysis. Expression is referred as increases fold related to wild type control samples (time 0), using *actin* as reference gene. The results are expressed as average (± one standard deviation) of three independent biological repetitions ($p<0.05$(*); $p<0.01$(**)).

The expression of FOXG_02405 was imperceptible (data not shown). By contrast, FOXG_08697 gene (hereafter, *catA*) was highly expressed in the wild-type strain after 15 minutes exposure to osmotic stress (1.2M or 0.6M NaCl) (Figure 36). Interestingly, after treatment with 0.6M NaCl, induction of *catA* in the *Δptc1* mutant was about 2-fold higher than in the wild-type strain. These results suggest that the lack of *ptc1* and the consequent increased

phosphorylation level of Hog1 are behind the higher *catA* expression in *Δptc1* mutant strain.

4.2.6 *F. oxysporum hog1* and *ptc3* expression respond to osmotic stress mediated by Ptc1

It is known that the magnitude by which osmotic stress affects gene expression varies according to the severity and the time after the shock induction (Posas, 2000 #254). *F. oxysporum Hog1* transcription levels was also dependent on the extracellular concentration of salt (Figure 37A).

A rapid expression induction was detected in response to lower salt stress (0.6M), both in the wild-type and mutant strains, with a maximum mRNA accumulation 15 minutes after treatment. The higher toxic concentration 1.2M NaCl induced a high *hog1* expression in the Δ*ptc1* mutant and, to a much lower extend, in the wild-type strain. The result indicated a transcriptional response rather early and largely transient in the presence of 0.6M NaCl compared to the higher salt concentration response. Taken together our results indicated that Ptc1 is involved in the regulation of *hog1* expression upon osmotic stress induction.

To investigate the impact of the Δ*ptc1* mutation on the transcriptional accumulation of other PP2C phosphatases, was assessed the expression of the *S. cerevisiae PTC3* orthologous gene in the different strains after exposure to NaCl. We observed that *ptc3* induction was significantly higher in the Δ*ptc1* mutant than in wild-type strain, especially after treatment with 1.2M NaCl, where no significant *ptc3* induction was detected in the wild-type background (Figure 37B).The fact that the *ptc3* accumulation is higher in Δ*ptc1* than in wild type suggest a redundancy of the system as previously reported in *Aspergillus* (Winkelstroter *et al*., 2015a)

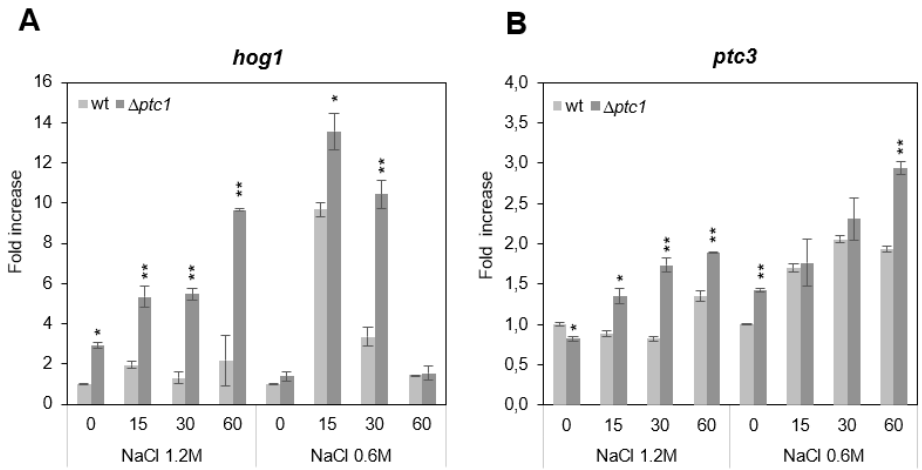

Figure 37. The *ptc1* null mutant shows higher expression of *hog1* and *ptc3* genes. Germlings of *F. oxysporum* wild type (Jin *et al.*) and Δ*ptc1* strains (15h growth) were transferred to PDB supplied with Sodium Choride (NaCl 1.2M or 0.6M) for 15, 30 and 60 min for RT-qPCR analysis. Expression is referred as increases fold related to wild type control samples (time 0), using *actin* as reference gene. The results are expressed as average (± one standard deviation) of three independent biological repetitions ($p<0.05$(*); $p<0.01$(**).

4.2.7 Vacuole fragmentation is constitutive in Δ*ptc1*

Vacuoles play a role in autophagy, osmoregulation, and storage of amino acids and ions. It has been previously reported that osmotic changes affect vacuole structure in yeast: hypotonic media promote vacuole fusion while hypertonic conditions induce rapid fragmentation (Klionsky *et al.*, 1990; Weisman *et al.,* 2003; Herrera *et al.,* 2017). Numerous genes have been reported recently to be involved in vacuole fragmentation (Michaillat *et al.*, 2013).

S. cerevisiae PTC1 has been identified as a protein required for maintaining the structure and function of the vacuole (Bonangelino *et al.*, 2002; Sambade *et al.*, 2005; Arino *et al.*, 2011). Based on these observations, we studied the role of *F. oxysporum* Ptc1 in vacuole dynamic upon osmotic stress. Vacuoles in *F. oxysporum* are large and round, although their size, shape and number varies depending on the hyphal developmental status, as reported in other filamentous fungi (Richards, 2010).

We analyzed the behavior of vacuoles after osmotic stress induction using the fluorescent vacuolar vital stain FM4-64 and microscopy analysis (Figure 38). When grown in rich medium, wild-type cells displayed large size vacuoles that were fragmented into small vesicles after transfer to osmotic stress medium (0.6M NaCl). By contrast, Δ*ptc1* cells contained fragmented vacuoles under both growth conditions (either with or without osmotic stress).

Our results suggest a role of Ptc1 in vacuole dynamics in *F. oxysporum*. The presence of fragmented vacuoles observed in the mutant strain would also support its increased tolerance to osmotic stress. It has been described that upon osmotic stress, cell lose water and the vacuolar volume is reduced maintaining the membrane surface. Fragmentation of the organelle can then readjust the surface to the volume under these conditions (Bonangelino *et al.*, 2002).

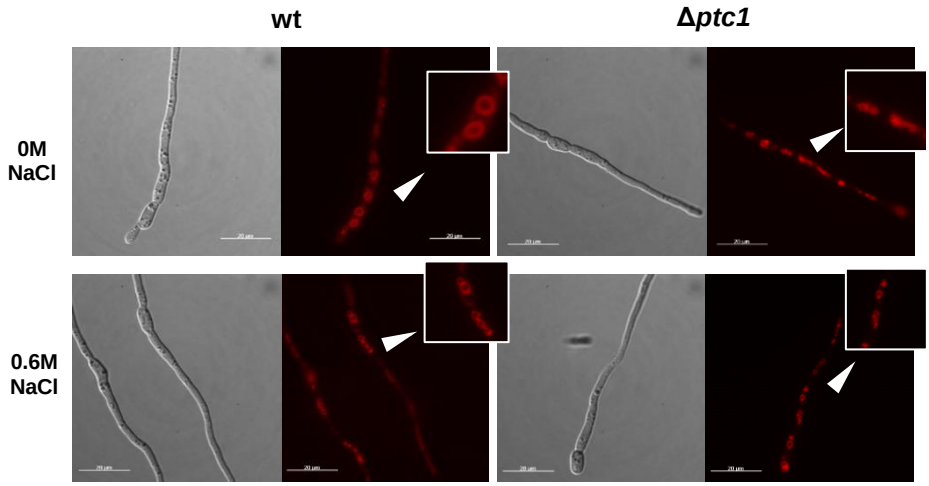

Figure 38. *Ptc1* is involved in vacuolar fragmentation dynamics. Representative micrographs showing wt and Δ*ptc1* hiphae after incubation for 15 min on the salt concentration indicated (left panel) and stained with FM4-64 (right panel). Barrs=20 µm.

5. Discussion

5. Discussion

5.1 Seven PP2C phosphatase encoding genes are present in *F. oxysporum* genome.

S. cerevisiae PP2C family of phosphatases is composed by seven proteins (PTC1-PTC7) that are involved in the regulation of different MAPK pathways. Some authors suggested the involvement of fungal phosphatases in key cellular processes, considering the abundance of filamentous fungi harbouring multiple PP2C encoding genes in their genome (Arino *et al*., 2011; Yang *et al.,* 2013; Winkelstroter *et al*., 2015a; Winkelstroter *et al.,* 2015b). Here we identified seven PP2C phosphatase encoding genes in the genome of *F. oxysporum* that are orthologous to the corresponding *S. cerevisiae* and *F. graminearum* genes. The protein products identified from the genes FOXG_11525, FOXG_05154, FOXG_07981, FOXG_11628, FOXG_07912, FOXG_09277 and FOXG_00617 were named Ptc1, Ptc3, Ptc5, Ptc5R, Ptc6, Ptc7, and Ptc7R, respectively.

Phylogenetic analysis confirmed the presence of the seven PP2C phosphatases clustering in five distinct clades as previously reported (Ariño, 2011; Jiang *et al*., 2011). Consistent with the previous finding, orthologous of *S. cerevisiae* PTC2 and PTC4 phosphatases were not found in *F. oxysporum* genome, neither in the other filamentous fungi species. It has been suggested that the lack of Ptc2 and Ptc4 phosphatases in filamentous fungi could be supply by other PP2C phosphatases (Ariño, 2011; Gosh *et al*., 2014). Additionally, it was confirmed the presence of *F. oxysporum* PP2C-related proteins on the subclade 5R for *Fusarium* spp and subclade 7R for filamentous fungi, as previously reported (Jiang *et al*., 2011).

S. cerevisiae PTC2 and PTC3 are proteins 75% identical that probably arose from a genome duplication event (Hughes and Friedman, 2003). This lack of this event in *F. oxysporum* and the RNAseq evidence of different *Ptc3* transcripts yielding five different protein isoforms, suggest that a structural

variation can somehow supply the lack of Ptc2 phosphatase. By alternative splicing fungal proteomes can be diversified, where one gene generates multiple distinct mRNAs that each encode a distinct protein (Marshall *et al*., 2013; Grützmann *et al*., 2014 Jin *et al*., 2017; Phasha *et al*., 2017). A similar pattern splicing variants of *S. cerevisiae* PTC3 orthologs in *F. oxysporum* and *F. graminearum* suggests that this mechanism can be conserved in between *Fusarium* spp.

The domain prediction analysis identified putative different domain composition on non-catalytical domains of *F. oxysporum* PP2Cs. In Ptc1 was predicted a Serine-rich region that can be target of protein phosphorylation by the kinases CK2, PKC, and cAMP- and cGMP-dependent protein kinase, suggesting a putative function on diverse kinase signaling pathways. The analysis also identified Microbodies C-terminal targeting signals in *F. oxysporum* Ptc5 and Ptc7 suggesting a putative localization to peroxisomes. that can be involved in targeting these proteins to the mitochondria where they could have a role on the regulation of the PDH complex and TCA cycle as reported in yeast (Krause-Buchhols *et al.*, 2006; Gey *et al.*, 2008; Vögtle *et al*., 2012) or activating coenzyme Q6 biosynthesis by dephosphorylation of demethoxy-Q6 hydroxylase Coq7p (Juneau *et al*., 2009; Martin-Montalvo *et al*., 2013; Guo *et al*., 2017; Gonzalez-Mariscal *et al.*, 2017). Additionally, *F. oxysporum* Ptc7R could be the responsible to code a protein with similar function to the yeast PTC7 nuclear isoform, since it contains a predicted N-terminal binuclear localization signal (Juneau *et al*., 2009).

5.2 *F. oxysporum* PP2C gene expression and disruption addresses putative roles on the regulation of MAPK pathways

Eukaryotes PP2C phosphatases have previously been reported as functionally redundant regulators of MAPK cascades by regulating basal levels or limiting the maximum activation of MAPK pathways after stress (Pearson *et al*., 2001, Warmka *et al*., 2001; Young *et al*., 2002; Mapes & Ota, 2004; Shitamukai *et al*., 2004; Ariño *et al*., 2011; Shi, 2009; Ghosh *et al*., 2014; Winkelstroter *et al*., 2015a; Winkelstroter *et al*., 2015b; Tatjer *et al*., 2016). Little

is known about the dynamics of gene expression of PP2Cs on fungi under stress and understanding the dynamics of expression of PP2C genes in stress responses can provide valuable information to unravel them biological role.

The presented gene expression analysis results support the idea of two major phosphatases PP2C of *F. oxysporum* involved in pathogenesis and filamentous growth and an orchestrate-like expression of genes under stresses that activate MAPK pathways illustrating that some of them are transcriptionally regulated. Higher amounts of the PP2Cs *ptc3* and *ptc7* transcripts were detected in filamentous growth and plant infection. The higher transcript levels of this genes in plant infection and their regulation in "invasive growth conditions" suggests possible roles on the pathogenesis of *F. oxysporum.* In response to cell wall and membrane stressors that activate the cell wall integrity pathway, *ptc1*, *ptc3, ptc6* and *ptc7* were transcriptionally regulated. The increase of transcript levels of *ptc7* was higher when compared to the others *F. oxysporum* PP2Cs along the time course, suggesting that *ptc7* is the main phosphatase that regulates the cell wall integrity pathway. Under stress responses that activate the Hog1 pathway, *ptc1 ptc7* and *ptc7R* were upregulated under osmotic stress while *ptc7*, *ptc5R* and *ptc6* under oxidative stress. The high levels of upregulation suggest a major role of Ptc1 under osmotic stress, and Ptc6 and Ptc7 as concomitant regulators of oxidative stress.

The involvement of PP2Cs as key regulators of MAPK cascades in *F. oxysporum*, was analyzed by western blot. The phosphorylation status of the MAPKs Mpk1, Fmk1 and Hog1 was investigated in wild-type and knockout mutant strains Δ*ptc1*, Δ*ptc5*, Δ*ptc5R*, Δ*ptc7*, and Δ*ptc7R*.

The reduced basal phosphorylation level of Mpk1 in *Δptc1* indicates that Ptc1 is a positive regulator of the cell wall integrity pathway in *F. oxysporum*. Interestingly, this result contrast with that obtained in *S. cerevisiae* where the lack of Ptc1 leads to hyperphosphorylation of Mpk1 (Du *et al*., 2006; Gonzalez *et al*., 2006). The sensibility to components of cell wall damage SDS and CR of the strain *Δptc1* can be attributed to the low quantity of Mpk1 protein and lower levels of phosphorylation leading to similar defects observed in the disruption

of Mpk1 (Segorbe *et al*., 2016). Previous studies reported an interplay between the HOG and CWI pathways (Liu *et al*., 2011; Rodriguez-Pena *et al*., 2010; Segorbe *et al*., 2017). Here it was found that in the Δ*ptc1* mutant the Mpk1 phosphorylation remained at a low level while the phosphorylation of Hog1 was highly increased, indicating that Ptc1 might be a positive regulator of the Mpk1 pathway and negative regulator of the Hog1 pathway. The function of Ptc1 in the Mpk1 pathway might be either direct or indirect through cross-talk between the Hog1 and Mpk1 pathways. Previous studies in the fungal pathogen *B. cinereae* reported a similar positive role of BcPtc1 on the CWI MAPK pathway suggesting that this control could be direct by the interplay of Sak1 on the Bmp3 cascade, or indirect by the action of phosphatases maintaining the equilibrium between MAPK phosphorylation (Liu *et al*., 2011; Yang *et al*., 2013).

The phosphorylation patterns of Mpk1 and Fmk1 in the *Δptc5* strain were quite similar to those observed after the disruption of *hog*1 in *F. oxysporum* that leads to an augmented phosphorylation of Fmk1 and Mpk1 (Segorbe *et al*., 2017), suggesting that this phosphatase act as negative regulator of both Fmk1 and Mpk1 pathways, and somehow can be involved on regulating a putative crosstalk. In agreement with the MAPKs phosphorylation, the Δ*ptc5* strain was more invasive at cellophane penetration assays and showed to be sensitive to the stressor SDS. The higher phosphorylation basal levels of Mpk1 and Fmk1 in the Δ*ptc5* were confirmed to keep higher levels than the wild type strain during the time course of the invasive growth assay. The augmented level of phosphorylation of Mpk1 can lead to altered composition of cell wall and membrane components to the *Δptc5* strain, as reported for PTC1, PTP2 and PTP3 in yeast (Du *et al*., 2006; Gonzalez *et al*., 2006), and could justify the somehow reduced virulence on tomato host.

An opposite role was shown for Ptc5R, the mutant strain *Δptc5R* showed an increment of the low phosphorylation basal levels of Mpk1 reaching wild-type levels, while Fmk1 did not show increase of phosphorylation. These results support a negative regulation of the Mpk1 pathway, and a positive role on regulation of the Fmk1 pathway. The virulence of this strain was probably reduced as result of lack of activation of Fmk1 pathway, in agreement with the

previously reports (Perez-Nadalez and Di Pietro, 2011; Turra *et al*., 2014; Miguel-Rojas and Hera, 2014; Perez-Nadalez and Di Pietro, 2015; Segorbe *et al*., 2017).

The phosphorylation MAPK levels in the lack of Ptc6 were reported to be unaltered, however Δ*ptc6* strain was shown to be more invasive on cellophane penetration assay, tolerant to oxidative stressor menadione, and shows reduced virulence on tomato (Nuñez and Hera, personal communication).

The low level of Mpk1 and Fmk1 phosphorylation in *Δptc7*strain was kept along the time course, not reaching wild type levels. The lack of Ptc7 reduced substantially the basal levels of phosphorylation of Mpk1, addressing the putative role on the positive regulation of this pathway, in agreement with the increased sensibility to cell wall stressors SDS and CR, this strain appear to be less invasive on cellophane penetration compared to the wild type on pH 7, however these differences were not so evident due to the reduction in radial growth of this strain. A delay on the mortality of plants was observed for *Δptc7*, maybe due to its slowly radial growth, however the mortality curve was not statistically different from the wild type.

The *Δptc7R* strain showed higher basal levels of phosphorylation of Mpk1 that were reduced along the time course. A fast and transient increment on Fmk1 was observed and can suggest that this shift leads to an increase invasive growth on the cellophane penetration assay. The *Δptc7R* strain presents also a faster radial growth, that can justify this increment in the penetration assay. Besides the phosphorylation level and higher penetration on cellophane sheets, the *Δptc7R* strains was not affected in pathogenesis.

In *S. cerevisiae*, PTC7 is a regulator of mitochondrial metabolism that is essential to maintain proper by regulating energy metabolism and oxidative stress resistance (Forsburg and Guarente, 1989; Abdulrehman *et al*., 2011; Ramos *et al*., 2000; Guo *et al*., 2017; Gonzalez-Mariscal *et al*., 2017). Significant increase in *PTC7* gene expression coinciding with the onset of respiratory metabolism and oxidative stress were reported, and overexpression improves cell growth in low oxygen environments (Ramos *et al*., 2000; Jiang et al., 2002, Runner and Brewster, 2003; Juneau *et al*., 2009). In plant pathogenic

fungi the functions of PTC7 orthologs is far to be elucidated, the first study was done in *F. graminearum,* and showed that the disruption of *FgPTC7* or *FgPTC7R* did not show aberrant phenotypic features when grown on PDA medium or inoculated on wheat head (Jiang *et al*., 2011).

In summary**,** the observed higher or lower phosphorylation levels of Fmk1 of the strains in the invasive growth immunoblot assay of the mutant PP2C strains could not justify alone that the activation/inactivation of the pathway having solely roles on the virulence of *F. oxysporum*. The present results suggest that an equilibrium in Mpk1 and Fmk1 MAPK pathways activation is required to pathogenesis, and both MAPKs contributes simultaneously. Fmk1 activation needs to be associated with Mpk1 activation at appropriate levels, since hyperactivation of Mpk1 can also lead to reduced virulence. The fact that the protein kinases are frequently regulated by multiple protein phosphatases difficult the identification of phosphatases roles on fungi by single gene deletion (Ghosh *et al*., 2014; Sacristán-Riviriego *et al*., 2015; Wilkelstroter *et al*., 2015b).

In *S. cerevisiae* other classes of phosphatases can be redundant players in fine-tune MAPKs phosphorylation, as the protein tyrosine phosphatases PTP2 and PTP3, by dephosphorylating tyrosine residues, and the dual specificity phosphatase MSG5 by dephosphorylating both Ser/Thr residues and Tyr residues (Palacios *et al*., 2011; Sacristán-Riviriego *et al*., 2015). In filamentous fungi, as *F. oxysporum*, the functionality of PP2Cs processes could be better elucidated in the future with further analysis of simultaneous disruption of PP2C genes (Sharmin *et al*., 2014; Tatjer *et al*., 2016), and with novel molecular techniques as RNAseq analysis of gene expression and phosphoproteomics, as recently performed in elucidating MAPK signaling in yeast (Mascaraque *et al*., 2013; Guo *et al*., 2017; Gonçalves *et al*., 2017; Romanov *et al*., 2017)

5.3 Ptc1 has a role on the High Osmolarity Glycerol and Cell Wall Integrity pathways in *F. oxysporum*

Altough p*tc1* disruption does not affect pathogenesis of *F. oxysporum*, other important processes were affected. Deletion of *ptc1* caused the opposite phenotype to Δ*hog1* in cellular adaptation to osmotic and oxidative stresses (Segorbe *et al*., 2017). In fact, Δ*ptc1* mutant showed increased tolerance to NaCl, KCl and Sorbitol and higher sensitivity to caffeine and menadione. In contrast to the results obtained in *F. graminearum* (Jiang *et al.*, 2010), we found higher tolerance of the Δ*ptc1* mutant to LiCl than the wild-type strain. Segorbe *et al.* (2017) reported that deletion of the *hog1* gene in *F. oxysporum* caused increased sensitivity to hyperosmotic stress and enhanced resistance to the fungicides iprodione and fludioxonil. They stated that these phenotypes are specific of Δ*hog1* because they were neither intensified nor lightened by additional deletion of other MAPKs.

Based on the stress responses observed in Δ*ptc1* and altered constitutive phosphorylation levels of Mpk1 and Hog1 levels, the phosphorylation levels were analysed under stress conditons. As expected, western blot analyses showed that phosphorylation levels of Hog1 increased in response to stress. These results suggest that Ptc1 acts as a phosphatase of Hog1 in *F. oxysporum*. Interestingly, the lack of Ptc1 produced a high and constant phosphorylation level of Hog1 in response to the cell membrane stressor SDS. This result is in agreement with those obtained in other fungi where the lack of Ptc1 is associated to a continuous phosphorylation of Hog1, indicating that Ptc1 dephosphorylates, at least in part, Hog1 MAPK (Arino *et al.*, 2011). It has been previously reported the involvement of HOG pathway in response to diverse cell stresses and the interplay between the HOG and CWI pathways (Rodriguez-Pena *et al*., 2010; Liu *et al*., 2011; Segorbe *et al*., 2017).

Consistent with a previous work (Miguel-Rojas & Hera, 2016), our results show that Mpk1 is rapidly phosphorylated after induction with SDS. By contrast, we found here that phosphorylation of Mpk1 remained at a low level in the Δ*ptc1* mutant, indicating that Ptc1 might be a positive regulator of the Mpk1 pathway. A previous work in the fungal pathogen *B. cinereae* reported a similar effect induced by CR, suggesting a positive role of BcPtc1 and BcPtc3 on the BcBmp3

(Mpk1 ortholog) pathway (Yang *et al*., 2013). The implication of Ptc1 on Mpk1 pathway might be direct or indirect through the interplay between Hog1 and Mpk1 pathways. It has been previously reported that during oxidative stress BcBmp3 was highly phosphorylated in a *B. cinereae* Δ*sak1* (Δhog1) mutant, suggesting a negative control of the Bmp3 phosphorylation by Sak1 under oxidative stress (Wang *et al.*, 2011). These authors suggest that this control could be direct by the action of Sak1 on the Bmp3 cascade or indirect by the action of phosphatases maintaining the equilibrium between the phosphorylated MAPKs.

It is currently proved that, in response to different stresses, HOG1 is phosphorylated and transported to the nucleus where it interacts with transcription factors to subsequently activate the expression of many genes (Rep *et al*., 2001; Rep *et al.*, 1999). Furthermore, it has been proved that HOG1 interacts with the elongation subunit of the RNApol II (Proft *et al*., 2004). On the other hand, downregulation of the pathway is required since the continuous activation of the HOG pathway is detrimental to cell growth (Maeda *et al.*, 1994). Several regulatory feedback loops exist in the HOG pathway where the proper Hog1 targets upstream components of the system (Hao *et al*., 2007; Hao *et al*., 2008). In addition, regulation of the HOG pathway has been associated with dephosphorylaton. Indeed, tyrosine phosphatases, Ptp2 and Ptp3, and threonine-serine phosphatases PP2C family (Ptc1) are important to counteract the pathway activation and adjust the dynamic range of response (Jacoby *et al*., 1997; Warmka *et al*., 2001; Mapes & Ota, 2004; Hohmann *et al*., 2007).

The presented results support the idea that Ptc1 mediates the expression of genes regulated by the Hog1 pathway in *F. oxysporum*. The increased tolerance to osmotic stress observed in the Δ*ptc1* mutant might be due to overexpression of cation transporters induced by salt treatment. It has been previously shown that the correct balance between influx and efflux of cations is carried out through transport across the cell membrane. Two cation transporters, the ENA1 ATPase and NHA1 antiporter, are crucial in yeast. The efflux of cations through the ENA ATPase is mainly regulated at the transcriptional level, where several signalling pathways allow fine-tuned control of its expression, including diverse kinases and phosphatases (Marquina *et al*.,

2012; Ruiz *et al*., 2007). Nevertheless, some authors proposed that Nha1 regulation is not mediated by transcriptional changes, but rather through Hog1-mediated phosphorylation of threonine residues (Kinclova-Zimmermannova, *et al*. 2006; Krauke *et al*., 2011; Proft *et al*., 2004).

It was found that the *ena5* ATPase was highly induced under salt stress conditions, and the induction was exacerbated in the mutant strain, suggesting the involvement of Ptc1 in the regulation of the gene expression. We propose that the sodium and lithium tolerance observed in the mutant cells could be caused by the increased efflux of lithium and sodium, mediated by the higher expression of *ena5*, although a decrease in the cation influx is also probably involved. In *S. cerevisiae*, the transcriptional regulated expression of ENA1 has been explained through the action of different signalling pathways involving several kinases (HOG1, PKA or SNF1) and phosphatases such as calcineurin, PTC1 or PPZ1/HAL3 (Martin-Urdiroz *et al.*, 2008).

An interesting finding in this work was that, in contrast to yeast, the *F. oxysporum* antiporter Nha1 was transcriptionally regulated, and similarly to *Ena5*, *Nha1* expression level was higher in the mutant than in the wild-type strain. This study revealed that expression levels of *ena5* and *nha1* were induced under salt stress in a Hog1-dependent manner. In *Cryptococcus neoformans*, Nha1 was also transcriptionally regulated in response to salt stress in a Hog1-dependent manner and also regulated by the Rim101-Nrg1 pathway (Jung *et al*., 2012).

Previous transcriptional analysis in yeast identified signalling transduction genes upregulated in response to saline stress, some of them involved in the HOG pathway, including *HOG1* (Posas *et al*., 2000). The authors reported that transcriptional induction of most genes that are strongly responsive to salt stress, was highly or fully dependent on the presence of HOG1, indicating that the HOG1 mediated signalling pathway plays a key role in global gene regulation under saline stress conditions. Our results indicated an important induction of *F. oxysporum hog1* in response to salt stress. This induction was higher in the Δ*ptc1* mutant in comparison with the wild-type

strain, suggesting a direct or indirect implication of Ptc1 in *hog1* expression upon stress.

As already mencioned, the expression of *Ptc1* was stress induced, specially under osmotic stress conditions, suggesting a putative role in response to this injuries. We found that expression of an additional PP2C gene, *Ptc3*, was slightly induced in the wild-type strain after NaCl treatment, and that this induction was higher in the Δ*ptc1* mutant. These results suggest that the lack of Ptc1 can be partially compensated by the action of Ptc3, similarly to the results previously obtained in *A. fumigatus* by Winkelstroter *et al*., (2015a) demonstrating that lack of PtcB phosphatase was supply by other PP2C phosphatases.

One of the most interesting aspects derived of our data is that the magnitude by which osmotic stress affects gene expression varies according to salt concentration and time after induction. *F. oxysporum CatA*, *Hog1* and *Ptc3* genes were highly expressed at lower salt concentration. This is in accordance with a previous report in yeast showing that treatment with low salt concentrations induced the expression of an important number of genes after 10 min incubation, whereas a small quantity of them remained upregulated after 20 min. By contrast, incubation with a higher salt concentration resulted in a higher number of genes induced after 20 min of treatment (Posas *et al*., 2000).

5.4 Vacuole fragmentation is regulated by Ptc1

Previous studies showed that PTC1 is required for the distribution of the mitochondria and the vacuole in yeast (Jin *et al.,* 2009; Roeder *et al*.,1998; Du *et al*., 2006). Additionally, vacuole fusion and fission appear to be HOG-regulated homeostatic mechanisms that restore the concentration of the cytosol. Here we demonstrated, for the first time, that hyperosmotic stress induced vacuole fragmentation in *F. oxysporum*, as it occurs in other fungi (Michaillat *et al*, 2013; Bone *et al*., 1998). We also showed that the lack of Ptc1 entailed a vacuolar system composed of small vacuoles mimicking osmotic stress conditions. In fact, no differences were observed between treated and non-treated mutant cells. A link between Ptc1 and vacuolar function in yeast

came from the finding that overexpression of VPS73, a protein involved in vacuole protein sorting, recues, beyond vacuolar fragmentation, other *ptc1* specific phenotypes (Gonzalez *et al*., 2006).

6.Conclusions

6. Conclusions

1. The genome of *F. oxysporum* f. sp. lycopersici codes for seven PP2C genes that are regulated during stress activating MAPK signalling.

2. *F. oxysporum* PP2C phosphatases have overlapping functions on the regulation of the basal phosphorylation levels of the MAPKs Mpk1, Hog1 and Fmk1.

3. Ptc1 is the major PP2C phosphatase implicated in the negative regulation of the High Osmolarity and Glycerol pathway in *F. oxyporum.*

4. Ptc1 has a role in the gene expression regulation of osmotic stress responsive genes in *F. oxysporum.*

5. Ptc1 presents a constitutive vacuolar fragmentation independent of osmotic stress.

7. References

7. References

Agrios, G. (2005) Plant diseases caused by fungi. Plant pathology, 4.

Alastruey-Izquierdo, A., M. Cuenca-Estrella, A. Monzon, E. Mellado & J. L. Rodriguez-Tudela (2008) Antifungal susceptibility profile of clinical Fusarium spp. isolates identified by molecular methods. J Antimicrob Chemother, 61, 805-9.

Alkan, N., E. A. Espeso & D. Prusky (2013) Virulence regulation of phytopathogenic fungi by pH. Antioxidants & redox signaling, 19, 1012-1025.

Andersen, J. N., O. H. Mortensen, G. H. Peters, P. G. Drake, L. F. Iversen, O. H. Olsen, P. G. Jansen, H. S. Andersen, N. K. Tonks & N. P. Moller (2001) Structural and evolutionary relationships among protein tyrosine phosphatase domains. Mol Cell Biol, 21, 7117-36.

Arie, T., I. Kaneko, T. Yoshida, M. Noguchi, Y. Nomura & I. Yamaguchi (2000) Mating-type genes from asexual phytopathogenic ascomycetes Fusarium oxysporum and Alternaria alternata. Molecular Plant-Microbe Interactions, 13, 1330-1339.

Arino, J., A. Casamayor & A. Gonzalez (2011) Type 2C protein phosphatases in fungi. Eukaryot Cell, 10, 21-33.

Baayen, R. P., K. O'Donnell, P. J. M. Bonants, E. Cigelnik, L. P. N. M. Kroon, E. J. A. Roebroeck & C. Waalwijk (2000) Gene Genealogies and AFLP Analyses in the Fusarium oxysporum Complex Identify Monophyletic and Nonmonophyletic Formae Speciales Causing Wilt and Rot Disease. Phytopathology, 90, 891-900.

Banuett, F. & I. Herskowitz (1994) Morphological Transitions in the Life Cycle of Ustilago maydis and Their Genetic Control by the a and b Loci. Experimental Mycology, 18, 247-266.

Bardwell, L. (2006) Mechanisms of MAPK signalling specificity. Biochem Soc Trans, 34, 837-41.

Barford, D., A. K. Das & M. P. Egloff (1998) The structure and mechanism of protein phosphatases: insights into catalysis and regulation. Annu Rev Biophys Biomol Struct, 27, 133-64.

Basse, C. W. & G. Steinberg (2004) Ustilago maydis, model system for analysis of the molecular basis of fungal pathogenicity. Mol Plant Pathol, 5, 83-92.

Bayram, O., O. S. Bayram, Y. L. Ahmed, J. Maruyama, O. Valerius, S. O. Rizzoli, R. Ficner, S. Irniger & G. H. Braus (2012) The Aspergillus nidulans MAPK module AnSte11-Ste50-Ste7-Fus3 controls development and secondary metabolism. PLoS Genet, 8, e1002816.

Beckman, C. H. 1987. The nature of wilt diseases of plants. APS press.

Bilsland, E., C. Molin, S. Swaminathan, A. Ramne & P. Sunnerhagen (2004) Rck1 and Rck2 MAPKAP kinases and the HOG pathway are required for oxidative stress resistance. Mol Microbiol, 53, 1743-56.

Bluhm, B. H., X. Zhao, J. E. Flaherty, J. R. Xu & L. D. Dunkle (2007) RAS2 regulates growth and pathogenesis in Fusarium graminearum. Mol Plant Microbe Interact, 20, 627-36.

Bodenmiller, B., S. Wanka, C. Kraft, J. Urban, D. Campbell, P. G. Pedrioli, B. Gerrits, P. Picotti, H. Lam, O. Vitek, M. Y. Brusniak, B. Roschitzki, C. Zhang, K. M. Shokat, R. Schlapbach, A. Colman-Lerner, G. P. Nolan, A. I. Nesvizhskii, M. Peter, R. Loewith, C. von Mering & R. Aebersold (2010) Phosphoproteomic analysis reveals interconnected system-wide responses to perturbations of kinases and phosphatases in yeast. Sci Signal, 3, rs4.

Bonangelino, C. J., E. M. Chavez & J. S. Bonifacino (2002) Genomic screen for vacuolar protein sorting genes in Saccharomyces cerevisiae. Molecular biology of the cell, 13, 2486-2501.

Boutati, E. I. & E. J. Anaissie (1997) Fusarium, a significant emerging pathogen in patients with hematologic malignancy: ten years' experience at a cancer center and implications for management. Blood, 90, 999-1008.

Bradshaw, N., V. M. Levdikov, C. M. Zimanyi, R. Gaudet, A. J. Wilkinson & R. Losick (2017) A widespread family of serine/threonine protein phosphatases shares a common regulatory switch with proteasomal proteases. Elife, 6.

Bravo-Ruiz, G., C. Ruiz-Roldan & M. I. Roncero (2013) Lipolytic system of the tomato pathogen Fusarium oxysporum f. sp. lycopersici. Mol Plant Microbe Interact, 26, 1054-67.

Brewster, J. L. & M. C. Gustin (2014) Hog1: 20 years of discovery and impact. Sci Signal, 7, re7.

Canero, D. C. & M. I. Roncero (2008) Functional analyses of laccase genes from Fusarium oxysporum. Phytopathology, 98, 509-18.

Caracuel, Z., A. L. Martinez-Rocha, A. Di Pietro, M. P. Madrid & M. I. Roncero (2005) Fusarium oxysporum gas1 encodes a putative beta-1,3-glucanosyltransferase required for virulence on tomato plants. Mol Plant Microbe Interact, 18, 1140-7.

Catlett, N. L., B.-N. Lee, O. C. Yoder & B. G. Turgeon (2003) Split-marker recombination for efficient targeted deletion of fungal genes. Fungal Genetics Reports, 50, 9-11.

Chang, L. & M. Karin (2001) Mammalian MAP kinase signalling cascades. Nature, 410, 37-40.

Chen, R. E. & J. Thorner (2007) Function and regulation in MAPK signaling pathways: lessons learned from the yeast Saccharomyces cerevisiae. Biochim Biophys Acta, 1773, 1311-40.

Cheng, A., K. E. Ross, P. Kaldis & M. J. Solomon (1999) Dephosphorylation of cyclin-dependent kinases by type 2C protein phosphatases. Genes Dev, 13, 2946-57.

Cho, Y., R. A. Cramer, Jr., K. H. Kim, J. Davis, T. K. Mitchell, P. Figuli, B. M. Pryor, E. Lemasters & C. B. Lawrence (2007) The Fus3/Kss1 MAP kinase homolog Amk1 regulates the expression of genes encoding hydrolytic enzymes in Alternaria brassicicola. Fungal Genet Biol, 44, 543-53.

Clarke, D. L., G. L. Woodlee, C. M. McClelland, T. S. Seymour & B. L. Wickes (2001) The Cryptococcus neoformans STE11alpha gene is similar to other fungal mitogen-activated protein kinase kinase kinase (MAPKKK) genes but is mating type specific. Mol Microbiol, 40, 200-13.

Cohen, P. (2000) The regulation of protein function by multisite phosphorylation--a 25 year update. Trends Biochem Sci, 25, 596-601.

Cohen, P. & P. T. Cohen (1989) Protein phosphatases come of age. J Biol Chem, 264, 21435-8.

Cousin, A., R. Mehrabi, M. Guilleroux, M. Dufresne, V. D. L. T, C. Waalwijk, T. Langin & G. H. Kema (2006) The MAP kinase-encoding gene MgFus3 of the non-appressorium phytopathogen Mycosphaerella graminicola is required for penetration and in vitro pycnidia formation. Mol Plant Pathol, 7, 269-78.

Cullen, P. J., W. Sabbagh, Jr., E. Graham, M. M. Irick, E. K. van Olden, C. Neal, J. Delrow, L. Bardwell & G. F. Sprague, Jr. (2004) A signaling mucin at the head of the Cdc42- and MAPK-dependent filamentous growth pathway in yeast. Genes Dev, 18, 1695-708.

Dagdas, Y. F. & T. O. Bozkurt (2015) Fungal Sex Receptors Recalibrated to Detect Host Plants. Cell Host Microbe, 18, 637-8.

Das, A. K., N. R. Helps, P. T. Cohen & D. Barford (1996) Crystal structure of the protein serine/threonine phosphatase 2C at 2.0 A resolution. Embo j, 15, 6798-809.

de Nadal, E. & F. Posas (2015) Osmostress-induced gene expression--a model to understand how stress-activated protein kinases (SAPKs) regulate transcription. Febs j, 282, 3275-85.

Dean, R., J. A. Van Kan, Z. A. Pretorius, K. E. Hammond-Kosack, A. Di Pietro, P. D. Spanu, J. J. Rudd, M. Dickman, R. Kahmann, J. Ellis & G. D. Foster (2012) The Top 10 fungal pathogens in molecular plant pathology. Mol Plant Pathol, 13, 414-30.

DeIulio, G. A., L. Guo, Y. Zhang, J. M. Goldberg, H. C. Kistler & L.-J. Ma (2018) Kinome Expansion in the Fusarium oxysporum Species Complex Driven by Accessory Chromosomes. mSphere, 3, e00231-18.

Delgado-Jarana, J., A. L. Martinez-Rocha, R. Roldan-Rodriguez, M. I. Roncero & A. Di Pietro (2005) Fusarium oxysporum G-protein beta subunit Fgb1 regulates hyphal growth, development, and virulence through multiple signalling pathways. Fungal Genet Biol, 42, 61-72.

Desjardins, A. E. 2006. Fusarium mycotoxins: chemistry, genetics, and biology. St. Paul: American Phytopathological Society (APS Press).

Desjardins, A. E., T. M. Hohn & S. P. McCormick (1993) Trichothecene biosynthesis in Fusarium species: chemistry, genetics, and significance. Microbiol Rev, 57, 595-604.

Di Pietro, A., F. I. García-Maceira, E. Meglecz & M. I. G. Roncero (2001) A MAP kinase of the vascular wilt fungus Fusarium oxysporum is essential for root penetration and pathogenesis. Molecular microbiology, 39, 1140-1152.

Di Pietro, A. & M. I. G. Roncero (1998) Cloning, expression, and role in pathogenicity of pg1 encoding the major extracellular endopolygalacturonase of the vascular wilt pathogen Fusarium oxysporum. Molecular plant-microbe interactions, 11, 91-98.

Di Pietro, A., M. I. G. Roncero & M. C. R. Roldán. 2009. From Tools of Survival to Weapons of Destruction: The Role of Cell Wall-Degrading Enzymes in Plant Infection. In Plant Relationships, ed. H. B. Deising, 181-200. Berlin, Heidelberg: Springer Berlin Heidelberg.

Diez-Orejas, R., G. Molero, F. Navarro-García, J. Pla, C. Nombela & M. Sanchez-Pérez (1997) Reduced virulence of Candida albicans MKC1 mutants: a role for mitogen-activated protein kinase in pathogenesis. Infection and Immunity, 65, 833.

Ding, Z., M. Li, F. Sun, P. Xi, L. Sun, L. Zhang & Z. Jiang (2015) Mitogen-activated protein kinases are associated with the regulation of physiological traits and virulence in Fusarium oxysporum f. sp. cubense. PLoS One, 10, e0122634.

Divon, H. H., C. Ziv, O. Davydov, O. Yarden & R. Fluhr (2006) The global nitrogen regulator, FNR1, regulates fungal nutrition-genes and fitness during Fusarium oxysporum pathogenesis. Mol Plant Pathol, 7, 485-97.

Dixon, K. P., J. R. Xu, N. Smirnoff & N. J. Talbot (1999) Independent signaling pathways regulate cellular turgor during hyperosmotic stress and appressorium-mediated plant infection by Magnaporthe grisea. Plant Cell, 11, 2045-58.

Dodds, P. N. & J. P. Rathjen (2010) Plant immunity: towards an integrated view of plant-pathogen interactions. Nat Rev Genet, 11, 539-48.

Dodou, E. & R. Treisman (1997) The Saccharomyces cerevisiae MADS-box transcription factor Rlm1 is a target for the Mpk1 mitogen-activated protein kinase pathway. Mol Cell Biol, 17, 1848-59.

Doehlemann, G., P. Berndt & M. Hahn (2006) Different signalling pathways involving a Galpha protein, cAMP and a MAP kinase control germination of Botrytis cinerea conidia. Mol Microbiol, 59, 821-35.

Du, Y., L. Walker, P. Novick & S. Ferro-Novick (2006) Ptc1p regulates cortical ER inheritance via Slt2p. The EMBO journal, 25, 4413-4422.

Duyvesteijn, R. G., R. van Wijk, Y. Boer, M. Rep, B. J. Cornelissen & M. A. Haring (2005) Frp1 is a Fusarium oxysporum F-box protein required for pathogenicity on tomato. Mol Microbiol, 57, 1051-63.

Elion, E. A. (1998) Routing MAP Kinase Cascades. Science, 281, 1625.

Elion, E. A., B. Satterberg & J. E. Kranz (1993) FUS3 phosphorylates multiple components of the mating signal transduction cascade: evidence for STE12 and FAR1. Mol Biol Cell, 4, 495-510.

Fan, J., M. Wu, L. Jiang & S.-H. Shen (2009) A serine/threonine protein phosphatase-like protein, CaPTC8, from Candida albicans defines a new PPM subfamily. Gene, 430, 64-76.

Feng, J., J. Zhao, J. Li, L. Zhang & L. Jiang (2010) Functional characterization of the PP2C phosphatase CaPtc2p in the human fungal pathogen Candida albicans. Yeast, 27, 753-64.

Fernandes, L., M. A. Araujo, A. Amaral, V. C. Reis, N. F. Martins & M. S. Felipe (2005) Cell signaling pathways in Paracoccidioides brasiliensis--inferred from comparisons with other fungi. Genet Mol Res, 4, 216-31.

Fuchs, B. B. & E. Mylonakis (2009) Our paths might cross: the role of the fungal cell wall integrity pathway in stress response and cross talk with other stress response pathways. Eukaryot Cell, 8, 1616-25.

Fujioka, T., O. Mizutani, K. Furukawa, N. Sato, A. Yoshimi, Y. Yamagata, T. Nakajima & K. Abe (2007) MpkA-Dependent and -independent cell wall integrity signaling in Aspergillus nidulans. Eukaryotic cell, 6, 1497-1510.

Furukawa, K. & S. Hohmann (2013) Synthetic biology: lessons from engineering yeast MAPK signalling pathways. Mol Microbiol, 88, 5-19.

Gawehns, F., P. M. Houterman, F. A. Ichou, C. B. Michielse, M. Hijdra, B. J. Cornelissen, M. Rep & F. L. Takken (2014) The Fusarium oxysporum effector Six6 contributes to virulence and suppresses I-2-mediated cell death. Mol Plant Microbe Interact, 27, 336-48.

Geiser, D. M., T. Aoki, C. W. Bacon, S. E. Baker, M. K. Bhattacharyya, M. E. Brandt, D. W. Brown, L. W. Burgess, S. Chulze, J. J. Coleman, J. C. Correll, S. F. Covert, P. W. Crous, C. A. Cuomo, G. S. De Hoog, A. Di Pietro, W. H. Elmer, L. Epstein, R. J. N. Frandsen, S. Freeman, T. Gagkaeva, A. E. Glenn, T. R. Gordon, N. F. Gregory, K. E. Hammond-Kosack, L. E. Hanson, M. d. M. Jímenez-Gasco, S. Kang, H. C. Kistler, G. A. Kuldau, J. F. Leslie, A. Logrieco, G. Lu, E. Lysøe, L.-J. Ma, S. P. McCormick, Q. Migheli, A. Moretti, F. Munaut, K. O'Donnell, L. Pfenning, R. C. Ploetz, R. H. Proctor, S. A. Rehner, V. A. R. G. Robert, A. P. Rooney, B. bin Salleh, M. M. Scandiani, J. Scauflaire, D. P. G. Short, E. Steenkamp, H. Suga, B. A. Summerell, D. A. Sutton, U. Thrane, F. Trail, A. Van Diepeningen, H. D. VanEtten, A. Viljoen, C. Waalwijk, T. J. Ward, M. J. Wingfield, J.-R. Xu, X.-B. Yang, T. Yli-Mattila & N. Zhang (2013) One Fungus, One Name: Defining the Genus Fusarium in a Scientifically Robust Way That Preserves Longstanding Use. Phytopathology, 103, 400-408.

Gey, U., C. Czupalla, B. Hoflack, G. Rodel & U. Krause-Buchholz (2008) Yeast pyruvate dehydrogenase complex is regulated by a concerted activity of two kinases and two phosphatases. J Biol Chem, 283, 9759-67.

Ghosh, A., J. A. Servin, G. Park & K. A. Borkovich (2014) Global analysis of serine/threonine and tyrosine protein phosphatase catalytic subunit genes in Neurospora crassa reveals interplay between phosphatases and the p38 mitogen-activated protein kinase. G3 (Bethesda), 4, 349-65.

Gold, S., G. Duncan, K. Barrett & J. Kronstad (1994) cAMP regulates morphogenesis in the fungal pathogen Ustilago maydis. Genes Dev, 8, 2805-16.

Gold, S. E., S. M. Brogdon, M. E. Mayorga & J. W. Kronstad (1997) The Ustilago maydis regulatory subunit of a cAMP-dependent protein kinase is required for gall formation in maize. Plant Cell, 9, 1585-94.

Gonzalez, A., C. Casado, J. Arino & A. Casamayor (2013) Ptc6 is required for proper rapamycin-induced down-regulation of the genes coding for ribosomal and rRNA processing proteins in S. cerevisiae. PLoS One, 8, e64470.

Gonzalez, A., A. Ruiz, A. Casamayor & J. Arino (2009) Normal function of the yeast TOR pathway requires the type 2C protein phosphatase Ptc1. Mol Cell Biol, 29, 2876-88.

González, A., A. Ruiz, R. Serrano, J. Ariño & A. Casamayor (2006) Transcriptional profiling of the protein phosphatase 2C family in yeast provides insights into the unique functional roles of Ptc1. Journal of Biological Chemistry, 281, 35057-35069.

Gower, E. W., L. J. Keay, R. A. Oechsler, A. Iovieno, E. C. Alfonso, D. B. Jones, K. Colby, S. S. Tuli, S. R. Patel, S. M. Lee, J. Irvine, R. D. Stulting, T. F. Mauger & O. D. Schein (2010) Trends in fungal keratitis in the United States, 2001 to 2007. Ophthalmology, 117, 2263-7.

Guarro, J. & J. Gene (1995) Opportunistic fusarial infections in humans. Eur J Clin Microbiol Infect Dis, 14, 741-54.

Guillemain, G., E. Ma, S. Mauger, S. Miron, R. Thai, R. Guerois, F. Ochsenbein & M. C. Marsolier-Kergoat (2007) Mechanisms of checkpoint kinase Rad53 inactivation after a double-strand break in Saccharomyces cerevisiae. Mol Cell Biol, 27, 3378-89.

Guo, X., N. M. Niemi, J. J. Coon & D. J. Pagliarini (2017a) Integrative proteomics and biochemical analyses define Ptc6p as the Saccharomyces cerevisiae pyruvate dehydrogenase phosphatase. Journal of Biological Chemistry, jbc. M117. 787341.

Guo, X., N. M. Niemi, P. D. Hutchins, S. G. Condon, A. Jochem, A. Ulbrich, A. J. Higbee, J. D. Russell, A. Senes & J. J. Coon (2017b) Ptc7p dephosphorylates select mitochondrial proteins to enhance metabolic function. Cell reports, 18, 307-313.

Haghnazari, E. & W. D. Heyer (2004) The Hog1 MAP kinase pathway and the Mec1 DNA damage checkpoint pathway independently control the cellular responses to hydrogen peroxide. DNA Repair (Amst), 3, 769-76.

Hamel, L. P., M. C. Nicole, S. Duplessis & B. E. Ellis (2012) Mitogen-activated protein kinase signaling in plant-interacting fungi: distinct messages from conserved messengers. Plant Cell, 24, 1327-51.

Hanaoka, N., Y. Takano, K. Shibuya, H. Fugo, Y. Uehara & M. Niimi (2008) Identification of the putative protein phosphatase gene PTC1 as a virulence-related gene using a silkworm model of Candida albicans infection. Eukaryotic cell, 7, 1640-1648.

Hogenhout, S. A., R. A. Van der Hoorn, R. Terauchi & S. Kamoun (2009) Emerging concepts in effector biology of plant-associated organisms. Mol Plant Microbe Interact, 22, 115-22.

Hohmann, S. (2009) Control of high osmolarity signalling in the yeast Saccharomyces cerevisiae. FEBS Lett, 583, 4025-9.

Hou, Z., C. Xue, Y. Peng, T. Katan, H. C. Kistler & J. R. Xu (2002) A mitogen-activated protein kinase gene (MGV1) in Fusarium graminearum is required for female fertility, heterokaryon formation, and plant infection. Mol Plant Microbe Interact, 15, 1119-27.

Houterman, P. M., B. J. Cornelissen & M. Rep (2008) Suppression of plant resistance gene-based immunity by a fungal effector. PLoS Pathog, 4, e1000061.

Houterman, P. M., L. Ma, G. van Ooijen, M. J. de Vroomen, B. J. Cornelissen, F. L. Takken & M. Rep (2009) The effector protein Avr2 of the xylem-colonizing fungus Fusarium oxysporum activates the tomato resistance protein I-2 intracellularly. Plant J, 58, 970-8.

Houterman, P. M., D. Speijer, H. L. Dekker, D. E. K. CG, B. J. Cornelissen & M. Rep (2007) The mixed xylem sap proteome of Fusarium oxysporum-infected tomato plants. Mol Plant Pathol, 8, 215-21.

Hruby, A., M. Zapatka, S. Heucke, L. Rieger, Y. Wu, U. Nussbaumer, S. Timmermann, A. Dunkler & N. Johnsson (2011) A constraint network of interactions: protein-protein interaction analysis of the yeast type II phosphatase Ptc1p and its adaptor protein Nbp2p. J Cell Sci, 124, 35-46.

Hu, G., A. Kamp, R. Linning, S. Naik & G. Bakkeren (2007) Complementation of Ustilago maydis MAPK mutants by a wheat leaf rust, Puccinia triticina homolog: potential for functional analyses of rust genes. Mol Plant Microbe Interact, 20, 637-47.

Huber, A., B. Bodenmiller, A. Uotila, M. Stahl, S. Wanka, B. Gerrits, R. Aebersold & R. Loewith (2009) Characterization of the rapamycin-sensitive phosphoproteome reveals that Sch9 is a central coordinator of protein synthesis. Genes & Development, 23, 1929-1943.

Igbaria, A., S. Lev, M. S. Rose, B. N. Lee, R. Hadar, O. Degani & B. A. Horwitz (2008) Distinct and combined roles of the MAP kinases of Cochliobolus heterostrophus in virulence and stress responses. Molecular plant-microbe interactions, 21, 769-780.

Imazaki, I., M. Kurahashi, Y. Iida & T. Tsuge (2007) Fow2, a Zn(II)2Cys6-type transcription regulator, controls plant infection of the vascular wilt fungus Fusarium oxysporum. Mol Microbiol, 63, 737-53.

Ito, S., T. Ihara, H. Tamura, S. Tanaka, T. Ikeda, H. Kajihara, C. Dissanayake, F. F. Abdel-Motaal & M. A. El-Sayed (2007) alpha-Tomatine, the major saponin in tomato, induces programmed cell death mediated by reactive oxygen species in the fungal pathogen Fusarium oxysporum. FEBS Lett, 581, 3217-22.

Ito, T., T. Chiba, R. Ozawa, M. Yoshida, M. Hattori & Y. Sakaki (2001) A comprehensive two-hybrid analysis to explore the yeast protein interactome. Proc Natl Acad Sci U S A, 98, 4569-74.

Jain, S., K. Akiyama, K. Mae, T. Ohguchi & R. Takata (2002) Targeted disruption of a G protein alpha subunit gene results in reduced pathogenicity in Fusarium oxysporum. Curr Genet, 41, 407-13.

James, A. G., R. M. Cook, S. M. West & J. G. Lindsay (1995) The pyruvate dehydrogenase complex of Saccharomyces cerevisiae is regulated by phosphorylation. FEBS Lett, 373, 111-4.

Jashni, M. K., I. H. Dols, Y. Iida, S. Boeren, H. G. Beenen, R. Mehrabi, J. Collemare & P. J. de Wit (2015) Synergistic Action of a Metalloprotease and a Serine Protease from Fusarium oxysporum f. sp. lycopersici Cleaves Chitin-Binding Tomato Chitinases, Reduces Their Antifungal Activity, and Enhances Fungal Virulence. Mol Plant Microbe Interact, 28, 996-1008.

Jenczmionka, N. J., F. J. Maier, A. P. Losch & W. Schafer (2003) Mating, conidiation and pathogenicity of Fusarium graminearum, the main causal agent of the head-blight disease of wheat, are regulated by the MAP kinase gpmk1. Curr Genet, 43, 87-95.

Jenczmionka, N. J. & W. Schafer (2005) The Gpmk1 MAP kinase of Fusarium graminearum regulates the induction of specific secreted enzymes. Curr Genet, 47, 29-36.

Jia, L. J. & W. H. Tang (2015) The omics era of Fusarium graminearum: opportunities and challenges. New Phytol, 207, 1-3.

Jiang, J., Y. Yun, Q. Yang, W. B. Shim, Z. Wang & Z. Ma (2011) A type 2C protein phosphatase FgPtc3 is involved in cell wall integrity, lipid metabolism, and virulence in Fusarium graminearum. PLoS One, 6, e25311.

Jiang, L., M. Whiteway, C. Ramos, J. R. Rodriguez-Medina & S. H. Shen (2002) The YHR076w gene encodes a type 2C protein phosphatase and represents the seventh PP2C gene in budding yeast. FEBS Lett, 527, 323-5.

Jiang, L., J. Yang, F. Fan, D. Zhang & X. Wang (2010) The type 2C protein phosphatase FgPtc1p of the plant fungal pathogen Fusarium graminearum is involved in lithium toxicity and virulence. Mol Plant Pathol, 11, 277-82.

Jin, K., L. Han & Y. Xia (2014) MaMk1, a FUS3/KSS1-type mitogen-activated protein kinase gene, is required for appressorium formation, and insect cuticle penetration of the entomopathogenic fungus Metarhizium acridum. J Invertebr Pathol, 115, 68-75.

Jin, Y., P. Taylor Eves, F. Tang & L. S. Weisman (2009) PTC1 is required for vacuole inheritance and promotes the association of the myosin-V vacuole-specific receptor complex. Molecular biology of the cell, 20, 1312-1323.

Joubert, A., N. Bataille-Simoneau, C. Campion, T. Guillemette, P. Hudhomme, B. Iacomi-Vasilescu, T. Leroy, S. Pochon, P. Poupard & P. Simoneau (2011) Cell wall integrity and high osmolarity glycerol pathways are required for adaptation of Alternaria brassicicola to cell wall stress caused by brassicaceous indolic phytoalexins. Cell Microbiol, 13, 62-80.

Journo, D., A. Mor & H. Abeliovich (2009) Aup1-mediated regulation of Rtg3 during mitophagy. J Biol Chem, 284, 35885-95.

Juneau, K., C. Nislow & R. W. Davis (2009) Alternative splicing of PTC7 in Saccharomyces cerevisiae determines protein localization. Genetics.

Jung, U. S., A. K. Sobering, M. J. Romeo & D. E. Levin (2002) Regulation of the yeast Rlm1 transcription factor by the Mpk1 cell wall integrity MAP kinase. Molecular Microbiology, 46, 781-789.

Kamada, Y., H. Qadota, C. P. Python, Y. Anraku, Y. Ohya & D. E. Levin (1996) Activation of yeast protein kinase C by Rho1 GTPase. J Biol Chem, 271, 9193-6.

Ketela, T., R. Green & H. Bussey (1999) Saccharomyces cerevisiae mid2p is a potential cell wall stress sensor and upstream activator of the PKC1-MPK1 cell integrity pathway. J Bacteriol, 181, 3330-40.

Kim, H. S., S. Y. Park, S. Lee, E. L. Adams, K. Czymmek & S. Kang (2011) Loss of cAMP-dependent protein kinase A affects multiple traits important for root pathogenesis by Fusarium oxysporum. Mol Plant Microbe Interact, 24, 719-32.

Klipp, E., B. Nordlander, R. Kruger, P. Gennemark & S. Hohmann (2005) Integrative model of the response of yeast to osmotic shock. Nat Biotechnol, 23, 975-82.

Kobayashi, T., M. Sadaie, M. Ohnishi, H. Wang, S. Ikeda, M. Hanada, Y. Yanagawa, T. Nakajima & S. Tamura (1998) Isoform-specific phosphorylation of fission yeast type 2C protein phosphatase. Biochem Biophys Res Commun, 251, 296-300.

Kojima, K., T. Kikuchi, Y. Takano, E. Oshiro & T. Okuno (2002) The mitogen-activated protein kinase gene MAF1 is essential for the early differentiation phase of appressorium formation in Colletotrichum lagenarium. Mol Plant Microbe Interact, 15, 1268-76.

Kojima, K., Y. Takano, A. Yoshimi, C. Tanaka, T. Kikuchi & T. Okuno (2004) Fungicide activity through activation of a fungal signalling pathway. Mol Microbiol, 53, 1785-96.

Kommedahl, T. 1966. RELATION OF EXUDATES OF PEA ROOTS TO GERMINATION OF SPORES IN RACES OF FUSARIUM OXYSPORUM F PISI. 721-+. AMER PHYTOPATHOLOGICAL SOC 3340 PILOT KNOB ROAD, ST PAUL, MN 55121 USA.

Kraus, P. R., D. S. Fox, G. M. Cox & J. Heitman (2003) The Cryptococcus neoformans MAP kinase Mpk1 regulates cell integrity in response to antifungal drugs and loss of calcineurin function. Molecular microbiology, 48, 1377-1387.

Krause-Buchholz, U., U. Gey, J. Wünschmann, S. Becker & G. Rödel (2006) YIL042c and YOR090c encode the kinase and phosphatase of the Saccharomyces cerevisiae pyruvate dehydrogenase complex. FEBS letters, 580, 2553-2560.

Krebs, E. G. & J. A. Beavo (1979) Phosphorylation-dephosphorylation of enzymes. Annu Rev Biochem, 48, 923-59.

Lairini, K., A. Perez-Espinosa, M. Pineda & M. Ruiz-Rubio (1996) Purification and characterization of tomatinase from Fusarium oxysporum f. sp. lycopersici. Appl Environ Microbiol, 62, 1604-9.

Lammers, T. & S. Lavi (2007) Role of type 2C protein phosphatases in growth regulation and in cellular stress signaling. Crit Rev Biochem Mol Biol, 42, 437-61.

Lawrence, C. L., C. H. Botting, R. Antrobus & P. J. Coote (2004) Evidence of a new role for the high-osmolarity glycerol mitogen-activated protein kinase pathway in yeast: regulating adaptation to citric acid stress. Mol Cell Biol, 24, 3307-23.

Leberer, E., D. Harcus, D. Dignard, L. Johnson, S. Ushinsky, D. Y. Thomas & K. Schroppel (2001) Ras links cellular morphogenesis to virulence by regulation of the MAP kinase and cAMP signalling pathways in the pathogenic fungus Candida albicans. Mol Microbiol, 42, 673-87.

Leng, Y. & S. Zhong (2015) The Role of Mitogen-Activated Protein (MAP) Kinase Signaling Components in the Fungal Development, Stress Response and Virulence of the Fungal Cereal Pathogen Bipolaris sorokiniana. PloS one, 10, e0128291-e0128291.

Leroy, C., S. E. Lee, M. B. Vaze, F. Ochsenbein, R. Guerois, J. E. Haber & M. C. Marsolier-Kergoat (2003) PP2C phosphatases Ptc2 and Ptc3 are required for DNA checkpoint inactivation after a double-strand break. Mol Cell, 11, 827-35.

Lesage, G., A.-M. Sdicu, P. Ménard, J. Shapiro, S. Hussein & H. Bussey (2004) Analysis of beta-1,3-glucan assembly in Saccharomyces cerevisiae using a synthetic interaction network and altered sensitivity to caspofungin. Genetics, 167, 35-49.

Lev, S., A. Sharon, R. Hadar, H. Ma & B. A. Horwitz (1999) A mitogen-activated protein kinase of the corn leaf pathogen Cochliobolus heterostrophus is involved in conidiation, appressorium formation, and pathogenicity: diverse roles for mitogen-activated protein kinase homologs in foliar pathogens. Proc Natl Acad Sci U S A, 96, 13542-7.

Levin, D. E. (2005) Cell wall integrity signaling in Saccharomyces cerevisiae. Microbiol Mol Biol Rev, 69, 262-91.

Li, G., X. Zhou & J.-R. Xu (2012) Genetic control of infection-related development in Magnaporthe oryzae. Current Opinion in Microbiology, 15, 678-684.

Lievens, B., P. M. Houterman & M. Rep (2009) Effector gene screening allows unambiguous identification of Fusarium oxysporum f. sp. lycopersici races and discrimination from other formae speciales. FEMS Microbiol Lett, 300, 201-15.

Lin, C. H. & K. R. Chung (2010) Specialized and shared functions of the histidine kinase- and HOG1 MAP kinase-mediated signaling pathways in Alternaria alternata, a filamentous fungal pathogen of citrus. Fungal Genet Biol, 47, 818-27.

Livak, K. J. & T. D. Schmittgen (2001) Analysis of relative gene expression data using real-time quantitative PCR and the 2(-Delta Delta C(T)) Method. Methods, 25, 402-8.

Lopez-Berges, M. S., D. I. P. A, M. J. Daboussi, H. A. Wahab, C. Vasnier, M. I. Roncero, M. Dufresne & C. Hera (2009) Identification of virulence genes in Fusarium oxysporum f. sp. lycopersici by large-scale transposon tagging. Mol Plant Pathol, 10, 95-107.

Lopez-Berges, M. S., J. Capilla, D. Turra, L. Schafferer, S. Matthijs, C. Jochl, P. Cornelis, J. Guarro, H. Haas & A. Di Pietro (2012) HapX-mediated iron homeostasis is essential for rhizosphere competence and virulence of the soilborne pathogen Fusarium oxysporum. Plant Cell, 24, 3805-22.

Lopez-Berges, M. S., C. Hera, M. Sulyok, K. Schafer, J. Capilla, J. Guarro & A. Di Pietro (2013) The velvet complex governs mycotoxin production and virulence of Fusarium oxysporum on plant and mammalian hosts. Mol Microbiol, 87, 49-65.

Lopez-Berges, M. S., K. Schafer, C. Hera & A. Di Pietro (2014) Combinatorial function of velvet and AreA in transcriptional regulation of nitrate utilization and secondary metabolism. Fungal Genet Biol, 62, 78-84.

Lu, G. & Y. Wang (2008) Functional diversity of mammalian type 2C protein phosphatase isoforms: new tales from an old family. Clin Exp Pharmacol Physiol, 35, 107-12.

Ma, L., P. M. Houterman, F. Gawehns, L. Cao, F. Sillo, H. Richter, M. J. Clavijo-Ortiz, S. M. Schmidt, S. Boeren, J. Vervoort, B. J. Cornelissen, M. Rep & F. L. Takken (2015) The AVR2-SIX5 gene pair is required to activate I-2-mediated immunity in tomato. New Phytol, 208, 507-18.

Ma, L. J., D. M. Geiser, R. H. Proctor, A. P. Rooney, K. O'Donnell, F. Trail, D. M. Gardiner, J. M. Manners & K. Kazan (2013) Fusarium pathogenomics. Annu Rev Microbiol, 67, 399-416.

Ma, L. J., H. C. van der Does, K. A. Borkovich, J. J. Coleman, M. J. Daboussi, A. Di Pietro, M. Dufresne, M. Freitag, M. Grabherr, B. Henrissat, P. M. Houterman, S. Kang, W. B. Shim, C. Woloshuk, X. Xie, J. R. Xu, J. Antoniw, S. E. Baker, B. H. Bluhm, A. Breakspear, D. W. Brown, R. A. Butchko, S. Chapman, R. Coulson, P. M. Coutinho, E. G. Danchin, A. Diener, L. R. Gale, D. M. Gardiner, S. Goff, K. E. Hammond-Kosack, K. Hilburn, A. Hua-Van, W. Jonkers, K. Kazan, C. D. Kodira, M. Koehrsen, L. Kumar, Y. H. Lee, L. Li, J. M. Manners, D. Miranda-Saavedra, M. Mukherjee, G. Park, J. Park, S. Y. Park, R. H. Proctor, A. Regev, M. C. Ruiz-Roldan, D. Sain, S. Sakthikumar, S. Sykes, D. C. Schwartz, B. G. Turgeon, I. Wapinski, O. Yoder, S. Young, Q. Zeng, S. Zhou, J. Galagan, C. A. Cuomo, H. C. Kistler & M. Rep (2010) Comparative genomics reveals mobile pathogenicity chromosomes in Fusarium. Nature, 464, 367-73.

Macias-Sanchez, K., J. Garcia-Soto, A. Lopez-Ramirez & G. Martinez-Cadena (2011) Rho1 and other GTP-binding proteins are associated with vesicles carrying glucose oxidase activity from Fusarium oxysporum f. sp. lycopersici. Antonie Van Leeuwenhoek, 99, 671-80.

Madden, K., Y. J. Sheu, K. Baetz, B. Andrews & M. Snyder (1997) SBF cell cycle regulator as a target of the yeast PKC-MAP kinase pathway. Science, 275, 1781-4.

Madhani, H. D. & G. R. Fink (1997) Combinatorial control required for the specificity of yeast MAPK signaling. Science, 275, 1314-7.

Madrid, M. P., A. Di Pietro & M. I. Roncero (2003) Class V chitin synthase determines pathogenesis in the vascular wilt fungus Fusarium oxysporum and mediates resistance to plant defence compounds. Mol Microbiol, 47, 257-66.

Maeda, T., A. Y. Tsai & H. Saito (1993) Mutations in a protein tyrosine phosphatase gene (PTP2) and a protein serine/threonine phosphatase gene (PTC1) cause a synthetic growth defect in Saccharomyces cerevisiae. Mol Cell Biol, 13, 5408-17.

Maeda, T., S. M. Wurgler-Murphy & H. Saito (1994) A two-component system that regulates an osmosensing MAP kinase cascade in yeast. Nature, 369, 242-5.

Maerz, S., C. Ziv, N. Vogt, K. Helmstaedt, N. Cohen, R. Gorovits, O. Yarden & S. Seiler (2008) The nuclear Dbf2-related kinase COT1 and the mitogen-activated protein kinases MAK1 and MAK2 genetically interact to regulate filamentous growth, hyphal fusion and sexual development in Neurospora crassa. Genetics, 179, 1313-1325.

Malleshaiah, M. K., V. Shahrezaei, P. S. Swain & S. W. Michnick (2010) The scaffold protein Ste5 directly controls a switch-like mating decision in yeast. Nature, 465, 101-5.

Manning, B. D., A. R. Tee, M. N. Logsdon, J. Blenis & L. C. Cantley (2002) Identification of the tuberous sclerosis complex-2 tumor suppressor gene product tuberin as a target of the phosphoinositide 3-kinase/akt pathway. Mol Cell, 10, 151-62.

Mapes, J. & I. M. Ota (2004) Nbp2 targets the Ptc1-type 2C Ser/Thr phosphatase to the HOG MAPK pathway. The EMBO journal, 23, 302-311.

Marasas, W. F. O., P. E. Nelson & T. A. Toussoun. 1984. Toxigenic Fusarium species. Identity and mycotoxicology. University Park: Pennsylvania State University.

Marin, M. J., M. Flandez, C. Bermejo, J. Arroyo, H. Martin & M. Molina (2009) Different modulation of the outputs of yeast MAPK-mediated pathways by distinct stimuli and isoforms of the dual-specificity phosphatase Msg5. Mol Genet Genomics, 281, 345-59.

Markovich, S., A. Yekutiel, I. Shalit, Y. Shadkchan & N. Osherov (2004) Genomic approach to identification of mutations affecting caspofungin susceptibility in Saccharomyces cerevisiae. Antimicrobial agents and chemotherapy, 48, 3871-3876.

Marsolier, M. C., P. Roussel, C. Leroy & C. Mann (2000) Involvement of the PP2C-like phosphatase Ptc2p in the DNA checkpoint pathways of Saccharomyces cerevisiae. Genetics, 154, 1523-32.

Martin-Udiroz, M., M. P. Madrid & M. I. Roncero (2004) Role of chitin synthase genes in Fusarium oxysporum. Microbiology, 150, 3175-87.

Martin-Urdiroz, M., M. I. Roncero, J. A. Gonzalez-Reyes & C. Ruiz-Roldan (2008) ChsVb, a class VII chitin synthase involved in septation, is critical for pathogenicity in Fusarium oxysporum. Eukaryot Cell, 7, 112-21.

Martinez-Rocha, A. L., M. I. Roncero, A. Lopez-Ramirez, M. Marine, J. Guarro, G. Martinez-Cadena & A. Di Pietro (2008) Rho1 has distinct functions in morphogenesis, cell wall biosynthesis and virulence of Fusarium oxysporum. Cell Microbiol, 10, 1339-51.

Mattern, I. E., P. J. Punt & C. Van den Hondel (1988) A vector for Aspergillus transformation conferring phleomycin resistance. Fungal Genetics Reports, 35, 25.

Mehrabi, R., T. Van der Lee, C. Waalwijk & H. J. Gert (2006) MgSlt2, a cellular integrity MAP kinase gene of the fungal wheat pathogen Mycosphaerella graminicola, is dispensable for penetration but essential for invasive growth. Mol Plant Microbe Interact, 19, 389-98.

Mey, G., K. Held, J. Scheffer, K. B. Tenberge & P. Tudzynski (2002) CPMK2, an SLT2-homologous mitogen-activated protein (MAP) kinase, is essential for pathogenesis of Claviceps purpurea on rye: evidence for a second conserved pathogenesis-related MAP kinase cascade in phytopathogenic fungi. Mol Microbiol, 46, 305-18.

Michielse, C. B., L. Reijnen, C. Olivain, C. Alabouvette & M. Rep (2012) Degradation of aromatic compounds through the beta-ketoadipate pathway is required for pathogenicity of the tomato wilt pathogen Fusarium oxysporum f. sp. lycopersici. Mol Plant Pathol, 13, 1089-100.

Michielse, C. B. & M. Rep (2009) Pathogen profile update: Fusarium oxysporum. Mol Plant Pathol, 10, 311-24.

Michielse, C. B., R. van Wijk, L. Reijnen, B. J. Cornelissen & M. Rep (2009a) Insight into the molecular requirements for pathogenicity of Fusarium oxysporum f. sp. lycopersici through large-scale insertional mutagenesis. Genome Biol, 10, R4.

Michielse, C. B., R. van Wijk, L. Reijnen, E. M. Manders, S. Boas, C. Olivain, C. Alabouvette & M. Rep (2009b) The nuclear protein Sge1 of Fusarium oxysporum is required for parasitic growth. PLoS Pathog, 5, e1000637.

Miguel-Rojas, C. & C. Hera (2013) Proteomic identification of potential target proteins regulated by the SCFFbp1-mediated proteolysis pathway in Fusarium oxysporum. Molecular Plant Pathology, 14, 934-945.

Miguel-Rojas, C. & C. Hera (2015) The F-box protein Fbp1 functions in the invasive growth and cell wall integrity mitogen-activated protein kinase (MAPK) pathways in Fusarium oxysporum. Molecular Plant Pathology.

Mirocha, C. J., H. K. Abbas, T. Kommedahl & B. B. Jarvis (1989) Mycotoxin production by Fusarium oxysporum and Fusarium sporotrichioides isolated from Baccharis spp. from Brazil. Applied and Environmental Microbiology, 55, 254-255.

Mitchell, T. K. & R. A. Dean (1995) The cAMP-dependent protein kinase catalytic subunit is required for appressorium formation and pathogenesis by the rice blast pathogen Magnaporthe grisea. Plant Cell, 7, 1869-78.

Moorhead, G. B., L. Trinkle-Mulcahy & A. Ulke-Lemee (2007) Emerging roles of nuclear protein phosphatases. Nat Rev Mol Cell Biol, 8, 234-44.

Moretti, A., L. Ferracane, S. Somma, V. Ricci, G. Mule, A. Susca, A. Ritieni & A. Logrieco (2010) Identification, mycotoxin risk and pathogenicity of Fusarium species associated to fig endosepsis in Apulia. Food Additives and Contaminants, 27, 718-728.

Moriwaki, A., E. Kubo, S. Arase & J. Kihara (2006) Disruption of SRM1, a mitogen-activated protein kinase gene, affects sensitivity to osmotic and ultraviolet stressors in the phytopathogenic fungus Bipolaris oryzae. FEMS Microbiol Lett, 257, 253-61.

Mosch, H. U., R. L. Roberts & G. R. Fink (1996) Ras2 signals via the Cdc42/Ste20/mitogen-activated protein kinase module to induce filamentous growth in Saccharomyces cerevisiae. Proc Natl Acad Sci U S A, 93, 5352-6.

Muñoz, I., E. Simón, N. Casals, J. Clotet & J. Ariño (2002) Identification of multicopy suppressors of cell cycle arrest at the G1–S transition in Saccharomyces cerevisiae. Yeast, 20, 157-169.

Navarro-Velasco, G. Y., R. C. Prados-Rosales, A. Ortiz-Urquiza, E. Quesada-Moraga & A. Di Pietro (2011) Galleria mellonella as model host for the trans-kingdom pathogen Fusarium oxysporum. Fungal Genet Biol, 48, 1124-9.

Nucci, M. & E. Anaissie (2007) Fusarium infections in immunocompromised patients. Clinical microbiology reviews, 20, 695-704.

O'Donnell, K., H. C. Kistler, E. Cigelnik & R. C. Ploetz (1998) Multiple evolutionary origins of the fungus causing Panama disease of banana: concordant evidence from nuclear and mitochondrial gene genealogies. Proc Natl Acad Sci U S A, 95, 2044-9.

O'Donnell, K., A. P. Rooney, R. H. Proctor, D. W. Brown, S. P. McCormick, T. J. Ward, R. J. Frandsen, E. Lysoe, S. A. Rehner, T. Aoki, V. A. Robert, P. W. Crous, J. Z. Groenewald, S. Kang & D. M. Geiser (2013) Phylogenetic analyses of RPB1 and RPB2 support a middle Cretaceous origin for a clade comprising all agriculturally and medically important fusaria. Fungal Genet Biol, 52, 20-31.

Odds, F. C., F. Van Gerven, A. Espinel-Ingroff, M. S. Bartlett, M. A. Ghannoum, M. V. Lancaster, M. A. Pfaller, J. H. Rex, M. G. Rinaldi & T. J. Walsh (1998) Evaluation of possible correlations between antifungal susceptibilities of filamentous fungi in vitro and antifungal treatment outcomes in animal infection models. Antimicrob Agents Chemother, 42, 282-8.

Ohkuni, K., A. Okuda & A. Kikuchi (2003) Yeast Nap1-binding protein Nbp2p is required for mitotic growth at high temperatures and for cell wall integrity. Genetics, 165, 517-529.

Olivain, C. & C. Alabouvette (1999) Process of tomato root colonization by a pathogenic strain of Fusarium oxysporum f. sp. lycopersici in comparison with a non-pathogenic strain. The New Phytologist, 141, 497-510.

Oliveira, A. P., C. Ludwig, P. Picotti, M. Kogadeeva, R. Aebersold & U. Sauer (2012) Regulation of yeast central metabolism by enzyme phosphorylation. Mol Syst Biol, 8, 623.

Ortoneda, M., J. Guarro, M. P. Madrid, Z. Caracuel, M. I. Roncero, E. Mayayo & A. Di Pietro (2004) Fusarium oxysporum as a multihost model for the genetic dissection of fungal virulence in plants and mammals. Infect Immun, 72, 1760-6.

Ozaki, K., K. Tanaka, H. Imamura, T. Hihara, T. Kameyama, H. Nonaka, H. Hirano, Y. Matsuura & Y. Takai (1996) Rom1p and Rom2p are GDP/GTP exchange proteins (GEPs) for the Rho1p small GTP binding protein in Saccharomyces cerevisiae. Embo j, 15, 2196-207.

Palacios, L., R. J. Dickinson, A. Sacristán-Reviriego, M. P. Didmon, M. J. Marín, H. Martín, S. M. Keyse & M. Molina (2011) Distinct docking mechanisms mediate interactions between the Msg5 phosphatase and mating or cell integrity mitogen-activated protein kinases (MAPKs) in Saccharomyces cerevisiae. The Journal of biological chemistry, 286, 42037-42050.

Pan, C., J.-y. Tang, Y.-f. Xu, P. Xiao, H.-d. Liu, H.-a. Wang, W.-b. Wang, F.-g. Meng, X. Yu & J.-p. Sun (2015) The catalytic role of the M2 metal ion in PP2Cα. Scientific Reports, 5, 8560.

Pao, L. I., K. Badour, K. A. Siminovitch & B. G. Neel (2007) Nonreceptor protein-tyrosine phosphatases in immune cell signaling. Annu Rev Immunol, 25, 473-523.

Pareja-Jaime, Y., M. Martin-Urdiroz, M. I. Roncero, J. A. Gonzalez-Reyes & C. Roldan Mdel (2010) Chitin synthase-deficient mutant of Fusarium oxysporum elicits tomato plant defence response and protects against wild-type infection. Mol Plant Pathol, 11, 479-93.

Pareja-Jaime, Y., M. I. Roncero & M. C. Ruiz-Roldan (2008) Tomatinase from Fusarium oxysporum f. sp. lycopersici is required for full virulence on tomato plants. Mol Plant Microbe Interact, 21, 728-36.

Park, G., S. Pan & K. A. Borkovich (2008) Mitogen-activated protein kinase cascade required for regulation of development and secondary metabolism in Neurospora crassa. Eukaryot Cell, 7, 2113-22.

Park, G., C. Xue, X. Zhao, Y. Kim, M. Orbach & J.-R. Xu (2006) Multiple upstream signals converge on the adaptor protein Mst50 in Magnaporthe grisea. The Plant Cell, 18, 2822-2835.

Park, S. M., E. S. Choi, M. J. Kim, B. J. Cha, M. S. Yang & D. H. Kim (2004) Characterization of HOG1 homologue, CpMK1, from Cryphonectria parasitica and evidence for hypovirus-mediated perturbation of its phosphorylation in response to hypertonic stress. Mol Microbiol, 51, 1267-77.

Parsons, A. B., R. L. Brost, H. Ding, Z. Li, C. Zhang, B. Sheikh, G. W. Brown, P. M. Kane, T. R. Hughes & C. Boone (2004) Integration of chemical-genetic and genetic interaction data links bioactive compounds to cellular target pathways. Nat Biotechnol, 22, 62-9.

Perez-Nadales, E. & A. Di Pietro (2015) The transmembrane protein Sho1 cooperates with the mucin Msb2 to regulate invasive growth and plant infection in Fusarium oxysporum. Mol Plant Pathol, 16, 593-603.

Perez-Nadales, E., M. F. Nogueira, C. Baldin, S. Castanheira, M. El Ghalid, E. Grund, K. Lengeler, E. Marchegiani, P. V. Mehrotra, M. Moretti, V. Naik, M. Oses-Ruiz, T. Oskarsson, K. Schafer, L. Wasserstrom, A. A. Brakhage, N. A. Gow, R. Kahmann, M. H. Lebrun, J. Perez-Martin, A. Di Pietro, N. J. Talbot, V. Toquin, A. Walther & J. Wendland (2014) Fungal model systems and the elucidation of pathogenicity determinants. Fungal Genet Biol, 70, 42-67.

Posas, F. & H. Saito (1998) Activation of the yeast SSK2 MAP kinase kinase kinase by the SSK1 two-component response regulator. Embo j, 17, 1385-94.

Posas, F., S. M. Wurgler-Murphy, T. Maeda, E. A. Witten, T. C. Thai & H. Saito (1996) Yeast HOG1 MAP kinase cascade is regulated by a multistep phosphorelay mechanism in the SLN1-YPD1-SSK1 "two-component" osmosensor. Cell, 86, 865-75.

Prados-Rosales, R. C. & A. Di Pietro (2008) Vegetative hyphal fusion is not essential for plant infection by Fusarium oxysporum. Eukaryotic Cell, 7, 162-171.

Pryciak, P. M. & F. A. Huntress (1998) Membrane recruitment of the kinase cascade scaffold protein Ste5 by the Gbetagamma complex underlies activation of the yeast pheromone response pathway. Genes Dev, 12, 2684-97.

Ptacek, J., G. Devgan, G. Michaud, H. Zhu, X. Zhu, J. Fasolo, H. Guo, G. Jona, A. Breitkreutz, R. Sopko, R. R. McCartney, M. C. Schmidt, N. Rachidi, S. J. Lee, A. S. Mah, L. Meng, M. J. Stark, D. F. Stern, C. De Virgilio, M. Tyers, B. Andrews, M. Gerstein, B. Schweitzer, P. F. Predki & M. Snyder (2005) Global analysis of protein phosphorylation in yeast. Nature, 438, 679-84.

Punt, P. J., R. P. Oliver, M. A. Dingemanse, P. H. Pouwels & C. A. van den Hondel (1987) Transformation of Aspergillus based on the hygromycin B resistance marker from Escherichia coli. Gene, 56, 117-24.

Pérez-Nadales, E. & A. Di Pietro (2011) The membrane mucin Msb2 regulates invasive growth and plant infection in Fusarium oxysporum. The Plant Cell, tpc. 110.075093.

López-Berges M.S.[1], Rispail N., Prados-Rosales R.C., A. Di Pietro. (2012) Signaling of Infectious Growth in Fusarium oxysporum. In Morphogenesis and Pathogenicity in Fungi, 61-79. Springer.

Qi, M. & E. A. Elion (2005) MAP kinase pathways. J Cell Sci, 118, 3569-72.

Ram, A. F., A. Wolters, R. Ten Hoopen & F. M. Klis (1994) A new approach for isolating cell wall mutants in Saccharomyces cerevisiae by screening for hypersensitivity to calcofluor white. Yeast, 10, 1019-30.

Ramamoorthy, V., X. Zhao, A. K. Snyder, J. R. Xu & D. M. Shah (2007) Two mitogen-activated protein kinase signalling cascades mediate basal resistance to antifungal plant defensins in Fusarium graminearum. Cell Microbiol, 9, 1491-506.

Ramos, B., F. M. Alves-Santos, M. A. Garcia-Sanchez, N. Martin-Rodrigues, A. P. Eslava & J. M. Diaz-Minguez (2007) The gene coding for a new transcription factor (ftf1) of Fusarium oxysporum is only expressed during infection of common bean. Fungal Genet Biol, 44, 864-76.

Ramos, C. W., U. Guldener, S. Klein, J. H. Hegemann, S. Gonzalez & J. R. Rodriguez-Medina (2000) Molecular analysis of the Saccharomyces cerevisiae YHR076w gene. IUBMB Life, 50, 371-7.

Rauyaree, P., M. D. Ospina-Giraldo, S. Kang, R. G. Bhat, K. V. Subbarao, S. J. Grant & K. F. Dobinson (2005) Mutations in VMK1, a mitogen-activated protein kinase gene, affect microsclerotia formation and pathogenicity in Verticillium dahliae. Curr Genet, 48, 109-16.

Rep, M., M. Meijer, P. M. Houterman, H. C. van der Does & B. J. Cornelissen (2005) Fusarium oxysporum evades I-3-mediated resistance without altering the matching avirulence gene. Mol Plant Microbe Interact, 18, 15-23.

Rep, M., H. C. van der Does, M. Meijer, R. van Wijk, P. M. Houterman, H. L. Dekker, C. G. de Koster & B. J. Cornelissen (2004) A small, cysteine-rich protein secreted by Fusarium oxysporum during colonization of xylem vessels is required for I-3-mediated resistance in tomato. Mol Microbiol, 53, 1373-83.

Rispail, N., D. M. Soanes, C. Ant, R. Czajkowski, A. Grunler, R. Huguet, E. Perez-Nadales, A. Poli, E. Sartorel, V. Valiante, M. Yang, R. Beffa, A. A. Brakhage, N. A. Gow, R. Kahmann, M. H. Lebrun, H. Lenasi, J. Perez-Martin, N. J. Talbot, J. Wendland & A. Di Pietro (2009) Comparative genomics of MAP kinase and calcium-calcineurin signalling components in plant and human pathogenic fungi. Fungal Genet Biol, 46, 287-98.

Rodríguez-Gálvez, E. & K. Mendgen (1995) The infection process ofFusarium oxysporum in cotton root tips. Protoplasma, 189, 61-72.

Roeder, A. D., G. J. Hermann, B. R. Keegan, S. A. Thatcher & J. M. Shaw (1998) Mitochondrial inheritance is delayed in Saccharomyces cerevisiae cells lacking the serine/threonine phosphatase PTC1. Molecular biology of the cell, 9, 917-930.

Ruan, H., Z. Yan, H. Sun & L. Jiang (2006) The YCR079w gene confers a rapamycin-resistant function and encodes the sixth type 2C protein phosphatase in Saccharomyces cerevisiae. FEMS yeast research, 7, 209-215.

Ruan H., Yan Z., Sun H., Jiang L. (2007) The YCR079w gene confers a rapamycin-resistant function and encodes the sixth type 2C protein phosphatase in Saccharomyces cerevisiae. FEMS Yeast Res, 7, 209-15.

Rui, O. & M. Hahn (2007) The Slt2-type MAP kinase Bmp3 of Botrytis cinerea is required for normal saprotrophic growth, conidiation, plant surface sensing and host tissue colonization. Mol Plant Pathol, 8, 173-84.

Ruiz, A., A. González, R. García-Salcedo, J. Ramos & J. Ariño (2006) Role of protein phosphatases 2C on tolerance to lithium toxicity in the yeast Saccharomyces cerevisiae. Molecular microbiology, 62, 263-277.

Ruiz, A., X. Xu & M. Carlson (2013) Ptc1 protein phosphatase 2C contributes to glucose regulation of SNF1/AMP-activated protein kinase (AMPK) in Saccharomyces cerevisiae. J Biol Chem, 288, 31052-8.

Ruiz-Roldan, C., Y. Pareja-Jaime, J. A. Gonzalez-Reyes & M. I. Roncero (2015) The Transcription Factor Con7-1 Is a Master Regulator of Morphogenesis and Virulence in Fusarium oxysporum. Mol Plant Microbe Interact, 28, 55-68.

Ruiz-Roldan, M. C., F. J. Maier & W. Schafer (2001) PTK1, a mitogen-activated-protein kinase gene, is required for conidiation, appressorium formation, and pathogenicity of Pyrenophora teres on barley. Mol Plant Microbe Interact, 14, 116-25.

Runner, V. M. & J. L. Brewster (2003) A genetic screen for yeast genes induced by sustained osmotic stress. Yeast, 20, 913-20.

Sacristán-Reviriego, A., H. Martín & M. Molina (2015) Identification of putative negative regulators of yeast signaling through a screening for protein phosphatases acting on cell wall integrity and mating MAPK pathways. Fungal Genetics and Biology, 77, 1-11.

Saito, H. & F. Posas (2012) Response to hyperosmotic stress. Genetics, 192, 289-318.

Sambade, M., M. Alba, A. M. Smardon, R. W. West & P. M. Kane (2005) A genomic screen for yeast vacuolar membrane ATPase mutants. Genetics, 170, 1539-1551.

Sambrook, J., E. F. Fritsch & T. Maniatis. 1989. Molecular cloning: a laboratory manual. Cold spring harbor laboratory press.

Schafer, K., A. Di Pietro, N. A. Gow & D. MacCallum (2014) Murine model for Fusarium oxysporum invasive fusariosis reveals organ-specific structures for dissemination and long-term persistence. PLoS One, 9, e89920.

Schweighofer, A., H. Hirt & I. Meskiene (2004) Plant PP2C phosphatases: emerging functions in stress signaling. Trends Plant Sci, 9, 236-43.

Schweighofer, A., V. Shubchynskyy, V. Kazanaviciute, A. Djamei & I. Meskiene (2014) Bimolecular fluorescent complementation (BiFC) by MAP kinases and MAPK phosphatases. Methods Mol Biol, 1171, 147-58.

Seeley, E. S., M. Kato, N. Margolis, W. Wickner & G. Eitzen (2002) Genomic analysis of homotypic vacuole fusion. Molecular biology of the cell, 13, 782-794.

Segmuller, N., U. Ellendorf, B. Tudzynski & P. Tudzynski (2007) BcSAK1, a stress-activated mitogen-activated protein kinase, is involved in vegetative differentiation and pathogenicity in Botrytis cinerea. Eukaryot Cell, 6, 211-21.

Segorbe, D., A. Di Pietro, E. Perez-Nadales & D. Turra (2017) Three Fusarium oxysporum mitogen-activated protein kinases (MAPKs) have distinct and complementary roles in stress adaptation and cross-kingdom pathogenicity. Mol Plant Pathol, 18, 912-924.

Seitomer, E., B. Balar, D. He, P. R. Copeland & T. G. Kinzy (2008) Analysis of Saccharomyces cerevisiae null allele strains identifies a larger role for DNA damage versus oxidative stress pathways in growth inhibition by selenium. Mol Nutr Food Res, 52, 1305-15.

Serber, Z. & J. E. Ferrell, Jr. (2007) Tuning bulk electrostatics to regulate protein function. Cell, 128, 441-4.

Serrano, R., D. Bernal, E. Simon & J. Arino (2004) Copper and iron are the limiting factors for growth of the yeast Saccharomyces cerevisiae in an alkaline environment. J Biol Chem, 279, 19698-704.

Serrano, R., H. Martin, A. Casamayor & J. Arino (2006) Signaling alkaline pH stress in the yeast Saccharomyces cerevisiae through the Wsc1 cell surface sensor and the Slt2 MAPK pathway. J Biol Chem, 281, 39785-95.

Sharmin, D., Y. Sasano, M. Sugiyama & S. Harashima (2014) Effects of deletion of different PP2C protein phosphatase genes on stress responses in Saccharomyces cerevisiae. Yeast, 31, 393-409.

Sharmin, D., Y. Sasano, M. Sugiyama & S. Harashima (2015) Type 2C protein phosphatase Ptc6 participates in activation of the Slt2-mediated cell wall integrity pathway in Saccharomyces cerevisiae. J Biosci Bioeng, 119, 392-8.

Shi, Y. (2009) Serine/threonine phosphatases: mechanism through structure. Cell, 139, 468-484.

Shitamukai, A., D. Hirata, S. Sonobe & T. Miyakawa (2004) Evidence for antagonistic regulation of cell growth by the calcineurin and high osmolarity glycerol pathways in Saccharomyces cerevisiae. J Biol Chem, 279, 3651-61.

Short, D. P., K. O'Donnell, N. Zhang, J. H. Juba & D. M. Geiser (2011) Widespread occurrence of diverse human pathogenic types of the fungus Fusarium detected in plumbing drains. J Clin Microbiol, 49, 4264-72.

Si, Y., Y. Yuan, Y. Wang, J. Gao, Y. Hu, S. Feng & J. Su (2016) Structural and Biochemical Characterization of a Cyanobacterial PP2C Phosphatase Reveals Insights into Catalytic Mechanism and Substrate Recognition. Catalysts, 6.

Smith, S. A., J. M. Beaulieu & M. J. Donoghue (2010) An uncorrelated relaxed-clock analysis suggests an earlier origin for flowering plants. Proc Natl Acad Sci U S A, 107, 5897-902.

Smith, S. N. & W. C. Snyder (1972) Germination of Fusarium oxysporum chlamydospores in soils favorable and unfavorable to wilt establishment. Phytopathology.

Snyder, W. C. & H. N. Hansen (1940) THE SPECIES CONCEPT IN FUSARIUM. American Journal of Botany, 27, 64-67.

So, K. K., Y. H. Ko, J. Chun, J. M. Kim & D. H. Kim (2017) Mutation of the Slt2 ortholog from Cryphonectria parasitica results in abnormal cell wall integrity and sectorization with impaired pathogenicity. Sci Rep, 7, 9038.

Solomon, P. S., O. D. Waters, J. Simmonds, R. M. Cooper & R. P. Oliver (2005) The Mak2 MAP kinase signal transduction pathway is required for pathogenicity in Stagonospora nodorum. Curr Genet, 48, 60-8.

Sperschneider, J., D. M. Gardiner, L. F. Thatcher, R. Lyons, K. B. Singh, J. M. Manners & J. M. Taylor (2015) Genome-Wide Analysis in Three Fusarium Pathogens Identifies Rapidly Evolving Chromosomes and Genes Associated with Pathogenicity. Genome biology and evolution, 7, 1613-1627.

Staleva, L., A. Hall & S. J. Orlow (2004) Oxidative stress activates FUS1 and RLM1 transcription in the yeast Saccharomyces cerevisiae in an oxidant-dependent Manner. Mol Biol Cell, 15, 5574-82.

Stanger, K., M. Gorelik & A. R. Davidson (2012) Yeast adaptor protein, Nbp2p, is conserved regulator of fungal Ptc1p phosphatases and is involved in multiple signaling pathways. The Journal of biological chemistry, 287, 22133-22141.

Stark, M. J. (1996) Yeast protein serine/threonine phosphatases: multiple roles and diverse regulation. Yeast, 12, 1647-75.

Szyjka, S. J., J. G. Aparicio, C. J. Viggiani, S. Knott, W. Xu, S. Tavaré & O. M. Aparicio (2008) Rad53 regulates replication fork restart after DNA damage in Saccharomyces cerevisiae. Genes & development, 22, 1906-1920.

Takano, Y., T. Kikuchi, Y. Kubo, J. E. Hamer, K. Mise & I. Furusawa (2000) The Colletotrichum lagenarium MAP kinase gene CMK1 regulates diverse aspects of fungal pathogenesis. Mol Plant Microbe Interact, 13, 374-83.

Takken, F. & M. Rep (2010) The arms race between tomato and Fusarium oxysporum. Mol Plant Pathol, 11, 309-14.

Tal, R., G. Winter, N. Ecker, D. J. Klionsky & H. Abeliovich (2007) Aup1p, a yeast mitochondrial protein phosphatase homolog, is required for efficient stationary phase mitophagy and cell survival. J Biol Chem, 282, 5617-24.

Tatjer, L., A. Gonzalez, A. Serra-Cardona, A. Barcelo, A. Casamayor & J. Arino (2016a) The Saccharomyces cerevisiae Ptc1 protein phosphatase attenuates G2-M cell cycle blockage caused by activation of the cell wall integrity pathway. Mol Microbiol, 101, 671-87.

Tatjer, L., A. Sacristan-Reviriego, C. Casado, A. Gonzalez, B. Rodriguez-Porrata, L. Palacios, D. Canadell, A. Serra-Cardona, H. Martin, M. Molina & J. Arino (2016b) Wide-Ranging Effects of the Yeast Ptc1 Protein Phosphatase Acting Through the MAPK Kinase Mkk1. Genetics, 202, 141-56.

Torres, A. M., N. F. Weeden & A. Martin (1993) Linkage among isozyme, RFLP and RAPD markers in Vicia faba. Theor Appl Genet, 85, 937-45.

Turra, D., D. Segorbe & A. Di Pietro (2014) Protein kinases in plant-pathogenic fungi: conserved regulators of infection. Annu Rev Phytopathol, 52, 267-88.

Tyson, J. J. & B. Novak (2008) Temporal organization of the cell cycle. Curr Biol, 18, R759-r768.

Uetz, P., L. Giot, G. Cagney, T. A. Mansfield, R. S. Judson, J. R. Knight, D. Lockshon, V. Narayan, M. Srinivasan, P. Pochart, A. Qureshi-Emili, Y. Li, B. Godwin, D. Conover, T. Kalbfleisch, G. Vijayadamodar, M. Yang, M. Johnston, S. Fields & J. M. Rothberg (2000) A comprehensive analysis of protein-protein interactions in Saccharomyces cerevisiae. Nature, 403, 623-7.

Urban, M., E. Mott, T. Farley & K. Hammond-Kosack (2003) The Fusarium graminearum MAP1 gene is essential for pathogenicity and development of perithecia. Mol Plant Pathol, 4, 347-59.

Valiante, V., R. Jain, T. Heinekamp & A. A. Brakhage (2009) The MpkA MAP kinase module regulates cell wall integrity signaling and pyomelanin formation in Aspergillus fumigatus. Fungal Genetics and Biology, 46, 909-918.

Valiante, V., J. Macheleidt, M. Foge & A. A. Brakhage (2015) The Aspergillus fumigatus cell wall integrity signaling pathway: drug target, compensatory pathways, and virulence. Front Microbiol, 6, 325.

van Dam, P., L. Fokkens, S. M. Schmidt, J. H. Linmans, H. C. Kistler, L. J. Ma & M. Rep (2016) Effector profiles distinguish formae speciales of Fusarium oxysporum. Environ Microbiol, 18, 4087-4102.

Van Thuat, N., W. Schafer & J. Bormann (2012) The stress-activated protein kinase FgOS-2 is a key regulator in the life cycle of the cereal pathogen Fusarium graminearum. Mol Plant Microbe Interact, 25, 1142-56.

VanEtten, H. D., J. W. Mansfield, J. A. Bailey & E. E. Farmer (1994) Two Classes of Plant Antibiotics: Phytoalexins versus "Phytoanticipins". The Plant Cell, 6, 1191.

Vartivarian, S. E., E. J. Anaissie & G. P. Bodey (1993) Emerging fungal pathogens in immunocompromised patients: classification, diagnosis, and management. Clin Infect Dis, 17 Suppl 2, S487-91.

Vidanes, G. M., F. D. Sweeney, S. Galicia, S. Cheung, J. P. Doyle, D. Durocher & D. P. Toczyski (2010) CDC5 inhibits the hyperphosphorylation of the checkpoint kinase Rad53, leading to checkpoint adaptation. PLoS biology, 8, e1000286-e1000286.

Wang, C., S. Zhang, R. Hou, Z. Zhao, Q. Zheng, Q. Xu, D. Zheng, G. Wang, H. Liu, X. Gao, J. W. Ma, H. C. Kistler, Z. Kang & J. R. Xu (2011) Functional analysis of the kinome of the wheat scab fungus Fusarium graminearum. PLoS Pathog, 7, e1002460.

Wang, J., Z. Yan, S. H. Shen, M. Whiteway & L. Jiang (2007) Expression of CaPTC7 is developmentally regulated during serum-induced morphogenesis in the human fungal pathogen Candida albicans. Can J Microbiol, 53, 237-44.

Wang, M., Q. Zhao, J. Yang, B. Jiang, F. Wang, K. Liu & X. Fang (2013) A mitogen-activated protein kinase Tmk3 participates in high osmolarity resistance, cell wall integrity maintenance and cellulase production regulation in Trichoderma reesei. PLoS One, 8, e72189.

Wang, Y. & H. G. Dohlman (2004) Pheromone signaling mechanisms in yeast: a prototypical sex machine. Science, 306, 1508-9.

Warmka, J., J. Hanneman, J. Lee, D. Amin & I. Ota (2001) Ptc1, a type 2C Ser/Thr phosphatase, inactivates the HOG pathway by dephosphorylating the mitogen-activated protein kinase Hog1. Molecular and cellular biology, 21, 51-60.

Watanabe, Y., G. Takaesu, M. Hagiwara, K. Irie & K. Matsumoto (1997) Characterization of a serum response factor-like protein in Saccharomyces cerevisiae, Rlm1, which has transcriptional activity regulated by the Mpk1 (Slt2) mitogen-activated protein kinase pathway. Molecular and cellular biology, 17, 2615-2623.

Widmann, C., S. Gibson, M. B. Jarpe & G. L. Johnson (1999) Mitogen-activated protein kinase: conservation of a three-kinase module from yeast to human. Physiol Rev, 79, 143-80.

Wiebe, M. G. (2002) Myco-protein from Fusarium venenatum: a well-established product for human consumption. Appl Microbiol Biotechnol, 58, 421-7.

Williams, A. H., M. Sharma, L. F. Thatcher, S. Azam, J. K. Hane, J. Sperschneider, B. N. Kidd, J. P. Anderson, R. Ghosh, G. Garg, J. Lichtenzveig, H. C. Kistler, T. Shea, S. Young, S. A. Buck, L. G. Kamphuis, R. Saxena, S. Pande, L. J. Ma, R. K. Varshney & K. B. Singh (2016) Comparative genomics and prediction of conditionally dispensable sequences in legume-infecting Fusarium oxysporum formae speciales facilitates identification of candidate effectors. BMC Genomics, 17, 191.

Winkelstroter, L. K., V. L. Bom, P. A. de Castro, L. N. Ramalho, M. H. Goldman, N. A. Brown, R. Rajendran, G. Ramage, E. Bovier, T. F. Dos Reis, M. Savoldi, D. Hagiwara & G. H. Goldman (2015a) High osmolarity glycerol response PtcB phosphatase is important for Aspergillus fumigatus virulence. Mol Microbiol, 96, 42-54.

Winkelstroter, L. K., S. K. Dolan, T. Fernanda Dos Reis, V. L. Bom, P. Alves de Castro, D. Hagiwara, R. Alowni, G. W. Jones, S. Doyle, N. A. Brown & G. H. Goldman (2015b) Systematic Global Analysis of Genes Encoding Protein Phosphatases in Aspergillus fumigatus. G3 (Bethesda), 5, 1525-39.

Wolfe, K. H. & D. C. Shields (1997) Molecular evidence for an ancient duplication of the entire yeast genome. Nature, 387, 708.

Wollenweber, H. W. (1931) Fusarium-Monographie. Zeitschrift für Parasitenkunde, 3, 269-516.

Wollenweber, H. W. & O. A. Reinking. 1935. Die fusarien, ihre beschreibung, schadwirkung und bekämpfung. P. Parey.

Woloshuk, C. P. & W. B. Shim (2013) Aflatoxins, fumonisins, and trichothecenes: a convergence of knowledge. FEMS Microbiol Rev, 37, 94-109.

Xie, M. W., F. Jin, H. Hwang, S. Hwang, V. Anand, M. C. Duncan & J. Huang (2005) Insights into TOR function and rapamycin response: chemical genomic profiling by using a high-density cell array method. Proc Natl Acad Sci U S A, 102, 7215-20.

Xu, C., R. Liu, Q. Zhang, X. Chen, Y. Qian & W. Fang (2017) The Diversification of Evolutionarily Conserved MAPK Cascades Correlates with the Evolution of Fungal Species and Development of Lifestyles. Genome Biol Evol, 9, 311-322.

Xu, J. R. (2000) Map kinases in fungal pathogens. Fungal Genet Biol, 31, 137-52.

Xu, J. R. & J. E. Hamer (1996) MAP kinase and cAMP signaling regulate infection structure formation and pathogenic growth in the rice blast fungus Magnaporthe grisea. Genes Dev, 10, 2696-706.

Xu, J. R., C. J. Staiger & J. E. Hamer (1998) Inactivation of the mitogen-activated protein kinase Mps1 from the rice blast fungus prevents penetration of host cells but allows activation of plant defense responses. Proc Natl Acad Sci U S A, 95, 12713-8.

Xue, T., D. Wang, S. Zhang, J. Ehlting, F. Ni, S. Jakab, C. Zheng & Y. Zhong (2008) Genome-wide and expression analysis of protein phosphatase 2C in rice and Arabidopsis. BMC Genomics, 9, 550.

Yang, L., L. Ukil, A. Osmani, F. Nahm, J. Davies, C. P. De Souza, X. Dou, A. Perez-Balaguer & S. A. Osmani (2004) Rapid production of gene replacement constructs and generation of a green fluorescent protein-tagged centromeric marker in Aspergillus nidulans. Eukaryot Cell, 3, 1359-62.

Yang, Q., J. Jiang, C. Mayr, M. Hahn & Z. Ma (2013) Involvement of two type 2C protein phosphatases BcPtc1 and BcPtc3 in the regulation of multiple stress tolerance and virulence of Botrytis cinerea. Environ Microbiol, 15, 2696-711.

Yoshimi, A., K. Kojima, Y. Takano & C. Tanaka (2005) Group III Histidine Kinase Is a Positive Regulator of Hog1-Type Mitogen-Activated Protein Kinase in Filamentous Fungi. Eukaryotic Cell, 4, 1820.

Young, C., J. Mapes, J. Hanneman, S. Al-Zarban & I. Ota (2002) Role of Ptc2 type 2C Ser/Thr phosphatase in yeast high-osmolarity glycerol pathway inactivation. Eukaryot Cell, 1, 1032-40.

Yu, L., J. Zhao, J. Feng, J. Fang, C. Feng, Y. Jiang, Y. Cao & L. Jiang (2010) Candida albicans CaPTC6 is a functional homologue for Saccharomyces cerevisiae ScPTC6 and encodes a type 2C protein phosphatase. Yeast, 27, 197-206.

Zhang, D., F. Fan, J. Yang, X. Wang, D. Qiu & L. Jiang (2010) FgTep1p is linked to the phosphatidylinositol-3 kinase signalling pathway and plays a role in the virulence of Fusarium graminearum on wheat. Mol Plant Pathol, 11, 495-502.

Zhang, W. & L. Shi (2004) Evolution of the PPM-family protein phosphatases in Streptomyces: duplication of catalytic domain and lateral recruitment of additional sensory domains. Microbiology, 150, 4189-97.

Zhang, Y. & L. J. Ma (2017) Deciphering Pathogenicity of Fusarium oxysporum From a Phylogenomics Perspective. Adv Genet, 100, 179-209.

Zhao, J., X. Sun, J. Fang, W. Liu, C. Feng & L. Jiang (2010) Identification and characterization of the type 2C protein phosphatase Ptc4p in the human fungal pathogen Candida albicans. Yeast, 27, 149-57.

Zheng, D., Y. Wang, Y. Han, J.-R. Xu & C. Wang (2016) UvHOG1 is important for hyphal growth and stress responses in the rice false smut fungus Ustilaginoidea virens. Scientific reports, 6, 24824-24824.

Zheng, L., M. Campbell, J. Murphy, S. Lam & J.-R. Xu (2000) The BMP1 gene is essential for pathogenicity in the gray mold fungus Botrytis cinerea. Molecular Plant-Microbe Interactions, 13, 724-732.

Fungal Genetics and Biology 118 (2018) 10–20

Contents lists available at ScienceDirect

Fungal Genetics and Biology

journal homepage: www.elsevier.com/locate/yfgbi

Regular Articles

Role of the phosphatase Ptc1 in stress responses mediated by CWI and HOG pathways in *Fusarium oxysporum*

Pedro Lemos, Carmen Ruiz-Roldán, Concepción Hera*

Departamento de Genética, Campus de Excelencia Internacional Agroalimentario ceiA3, Universidad de Córdoba, 14071 Córdoba, Spain

ARTICLE INFO

Keywords:
Fusarium oxysporum
PP2C phosphatases
MAPK
Stress response

ABSTRACT

Reversible protein phosphorylation is crucial for cell signal transduction in stress response. *Fusarium oxysporum* is a soil inhabiting fungus that can adapt to a wide range of ecological niches and environmental conditions. Three mitogen activated protein kinase (MAPK) cascades have been shown to orchestrate the response of the fungus to external insults such as high temperature, cell wall, oxidative or hyperosmotic stress in *F. oxysporum*. However, the protein phosphatases that fine-tune phosphorylation levels of different MAPKs in this fungus are unknown. In this study we show that the serine/threonine phosphatase Ptc1 regulates phosphorylation of the high osmolarity glycerol response (HOG) MAPK Hog1 and the cell wall integrity (CWI) MAPK Mpk1. A Δ*ptc1* mutant showed decreased phosphorylation levels of the Mpk1 and was more sensitive to cell wall damaging agents in comparison to the wild type strain. In contrast, this mutant exhibited higher phosphorylation levels of the p38 MAPK Hog1, increased tolerance to osmotic stress compounds and higher expression of genes induced by osmotic stress. Moreover, Δ*ptc1* contained fragmented vacuoles even in absence of the osmotic stressor, supporting the involvement of Ptc1 in the HOG pathway.

1. Introduction

Fungal pathogens can sense and respond to numerous stimuli from their environment including their host organism. Molecular perception of these stimuli is usually mediated by MAPK cascades, conserved three-tiered protein kinase modules composed of a MAPK kinase kinase (MAPKKK) that phosphorylates a downstream MAPK kinase (MAPKK) which activates the MAPK for the downstream activation of cellular signals (Segorbe et al., 2017; Turra et al., 2014; Widmann et al., 1999). Reversible phosphorylation of proteins, catalysed by the action of protein kinases and phosphatases, is at the midpoint of regulation of many biological processes (Arino et al., 2011; Pearson et al., 2001; Rispail and Di Pietro, 2010; Rispail et al., 2009; Shi, 2009). In eukaryotes, most phosphorylation events occur at serine and threonine residues, although tyrosine residues are also involved in phospho-regulation. Based on substrate specificity, protein phosphatases are classified into two major classes: serine/threonine (S/T) phosphatases and tyrosine phosphatases (PTP). There are three subfamilies in the S/T phosphatases: phosphoprotein phosphatases (PPPs), metal-dependent protein phosphatases (PPMs) and aspartate-based protein phosphatases (Shi, 2009). Type 2C protein phosphatases (PP2C) constitute a PPM subfamily of monomeric enzymes that dephosphorylate S/T residues and require metal cations $Mn2+$ or $Mg2+$ for their activity (Arino et al., 2011; Cohen, 1989; Jiang et al., 2011; Shi, 2009). These protein phosphatases are involved in a variety of cellular functions both in prokaryotes and eukaryotes (Aburai et al., 2013; Das et al., 1996; Lammers and Lavi, 2007; Lu and Wang, 2008).

Fusarium oxysporum is a soil pathogen that causes vascular wilt disease in a large number of field and greenhouse crops and has also been reported as an emerging human pathogen causing lethal systemic infection on immunocompromised patients (Dean et al., 2012; Nucci and Anaissie, 2007). Previous studies identified three MAPK pathways involved in *F. oxysporum* cell wall integrity (Mpk1), hyperosmotic stress response (Hog1) and invasive growth (Fmk1) (Di Pietro et al., 2001; Turra et al., 2014). A recent report indicated a positive and negative crosstalk between the three MAPK pathways regulating stress adaptation, virulence and development in *F. oxysporum* (Segorbe et al., 2017). However, the phosphatases controlling the equilibrium between phosphorylated and dephosphorylated MAPK status are still unknown.

The role of PP2C enzymes in fungi has been mainly explored in *Saccharomyces cerevisiae*, which contains seven genes (PTC1–PTC7) encoding PP2C phosphatases (Cheng et al., 1999; Ruan et al., 2007). All these proteins share a conserved PP2C catalytic domain accompanied by amino-terminal or carboxy-terminal extensions (Arino et al., 2011).

Abbreviations: CFW, calcofluor white; CWI, cell wall integrity; CR, congo red; HOG, high-osmolarity glycerol; SDS, sodium dodecyl sulphate

* Corresponding author.
E-mail address: ge1hedic@uco.es (C. Hera).

https://doi.org/10.1016/j.fgb.2018.05.004
Received 6 February 2018; Received in revised form 24 April 2018; Accepted 27 May 2018
Available online 02 June 2018

Yeast PP2Cs have been initially involved in the regulation of cell growth and stress signalling. The best characterized PP2C, PTC1, plays specific functional roles that are not shared by other family members (Gonzalez et al., 2006). Previous studies have shown that PTC1 negatively regulates the high-osmolarity glycerol (HOG) pathway through interaction with the adaptor protein Nbp2 (Mapes and Ota, 2004; Uetz et al., 2000). In addition to inactivating the HOG pathway, PTC1 negatively regulates the CWI pathway by inactivating MPK1 cascade and positively regulates the pheromone response FUS3 cascade (Arino et al., 2011). Nevertheless, recent evidence suggests that PP2C functions may be much more diverse. In addition to dephosphorylating HOG1, PTC1 was found to be involved in the regulation of cell wall integrity, tRNA splicing, sporulation, lithium tolerance, vacuolar endoplasmic reticulum dynamics and during cell division. Finally, PTC1 is also linked to the nutrient response regulated by the TOR pathway (Gonzalez et al., 2009).

Genome analysis of different filamentous fungi including *Aspergillus* spp., *F. graminearum*, *Neurospora crassa*, *Magnaporthe oryzae* and *Botritis cinerea* revealed the presence of multiple genes encoding putative PP2Cs (Arino et al., 2011; Yang et al., 2013) The wide distribution of PP2C in filamentous fungi suggests that they have conserved functions in a number of cellular processes. Here we characterised the role of phosphatase Ptc1 in *F. oxysporum*. We demonstrate that Ptc1 plays a dual role in the positive regulation of the Mpk1 cell integrity pathway and the negative regulation of the Hog1 pathway, as well as in the subsequent regulation of gene expression in response to osmotic stress.

2. Material and methods

2.1. Fungal isolates and culture conditions

Fusarium oxysporum f. sp. *lycopersici* race 2 wild-type 4287 (FGSC 9935) was used in all experiments. Fungal strains were stored at −80 °C with 30% glycerol as microconidia suspensions. For microconidia production and fungal development studies, cultures were grown in liquid potato dextrose broth (PDB) at 28 °C with shaking at 170 rpm (Di Pietro and Roncero, 1998).

2.2. Targeted gene deletion and gene complementation

Targeted gene replacement of *ptc1* gene in the wild-type background was performed by the split-marker strategy, as described previously (Lopez-Berges et al., 2010), using the hygromicin B resistance (Hyg^R) cassette as selectable marker. Complemented strains were obtained by cotransformation of Δ*ptc1* protoplasts with the wild type allele and the phleomycin resistance ($Phle^R$) cassette. Fig. S1 and Table S1 (See supporting information) summarizes the strategy for gene deletion and the oligonucleotides used to generate the PCR fragments for gene knock-out. PCRs were routinely performed in a BioRad T100 thermal cycler (Bio-Rad, Alcobendas, Spain) using Velocity DNA polymerase (Bioline, London, United Kingdom). The *ptc1* amplified flanking sequences were PCR fused with partially overlapping fragments of the Hyg^R cassette. Selection of transformants was performed on hygromycin- or phleomycin-containing plates isolating monoconidial colonies. The gDNA of the transformants was analysed by PCR and Southern blot to verify homologous insertion of the construct.

2.3. Growth assays on plate and liquid media

For the phenotypic analysis of colony growth, water droplets from serial dilutions containing 10^4, 5×10^3, 10^3, 2×10^2, 10^2 freshly obtained microconidia were plated onto agar plates containing complete rich medium YPD. Cell wall and membrane stress were performed on YPD plates supplemented with Sodium-dodecyl-sulfate (SDS 0.0125%) prepared in water; calcofluor white (CFW 50 μg/ml) prepared in 0.5% KOH, 83% glycerol (both from Sigma-Aldrich); congo red (CR 100 μg/ml) prepared in water. For oxidative stress YPDA plates were supplemented with menadione (20 μg/ml) prepared in DMSO and caffeine (5 mM) in water. Fungicide sensibility assays were performed on YPDA containing iprodione (20 μg/ml) and fludioxonil (20 μg/ml) prepared in ethanol or DMSO respectively. For hyperosmotic stress, YPDA plates were supplemented with Sodium chloride (NaCl 1.2 M), Sorbitol (1.25 M) and Potassium chloride (KCl 1.2 M). To measure metal tolerance YPD plates contained calcium chloride ($CaCl_2$ 0.3 M) or lithium chloride (LiCl 0.3 M). Plates were incubated at 28 °C and scanned. Colony area was measured using ImageJ software. Relative colony growth was calculated using the formula: Relative growth (%) = (growth area on stress media / growth area on YPGA) * 100. The average of three biological replicates was used to perform statistic significance test (*t-test*) comparing the strains Δ*ptc1* and *CΔptc1* with the wild-type strain. Heat tolerance was measured by inoculation of 5×10^4 fresh microconidia on PDA followed by incubation at 28 °C or 33 °C. For acetic acid tolerance assays, water droplets containing 5×10^4 fresh microconidia were inoculated on PDA plates and incubated at 28 °C. All plate assays included three replica plates and were performed three times with similar results.

For conidiation assays 1.25×10^8 fresh conidia were inoculated on 25 ml of PDB media and incubated 48 h at 28 °C with shaking (170 rpm). Aliquots of 1 ml were taken from each replicate to perform quantification of the conidia on a Leica DMR microscope using an haemocytometer (Marienfiend, Baden-Württemberg, Germany).

Germination was measured 13 h after inoculation of 3.19×10^6 conidia on 1 ml of diluted 1:10 minimal medium (MM) (0.05% KCl, 0.05% $MgSO_4$, 0.1% KH_2PO_4, 0.2124% $NaNO_3$, 0.1% Sacarose) (Puhalla, 1985), supplemented with 25 mM $NaNO_3$. One hundred events were counted by sample using a Leica DMR microscope (germinated or not germinated microconidia). Germination rate was calculated using the formula: Germination (%) = (germinated microconidia/total microconidia) * 100. Statistical analysis (*t-test*) was performed to compare the strains Δ*ptc1* and *CΔptc1* with the wild-type strain.

For protein and RNA extraction, 2.5×10^8 microconidia from each strain were inoculated on 50 ml of PDB. After 15 h of incubation at 28 °C and 170 rpm, the obtained germlings were filtered to remove completely the media, washed with sterile PDB, and then transferred to PDB supplemented with stress compounds. After stress treatment, mycelia were rapidly recovered, and frozen in liquid nitrogen. All liquid assays were repeat at least three time with similar results.

2.4. Protein purification and western blot analysis

Mycelial samples were obtained as described above, protein extraction and western blot analysis were performed as described previously (Miguel-Rojas and Hera, 2016; Segorbe et al., 2017). Equal amounts of protein were loaded to a 14% Tris-glycine 10% polyacrylamide gel using standard protocols (Sambrook and Maniatis, 2001). After electrophoresis separation, proteins were transferred to a 0.45 μm nitrocellulose membrane (Bio-Rad, Hercules, CA, USA) in a Trans-Blot Turbo Transfer System (Bio-Rad, Hercules, CA, USA) using the Trans-Blot RTA Transfer Kit, following manufacturer's instructions. The membranes were blocked using 5% Skim-Milk (Difco, Detroit, MI, USA) on PBS-Tween for 45 min and then incubated overnight with monoclonal antibodies on 1% BSA PBS-Tween to detect the phosphorylated and total MAPK proteins Mpk1 and Hog1 and Tubulin (loading control) as previously described (Miguel-Rojas and Hera, 2016; Perez-Nadales and Di Pietro, 2011; Segorbe et al., 2017). Phosphorylated Mpk1 and Fmk1 were detected using the Phospho-p44/42 MAPK (Erk1/2) (Thr202/Tyr204) (D13.14.4E) XPV R Rabbit monoclonal antibody (no. 4370) (Cell Signalling Technology, Danvers, MA, USA). Unphosphorylated Mpk1 and Fmk1 were detected using anti-Mpk1 (yN-19) (sc-6802) and anti-Fus3 (γN-19) (sc6772) respectively (Santa Cruz Biotechnology, Heidelberg, Germany). Phosphorylated

Hog1 was detected using the Phospho-p38 MAPK (Erk1/2) (Thr180/Tyr182) Rabbit monoclonal antibody (no. 9211S) (Cell Signalling Technology, Danvers, MA, USA). Unphosphorylated Hog1 was detected using anti-Hog1 Rabbit monoclonal antibody (y-215) (sc-9079) ((Santa Cruz Biotechnology, Heidelberg, Germany). Tubulin was detected using αTub Mouse monoclonal antibody (3H3087) (Santa Cruz Biotechnology, Heidelberg, Germany). Horseradish peroxidase (HRP)-conjugated anti-rabbit (no. 7074) (Cell Signalling Technology, Danvers, MA, USA), Horseradish peroxidase (HRP)-conjugated anti-mouse (no. 7076) (Cell Signalling Technology, Danvers, MA, USA), and donkey anti-goat IgG-HRP (sc2020) (Santa Cruz Biotechnology, Heidelberg, Germany) were used as secondary antibodies. After overnight incubation, the membranes were washed three times with PBS-Tween (10 min), incubated for 1 h with the correspondent secondary antibody, washed three times with PBS-Tween (10 min), and then visualized using the ECL Select western blotting detection reagent (GE Healthcare, Madrid, Spain) on LAS-1000 Intelligent Dark-box (Fuji Photo Film co, Tokyo, Japan).

Band intensity was quantified with Image J software v. 1.08 (National Health Institute, United States of America). The phosphorylation level was calculated by the ratio of phosphorylated protein versus non phosphorylated protein. Wild-type (time 0) was used to standardize the samples.

2.5. Nucleic acid purification, RT-PCR and RT-qPCR analyses

Total RNA and genomic DNA isolation from mycelia of *F. oxysporum* strains were performed following previously described protocols (Chomczynski and Sacchi, 1987; Raeder and Broda, 1985). Nucleic acid quality and quantity were determined by gel electrophoresis on ethidium bromide-stained agarose 1% gels and by spectrophotometric analysis in a NanoDrop ND-1000 spectrophotometer (NanoDrop Technologies, Wilmington, DE, USA).

First strand cDNA was synthesized from 2 μg of total RNA, using the Transcriptor cDNA Master (Roche Diagnostics, Basel, Switzerland). The RNA samples were previously treated with DNase I (Roche Diagnostics, Basel, Switzerland). RT-PCR tested assessment of genomic DNA contamination and quality of cDNA samples with primers *Act*-q7 and *Act*-q9 (primers designed flanking an intron on the *Actin* gene RNA transcript) and Expand high fidelity Taq DNA polymerase (Roche Diagnostics, Basel, Switzerland). DNase, cDNA synthesis, and RT-PCR reactions were prepared following the manufacturer's instructions. The resulting cDNA samples were diluted 1:1 on ultrapure deionized water for RT-qPCR assays.

RT-qPCR was performed using 7.5 μl FastStart Essential DNA Green master (Roche Diagnostics, Basel, Switzerland), 5 μl of cDNA (1:1) and 0.3 μl of each gene specific primer on a final volume of 15 μl. Analyses were performed using primers flanking an intron of each gene when possible (Table S1). The following PCR program was used for all reactions: an initial step of denaturation (10 min, 95 °C), followed by 40 cycles of 10 s at 95 °C, 10 s at 62 °C and 20 s at 72 °C, 5 s at 80 °C (Plate read), in a CFX-Connect Real Time System (Bio-Rad, Hercules, CA, USA). Gene expression fold-increase levels were calculated with the formula $2^{-\Delta\Delta Ct}$ (Livak and Schmittgen, 2001) related to the non-treated wild-type strain, using *actin* as reference gene. All experiments included three biological replicates and three technical replicates for each biological sample. Data were subjected to statistic significance test (*t-test*) comparing the expression levels with the non-treated wild-type strain level (time 0).

2.6. Vacuole staining and fluorescence microscopy

For vacuole analyses, 3.19×10^6 fresh conidia were inoculated on 1 ml diluted 1:10 MM supplied with 25 mM $NaNO_3$. After 13 h incubation at 28 °C 170 rpm shaking, germling aggregation was eliminated by 1 min vortexing and vacuoles were stained for 15 min in the dark using the fluorescent dye FM4-64 (T13320) (Invitrogen, Thermo Fisher Scientific co, Whaltan, MA, USA) at a final concentration of 4 mM FM4-64 dye. Samples were centrifuged for 5 min at 7000 rpm and 250 μl aliquots of the supernatant were incubated in the presence of 0.6 M NaCl. Un-treated control samples were supplemented with equal volume of fresh MM. After 15 min treatment at 28 °C samples were observed under optical and epifluorescence microscopy analysis using the Nomarsky technique or the appropriate filter set, respectively, in a Zeiss Axio Imager M2 Dual Cam microscope (Carl Zeiss MicroImaging GmbH, Göttingen, Germany). Examination using epifluorescence was performed with UV-light 340–380 nm and a filter block (BP 560/40, FT 585, BP 630/75). Images were captured with an Evolve Photometrics PV Cam digital camera using the Axiovision 4.8 software. Images were processed using Adobe Photoshop CS3 (Adobe Systems, Mountain views, CA, USA).

2.7. Plant infection and virulence-related phenotype assays

Tomato root infection assay was performed as described (Di Pietro et al., 2001), using the susceptible cultivar Monika (Syngenta Seeds, Almeria, Spain). Briefly, 2-week-old tomato seedlings were inoculated by submerging roots for 30 min in a suspension of 5×10^6 microconidia/mL of the different *F. oxysporum* strains, planted in vermiculite and maintained in a growth chamber (28 °C; photoperiod 14 h light/10 h dark). Ten plants were used for each treatment. Plant survival was recorded for 35 days. A Long-rank (Mantel-Cox) test was used to assess the statistical significance of the differences in survival among groups. Data were plotted using the software GraphPad Prism version 5. (GraphPad Software, La Jolla, CA, United States of America). $P < 0.05$ was considered to be significant. Experiments were performed three times with similar results.

For adhesion assays, the roots of tomato seedlings were placed in flasks containing a suspension of microconidia in PDB diluted 1:50 with water and supplemented with 20 mM glutamic acid. After 72 h incubation at 28 °C and 170 rpm, roots were photographed. The experiments were performed at least three times with similar results.

Invasive growth assays on cellophane membranes were performed as described (Lopez-Berges et al., 2010; Prados Rosales and Di Pietro, 2008) with some modifications, using solid MM supplemented with 50 mM NaNO3 and buffered with 100 mM MES. The pH of the media (5 or 7) were adjusted with 10 M NaOH.

3. Results

3.1. F. oxysporum FOXG_11525 encodes a PP2C phosphatase orthologous to S. cervisiae Ptc1.

The *F. graminearum* genome was reported to contain seven predicted PP2C phosphatase genes orthologous to the PP2C genes of *S. cerevisiae* (Jiang et al., 2011, 2010). Likewise, BLASTp searches in the *F. oxysporum* genome identified seven genes showing different levels of homology to *S. cerevisiae* PP2C genes (Table S2). Single orthologues to *S. cerevisiae* PTC1, PTC3, and PTC6 were found in the survey. Additionally, we found two predicted orthologues each for *S. cerevisiae PTC5* and *PTC7* (named *ptc5* and *ptc5R* and *ptc7* and *ptc7R*, respectively), as previously described in *F. graminearum* (Jiang et al., 2011). However, no *F. oxysporum* orthologues were detected in the blast analysis for *S. cerevisiae* PTC2 and PTC4.

The single *ptc1* orthologue, *FOXG_11525*, encodes a predicted 576 amino acid protein showing 43% identity to *S. cerevisiae* Ptc1 and 92% to *F. graminearum* Ptc1. Data from RNAseq analysis available at http://fungidb.org/fungidb/, revealed the presence of two different *ptc1* transcripts in *F. oxysporum*. The nucleotide sequence contained two introns, one of 521 nucleotides located at the 5′UTR region and a smaller intron of 52 nucleotides sited within the ORF.

As a first approach to unravel the biological role of Ptc1 in *F.*

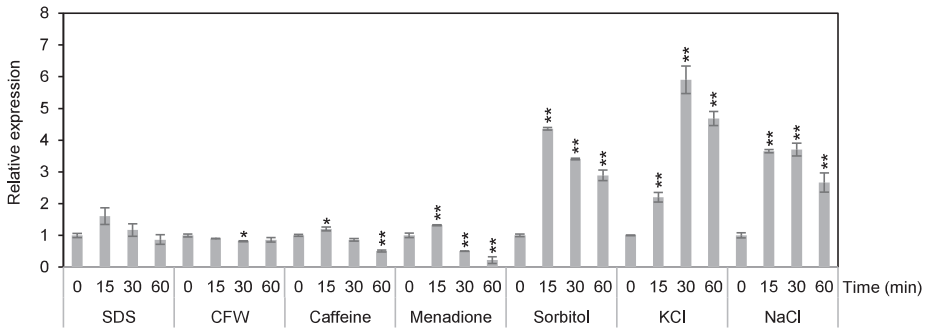

Fig. 1. Expression of *ptc1* is induced under oxidative and hyperosmotic stress. Germlings were transferred to potato dextrose broth (PDB) supplemented with the indicated stress compounds and RNA was obtained at the indicated time points. SDS (0.0125%), CFW (50 μg/ml); Caffeine (5 mM); Menadione (20 μg/ml); Sorbitol (1.25 M); KCl (1.2 M) and NaCl (0.6 M). Transcript levels are indicated as time-fold increase related to control samples (time 0), using *actin* as reference gene. The results are expressed as average (± standard deviation) of three independent biological repeats ($p < 0.05$(*); $p < 0.01$(**). Bars represent standard error.

oxysporum, we studied its expression in response to different stress conditions using RT-qPCR (Fig. 1). Although *ptc1* expression levels were low in all conditions tested, we found an increase of *ptc1* transcript in response to both hyperosmotic and salt stress (1M sorbitol, 1.2 M KCl, 0.6 M NaCl). By contrast, exposure to oxidative stress compounds (10 mM caffeine or 20 μg/ml menadione) led to a reduction in *ptc1* transcript levels. These results prompted us to further investigate the involvement of Ptc1 in the response to osmotic, oxidative and cell wall stresses.

3.2. Deletion of ptc1 leads to growth and developmental defects

To gain insight into the function of Ptc1, a null mutant was generated by replacing the entire coding region with the hygromycin resistance cassette. The selected transformants were analysed by PCR and Southern blot, to confirm that a homologous recombination event had occurred and that a single copy of the construct was introduced into the genome (Fig. S1). A Δ*ptc1* knockout strain was complemented with the *ptc1* wild-type allele by co-transformation with the phleomycin resistance cassette. PCR analysis of the resulting transformants using gene-specific primers yielded an amplification product identical to that obtained from the wild-type strain in five independent transformants, but not in the Δ*ptc1* mutant, suggesting that these strains had integrated an intact copy of the gene (Fig. S1).

To test the role of Ptc1 in vegetative hyphal growth, colony diameter of the different strains was measured in two different media: nutrient-rich PDA medium and nutrient-poor minimal medium (MM). Colony growth rate was not affected in the Δ*ptc1* mutant in comparison to the wild type strain, suggesting that Ptc1 is not involved in hyphal growth. Nevertheless, formation of growth sectors showing increased aerial hyphae formation was observed in the Δ*ptc1* mutant colonies grown on PDA or MM (Fig. 2A).

Two days after inoculation in liquid PDB medium we observed a 44% reduction of microconidia production in the Δ*ptc1* strain (Fig. 2B). Additionally, the conidial germination rate was significantly decreased in the mutant strain (Fig. 2C). These results suggest a role of Ptc1 in developmental processes of *F. oxysporum*.

3.3. Ptc1 contributes in response to cell wall, oxidative and acidity stress

The implication of Ptc1 in the cell wall integrity stress response pathway was reported in several fungi (Arino et al., 2011). To further investigate the biological role of *F. oxysporum* Ptc1, we determined the tolerance of Δ*ptc1* mutant to a range of stresses using plate dilution assays on YPGA medium supplemented with different compounds. Sensitivity of the Δ*ptc1* mutant to cell wall (calcofluor white, CFW and congo red, CR), membrane (sodium dodecyl sulphate, SDS) and oxidative stresses (menadione) was increased in comparison to the wild-type and complemented strains (Fig. 3 and Fig. S2). Here we found that loss of Ptc1 in *F. oxysporum* also reduced tolerance to calcium ions (Fig. 3 and Fig. S2). In *S. cerevisiae*, Δ*ptc1* mutant cells are highly sensitive to calcium ions, possibly due to hyperactivation of the phosphatase calcineurin (Gonzalez et al., 2006).

We next analysed the tolerance to acetic acid, since addition of acetic acid at low pH values was reported to activate the Hog1 and Slt2 pathways in yeast (Fuchs and Mylonakis, 2009; Hohmann, 2009). Indeed, growth of the Δ*ptc1* mutant was completely abolished on 0.05% acetic acid, in contrast to the wild-type strain that was still able to germinate and form a visible colony after 4 days (Fig. 3C). Finally, we observed that loss of Ptc1 resulted in increased tolerance to high temperature (Fig. 3C).

3.4. Ptc1 is involved in sensitivity to saline and osmotic stress

In order to know the role of Ptc1 in osmotic stress response, high concentration of salt (NaCl, KCl and LiCl) and osmolytes (sorbitol) was added to YPGA plates. Tolerance to the mentioned compounds was increased in Δ*ptc1* mutant compared to the wild-type strain. Moreover, the Δ*ptc1* mutant was more sensitive to the fungicide fludioxonil but more tolerant to iprodione (Fig. 3 and Fig. S2). In several fungi, resistance to fludioxonil was linked to sensitivity to hyperosmotic stress of Δ*hog1* mutants (Liu et al., 2017; Segorbe et al., 2017). Collectively, our results suggest a role of Ptc1 in the HOG response as previously reported in yeast and other fungi (Arino et al., 2011; Liu et al., 2017).

We next asked if the increased tolerance to salt and osmotic stress observed in Δ*ptc1* mutant strain was correlated with the expression of sodium and lithium transporters. In *S. cerevisiae,* two main mechanisms are used for the elimination of monovalent cations. The first is based on a P-type ATPase pump encoded by the ENA system (Arino et al., 2010). ENA genes are likely to exist in all fungal genomes, often as a gene family encoding similar proteins. Ena1 is involved in tolerance to high levels of monovalent cations such as Na^+ and Li^+ or alkaline pH, both in yeast and filamentous fungi (Caracuel et al., 2003; Krauke and Sychrova, 2011; Petrezselyova et al., 2016).

A recent paper identified FgENA5 as the most important ENA protein for extruding the excess of sodium in *F. graminearum* (Son et al., 2015). A BLAST search with the *ENA5* gene from *F. graminearum* identified *FOXG_09046* as the orthologous gene in *F. oxysporum*, named *ena5*. A strong induction of *ena5* expression was observed 15 min after exposure to 1.2 M NaCl, showing a gradual increase during the rest of the time course analysed (Fig. 4A). The expression level was slightly but significantly higher in the Δ*ptc1* mutant in comparison to the wild-type strain. Expression of *ena5* gene was exacerbated at lower and less toxic sodium concentration (0.6 M), reaching a maximum transcript amount

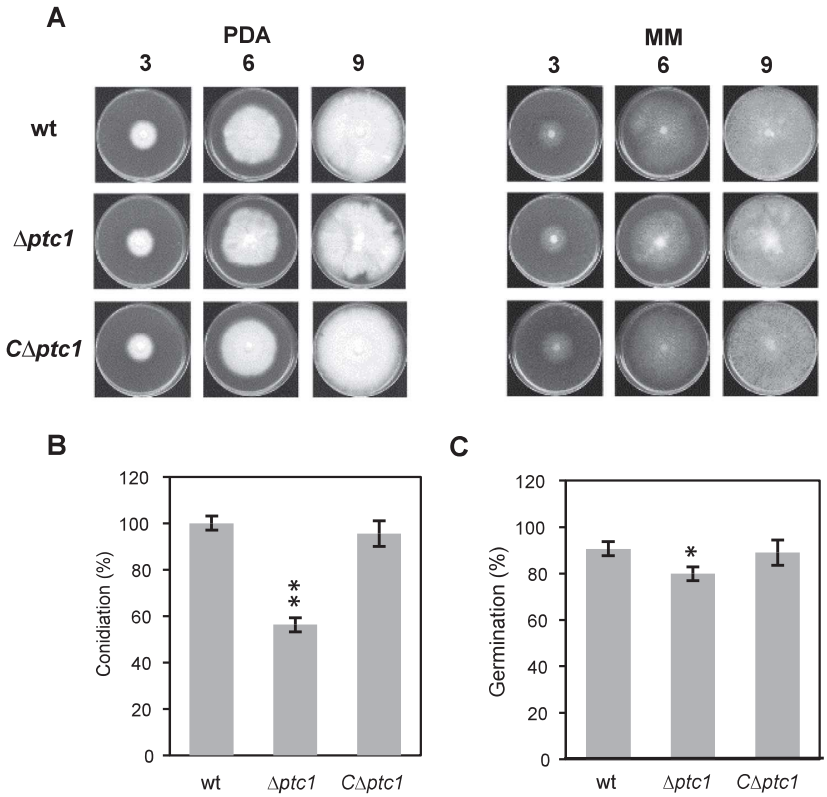

Fig. 2. Deletion of *ptc1* affects growth, conidiation and germination of *F. oxysporum*. (A) Aliquots of 5×10^4 fresh conidia of the wild-type (wt), Δ*ptc1* and CΔ*ptc1* strains were spot inoculated on potato dextrose agar (PDA) or minimal medium (MMP) plates. Growth was monitored 3, 6 and 9 days after inoculation. (B) Microconidia were counted 48h after inoculation on PDB medium. Conidiation rates are referred to wt levels (100%) (C) Germination rates were determined 13h after inoculation of fresh microconidia into diluted MM supplemented with 25 mM $NaNO_3$. (B–C) The results are expressed as average (± standard deviation) of three independent biological repeats ($p < 0.05$(*); $p < 0.01$(**). Statistical significance test (*t-test*) was performed comparing Δ*ptc1* and CΔ*ptc1* with wild-type strain. Bars represent standard error.

30 min after transfer to sodium containing medium in both strains. Importantly, the mutant lacking Ptc1 showed a twofold increase in *ena5* transcript levels after NaCl induction, suggesting that the Na^+-ATPase Ena5 is, at least in part, responsible for the increased tolerance of the Δ*ptc1* mutant to NaCl and LiCl.

A second strategy of *S. cerevisiae* to extrude monovalent cations is based on the H^+/Na^+ antiporter encoded by NHA1, which exchanges protons with Na^+, Li^+, and K^+ cations and is expressed constitutively at low levels (Arino et al., 2010). We measured the transcript levels of the predicted *F. oxysporum NHA1* orthologue *FOXG_11541*. Although the transcript levels were low throughout the time course experiment, an increase of expression in response to NaCl treatment was observed, which was significantly higher in the Δ*ptc1* mutant than in the wild-type strain (Fig. 4B).

3.5. Ptc1 regulates phosphorylation levels of the MAPKs Hog1 and Mpk1

Previous work revealed an interplay in stress responses between the three MAPK pathways in *F. oxysporum* (Segorbe et al., 2017). To investigate the role of Ptc1 in MAPK regulation, we monitored the phosphorylation status of Mpk1 and Hog1 using western blot of total proteins from mycelia treated with 0.0125% SDS. In the wild-type strain, Mpk1 phosphorylation was rapidly induced upon treatment with SDS (Fig. 5A). By contrast, the Δ*ptc1* mutant showed a significant reduction and delay in the phosphorylation level of Mpk1, suggesting that Ptc1 positively regulates the Mpk1 pathway. This is in line with the increased sensitivity of the mutant strain to SDS shown above (Fig. 3A and Fig. S2).

By contrast, we observed increased phosphorylation levels of Hog1 in the Δ*ptc1* mutant, both before and after SDS treatment. The high Hog1 phosphorylation level was continuous during the 60 min of the time course. Next, Hog1 phosphorylation levels were determined after treatment with high salt concentrations, which generate osmotic stress to the cell. We observed a strong induction of phosphorylation in the wild-type upon exposure to LiCl or NaCl (Fig. 5B). Again, in the Δ*ptc1* mutant Hog1 was constitutively phosphorylated even before induction, and the high phosphorylation level was maintained until 1 h after induction. Taken together, these findings strongly suggest that Ptc1 contributes to inactivation of the Hog1 pathway.

3.6. F. oxysporum Ptc1 regulates catalase gene expression

Catalase plays a role in oxidative, osmotic and pH stress responses and its transcriptional induction is dependent on the Hog1 pathway (Winkelstroter et al., 2015a). BLAST searches with the *Aspergillus* CatA and CatB genes detected two catalase orthologues in the genome of *F. oxysporum*, *FOXG_08697* and *FOXG_02405*. While the expression level of *FOXG_02405* was very low (data not shown), *FOXG_08697* (hereafter named *catA*) was markedly upregulated after 15 min exposure to 0.6 M NaCl (Fig. 6). Interestingly, induction of *catA* was about 2-fold higher in the Δ*ptc1* mutant than in the wild-type strain. These results suggest that increased phosphorylation level of Hog1 could be related to the higher *catA* expression observed in Δ*ptc1* mutant.

3.7. F. oxysporum hog1 and ptc3 expression levels respond to osmotic stress mediated by Ptc1

We found that *F. oxysporum hog1* transcript levels are also dependent on extracellular salt concentration, since a rapid induction was detected in response to 0.6 M NaCl, both in the wild-type and in the mutant strain, with a peak at 15 min after treatment (Fig. 7A). A higher, toxic concentration of 1.2 M NaCl triggered a strong increase of *hog1*

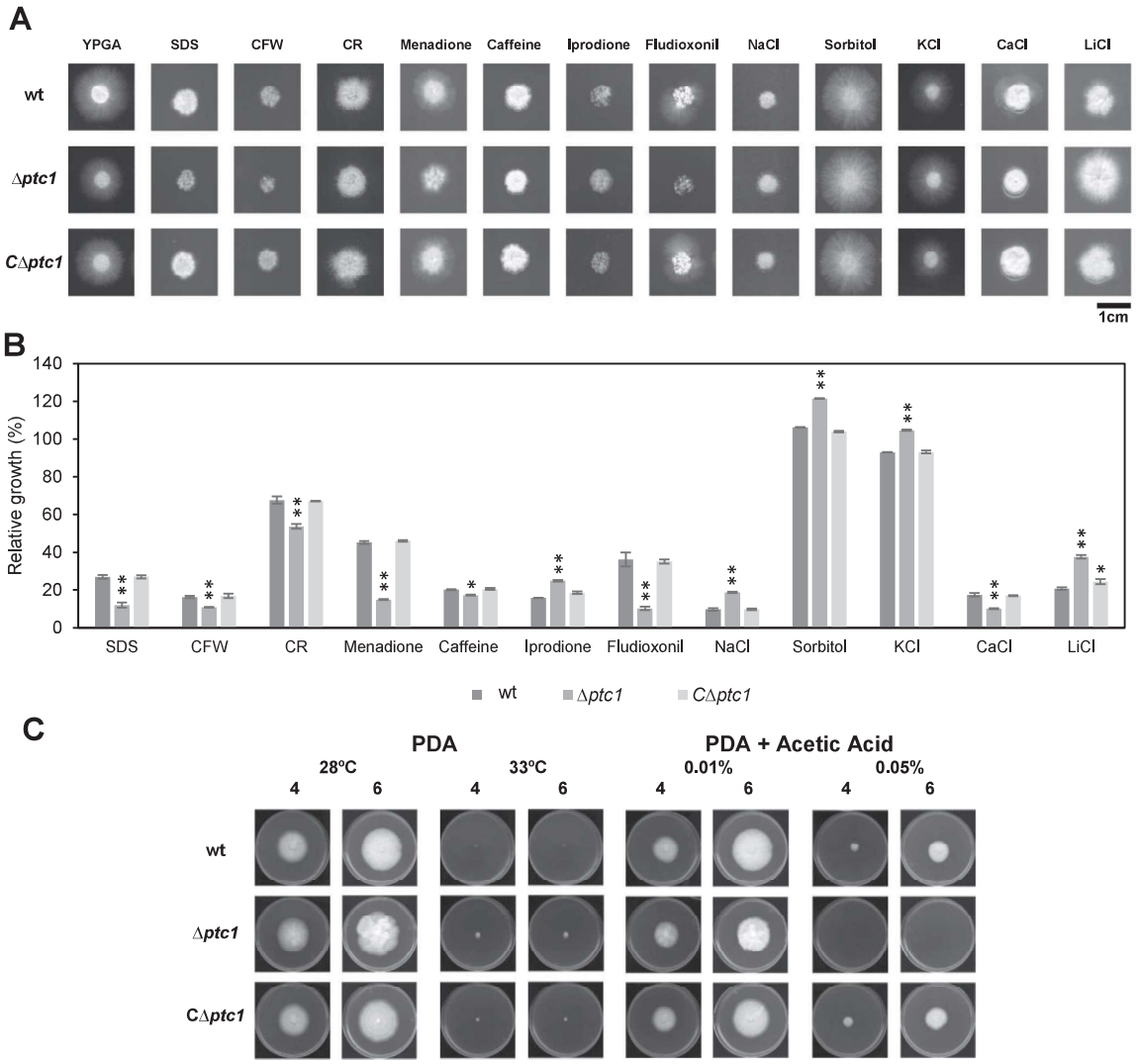

Fig. 3. Ptc1 functions in stress response (A) Aliquots containing 10^3 fresh microconidia of the wild-type (wt), Δ*ptc1* and CΔ*ptc1* strains were spot inoculated on YPGA plates supplemented with the indicated stress agents: SDS (0.0125%), CFW (50 μg/ml), CR (100 μg/ml), Menadione (20 μg/ml), Caffeine (5 mM), Iprodione (20 μg/ml), Fludioxonil (20 μg/ml), NaCl (1,2 M), Sorbitol (1.25 M), KCl (1.2 M), CaCl (0.3 M) and LiCl (0.3 M). Plates were scanned 48 h (KCl and iprodione); 72 h (SDS, CFW, CR, Menadione, Caffeine, Fludioxonil, NaCl, Sorbitol and CaCl); and 96 h (LiCl) after inoculation. Growth on YPGA media was measured after 48, 72 and 96 h (Fig S2) (B) Relative growth (%) of the different strains in the presence of the indicated stressors was calculated as the colony area on stressor-containing medium versus colony area on YPDA. Colony area was measured using the ImageJ software. Three biological replicates were used to perform statistical significance test (*t-test*) comparing Δ*ptc1* and *C* Δ*ptc1* with the wild-type strain, represented by $p < 0.05$(*); $p < 0.01$(**). (C) Growth of the indicated strains on PDA at 28 °C or 33 °C, or on PDA containing 0.05% and 0.01% Acetic Acid at 28 °C, was monitored 4 and 6 days after inoculation.

expression in the Δ*ptc1* mutant, but to a much lesser extent in the wild-type strain, indicating that the transcriptional response is fast and largely transient in the presence of 0.6 M NaCl compared to a higher salt concentration. It is known that the magnitude by which hyperosmotic stress affects gene expression depends on the severity and the time of the shock (Posas et al., 2000). Taken together our results indicate that Ptc1 regulates *hog1* expression upon osmotic stress induction.

To investigate the role of Ptc1 in the regulation of other PP2C phosphatases, we measured the expression of the *S. cerevisiae* PTC3 orthologue *FOXG_05154* in the wild-type and knockout strains after exposure to NaCl. We found that *ptc3* induction was significantly higher in the Δ*ptc1* mutant than in wild-type, especially after treatment with 1.2 M NaCl where no significant *ptc3* induction was detected in the wild-type background (Fig. 7B). The fact that Ptc3 accumulation is higher in Δ*ptc1* than in wild-type suggest a partial redundancy of the PP2C system as previously reported in *Aspergillus* (Winkelstroter et al., 2015b).

3.8. Constitutive vacuole fragmentation in Δptc1

In *S. cerevisiae,* PTC1 has been identified as a protein required for maintaining the structure and function of the vacuole (Arino et al., 2011; Bonangelino et al., 2002; Sambade et al., 2005). Vacuoles play a role in autophagy, osmoregulation and storage of amino acids and ions,

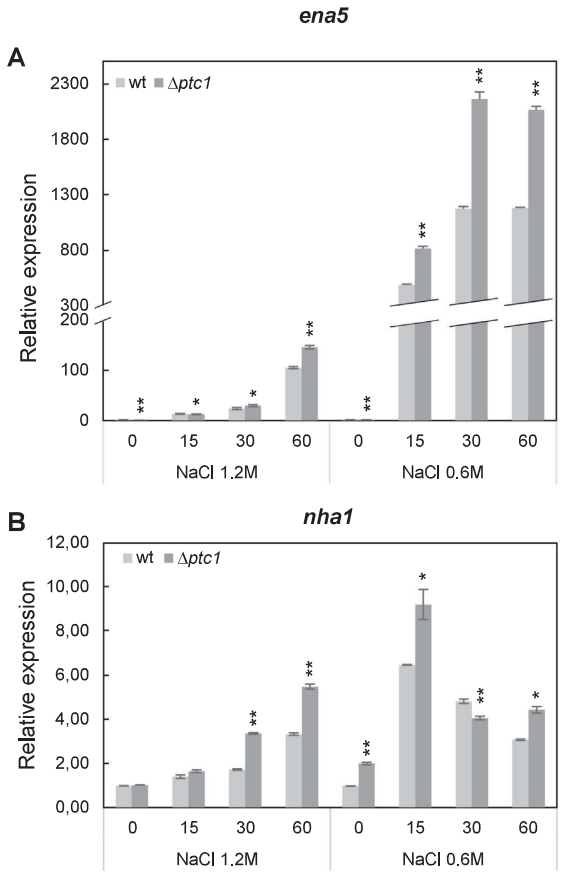

Fig. 4. Expression of *ena5* and *nha1* genes is induced by NaCl and regulated by Ptc1. Germlings of the wild-type (wt) strain and Δ*ptc1* mutant were transferred to PDB supplemented or not with NaCl 1.2 M or 0.6M for 15, 30 and 60 min. RT-qPCR analysis was performed using *ena5* (A) or *nha1* (B) gene specific primers. Expression is referred as time-fold increase relative to wild-type control (time 0), using *actin* as reference gene. The results are expressed as average (± standard deviation) of three independent biological repeats ($p < 0.05$(*); $p < 0.01$(**). Bars represent standard error.

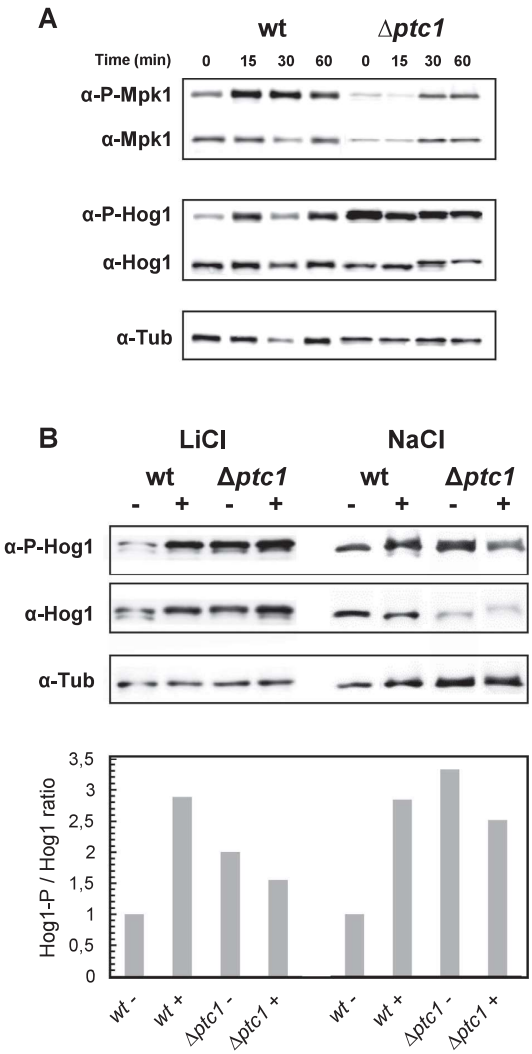

Fig. 5. Ptc1 regulates Mpk1 and Hog1 phosphorylation. Germlings of the wild-type (wt) strain and Δ*ptc1* mutant were transferred to (A) PDB supplemented with SDS (0.0125%) for 15, 30 and 60 min or (B) PDB with (+) or without (−) LiCl (0.3 M) or NaCl (1.2 M) for 60 min. Mycelia were frozen in liquid nitrogen before protein extraction and western-blot analysis to detect the phosphorylated and total MAPK levels (A) Mpk1 and Hog1, (B) Hog1. (A–B) Tubulin was used as loading control. Relative amount of phosphorylated versus non phosphorylated Hog1 is shown in the graph. Experiments were performed twice with similar results. The figure shows results from one representative experiment.

and it was previously reported that hypoosmotic conditions promote vacuole fusion while hyperosmotic conditions induce rapid vacuolar fragmentation (Herrera et al., 2017; Klionsky et al., 1990; Weisman, 2003). Numerous genes were reported recently to be involved in vacuole fragmentation (Michaillat and Mayer, 2013). Here we examined the role of Ptc1 in vacuole dynamics of *F. oxysporum* upon osmotic stress. Vacuoles in *F. oxysporum* are large and round, although their size, shape and number can vary depending on the developmental status, as reported in other filamentous fungi (Richards et al., 2010). We analysed the behaviour of vacuoles after osmotic stress induction using the fluorescent vacuolar vital stain FM4-64 (Fig. 8). Wild-type cells displayed large vacuoles that were fragmented into small vesicles after exposure to osmotic stress (0.6 M NaCl). By contrast, Δ*ptc1* cells contained constitutively fragmented vacuoles even in the absence of osmotic stress. These results suggest a role of Ptc1 in vacuole dynamics in *F. oxysporum*.

3.9. Ptc1 is not involved in virulence of F. oxysporum

In order to investigate the role of Ptc1 in pathogenesis, tomato plants were inoculated with 5×10^6 microconidia of the wild type, mutant or complemented strains. No significant differences were observed in the evolution of the disease symptoms (Fig. S4A). We then analysed the root adhesion ability of the three strains by submerging the roots in a microconidia suspension (5×10^6 microconidia/mL). After 72 h, no differences were observed in the adhesion of germlings of the wild type, mutant and complemented strains (Fig. S4B). Finally, we analysed the ability of the mutant strain to penetrate cellophane sheets, an assay that indicates the capability of the fungus to invade a solid surface (Prados Rosales and Di Pietro, 2008). Our results indicated no differences between the three analysed strains (Fig. S4C). Altogether

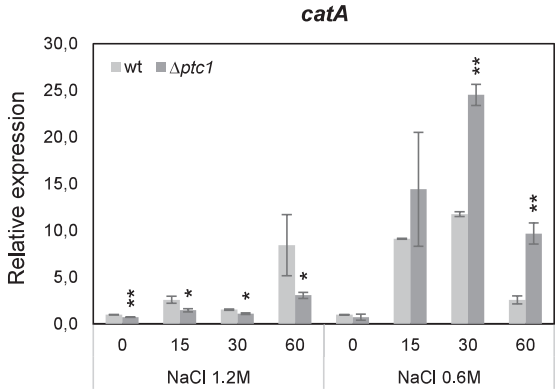

Fig. 6. The *ptc1* null mutant shows higher expression of the osmostress-induced gene *catA*. Germlings of the wild-type strain (wt) or Δ*ptc1* mutant were transferred to PDB supplemented with NaCl (1.2 M or 0.6 M) for 15, 30 and 60 min. RT-qPCR analysis was done using *catA* gene specific primers. Expression is referred as fold increase relative to wild-type control (time 0), using *actin* as reference gene. The results are expressed as average (± standard deviation) of three independent biological repeats ($p < 0.05$(*); $p < 0.01$(**). Bars represent standard error.

these results indicated that Ptc1 is not important for the pathogenesis in *F. oxysporum*.

4. Discussion

4.1. Ptc1 is a PP2C phosphatase that participates in stress response by acting on the CWI and HOG MAPK pathways

The *S. cerevisiae* PP2C family of phosphatases is composed by seven proteins (PTC1-PTC7) that participate in the regulation of different MAPK pathways. Several studies reported the role of PTC1 in dephosphorylation of Hog1, demonstrating the importance of this phosphatase for the correct functioning of the HOG pathway in yeast (Arino et al., 2011). Given the abundance of filamentous fungi harbouring multiple PP2C genes, a number of authors have suggested their involvement in key cellular processes, similar to yeast (Arino et al., 2011; Winkelstroter et al., 2015a; Winkelstroter et al., 2015b; Yang et al., 2013). We identified seven putative PP2C phosphatase genes in the genome of *F. oxysporum* that are orthologous to *S. cerevisiae* genes. Here we focused on the *F. oxysporum* orthologue of PTC1, encoded by the *FOX_11525* gene.

Similar to other fungi, three MAPK cascades interact in *F. oxysporum* to orchestrate the response to external insults including high temperature, cell wall, oxidative and hyperosmotic stress (Miguel-Rojas and Hera, 2016; Segorbe et al., 2017). For example, Segorbe et al. (2017) reported that deletion of the *hog1* gene in *F. oxysporum* causes increased sensitivity to hyperosmotic stress and enhanced resistance to the fungicides iprodione and fludioxonil. These phenotypes were specific of Δ*hog1* since they were neither exacerbated nor relieved by deletion of additional MAPKs. Here we found that deletion of *ptc1* causes a phenotype opposite to that of Δ*hog1* in cellular adaptation to osmotic and oxidative stress: a Δ*ptc1* mutant showed increased tolerance to NaCl, KCl and Sorbitol and higher sensitivity to caffeine and menadione. In contrast to the results obtained in *F. graminearum* (Jiang et al., 2010), we also observed higher tolerance of the Δ*ptc1* mutant to LiCl. In accordance with these findings, phosphorylation levels of Hog1 in the Δ*ptc1* mutant were notably higher, even in the absence of hyperosmotic or membrane stress, suggesting that Ptc1 acts as a phosphatase of Hog1 in *F. oxysporum*. This result is in agreement with those obtained in other fungi where the loss of Ptc1 is associated with constitutive

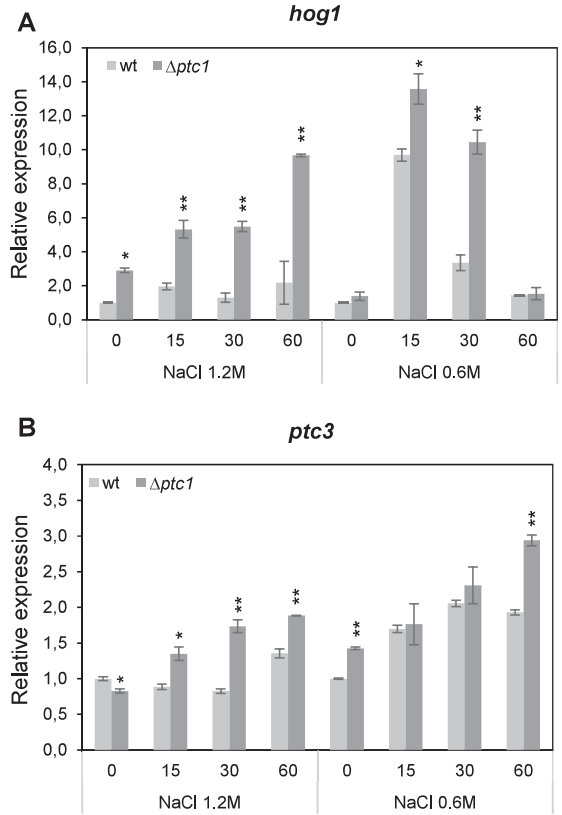

Fig. 7. The *ptc1* null mutant shows increased expression of *hog1* and *ptc3* genes. Germlings of the wild-type strain (wt) and Δ*ptc1* mutant were transferred to PDB supplemented with NaCl (1.2 M or 0.6 M) for 15, 30 and 60 min. RT-qPCR analysis was done using *hog1* (A) or *ptc3* (B) gene specific primers. Expression is referred as fold increase relative to wild-type control (time 0), using *actin* as reference gene. The results are expressed as average (± standard deviation) of three independent biological repeats ($p < 0.05$(*); $p < 0.01$(**). Bars represent standard error.

phosphorylation of Hog1 (Arino et al., 2011).

Previous studies reported an interplay between the HOG and CWI pathways (Liu et al., 2011; Rodriguez-Pena et al., 2010; Segorbe et al., 2017). Here we found that, while Mpk1 is rapidly phosphorylated in response to SDS as reported (Miguel-Rojas and Hera, 2016), phosphorylation of Mpk1 remained at a low level in the Δ*ptc1* mutant, indicating that Ptc1 might be a positive regulator of the Mpk1 pathway. A previous study in the fungal pathogen *B. cinereae* reported a similar result in response to CR, suggesting a positive role of BcPtc1 and BcPtc3 on the CWI MAPK pathway (Yang et al., 2013). The function of Ptc1 in the Mpk1 pathway might be either direct or indirect through cross-talk between the Hog1 and Mpk1 pathways. In a *B. cinereae* Δ*sak1* (Δhog1) mutant, BcBmp3 was highly phosphorylated during oxidative stress, suggesting a negative control of Bmp3 phosphorylation by Sak1 (Liu et al., 2011). It was suggested that this control could be direct by the action of Sak1 on the Bmp3 cascade or indirect by the action of phosphatases maintaining the equilibrium between MAPK phosphorylation.

4.2. Role of Ptc1 in regulation of stress response genes

Numerous studies contributed to the dissection of the HOG pathway in *S. cerevisiae* (Brewster and Gustin, 2014; de Nadal and Posas, 2010, 2015; Hohmann et al., 2007; Nadal-Ribelles et al., 2012; Saito and

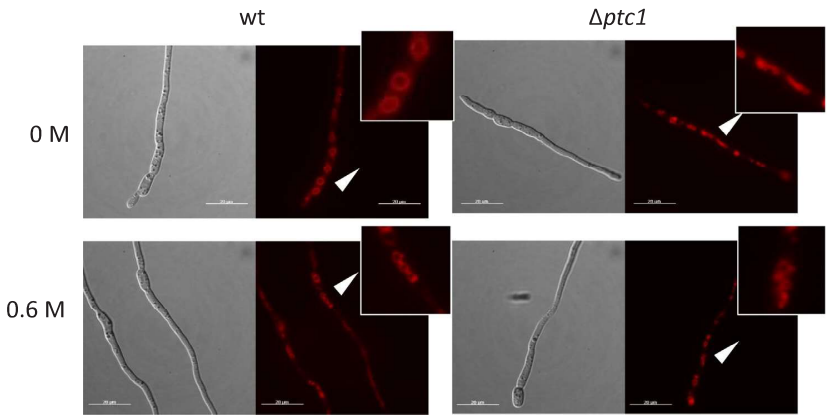

Fig. 8. *Ptc1* negatively regulates stress-induced vacuolar fragmentation. Representative micrographs showing wild-type (wt) and Δ*ptc1* hyphae after 15 min incubation at the indicated salt concentrations (left panel), stained with the membrane-specific dye FM4-64 (right panel). Bar = 20 μm.

Posas, 2012; Saito and Tatebayashi, 2004). It is currently accepted that, in response to different stresses, HOG1 is phosphorylated and transported to the nucleus where it interacts with transcription factors to activate the expression of many genes (Rep et al., 2001, 1999). Furthermore, it was shown that HOG1 interacts with the elongation subunit of the RNA pol II (Alepuz et al., 2001; Proft and Struhl, 2004). On the other hand, downregulation of the HOG pathway is essential since constitutive activation is detrimental to cell growth (Maeda et al., 1994). Several regulatory feedback loops exist in the HOG pathway where Hog1 targets upstream components of the system (Hao et al., 2007, 2008). In addition, regulation of the HOG pathway has been associated with protein dephosphorylation by the tyrosine phosphatases, Ptp2 and Ptp3 and the S/T phosphatase PP2C family (Ptc1), which counteract the pathway activation and adjust the dynamic range of response (Hohmann et al., 2007; Jacoby et al., 1997; Mapes and Ota, 2004; Warmka et al., 2001).

The results presented here support the idea that *F. oxysporum* Ptc1 modulates the expression of genes regulated by the Hog1 pathway. It is known that the correct balance between influx and efflux of cations is maintained through their transport across the cell membrane. Two key cation transporters in yeast are the *ENA*1 ATPase and the NHA1 antiporter. While *ENA1* is mainly regulated at the transcriptional level (Marquina et al., 2012; Ruiz and Arino, 2007), it was proposed that *NHA1* regulation is not mediated by transcriptional changes, but rather through Hog1-dependent phosphorylation of threonine residues (Kinclova-Zimmermannova and Sychrova, 2006; Krauke and Sychrova, 2011; Proft and Struhl, 2004) Here we found that the *F. oxysporum ena5* orthologue was highly induced under salt stress conditions, and that this induction was exacerbated in the Δ*ptc1* mutant. Thus, the increased sodium and lithium tolerance observed in the mutant cells could be due to increased efflux of these cations, mediated by Ena5, although a decrease in the cation influx cannot be discarded. In *S. cerevisiae*, transcriptional regulation of *ENA1* was explained through the action of different signalling pathways involving several kinases (Hog1, Pka or Snf1) and phosphatases (calcineurin, Ptc1 or Ppz1/Hal3) (Ruiz and Arino, 2007).

An interesting finding from our work is that, in contrast to yeast, the *F. oxysporum* antiporter Nha1 is transcriptionally regulated, and similar to *ena5*, *nha1* expression is higher in the Δ*ptc1* mutant than in the wild-type. In our study, expression levels of *ena5* and *nha1* were induced under salt stress in a Hog1-dependent manner. In *Cryptococcus neoformans*, Nha1 was transcriptionally upregulated in response to salt stress in a Hog1-dependent manner via the Rim101-Nrg1 pathway (Jung et al., 2012).

Transcriptional analysis in yeast identified signalling genes upregulated in response to salt stress, including genes involved in the HOG pathway such as *hog1* (Posas et al., 2000). The authors reported that transcriptional induction of most genes was largely or fully dependent on the presence of Hog1, indicating that the Hog1 plays a key role in global gene regulation under salt stress conditions. Here we found induction of *F. oxysporum hog1* transcript levels in response to salt stress, which was higher in the Δ*ptc1* mutant than in the wild-type, suggesting a direct or indirect role of Ptc1 in *hog1* expression. Moreover, expression of *ptc1* was stress-induced, particularly under hyperosmotic conditions, reinforcing a putative role in response to these stresses. Interestingly, expression of another PP2C gene, *ptc3*, was slightly induced after NaCl treatment, and this induction was also increased in the Δ*ptc1* mutant. This suggests that loss of Ptc1 can be partially compensated by the action of Ptc3. Similarly, in *A. fumigatus* loss of the PtcB phosphatase was supplied by other PP2C phosphatases (Winkelstroter et al., 2015a).

One of the most interesting aspects derived from our data is that the magnitude by which osmotic stress affects gene expression varies according to the salt concentration and the time after induction. Thus, *F. oxysporum catA*, *hog1* and *ptc3* genes were highly induced at lower (0.6 M) salt concentration. This is in accordance with a previous report in yeast showing that treatment with low salt concentrations induces the expression of a large number of genes after 10 min incubation, whereas only a low number of these remains upregulated after 20 min. By contrast, a higher salt concentration resulted in a larger number of genes remaining upregulated after 20 min of treatment (Posas et al., 2000).

4.3. Stress-induced vacuolar fragmentation is regulated by Ptc1

Vacuole fusion and fission are HOG-regulated homeostatic mechanisms that restore the osmolyte concentration of the cytosol (Bone et al., 1998). Here we show for the first time that hyperosmotic stress induces vacuole fragmentation in *F. oxysporum*, as shown in other fungi (Bone et al., 1998; Michaillat and Mayer, 2013). We further demonstrate that loss of Ptc1 leads to a vacuolar system composed of small vacuoles, mimicking those observed under hyperosmotic stress conditions. In fact, no difference in vacuole morphology was observed in the Δ*ptc1* mutant between NaCl-treated and non-treated cells. The constitutive presence of fragmented vacuoles could partially explain its increased tolerance to osmotic stress. It was described that upon osmotic stress, cell loses water and the vacuolar volume is reduced maintaining the membrane surface. Fragmentation of the organelle can thus readjust the surface to the volume under such conditions (Bonangelino et al., 2002).

In summary, our results demonstrate an important role of *F. oxysporum* Ptc1 in the response to stresses through the regulation of phosphorylation levels of two MAPK pathways and the subsequent regulation of gene expression and vacuolar dynamics.

Acknowledgements

The authors are grateful to E. Martínez Aguilera for technical assistance and to A. Di Pietro for helpful discussions and critical revision of the manuscript. This work was supported by grants BIO2013-47870R and BIO2016-78923-R from the Spanish Ministerio de Innovación y Competitividad (MINECO) and BIO-296 from Junta de Andalucia. PFL Student PhD was supported by Science Without Borders programme (CAPES, Ministry of Education and Ministry of Science and Technology), Federal Government of Brazil.

Appendix A. Supplementary material

Supplementary data associated with this article can be found, in the online version, at https://doi.org/10.1016/j.fgb.2018.05.004.

References

Aburai, N., et al., 2013. Pisiferdiol restores the growth of a mutant yeast suffering from hyperactivated Ca2+ signalling through calcineurin inhibition. FEMS Yeast Res. 13, 16–22.
Alepuz, P.M., et al., 2001. Stress-induced map kinase Hog1 is part of transcription activation complexes. Mol Cell. 7, 767–777.
Arino, J., et al., 2011. Type 2C protein phosphatases in fungi. Eukaryot Cell. 10, 21–33.
Arino, J., et al., 2010. Alkali metal cation transport and homeostasis in yeasts. Microbiol. Mol. Biol. Rev. 74, 95–120.
Bonangelino, C.J., et al., 2002. Genomic screen for vacuolar protein sorting genes in Saccharomyces cerevisiae. Mol. Biol. Cell. 13, 2486–2501.
Bone, N., et al., 1998. Regulated vacuole fusion and fission in Schizosaccharomyces pombe: an osmotic response dependent on MAP kinases. Curr. Biol. 8, 135–144.
Brewster, J.L., Gustin, M.C., 2014. Hog1: 20 years of discovery and impact. Sci Signal. 7, re7.
Caracuel, Z., et al., 2003. pH response transcription factor PacC controls salt stress tolerance and expression of the P-Type Na+ -ATPase Ena1 in Fusarium oxysporum. Eukaryot Cell. 2, 1246–1252.
Cohen, P., 1989. The structure and regulation of protein phosphatases. Annu. Rev. Biochem. 58, 453–508.
Cheng, A., et al., 1999. Dephosphorylation of cyclin-dependent kinases by type 2C protein phosphatases. Genes Dev. 13, 2946–2957.
Chomczynski, P., Sacchi, N., 1987. Single-step method of RNA isolation by acid guanidinium thiocyanate-phenol-chloroform extraction. Anal. Biochem. 162, 156–159.
Das, A.K., et al., 1996. Crystal structure of the protein serine/threonine phosphatase 2C at 2.0 A resolution. Embo J. 15, 6798–6809.
de Nadal, E., Posas, F., 2010. Multilayered control of gene expression by stress-activated protein kinases. EMBO J. 29, 4–13.
de Nadal, E., Posas, F., 2015. Osmostress-induced gene expression–a model to understand how stress-activated protein kinases (SAPKs) regulate transcription. FEBS J. 282, 3275–3285.
Dean, R., et al., 2012. The Top 10 fungal pathogens in molecular plant pathology. Mol. Plant. Pathol. 13, 414–430.
Di Pietro, A., et al., 2001. A MAP kinase of the vascular wilt fungus Fusarium oxysporum is essential for root penetration and pathogenesis. Mol. Microbiol. 39, 1140–1152.
Di Pietro, A., Roncero, M.I., 1998. Cloning, expression, and role in pathogenicity of pg1 encoding the major extracellular endopolygalacturonase of the vascular wilt pathogen Fusarium oxysporum. Mol. Plant. Microbe Interact. 11, 91–98.
Fuchs, B.B., Mylonakis, E., 2009. Our paths might cross: the role of the fungal cell wall integrity pathway in stress response and cross talk with other stress response pathways. Eukaryot Cell. 8, 1616–1625.
Gonzalez, A., et al., 2009. Normal function of the yeast TOR pathway requires the type 2C protein phosphatase Ptc1. Mol. Cell Biol. 29, 2876–2888.
Gonzalez, A., et al., 2006. Transcriptional profiling of the protein phosphatase 2C family in yeast provides insights into the unique functional roles of Ptc1. J. Biol. Chem. 281, 35057–35069.
Hao, N., et al., 2007. A systems-biology analysis of feedback inhibition in the Sho1 osmotic-stress-response pathway. Curr Biol. 17, 659–667.
Hao, N., et al., 2008. Control of MAPK specificity by feedback phosphorylation of shared adaptor protein Ste50. J. Biol. Chem. 283, 33798–33802.
Herrera, R., et al., 2017. Vacuolar control of subcellular cation distribution is a key parameter in the adaptation of Debaryomyces hansenii to high salt concentrations. Fungal Genet. Biol. 100, 52–60.
Hohmann, S., 2009. Control of high osmolarity signalling in the yeast Saccharomyces cerevisiae. FEBS Lett. 583, 4025–4029.
Hohmann, S., et al., 2007. Yeast osmoregulation. Methods Enzymol. 428, 29–45.
Jacoby, T., et al., 1997. Two protein-tyrosine phosphatases inactivate the osmotic stress response pathway in yeast by targeting the mitogen-activated protein kinase, Hog1. J. Biol. Chem. 272, 17749–17755.
Jiang, J., et al., 2011. A type 2C protein phosphatase FgPtc3 is involved in cell wall integrity, lipid metabolism, and virulence in Fusarium graminearum. PLoS One 6, e25311.
Jiang, L., et al., 2010. The type 2C protein phosphatase FgPtc1p of the plant fungal pathogen Fusarium graminearum is involved in lithium toxicity and virulence. Mol. Plant. Pathol. 11, 277–282.
Jung, K.W., et al., 2012. Two cation transporters Ena1 and Nha1 cooperatively modulate ion homeostasis, antifungal drug resistance, and virulence of Cryptococcus neoformans via the HOG pathway. Fungal Genet. Biol. 49, 332–345.
Kinclova-Zimmermannova, O., Sychrova, H., 2006. Functional study of the Nha1p C-terminus: involvement in cell response to changes in external osmolarity. Curr. Genet. 49, 229–236.
Klionsky, D.J., et al., 1990. The fungal vacuole: composition, function, and biogenesis. Microbiol. Rev. 54, 266–292.
Krauke, Y., Sychrova, H., 2011. Cnh1 Na(+) /H(+) antiporter and Ena1 Na(+) -ATPase play different roles in cation homeostasis and cell physiology of Candida glabrata. FEMS Yeast Res. 11, 29–41.
Lammers, T., Lavi, S., 2007. Role of type 2C protein phosphatases in growth regulation and in cellular stress signaling. Crit. Rev. Biochem. Mol. Biol. 42, 437–461.
Liu, J., et al., 2017. Characterization of the Hog1 MAPK pathway in the entomopathogenic fungus Beauveria bassiana. Environ. Microbiol. 19, 1808–1821.
Liu, W., et al., 2011. The osmosensing signal transduction pathway from Botrytis cinerea regulates cell wall integrity and MAP kinase pathways control melanin biosynthesis with influence of light. Fungal Genet. Biol. 48, 377–387.
Livak, K.J., Schmittgen, T.D., 2001. Analysis of relative gene expression data using real-time quantitative PCR and the 2(-Delta Delta C(T)) Method. Methods 25, 402–408.
Lopez-Berges, M.S., et al., 2010. A nitrogen response pathway regulates virulence functions in Fusarium oxysporum via the protein kinase TOR and the bZIP protein MeaB. Plant Cell. 22, 2459–2475.
Lu, G., Wang, Y., 2008. Functional diversity of mammalian type 2C protein phosphatase isoforms: new tales from an old family. Clin. Exp. Pharm. Physiol. 35, 107–112.
Maeda, T., et al., 1994. A two-component system that regulates an osmosensing MAP kinase cascade in yeast. Nature 369, 242–245.
Mapes, J., Ota, I.M., 2004. Nbp2 targets the Ptc1-type 2C Ser/Thr phosphatase to the HOG MAPK pathway. EMBO J. 23, 302–311.
Marquina, M., et al., 2012. Modulation of yeast alkaline cation tolerance by Ypi1 requires calcineurin. Genetics 190, 1355–1364.
Michaillat, L., Mayer, A., 2013. Identification of genes affecting vacuole membrane fragmentation in Saccharomyces cerevisiae. PLoS One 8, e54160.
Miguel-Rojas, C., Hera, C., 2016. The F-box protein Fbp1 functions in the invasive growth and cell wall integrity mitogen-activated protein kinase (MAPK) pathways in Fusarium oxysporum. Mol. Plant. Pathol. 17, 55–64.
Nadal-Ribelles, M., et al., 2012. Hog1 bypasses stress-mediated down-regulation of transcription by RNA polymerase II redistribution and chromatin remodeling. Genome. Biol. 13, R106.
Nucci, M., Anaissie, E., 2007. Fusarium infections in immunocompromised patients. Clin. Microbiol. Rev. 20, 695–704.
Pearson, G., et al., 2001. Mitogen-activated protein (MAP) kinase pathways: regulation and physiological functions. Endocr. Rev. 22, 153–183.
Perez-Nadales, E., Di Pietro, A., 2011. The membrane mucin Msb2 regulates invasive growth and plant infection in Fusarium oxysporum. Plant Cell 23, 1171–1185.
Petrezselyova, S., et al., 2016. Regulation of the Na+/K+-ATPase Ena1 Expression by Calcineurin/Crz1 under High pH Stress: a quantitative study. PLoS One 11, e0158424.
Posas, F., et al., 2000. The transcriptional response of yeast to saline stress. J. Biol. Chem. 275, 17249–17255.
Prados Rosales, R.C., Di Pietro, A., 2008. Vegetative hyphal fusion is not essential for plant infection by Fusarium oxysporum. Eukaryot Cell. 7, 162–171.
Proft, M., Struhl, K., 2004. MAP kinase-mediated stress relief that precedes and regulates the timing of transcriptional induction. Cell 118, 351–361.
Puhalla, J.E., 1985. Classification of Fusarium oxysporum on the basis of vegetative compatibility. Can. J. Botany 63, 179–183.
Raeder, U., Broda, P., 1985. Rapid preparation of DNA from filamentous fungi. Lett. Appl. Microbiol. 1, 17–20.
Rep, M., et al., 2001. The Saccharomyces cerevisiae Sko1p transcription factor mediates HOG pathway-dependent osmotic regulation of a set of genes encoding enzymes implicated in protection from oxidative damage. Mol. Microbiol. 40, 1067–1083.
Rep, M., et al., 1999. Osmotic stress-induced gene expression in Saccharomyces cerevisiae requires Msn1p and the novel nuclear factor Hot1p. Mol. Cell Biol. 19, 5474–5485.
Richards, A., Veses, V., Gow, N.A.R., 2010. Vacuole dynamics in fungi. Fungal Biol. Rev. 24, 13.
Rispail, N., Di Pietro, A., 2010. The two-component histidine kinase Fhk1 controls stress adaptation and virulence of Fusarium oxysporum. Mol. Plant. Pathol. 11, 395–407.
Rispail, N., et al., 2009. Comparative genomics of MAP kinase and calcium-calcineurin signalling components in plant and human pathogenic fungi. Fungal Genet. Biol. 46, 287–298.
Rodriguez-Pena, J.M., et al., 2010. The high-osmolarity glycerol (HOG) and cell wall integrity (CWI) signalling pathways interplay: a yeast dialogue between MAPK routes. Yeast 27, 495–502.
Ruan, H., et al., 2007. The YCR079w gene confers a rapamycin-resistant function and encodes the sixth type 2C protein phosphatase in Saccharomyces cerevisiae. FEMS Yeast Res. 7, 209–215.
Ruiz, A., Arino, J., 2007. Function and regulation of the Saccharomyces cerevisiae ENA sodium ATPase system. Eukaryot Cell. 6, 2175–2183.

Saito, H., Posas, F., 2012. Response to hyperosmotic stress. Genetics 192, 289–318.
Saito, H., Tatebayashi, K., 2004. Regulation of the osmoregulatory HOG MAPK cascade in yeast. J. Biochem. 136, 267–272.
Sambade, M., et al., 2005. A genomic screen for yeast vacuolar membrane ATPase mutants. Genetics 170, 1539–1551.
Sambrook, J.F., Maniatis, T.E.F., 2001. Molecular cloning: a laboratory manual.
Segorbe, D., et al., 2017. Three Fusarium oxysporum mitogen-activated protein kinases (MAPKs) have distinct and complementary roles in stress adaptation and cross-kingdom pathogenicity. Mol. Plant. Pathol. 18, 912–924.
Shi, Y., 2009. Serine/threonine phosphatases: mechanism through structure. Cell 139, 468–484.
Son, H., et al., 2015. Fss1 is involved in the regulation of an ENA5 homologue for sodium and lithium tolerance in Fusarium graminearum. Environ. Microbiol. 17, 2048–2063.
Turra, D., et al., 2014. Protein kinases in plant-pathogenic fungi: conserved regulators of infection. Annu. Rev. Phytopathol. 52, 267–288.
Uetz, P., et al., 2000. A comprehensive analysis of protein-protein interactions in Saccharomyces cerevisiae. Nature 403, 623–627.
Warmka, J., et al., 2001. Ptc1, a type 2C Ser/Thr phosphatase, inactivates the HOG pathway by dephosphorylating the mitogen-activated protein kinase Hog1. Mol. Cell Biol. 21, 51–60.
Weisman, L.S., 2003. Yeast vacuole inheritance and dynamics. Annu. Rev. Genet. 37, 435–460.
Widmann, C., et al., 1999. Mitogen-activated protein kinase: conservation of a three-kinase module from yeast to human. Physiol. Rev. 79, 143–180.
Winkelstroter, L.K., et al., 2015a. High osmolarity glycerol response PtcB phosphatase is important for Aspergillus fumigatus virulence. Mol. Microbiol. 96, 42–54.
Winkelstroter, L.K., et al., 2015b. Systematic Global Analysis of Genes Encoding Protein Phosphatases in Aspergillus fumigatus. G3 (Bethesda). vol. 5, pp. 1525–1539.
Yang, Q., et al., 2013. Involvement of two type 2C protein phosphatases BcPtc1 and BcPtc3 in the regulation of multiple stress tolerance and virulence of Botrytis cinerea. Environ. Microbiol. 15, 2696–2711.